Los Alamos
NATIONAL LABORATORY
EST. 1943

Associate Director for ESH
Environment, Safety, and Health
P.O. Box 1663, MS K491
Los Alamos, New Mexico 87545
505-667-4218/Fax 505-665-3811

National Nuclear Security Administration
Los Alamos Field Office, MS A316
Environmental Projects Office
Los Alamos, New Mexico 87544
(505) 667-4255/FAX (505) 606-2132

Date: JAN 29 2015
Refer To: ADESH-15-006
LAUR: 15-20165
Locates Action No.: N/A

John Kieling, Bureau Chief
Hazardous Waste Bureau
New Mexico Environment Department
2905 Rodeo Park Drive East, Building 1
Santa Fe, NM 87505-6303

Subject: Submittal of the Completion Report for Groundwater Extraction Well CrEX-1

Dear Mr. Kieling:

Enclosed please find two hard copies with electronic files of the Completion Report for Groundwater Extraction Well CrEX-1.

If you have any questions, please contact Stephani Swickley at (505) 606-1628 (sfuller@lanl.gov) or Cheryl Rodriguez at (505) 665-5330 (cheryl.rodriguez@nnsa.doe.gov).

Sincerely,

Michael T. Brandt, DrPH, CIH, Associate Director
Environment, Safety, and Health
Los Alamos National Laboratory

Sincerely,

Peter Maggiore, Assistant Manager
Environmental Projects Office
Los Alamos Field Office

MB/PM/DM/SS:sm

Enclosures: Two hard copies with electronic files – Completion Report for Groundwater Extraction Well CrEX-1

Cy: (w/enc.)
Hai Shen, DOE-NA-LA, MS A316
Cheryl Rodriguez, DOE-NA-LA, MS A316
Stephani Swickley, ADEP-ER Program, MS M992
Public Reading Room (EPRR)
ADESH Records (electronic copy)

Cy: (Letter and CD and/or DVD)
Laurie King, EPA Region 6, Dallas, TX
Steve Yanicak, NMED-DOE-OB, MS M894
Vern Christensen, Yellow Jacket Drilling
Ted Ball, ADEP-ER Program, MS M992
PRS Database

Cy: (w/o enc.)
Tom Skibitski, NMED-DOE-OB (date-stamped letter emailed)
lasomailbox@nnsa.doe.gov
Annette Russell, DOE-NA-LA (date-stamped letter emailed)
David Rhodes, DOE-NA-LA (date-stamped letter emailed)
Kimberly Davis Lebak, DOE-NA-LA (date-stamped letter emailed)
Dave McInroy, ADEP-ER Program (date-stamped letter emailed)
Randy Erickson, ADEP (date-stamped letter emailed)
Tony Grieggs, ADESH-ENV-CP (date-stamped letter emailed)
Alison Dorries, ADESH-ENV-CP (date-stamped letter emailed)
Michael Brandt, ADESH (date-stamped letter emailed)
Amy De Palma, PADOPS (date-stamped letter emailed)
Michael Lansing, PADOPS (date-stamped letter emailed)

LA-UR-15-20165
January 2015
EP2015-0005

Completion Report for Groundwater Extraction Well CrEX-1

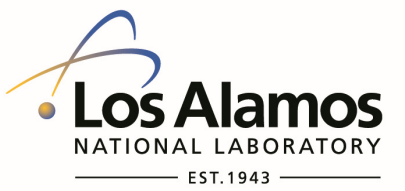

Prepared by the Environmental Programs Directorate

EP2015-0005

Completion Report for Groundwater Extraction Well CrEX-1

January 2015

Responsible project manager:

Printed Name	Signature	Title	Organization	Date
Stephani Swickley	Stephani Swickley	Project Manager	Environmental Programs	1/14/15

Responsible LANS representative:

Printed Name	Signature	Title	Organization	Date
Randall Erickson		Acting Associate Director	Environmental Programs	1/20/15

Responsible DOE representative:

Printed Name	Signature	Title	Organization	Date
Peter Maggiore	Peter Maggiore	Assistant Manager	DOE-NA-LA	1/29/15

EXECUTIVE SUMMARY

This completion report describes the drilling, installation, well development, aquifer testing, and pumping system installation for chromium extraction well 1 (CrEX-1), located in Technical Area 05 at Los Alamos National Laboratory.

CrEX-1 was installed as a hydraulic control well at the southern edge of the known plume of contamination. The work plan for installation of this extraction well was approved by the New Mexico Environment Department (NMED) in July 2014.

The CrEX-1 borehole was drilled using fluid-assisted dual-rotary drilling methods and mud-rotary methods. Drilling fluid additives included potable water, a foaming agent, and bentonite-based drilling mud. The drilling work plan for CrEX-1 proposed completion of a single-screen extraction well in the regional aquifer; however, a two-screen well was installed after review of the geophysical logs indicated the potential for water production from the upper part of the screen was minimal. In keeping with the objective of hydraulic capture as close to the top of the aquifer as possible, a two-screen approach was proposed to, and approved by, NMED. The well contains an upper screen 50 ft in length and a lower screen 20 ft in length, separated by 30 ft of blank pipe with a mechanical packer set between the screens. CrEX-1 was completed per the NMED-approved well design.

Following development, it was determined that the upper screen alone could produce the required amounts of water. Therefore, a mechanical packer was set between the upper and lower screened intervals, and the pumping campaign continued using only the upper screen. The pumping of CrEX-1 produces about 6.2 m (~20 ft) drawdown at the well within the pumped screen. However, the pumping test data do not suggest that the pumping produces a significant drawdown in the aquifer adjacent to the screen.

Geologic formations encountered during drilling included, in descending stratigraphic order, Tshirege Member of the Bandelier Tuff, Cerro Toledo interval, Otowi Member of the Bandelier Tuff (including the Guaje Pumice Bed), upper Puye Formation, Cerros del Rio volcanic series, the lower Puye Formation, Miocene pumiceous sediments, and Miocene riverine deposits.

The regional water table occurs within Miocene pumiceous sand and gravel at a depth of 997.2 ft below ground surface as measured in the completed well with a packer between the upper and lower screens.

CONTENTS

Figures

Tables

Appendixes

Acronyms and Abbreviations

amsl	above mean sea level
API	American Petroleum Institute
APS	accelerator porosity sonde
bgs	below ground surface
Consent Order	Compliance Order on Consent
EP	Environmental Programs (Directorate)
ESH	Environment, Safety, and Health (Directorate)
gpm	gallons per minute
hp	horsepower
HNGS	hostile natural gamma spectroscopy
I.D.	inside diameter
LANL	Los Alamos National Laboratory
MR	magnetic resonance
NAD	North American Datum
NMED	New Mexico Environment Department
NTU	nephelometric turbidity unit
O.D.	outside diameter
PVC	polyvinyl chloride
TA	technical area

TBD	to be determined
TD	total depth
VOA	volatile organic analysis

1.0 INTRODUCTION

This completion report summarizes the drilling, well construction, well development, aquifer testing, and pumping system installation for chromium extraction well 1 (CrEX-1). CrEX-1 was drilled and installed from July 4, 2014, to August 17, 2014, at Los Alamos National Laboratory (LANL or the Laboratory) for the Environmental Programs (EP) Directorate.

CrEX-1 is located within Technical Area 05 (TA-05) north of the narrow ridge that separates Mortandad and Cedro Canyons (Figure 1.0-1). The primary purpose of CrEX-1 is to attain hydraulic control of chromium-contaminated groundwater from beneath Mortandad Canyon and to prevent migration of this water farther southward towards San Ildefonso Pueblo. Water-quality and hydrologic data from CrEX-1 will also be used in conjunction with information from other wells in the area to assess where additional hydraulic control and source removal wells may be positioned in the future.

The work plan for installing CrEX-1 was approved by the New Mexico Environment Department (NMED) in its July 8, 2014, letter, "Approval Drilling Work Plan for Groundwater Extraction Well CrEX-1" (LANL 2014, 254824; NMED 2014, 525004). Earlier approval to begin work was received from NMED by e-mail on June 19, 2014 (Dale 2014, 600135). The approved work plan specified that a single screen up to 100 ft long would be installed in the regional aquifer. However, geophysical logging of the borehole indicated that the upper portion of the well might contribute only minimal water to the total well production. Therefore, a dual-screen design was proposed by the Laboratory and approved by NMED on August 8, 2014 (see Appendix A). The dual-screen design would allow for a packer to be inserted between the upper and lower screens if sufficient water production was achieved in the upper screen. The well screens were set between 1090 ft and 1070 ft below ground surface (bgs) and 1040 ft and 990 ft bgs. The water level was 997.2 ft bgs after development of both screens and placement of a packer between the upper and lower screened intervals.

Characterization during drilling included collection of cuttings samples at 10-ft intervals from ground surface to total depth (TD) for lithologic evaluation. Borehole logs included video and natural gamma logs conducted by the Laboratory and a full suite of geophysical logs conducted by Schlumberger.

Postinstallation activities included well development, aquifer testing, pumping system installation, and geodetic surveying. The aquifer testing demonstrated a relatively high permeability of the aquifer screened by CrEX-1. Future activities will include surface completion, site restoration, and continued waste management.

The information presented in this report was compiled from field reports and daily activity summaries. Records, including field reports, field logs, and survey information, are on file in the Laboratory's Electronic Document Management System. This report contains summary descriptions of activities and supporting figures, tables, and appendixes associated with the CrEX-1 well drilling and installation project.

2.0 ADMINISTRATIVE PREPARATION

The following documents were prepared to guide activities associated with the drilling, installation, and pumping of groundwater extraction well CrEX-1:

- "Drilling Work Plan for Groundwater Extraction Well CrEX-1" (LANL 2014, 254824)
- "Field Implementation Plan for Well CrEX-1" (LANL 2014, 600129)

- "[Integrated Work Document for] Implementation of the Drilling Work Plan for Groundwater Extraction Well CrEX-1" (Yellow Jacket Drilling 2014, 600131)
- "Spill Prevention Control and Countermeasures Plan for the ADEP Groundwater Monitoring Well Drilling Operations, Los Alamos National Laboratory, Revision 6" (North Wind Inc. 2011, 213292)
- "Waste Characterization Strategy Form for Chromium Well CrEX-1" (LANL 2014, 254859)
- "Application for Permit to Drill a Well with No Consumptive Use of Water" (OSE 2014, 600141)
- "Temporary Permission to Discharge, Treated Ground Water from Aquifer Testing at Pilot Pumping Well CrEX-1 (AI: 856, PRD20140007)" (NMED 2014, 600128)
- "Well Pump Tests Phase II in Sandia and Mortandad Canyons," U.S. Department of Energy Categorical Exclusion Determination Form (DOE 2014, 600140)

3.0 DRILLING ACTIVITIES

This section describes the drilling strategy and approach and provides a chronological summary of field activities conducted during the drilling of CrEX-1.

3.1 Drilling Approach

The CrEX-1 borehole was drilled using a Foremost DR-24HD dual-rotary drilling rig. The dual-rotary system allows for advancement of casing with the casing rotator while drilling with conventional air/mist/foam methods with the drill string. The Foremost DR-24HD drill rig was equipped with a 5.5-in.–outside diameter (O.D.) dual-wall reverse-circulation drill pipe, tricone bits, downhole hammer bits, and general drilling equipment. Casing sizes used in drilling activities included 20-in., 18-in., and 16-in. nominal diameters. Casing sizes were selected to ensure the required 3-in. minimum annular thickness of the filter pack would be achieved around an 8.62-in.-O.D. well screen, as recommended by the American Water Works Association for municipal well construction (standard A100). The dual-rotary and standard rotary (open-hole) techniques used filtered compressed air, fluid-assisted air, and bentonite-based drilling mud to evacuate cuttings from the borehole.

Drilling fluids, including compressed air, municipal water, and a mixture of municipal water with Baroid brand QUIK-FOAM foaming agent, were used as needed to advance the borehole to a depth of 820 ft bgs, just below the base of the Cerros del Rio volcanic series. The fluids were used to cool the bit and help lift cuttings from the borehole. At 820 ft bgs, the drilling subcontractor switched to a flooded reverse-circulation method using bentonite-based mud in an effort to drill the remainder of the borehole open hole. After trying to remedy lost circulation issues for several days, the drillers tried a modified flooded reverse-circulation system with the crossover subset in the drill string 50 ft above the bit. This approach was successful at advancing the borehole, maintaining borehole stability, returning cuttings to the surface, and achieving the planned TD of 1200 ft bgs.

3.2 Chronology of Drilling Activities

Decontamination of the drill rig and associated tools was performed before the crew arrived at the drill site. Drilling equipment and supplies were mobilized and prepared for drilling between June 30 and July 4, 2014. Drilling of the CrEX-1 borehole began on July 4, 2014, when a 20-in.-O.D. surface casing was installed with a 24-in.-diameter tricone bit and dual-rotary drilling method. The 24-in.-diameter borehole was advanced to 65 ft bgs. However, the 20-in.-O.D. casing could only be advanced to a depth of 35 ft bgs. The borehole was then filled from 65 ft to 35 ft bgs with cement grout, and the annular space

between the 20-in. casing and the 24-in.-diameter borehole wall was filled. The surface casing was set in unit 1v of the Tshirege Member of the Bandelier Tuff.

A 19-in.-diameter borehole was drilled to 475 ft bgs (top of the Cerros del Rio volcanic series) using casing-advance methods, including the use of potable water and foam. This portion of the well was cased with 18-in.-O.D. casing. Five feet of this casing, including the casing shoe, was cut off and left in the borehole from 475 ft to 470 ft bgs.

A 17-in.-diameter borehole was advanced from 475 ft to 816 ft bgs (bottom of the Cerros del Rio volcanic series) using casing-advance methods, including the use of potable water and foam. This portion of the well was cased with 16-in.-O.D. casing. Five feet of this casing, including the casing shoe, was cut off and left in the borehole from 816 ft to 811 ft bgs.

At 816 ft bgs, the drilling method was switched to flooded reverse-circulation using mud. However, circulation was lost at this depth and several days were spent changing the mud mixture and adding circulation-restoring additives (Baroid products BENSEAL and AQUAGUARD) to the mixture. On July 31, 2014, 8 yd of neat cement was placed downhole, allowed to set up for 12 h, and then drilled through. This appeared to stabilize the borehole but did not restore circulation. On August 2, 2014, a revised bottom-hole assembly with the crossover subset only 50 ft above the drill bit was used to successfully drill ahead to 1035 ft bgs. This approach used a modified reverse-circulation method by pumping drilling mud at a controlled rate from the top instead of flooding the borehole. The borehole was completed to a TD of 1211 ft bgs on August 4, 2014.

The borehole was logged by Schlumberger on August 6 and 7, 2014. A proposed well design was submitted by the Laboratory to NMED for review on August 8, 2014, and was approved the same day (Appendix A).

Well construction began on August 12, 2014.

4.0 SAMPLING ACTIVITIES

The following sections describe the cuttings sampling activities for CrEX-1. No groundwater samples were collected during drilling. All sampling activities were conducted in general accordance with applicable quality procedures.

4.1 Cuttings Sampling

Cuttings samples were collected at 10-ft intervals from the borehole beginning at 170 ft to the TD of 1211 ft bgs. At each interval, the drillers collected approximately 500 mL of bulk cuttings from the discharge cyclone, placed them in canvas or plastic bags, labeled them, and stored them on-site. Radiological control technicians screened cuttings before they were removed from the site, and screening measurements were within the range of background values. The cuttings were delivered to the Laboratory's Geology and Geochemistry Research Laboratory for binocular microscope analysis.

Section 5.1 of this report summarizes the stratigraphy encountered at well CrEX-1.

5.0 GEOLOGY AND HYDROGEOLOGY

A brief description of the geologic and hydrogeologic features encountered at CrEX-1 is presented below. The Laboratory's geology task leader and geologists examined the cuttings to determine the geologic

contacts and hydrogeologic conditions. Drilling observations, video logging, geophysics, and water-level measurements were used to characterize groundwater occurrences.

5.1 Stratigraphy

The stratigraphy and contacts presented below are based on lithologic descriptions of cuttings samples collected from the discharge cyclone, borehole geophysical logs, and video logs. Geologic units are described below in order of youngest to oldest geologic units. Figure 5.1-1 illustrates the stratigraphy at CrEX-1.

No cuttings were collected from 0 ft to 170 ft bgs, and no geophysical logs were run from 0 ft to 200 ft bgs, so contacts for the upper geologic units are based on depths predicted by the sitewide geologic model. Descriptions of these uncharacterized units are taken from nearby wells.

Unit 1v, Tshirege Member of the Bandelier Tuff, Qbt 1v (0 ft to 62 ft bgs)

Unit 1v of the Tshirege Member of the Bandelier Tuff consists of light and brownish-gray to dark yellowish-brown, poorly welded, crystal- and lithic-rich devitrified ash-flow tuff.

Unit 1g, Tshirege Member of the Bandelier Tuff, Qbt 1g (62 ft to 122 ft bgs)

Unit 1g of the Tshirege Member of the Bandelier Tuff consists of grayish-orange-pink to very pale orange to light brown, nonwelded to poorly welded vitric ash-flow tuff.

Cerro Toledo Interval, Qct (122 ft to 144 ft bgs)

The Cerro Toledo interval consists of light gray to light brownish-gray and pale red to light brown, poorly to well-sorted tuffaceous sedimentary deposits that occur between the Tshirege and Otowi Members of the Bandelier Tuff. The deposits are predominantly reworked tuff with minor silt, sands, granules, and gravels derived from Cerro Toledo rhyolites, Tschicoma dacites, and Otowi tuffs eroded from the Sierra de los Valles highlands west of the Pajarito Plateau. The formation commonly exhibits pervasive light pale orange to grayish-orange oxidation.

Otowi Member of the Bandelier Tuff, Qbo (144 ft to 433 ft bgs)

The Otowi Member of the Bandelier Tuff consists of white to light gray pumiceous, nonwelded to partly welded ash-flow tuff with vitric, fibrous pumices, phenocrysts, and lithic clasts that include a variety of pale brown and olive gray to brownish-gray intermediate-composition volcanic rocks.

Guaje Pumice Bed of the Otowi Member of the Bandelier Tuff, Qbog (433 ft to 450 ft bgs)

The Guaje Pumice Bed is white to gray and reddish-gray and contains pumice fragments with subordinate amounts of volcanic lithics and quartz and sanidine phenocrysts. The presence of this unit was difficult to determine based on drill cuttings alone. The unit boundaries were determined based on the high borehole gamma-ray response commonly found in this unit in nearby wells.

Puye Formation, Tpf (450 ft to 460 ft bgs)

The Puye Formation consists of unconsolidated, light brown, fairly sorted, volcaniclastic sand with a silty matrix of glassy shards and clay. These deposits contain abundant quartz and feldspar and minor pumice and dacite clasts up to 0.5 cm in size.

Cerros del Rio Volcanic Series, Tb4 (460 ft to 809 ft bgs)

The Cerros del Rio volcanic series consists of dark to medium gray, massive to vesicular basaltic lava flows separated by porous zones of interflow breccias. The basalts are sparsely porphyritic with phenocrysts of pyroxene, plagioclase, and altered olivine. Thin intervals of pinkish-gray claystone are intercalated with basalt in the lower part of the unit.

Puye Formation, Tpf (809 ft to 1054 ft bgs)

The Puye Formation consists of moderate brown and grayish-orange to very dusky red, poorly to moderately sorted volcaniclastic sediments with subangular to subrounded boulders, cobbles, gravels, sands, and silts. Clasts in these sedimentary deposits consist of dacitic detritus shed from the Tschicoma Formation exposed in the Sierra de los Valles highlands west of the Pajarito Plateau.

Mixed Miocene Deposits, Tjfp and Tcar (1054 ft to 1070 ft bgs)

The mixed Miocene deposits are a mixture of pumiceous sediments and riverine deposits that contain characteristics of both the Tjfp and Tcar units. The pumiceous sediments are represented by clasts of white crystal-poor vitric pumice and light gray rhyolite lavas. Riverine components include well-rounded lithic sands and gravels made up of intermediate-composition volcanics and minor (<5%) quartzite. The riverine sediments also include intervals of fine-grained crystal sand.

Miocene Pumiceous Sediments, Tjfp (1070 ft to 1155 ft bgs)

Miocene pumiceous sediments form an unassigned unit that consists of light brown and very light gray to tan tuffaceous silty sand with multicolored rhyolitic and dacitic gravel. Cuttings from this unit contain abundant, reworked, subrounded, white vitric pumice and gray vitric and devitrified rhyolite lava clasts in a silty and sandy matrix of rhyolite ash and fine-grained felsic crystals. Milky perlite and obsidian are minor but ubiquitous clasts in these deposits. Pumice clasts contain sparse biotite phenocrysts.

Miocene Riverine Deposits, Tcar (1155 ft to 1211 ft bgs)

Miocene riverine deposits consist of medium brown and grayish-orange-pink silty sand with subrounded to rounded gravel composed of dacite and minor quartzite. The sand fraction includes fine sand and silt dominated by rounded and frosted quartz and coarse lithic sand made up of intermediate volcanics. These deposits are probably correlative with the Chamita Formation of the Santa Fe Group.

5.2 Groundwater

No perched water was encountered during the drilling of CrEX-1. On August 8, 2014, after the well was drilled to a depth of 1211 ft bgs, a water level for the regional aquifer inside the drill casing was measured at 988 ft bgs. The depth to water in the open borehole at TD before well construction was 997 ft bgs. On September 24, 2014, after development of the upper and lower screens, the composite depth to water was measured at 995.8 ft bgs on a video log. On October 3, 2014, following well installation, well

development, installation of the packer between the upper and lower screens, and aquifer testing, the depth to water was 997.2 ft bgs in the completed well. The upper screen of CrEX-1 straddles the regional water table. This allows for effective assessment of the uppermost portion of the regional aquifer next to the regional water table where the highest contaminant concentrations are expected. The effective saturated thickness of the formation screened by the upper screen is approximately 43 ft (the bottom of the upper screen is 1040 ft bgs). The aquifer testing demonstrated a relatively high permeability of the aquifer screened by CrEX-1. The pumping of CrEX-1 produces about 6.2 m (~20 ft) drawdown at the well within the pumped screen. However, the pumping test data do not suggest that the pumping produces a significant drawdown in the aquifer adjacent to the screen. Potentially, borehole skin effects caused a substantial portion of the observed drawdown. Skin effect is an increase in the pressure drop at the pumping well when compared with aquifer pressure adjacent to the well. The increased pressure drop is thought to be caused by extra flow resistance near the wellbore because of imperfect hydraulic connection between the well and the aquifer.

5.2.1 Regional Aquifer Groundwater Elevations

Based upon the depth to water of 997.2 ft bgs measured on October 3, 2014, at CrEx-1 after installation, initial development, and aquifer testing, the water-level elevation was approximately 5834.13 ft above mean sea level ([amsl] the ground surface elevation is 6831.33 ft, and the water level in the well is 997.2 bgs). This elevation is approximately 1 ft to 1.5 ft lower than the expected elevation of about 5835 ft for CrEx-1 based on the current groundwater flow conditions in the aquifer. For example, the groundwater elevation at R-50 screen 1 was approximately 5834.6 ft when the CrEx-1 water level was measured. The general structure of groundwater flow is presented in Figure 5.2-1; the water-level contours in the figure are based on circa 2011 water-level data. (Note: There is a documented 0.6-ft average annual water-level decline in the area.) Based on the general groundwater flow direction, it is expected that the water-level elevation at R-50 screen 1 would be lower, not higher, than the water-level elevation at CrEX-1. The water level for CrEx-1 measured after well installation and hydraulic testing is a preliminary value, and the water level may fluctuate as pressures equilibrate in the newly installed well.

Water levels at CrEX-1 will continue to be monitored, and data will be incorporated in periodic updates of the water-table elevation map.

6.0 BOREHOLE LOGGING

The following sections describe the borehole logging conducted at CrEX-1. Table 6.0-1 presents a summary of all logging.

6.1 Video Logging

Laboratory personnel ran a video survey of the borehole from the surface to 750 ft bgs on July 30, 2014. The purpose of this survey was to observe the lost circulation zone at about 820 ft bgs. The survey was stopped at 750 ft bgs as a result of lost visibility because of highly turbid borehole fluids.

Laboratory personnel ran a video log of the CrEX-1 well after construction to confirm locations of the well screens. The video log was recorded on September 24, 2014, from ground surface to 1110.9 ft bgs to observe the screen locations and depth to water. Table 6.0-1 provides a description of the log. The video log is provided on DVD as Appendix B of this report.

6.2 Geophysical Logging

On August 6 to 7, 2014, Schlumberger ran a suite of geophysical logs in the upper (cased) part of the borehole from ground surface to 810 ft bgs, which included the following:

- accelerator porosity sonde (APS),
- natural gamma spectrometer,
- litho scanner elemental spectroscopy, and
- array induction tool.

For the lower (open) part of the borehole, the geophysical suite consisted of the following:

- microcylindrically focused log,
- magnetic resonance (MR) scanner,
- fullbore formation microimager,
- APS,
- natural gamma spectrometer, and
- litho scanner elemental spectroscopy.

On September 24, 2014, the Laboratory ran a natural gamma ray survey in the constructed CrEX-1 well from 945 ft to 1112 ft bgs to confirm the placement locations of the bentonite and filter-pack materials. Table 6.0-1 shows the depths of coverage for each type of log. The Laboratory and Schlumberger geophysical logs are included as Appendix C of this report (on CD).

7.0 WELL INSTALLATION

The CrEX-1 well was installed between August 12 and 17, 2014. The following sections summarize the well design and well construction activities.

7.1 Well Design

The CrEX-1 well was designed in accordance with the objectives and steps outlined in the field implementation plan (LANL 2014, 600129). The drill cuttings and drillers logs were reviewed and the results of the downhole geophysics were also reviewed, as well as the depth to water. The objectives in setting the screen were to

- establish a capture zone within the plume of elevated chromium concentrations in the upper 70 ft to 100 ft of the aquifer,
- optimize the removal of only chromium-contaminated water,
- reach downgradient towards R-50 during pumping if possible, and
- avoid drawing chromium contamination downwards within the aquifer.

Because the geophysical logs indicated that the upper part of the saturated zone may not be capable of producing the required volume of water needed for a successful extraction well as described in the work plan (i.e., 100 gallons per minute [gpm]), the design was revised to include a second zone, deeper within

the aquifer, that was more likely to produce the required volumes of water. The two zones were to be separated by a removable packer. A two-screen design was submitted to NMED on August 8, 2014, and approved later that day. The final CrEX-1 design and the NMED approval are included as Appendix A.

7.2 Well Construction

The CrEX-1 well was constructed of nominal 8-in.–inside diameter (I.D.)/8.62-in.-O.D. passivated type 304L stainless-steel welded casing fabricated to American Society for Testing and Materials standard A312. Figure 7.2-1 illustrates the final well construction details. The screened intervals consist of a 50-ft length of nominal 8-in.-I.D. rod-based, 0.040-in. slot, wire-wrapped well screen from 1040 ft to 990 ft bgs and a 20-ft length of nominal 8-in.-I.D. rod-based, 0.040-in. slot, wire-wrapped well screen from 1090 ft to 1070 ft bgs. Casing and screen were provided by the subcontractor and were steam-pressure washed before installation. A 2.5-in.-O.D. steel, flush-threaded tremie pipe string, also decontaminated before use, was used to deliver annular fill materials and potable water downhole during well construction.

The well was installed on August 12, 2014, and the screened intervals were placed at depths of 1090 ft to 1070 ft bgs and 1040 ft to 990 ft bgs. Before the well was constructed, the bottom of the borehole was measured at a depth of 1211 ft bgs. From a depth of 1211 ft to 1096.2 ft bgs, 3/8-in. bentonite chips were added to the borehole via tremie pipe and allowed to hydrate.

The primary filter pack for the lower screen (consisting of 10/20 sand) was emplaced via tremie pipe beginning on August 12. The filter pack was installed at depths of 1096.2 ft to 1066 ft bgs and swabbed to promote settling of the sand pack. The secondary filter pack consisting of 20/40 sand was emplaced via tremie pipe from depths of 1066 ft to 1063 ft bgs. A seal between the two screened intervals consisting of hydrated 3/8-in. bentonite chips was emplaced via tremie pipe at depths of 1063 ft to 1048 ft bgs and allowed to hydrate for 4 h. The primary filter pack for the upper screen (consisting of 10/20 sand) was emplaced via tremie pipe beginning on August 13. The filter pack was installed at depths of 1048 ft to 985.3 ft bgs and swabbed. The secondary filter pack consisting of 20/40 sand was emplaced via tremie pipe from depths of 985.3 ft to 979.3 ft bgs.

Additional bentonite was emplaced above the secondary filter pack from 816 ft to 979.3 ft bgs in multiple 10- to 20-ft-thick lifts and allowed to hydrate. The 16-in. drill casing was then removed from the borehole. Five feet of this casing, including the cutting shoe, were left behind in the borehole from 816 ft to 811 ft bgs. More bentonite was emplaced from 816 ft to 475 ft bgs in multiple lifts and allowed to hydrate. The 18-in. drill casing was then removed from the borehole. Five feet of this casing, including the cutting shoe, was left behind in the borehole from 475 ft to 470 ft bgs. More bentonite was then emplaced from 475 ft to 59.8 ft bgs in multiple lifts. A mixture consisting of 92% cement and 8% bentonite was emplaced from a depth of 59.8 ft to 4 ft bgs.

A summary of the annual fill materials is presented in Table 7.2-1.

8.0 POSTINSTALLATION ACTIVITIES

Following well installation at CrEX-1, the well was developed and tested, and the pumping system was installed. The well head and surface pad will be completed when weather permits. A geodetic survey will be completed on the surface pad, well head, and survey marker. Survey data will be sent to NMED in a separate submittal. Site restoration activities will be completed following the final disposition of contained drill cuttings and groundwater, per the NMED-approved waste disposal decision trees.

8.1 Well Development

Well development was conducted from August 25 to September 30, 2014. Well development began with swabbing and air-lifting to remove formation fines in the upper and lower filter packs and sump. AQUA-CLEAR was used from August 27 to August 29 in an effort to break down the bentonite wall cake and improve water delivery rates to the surface, which remained at about 1.5 gpm. AQUA-CLEAR and PENETROL were used together for the same purpose on August 30.

On September 1, 2014, the subcontractor decided that submergence of the tremie pipe was not adequate for effective air-lifting of water. Therefore, the decision was made to remove the tremie pipe and install a 10-horsepower (hp), 30-gpm pump to develop the well. The smaller-capacity pump was used because there was still no indication that the well could produce more than 1.5 gpm. Pumping and “rawhiding” with the 30-gpm pump was continued from September 1 to September 10 on both screened intervals of the well. At that point, the specific capacity had improved from 0.5 gpm/ft to 7.0 gpm/ft, and the well was producing 30 gpm. Rawhiding is the practice of removing the check valves in the riser pipe and pump, filling the riser pipe with water by pumping, then turning off the pump and allowing the water in the riser pipe to fall back down the riser pipe, through the pump, and into the filter pack—in effect back-flushing the screened intervals of the well.

On September 10, the 30-gpm pump was removed. On September 13, a 100-gpm pump was installed in the well, and the well was found to be capable of producing up to 168 gpm from the two screens. On September 14, the cuttings pit was full of development water, and pumping had to stop until the plumbing was complete to transfer the water to a treatment system located at nearby monitoring well R-28. Pumping resumed on September 17 and continued at near 100 gpm while the pump was moved up and down through the water column from the water table down to the sump. On September 23, the 100-gpm pump was removed from the well. On September 24, a video and gamma log was made of the entire well to confirm the placement of the well screens and the filter packs before a TAM single-set packer was inserted in the blank pipe between the screens.

On September 26, a TAM packer was installed in the well, and the 100-gpm development pump was put back into the well for additional, focused development of the upper screen. The upper screen was pumped at 60 gpm to 100 gpm from September 28 to September 30.

8.1.1 Well Development Field Parameters

The field parameters of turbidity, temperature, and pH were monitored via a flow-through cell at CrEX-1 during each phase of well development. The field parameter measurements at the end of development of both screens on September 22, 2014, were pH of 7.46, temperature of 19.3°C, and turbidity of 0.02 nephelometric turbidity units (NTU). Field parameters measured during the development of screen 1 alone were pH of 7.41, temperature of 19.21°C, and turbidity of 0.75 NTU on September 28, 2014. Field water-quality parameters are presented in Table 8.1-1.

8.2 Aquifer Testing

Aquifer pumping tests, including a step test and a 24-h test, were conducted at CrEx-1 between October 1 and 4, 2014, by Yellow Jacket Drilling, Inc. (Table 8.2-1). The aquifer testing was performed while pumping water from the upper 50-ft screen only; the lower screen was separated using a TAM packer. A 50-hp, 6-in.-diameter Grunfos submersible pump was used to perform the aquifer tests.

Five short-duration pumping intervals (steps), without recovery in between, were conducted on October 1. The primary objective of the short-duration step tests was to assess the hydraulic behavior of the system

and properly determine the optimal pumping rate for the 24-h test. The step tests demonstrated that the specific capacity of the well does not seem to depend on the pumping rate, which suggests the well is well developed. During the step tests, the specific capacity varied between 100 m^2/d and 120 m^2/d (5.5 gpm/ft and 6.6 gpm/ft). The pumping at the highest rate (96 gpm) produced about 5 m (~16 ft) drawdown at the well within the pumped screen. However, the well's specific capacity did not decline with the increase of the pumping rate (Appendix D). This suggests that borehole skin effects (imperfect hydraulic connection between the aquifer and the well) caused a portion of the drawdown. Nevertheless, the pumping caused a decline in the regional water table, and it is likely that vadose zone groundwater flow impacted the drawdowns observed in CrEx-1. Therefore, unconfined (phreatic) groundwater flow is occurring near the pumped well. However, the observed drawdowns are still small compared with the aquifer thickness (much greater than 100 ft), so it is acceptable to use analyses that interpret the groundwater flow as confined. In addition, analyses accounting for unconfined groundwater flow were also performed. The confined and unconfined analyses produced similar estimates for effective aquifer transmissivity and hydraulic conductivity.

A 24-h aquifer test was completed on October 4. The test was conducted at a pumping rate of 517.6 m^3/d (94.9 gpm). The 24-h aquifer test analyses suggested a formation transmissivity of approximately 490 m^2/d (40,000 gallons per day/ft). This transmissivity value is very similar to the estimate obtained by a recent R-28 aquifer test analysis conducted in 2014 (LANL 2014, 255110).

The saturated thickness corresponding to the transmissivity value is not known to estimate hydraulic conductivity. The saturated thickness is impacted by the pumping because the pumping causes a decline in the regional water table. Assuming the saturated thickness is the length of the initial saturated screened interval (~43 ft before the pumping started) minus half the observed drawdown (~10 ft), the estimated average hydraulic conductivity is about 49 m/d or 161 ft/d. This estimate is uncertain, but the value of hydraulic conductivity is consistent with the estimate obtained for R-28 (~120 ft/d).

The CrEX-1 transmissivity and hydraulic conductivity estimates suggest that the well is tapping a highly permeable zone of the regional aquifer. This helps achieve the CrEX-1 objective of hydraulic capture of contaminated groundwater.

8.3 Dedicated Pumping System Installation

A dedicated pumping system for CrEX-1 was initially installed on October 11, 2014. The system uses a single 50-hp Franklin Electric motor and 6-in. Grundfos submersible pump. The pump riser pipe consists of 3-in. threaded and coupled American Petroleum Institute (API) 5L galvanized steel. Two 1-in.-I.D. schedule 80 polyvinyl chloride (PVC) tubes are installed along with, and banded to, the pump column. A dedicated In-Situ Level Troll 500 transducer will be installed in one of the tubes, and the second tube will be used for manual water-level measurements. Both PVC tubes are equipped with a 0.5-ft section of 0.010-in. slotted screen and a closed bottom.

During electrical acceptance testing by Laboratory electricians, it was determined that the motor was initially functioning correctly but little water was delivered to the surface, and the system failed the test. In addition, it was found that the PVC transducer tubes were obstructed at a point about 50 ft above the water table. The pumping system and tubes were removed from the well on October 25, 2014. The problem was determined to be that the pump and transducer tubes had been set 100 ft above the water table. Once any water in the riser pipe had been pumped to the surface, the pump and motor overheated and were destroyed. Using the 50-hp, 6-in.-diameter Grundfos submersible pump from the development phase, the pump and motor were replaced on October 25, 2014, and the system retested. All systems worked correctly and the system was accepted.

Figure 8.3-1a shows details of the dedicated sampling system. Figure 8.3-1b presents technical notes describing the sampling system components. Figure 8.3-1c shows the Grundfos pump performance curve.

8.4 Wellhead Completion

A reinforced concrete surface pad, 10 ft × 24 ft × 9 in. thick, will be installed at the CrEX-1 wellhead when weather permits. The concrete pad will be slightly elevated above ground surface and crowned to promote runoff. The pad will provide long-term structural integrity for the well. A protective tent will be erected over the well. A brass monument marker will be embedded in the northwest corner of the pad. A 16-in.-O.D. steel protective casing will be installed around the stainless-steel well riser. A 0.25-in. weep hole will be drilled near the base of the protective casing to prevent water accumulation inside the protective casing. Pea gravel will be emplaced between the protective casing and well casing to a height of 1 ft above the weep hole. Six steel bollards, covered by high-visibility plastic sleeves, will be set at the outside edges of the pad to protect the well from accidental vehicle damage. They are designed for easy removal to allow access to the well. Figure 8.3-1a shows details of the proposed wellhead completion.

8.5 Geodetic Survey

A licensed professional land surveyor will conduct a geodetic survey once the wellhead is completed. The survey data will conform to Laboratory Information Architecture project standards IA-CB02, “GIS Horizontal Spatial Reference System,” and IA-D802, “Geospatial Positioning Accuracy Standard for A/E/C and Facility Management.” All coordinates will be expressed relative to New Mexico State Plane Coordinate System Central Zone 83 (North American Datum [NAD] 83); elevation will be expressed in feet amsl using the National Geodetic Vertical Datum of 1929. Survey points will include ground-surface elevation near the concrete pad, the top of the monument marker in the concrete pad, the top of the well casing, and the top of the protective casing.

8.6 Waste Management and Site Restoration

Waste generated from the CrEX-1 project includes drilling fluids and mud, purged groundwater, drill cuttings, decontamination water, and contact waste. A summary of the waste characterization samples collected during drilling, construction and development of the CrEX-1 well is presented in Table 8.6-1. All waste streams produced during drilling and development activities were sampled in accordance with the “Waste Characterization Strategy Form for Chromium Well CrEx-1” (LANL 2014, 254859). Development water was land-applied under a Temporary Permission to Discharge (NMED 2014, 600128).

Fluids produced during drilling and containerized in the pit will be evaporated on site. Evaporation activities began in October 2014.

Analytical results for fluids produced during well development and pump testing will be reviewed with the goal of land application. Data will be reviewed manually and within the automated waste disposition program per the waste characterization strategy form and ENV-RCRA-QP-010.3, Land Application of Groundwater. If it is determined that drilling fluids are nonhazardous but cannot meet the criteria for land application, the drilling fluids will be reevaluated for treatment and disposal at one of the Laboratory’s wastewater treatment facilities or other authorized disposal facility. If analytical data indicate the drilling fluids are hazardous/nonradioactive or mixed low-level waste, the drilling fluids will be either treated on-site or disposed of at an authorized facility.

Drilling mud was collected in a lined mud pit on the drill pad. This mud will be sampled in the spring once associated fluids are evaporated and a representative waste sample can be taken. Analytical results will be evaluated for waste characterization, and this mud will be disposed of at a Laboratory-approved off-site disposal facility.

Cuttings produced during drilling were sampled, and analytical results will be reviewed with the goal of land application. A sample submitted for volatile organic analysis (VOA) (sample ID WST05-14-84406) was damaged en route to the analytical laboratory. Once the fluids are evaporated or removed from the pit in the spring, a composite VOA sample of the cuttings will be taken and evaluated against land-application criteria (ENV-RCRA-QP-011.2, Land Application of Drill Cuttings). If cuttings meet land-application criteria, materials will be spread across the pad area and the site reseeded as required for site reclamation.

Decontamination fluids used for cleaning the well steel were containerized and staged at the CrEX-1 well pad. This fluid waste will be sampled, and a waste profile form will be completed. This decontamination waterwaste will be shipped for disposal at a Laboratory-approved off-site disposal facility.

Characterization of contact waste will be based upon acceptable knowledge, referencing the analyses of the waste samples collected from the drilling fluids, drill cuttings, and decontamination fluids. A waste profile form will be completed, and the contact wastes will be removed from the site following land application of the pit-contained drill cuttings. The pit liner will be included in the contact waste disposal materials.

Site restoration activities are conducted by Maintenance and Site Services personnel at the Laboratory. Activities include evaporating drilling fluids, removing cuttings from the pit, and managing the development/pump test fluids in accordance with applicable procedures. The polyethylene liner will be removed following land application of the cuttings, and the containment area berms will be removed and leveled. Activities also include backfilling and regrading the containment area, as appropriate.

9.0 DEVIATIONS FROM PLANNED ACTIVITIES

Drilling, construction, and development were performed in general accordance with the “Field Implementation Plan for Well CrEX-1” (LANL 2014, 600129). Two significant deviations from the plan occurred.

The first deviation from the plan was changing the design from a single 100-ft-long screen to an upper 50-ft-long screen and a lower 20-ft-long screen separated by 30 ft of blank pipe. The change was made because the upper part of the well appeared on the geophysical logs to be significantly less productive than the lower part of the well. To address one of the main objectives of the well, collecting chromium-contaminated water from the top of the regional aquifer and not drawing contaminated water down into the regional aquifer, the two-screen approach was proposed to, and approved by, NMED. Once the upper screen demonstrated that it could produce the required amounts of water, a packer was set between the screens.

The second deviation from the plan was the loss of 14 d of pumping because the pump was set above the water table; the completion rig left the site before acceptance testing could be conducted, and the rig could not return to the Laboratory for 13 d.

10.0 ACKNOWLEDGMENTS

Yellow Jacket Drilling drilled the CrEX-1 borehole, installed the well, and conducted the well development and aquifer testing.

Laboratory personnel ran downhole video and natural gamma logging equipment.

Schlumberger ran a suite of geophysical logs.

Laboratory personnel analyzed the data for the aquifer testing (Appendix D).

11.0 REFERENCES AND MAP DATA SOURCES

11.1 References

The following list includes all documents cited in this report. Parenthetical information following each reference provides the author(s), publication date, and ER ID or ESH ID. This information is also included in text citations. ER IDs were assigned by the EP Directorate's Records Processing Facility (IDs through 599999), and ESH IDs are assigned by the Environment, Safety, and Health (ESH) Directorate (IDs 600000 and above). IDs are used to locate documents in the Laboratory's Electronic Document Management System and, where applicable, in the master reference set.

Copies of the master reference set are maintained at the NMED Hazardous Waste Bureau and the ESH Directorate. The set was developed to ensure that the administrative authority has all material needed to review this document, and it is updated with every document submitted to the administrative authority. Documents previously submitted to the administrative authority are not included.

Dale, M., June 19, 2014. FW: Extraction Well CrEX-1 start up notification. E-mail message to H. Shen (NMED) and D. Katzman (LANL) from M. Dale (NMED), Santa Fe, New Mexico. (Dale 2014, 600135)

DOE (U.S. Department of Energy), May 19, 2014. "Well Pump Tests Phase II in Sandia and Mortandad Canyons," U.S. Department of Energy Categorical Exclusion Determination Form, Los Alamos Site Office, Los Alamos, New Mexico. (DOE 2014, 600140)

LANL (Los Alamos National Laboratory), February 28, 2014. "Waste Characterization Strategy Form for Chromium Well CrEx-1," Los Alamos National Laboratory, Los Alamos, New Mexico. (LANL 2014, 254859)

LANL (Los Alamos National Laboratory), March 2014. "Drilling Work Plan for Groundwater Extraction Well CrEX-1," Los Alamos National Laboratory document LA-UR-14-21478, Los Alamos, New Mexico. (LANL 2014, 254824)

LANL (Los Alamos National Laboratory), March 2014. "Summary Report for the 2013 Chromium Groundwater Aquifer Tests at R-42, R-28, and SCI-2," Los Alamos National Laboratory document LA-UR-14-21642, Los Alamos, New Mexico. (LANL 2014, 255110)

LANL (Los Alamos National Laboratory), June 2014. "Field Implementation Plan for CrEX-1," Los Alamos National Laboratory, Los Alamos, New Mexico. (LANL 2014, 600129)

NMED (New Mexico Environment Department), July 8, 2014. “Approval, Drilling Work Plan for Groundwater Extraction Well CrEX-1,” New Mexico Environment Department letter to P. Maggiore (DOE-NA-LA) and J.D. Mousseau (LANL) from J.E. Kieling (NMED-HWB), Santa Fe, New Mexico. (NMED 2014, 525004)

NMED (New Mexico Environment Department), August 8, 2014. “Temporary Permission to Discharge, Treated Ground Water from Aquifer Testing at Pilot Pumping Well CrEX-1 (AI: 856, PRD20140007),” New Mexico Environment Department letter to A. Dorries (LANL) and G. Turner (DOE) from J. Schoeppner (NMED-GWQB), Santa Fe, New Mexico. (NMED 2014, 600128)

North Wind Inc., July 2011. “Spill Prevention Control and Countermeasures Plan for the ADEP Groundwater Monitoring Well Drilling Operations, Los Alamos National Laboratory, Revision 6,” plan prepared for Los Alamos National Laboratory, Los Alamos, New Mexico. (North Wind, Inc., 2011, 213292)

OSE (New Mexico Office of the State Engineer), July 21, 2014. “Application for Permit to Drill a Well with No Consumptive Use of Water,” OSE File No. RG 94875, Santa Fe, New Mexico. (OSE 2014, 600141)

Yellow Jacket Drilling, June 27, 2014. “Integrated Work Document for Drilling and Installation of LANL Well [CrEX-1],” Gilbert, Arizona. (Yellow Jacket Drilling 2014, 600131)

11.2 Map Data Sources

Coarse Scale Drainage Arcs; Los Alamos National Laboratory, Water Quality and Hydrology Group of the Risk Reduction and Environmental Stewardship Program; as published 03 June 2003.

Dirt Road Arcs; Los Alamos National Laboratory, KSL Site Support Services, Planning, Locating and Mapping Section; 19 March 2008; as published 04 January 2008.

Hypsography, 100 ft Contour Interval; Los Alamos National Laboratory, ENV Environmental Remediation and Surveillance Program; 1991.

Inactive Outfalls; Los Alamos National Laboratory, Water Quality and Hydrology Group of the Environmental Stewardship Division at Los Alamos National Laboratory Los Alamos New Mexico; 01 September 2003.

Paved Road Arcs; Los Alamos National Laboratory, KSL Site Support Services, Planning, Locating and Mapping Section; 19 March 2008; as published 04 January 2008.

Penetrations; Los Alamos National Laboratory, Environment and Remediation Support Services, ER2006-0664; 1:2,500 Scale Data, 01 July 2006.

Structures; Los Alamos National Laboratory, KSL Site Support Services, Planning, Locating and Mapping Section; 19 March 2008; as published 04 January 2008.

Technical Area Boundaries; Los Alamos National Laboratory, Site Planning and Project Initiation Group, Infrastructure Planning Division; 19 September 2007.

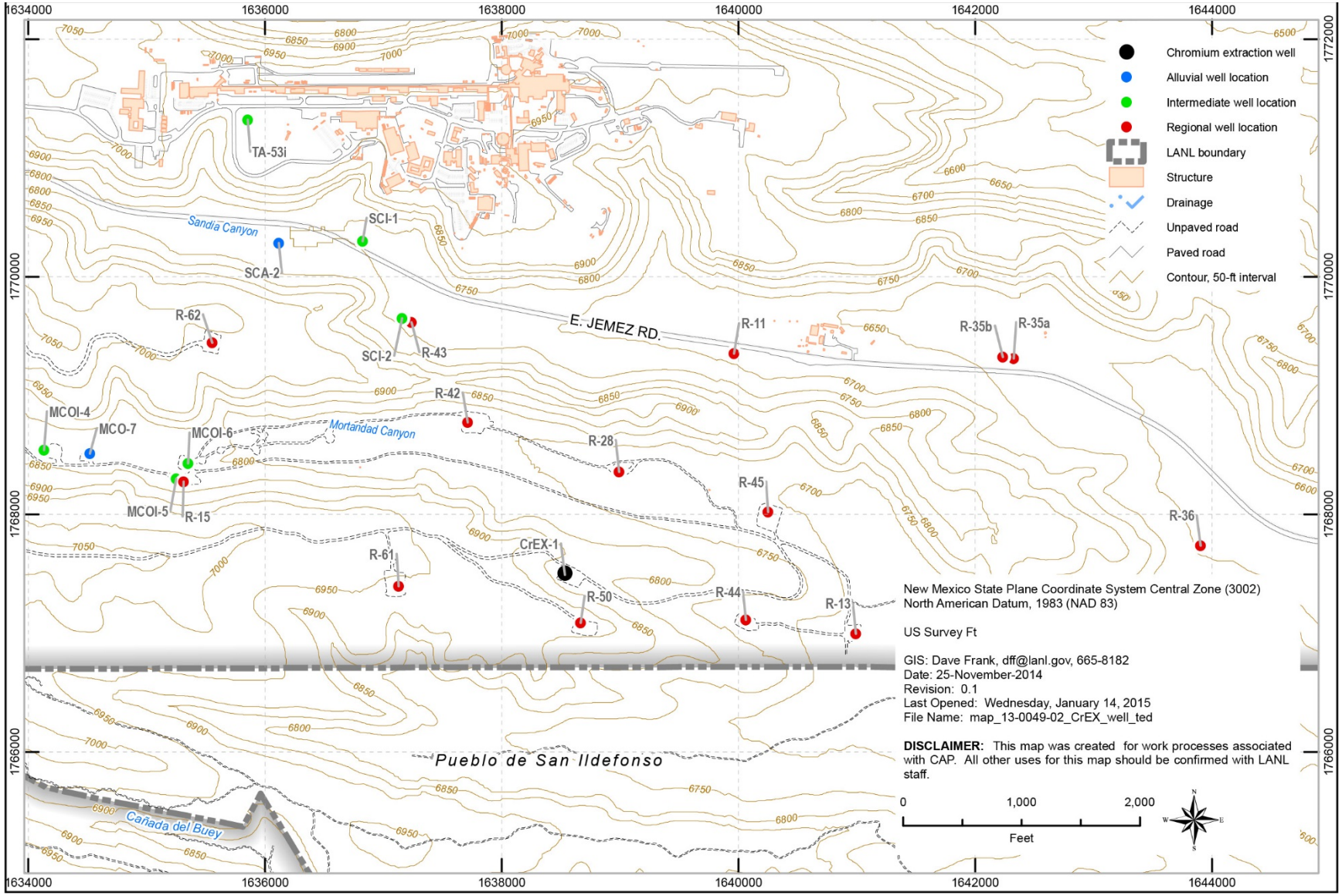

Figure 1.0-1 Location of well CrEX-1

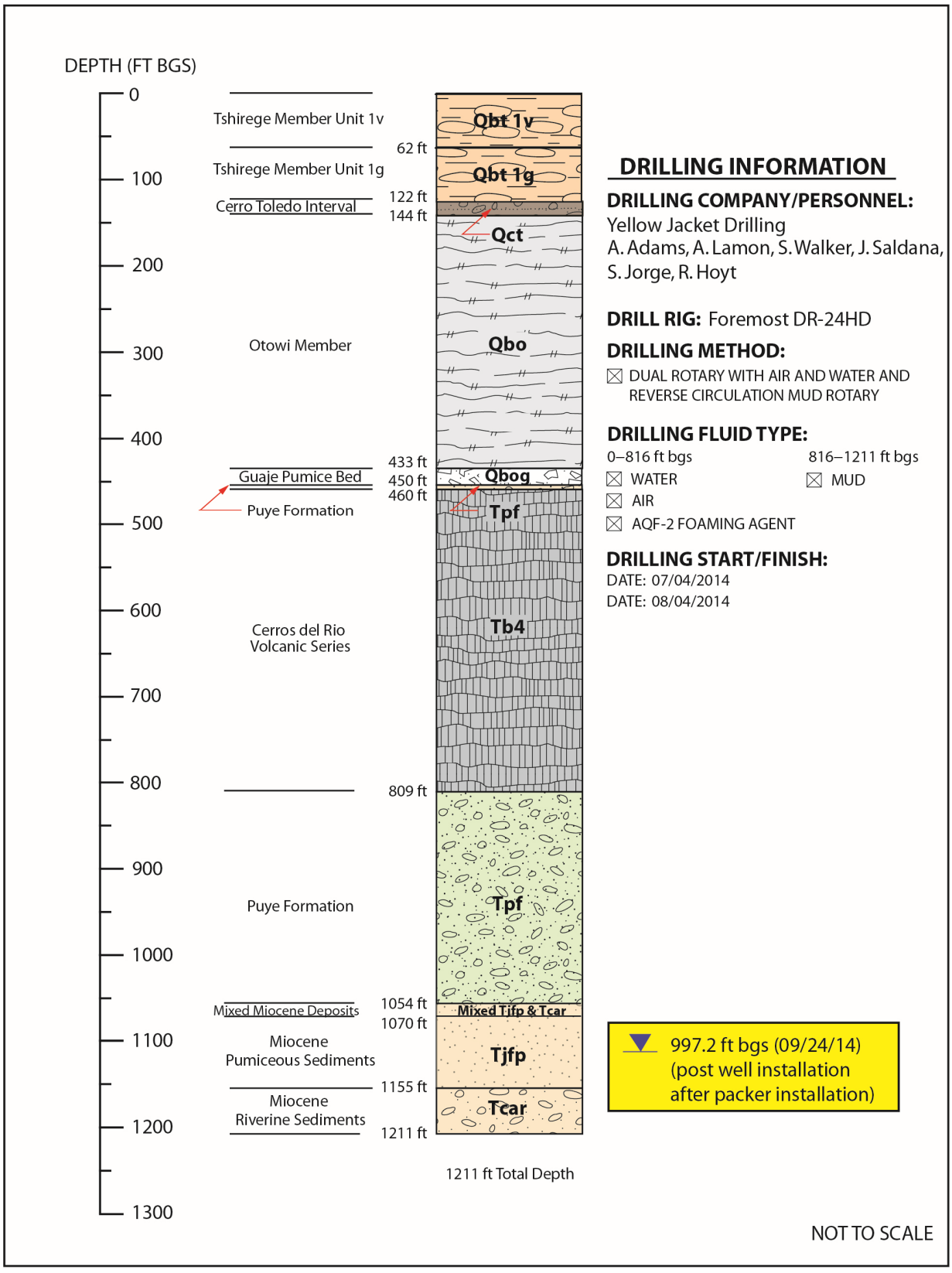

Figure 5.1-1 CrEX-1 borehole stratigraphy

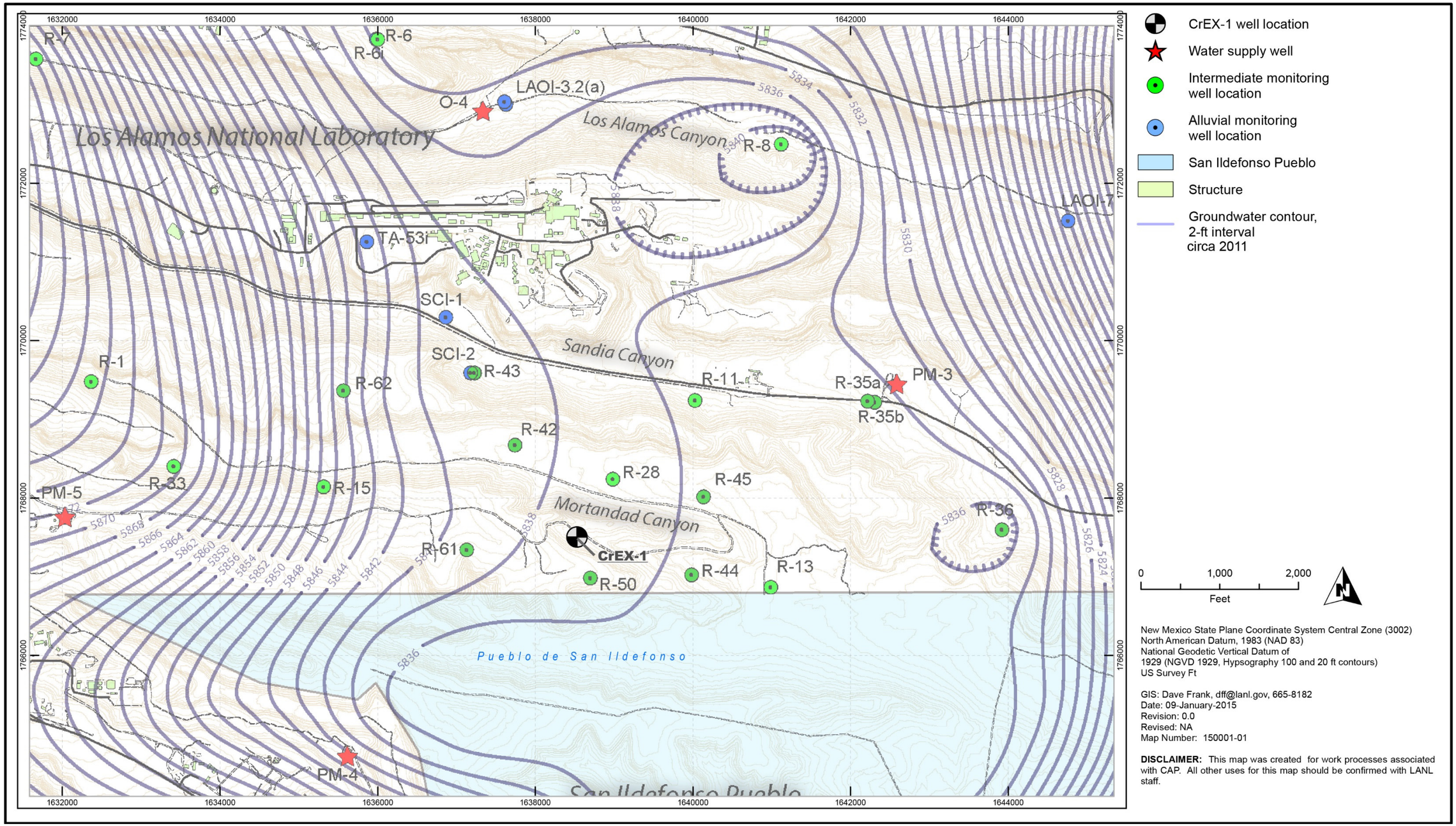

New Mexico State Plane Coordinate System Central Zone (3002)
North American Datum, 1983 (NAD 83)
National Geodetic Vertical Datum of
1929 (NGVD 1929, Hypsography 100 and 20 ft contours)
US Survey Ft

GIS: Dave Frank, dff@lanl.gov, 665-8182
Date: 09-January-2015
Revision: 0.0
Revised: NA
Map Number: 150001-01

DISCLAIMER: This map was created for work processes associated with CAP. All other uses for this map should be confirmed with LANL staff.

Figure 5.2-1 Regional aquifer groundwater elevations

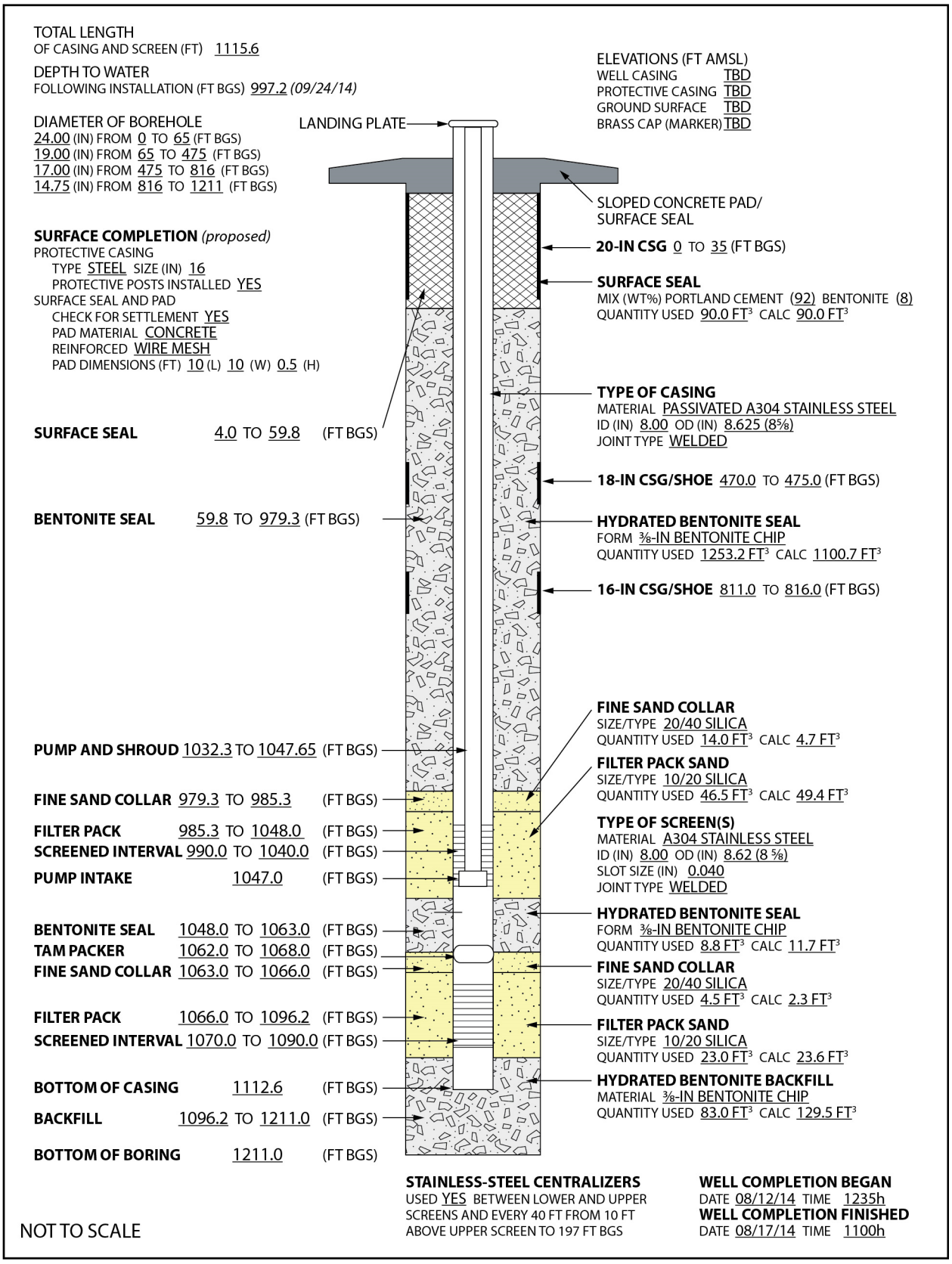

Figure 7.2-1 As-built construction diagram for well CrEX-1

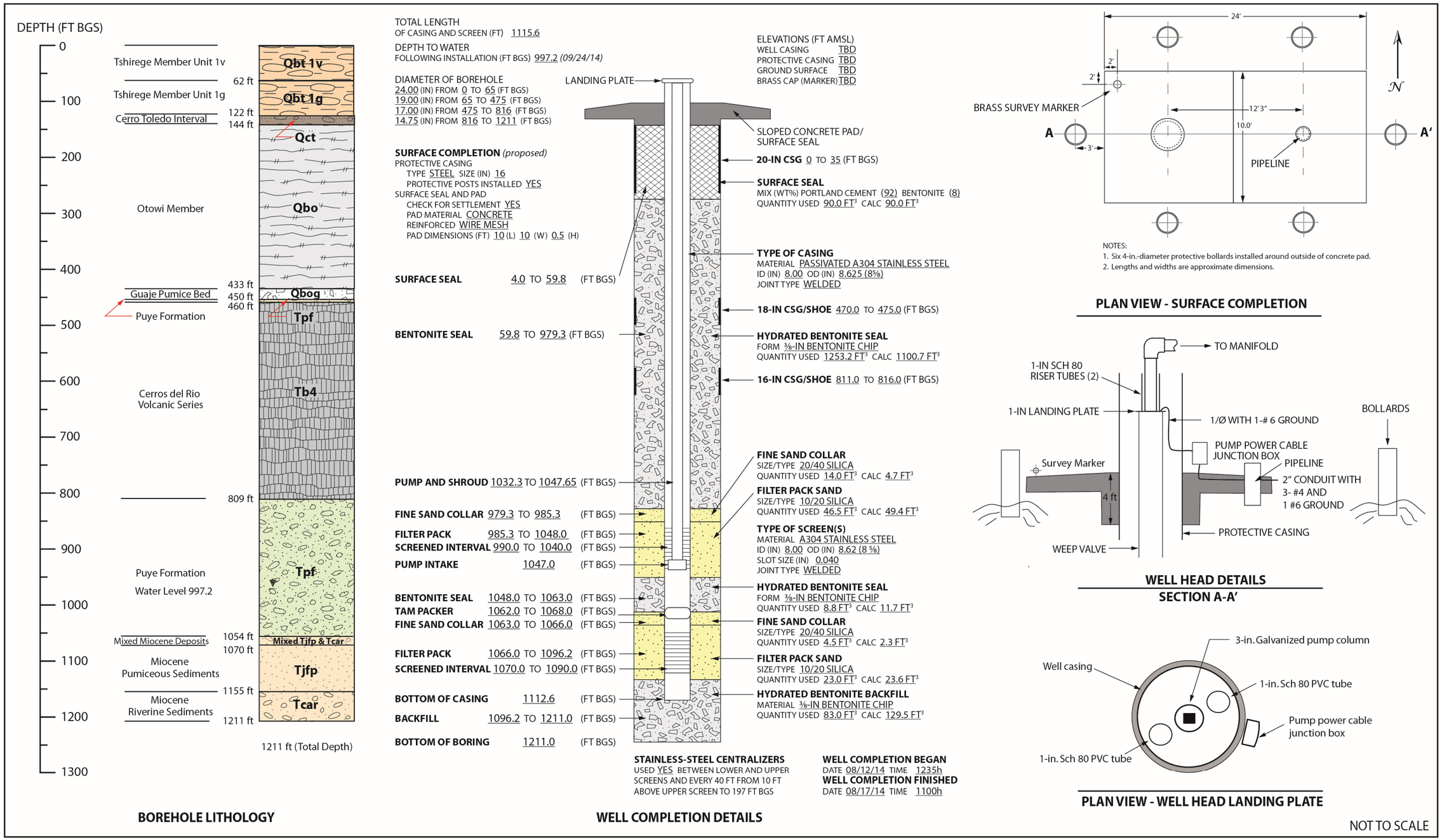

Figure 8.3-1a As-built schematic for well CrEX-1

CrEX-1 TECHNICAL NOTES:

SURVEY INFORMATION*

Brass Marker

Northing:	TBD
Easting:	TBD
Elevation:	TBD

Well Casing (top of stainless steel)

Northing:	TBD
Easting:	TBD
Elevation:	TBD

BOREHOLE GEOPHYSICAL LOGS

LANL: Natural gamma ray, induction
Schlumberger: APS, FMI, natural gamma ray, litho scanner, MR scanner, array induction

DRILLING INFORMATION

Drilling Company
Yellow Jacket Drilling, Inc.

Drill Rig
Foremost DR-24HD

Drilling Methods
Dual rotary foam-assisted air rotary and flooded reverse mud rotary,

Drilling Fluids
Air, potable water, AQF-2 Foam (to 810 ft bgs)
Potable water, soda ash, QUIK-TROL, bentonite (810 ft bgs to TD)

MILESTONE DATES

Drilling

Start:	07/04/2014
Finished:	08/04/2014

Well Completion

Start:	08/12/2014
Finished:	08/17/2014

Well Development

Start:	08/25/2014
Finished:	09/30/2014

WELL DEVELOPMENT

Development Methods
Performed swabbing, bailing, air-lifting, and pumping
Total Volume Purged: 178,090 gal.

Parameter Measurements (Final)

pH:	7.41
Temperature:	19.21˚C
Specific Conductance:	Not available
Turbidity:	0.75 NTU

AQUIFER TESTING

24-h Constant-Rate Pumping Test

Water Produced:	173,670 gal.
Average Flow Rate:	94.94 gpm
Performed on:	10/3/14–10/4/14

DEDICATED SAMPLING SYSTEM

Pump (Shrouded)
Make: Grundfos
Model: 150S500-28

Motor
Make: Franklin Electric
Model: Submersible Sand Fighter
50 hp, 3 phase, 460 V

Pump Column
Flomatic model # 80DI check valves at 760 and 1030 ft bgs

Transducer Tubes
2 × 1.0-in. flush threaded schd. 80 PVC tubing
0.020-in. slot screens at 1031.0–1031.5 ft bgs

Transducer
Make: In-Situ Level TROLL
Model: LT 500
PSIG range: Max 100 PSI / 231 ft
S/N: 379843

NOTE:
* Coordinates based on New Mexico State Plane Grid Coordinates, Central Zone (NAD83); Elevation expressed in feet amsl using the National Geodetic Vertical Datum of 1929.

Figure 8.3-1b Technical notes for well CrEX-1

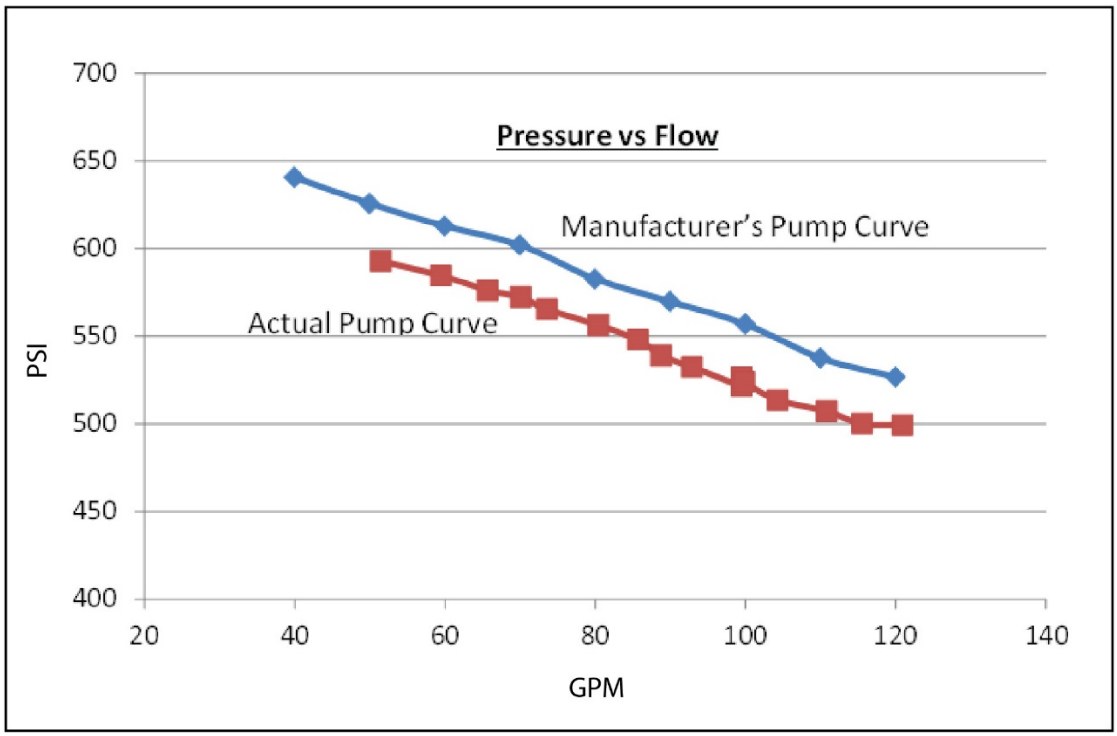

Figure 8.3-1c Pump performance curve

Table 6.0-1
Logging Runs

Date(s)	Type of Log	Depth (ft bgs)	Description
7/30/14	Video	0–750	LANL video from ground surface to 750 ft bgs. Attempted to observe lost circulation zone, thought to be above water table. However, muddy water remained in the borehole at 750 ft bgs, and survey was stopped before reaching the depth of interest.
8/6/14–8/7/14	APS	200–1208	Schlumberger geophysical log
8/6/14–8/7/14	Natural gamma/HNGS*	200–1208	Schlumberger geophysical log
8/6/14–8/7/14	Litho scanner	200–1180	Schlumberger geophysical log
8/6/14–8/7/14	Array induction tool	200–1180	Schlumberger geophysical log
8/6/14–8/7/14	Microcylindrically focused log	816–1211	Schlumberger geophysical log
8/6/14–8/7/14	MR scanner	858–1196	Schlumberger geophysical log
8/6/14–8/7/14	Fullbore formation microimager	840–1210	Schlumberger geophysical log
9/24/14	Video	0–1111	LANL video to confirm well screen placement and condition and water level
9/24/14	Gamma log	945–1112	LANL gamma log to confirm position of bentonite backfill and sand pack materials

*HNGS = Hostile natural gamma spectroscopy.

Table 7.2-1
CrEX-1 Annular Fill Materials

Material	Volume (ft^3)
Surface seal: 92% Portland cement, 8% bentonite	90.0
Upper seal: 0.375-in. bentonite chips	1253.2
Upper screen transition sand collar: 20/40 silica sand	14.0
Upper screen primary filter pack sand: 10/20 silica sand	46.5
Separating seal: 0.375-in. bentonite chips	8.8
Lower screen transition sand collar: 20/40 silica sand	4.5
Lower screen primary filter pack sand: 10/20 silica sand	23.0
Lower seal: 0.375-in. bentonite chips	83.0

Table 8.1-1
Field Water-Quality Parameters and Well Performance for Development of Well CrEX-1

Status	Screen	Time	Pumping Rate (gpm)	Depth to Water (ft bgs)	Draw Down (ft)	Cumulative Purge Volume (gal.)	pH	Specific Capacity (gpm/ft)	Turbidity (NTU)	Temp (°C)
9/19/14										
On	1 & 2	9:45	n/a[a]	990.63	n/a	0	n/a	n/a	n/a	n/a
		9:50	150	1012.13	21.5	920	na[b]	6.98	29.9	21.5
		9:55	150	1012.63	22	1260	na	6.82	10.72	22
		10:00	150	1012.43	21.8	920	na	6.88	9.32	21.8
		10:15	150.4	1012.03	21.4	4,240	na	7.03	6.92	21.4
		10:30	142.6	1012.93	22.3	6380	na	6.39	4.16	22.3
		11:00	143	1012.83	22.2	10,670	na	6.44	3.43	22.4
		11:30	148	1013.03	22.4	15,110	na	6.61	0.39	22.4
Off	1 & 2	12:00	135	1012.83	22.2	19,180	na	6.08	0.92	22.2
9/22/14										
On	1 & 2	10:15	n/a	989.66	0.00	54,880	n/a	n/a	n/a	n/a
		10:30	na	1009.56	19.90	57,060	7.22	0	1.18	19.15
		10:45	147.33	1009.69	20.03	61,450	7.3	7.36	1.25	19.17
		11:00	146	1009.72	20.06	68,030	7.35	7.28	0	19.46
		11:15	147	1009.8	20.14	69,210	7.36	7.30	0	19.68
		11:30	149	1009.82	20.16	70,320	7.37	7.39	0.03	19.28
		11:45	148	1009.83	20.17	71,640	7.38	7.34	0.02	19.45
		12:00	138	1009.82	20.16	73,180	7.39	6.85	0.02	19.24
		12:15	158	1009.76	20.10	74,950	7.41	7.86	0.02	19.38
		12:30	149.33	1009.76	20.10	76,940	7.4	7.43	0.03	19.28
		13:05	147.42	1009.74	20.08	79,450	7.42	7.34	0.04	19.27
		13:30	148.8	1009.82	20.16	82,340	7.46	7.38	0.03	19.32

Table 8.1-1 (continued)

Status	Screen	Time	Pumping Rate (gpm)	Depth to Water (ft bgs)	Draw Down (ft)	Cumulative Purge Volume (gal.)	pH	Specific Capacity (gpm/ft)	Turbidity (NTU)	Temp (°C)
		14:00	147.67	1009.74	20.08	85,660	4.46	7.35	0.03	19.3
		14:30	148.33	1009.77	20.11	89,430	7.45	7.38	0.02	19.31
		15:00	148	1009.81	20.15	93,650	7.46	7.34	0.02	19.3
		15:30	147.33	1009.81	20.15	101,450	7.46	7.31	0.02	19.31
Off	1 & 2	16:00	148.33	1009.81	20.15	105,900	7.46	7.36	0.02	19.3
9/28/14										
On	1	8:45	n/a	986.83	0	116,180	n/a	n/a	n/a	n/a
		9:00	100	1008.28	21.45	117,770	7.19	4.66	19.6	18.99
		9:15	100	1006.43	19.6	119,120	7.28	5.10	2.26	19.35
		9:32	94.68	1007.28	20.45	120,590	7.33	4.63	1.01	19.38
		9:45	101.54	1007.43	20.6	121,910	7.35	4.93	0.3	19.12
		10:00	94	1007.58	20.75	123,320	7.36	4.53	na	19.25
		10:15	93.33	1007.63	20.8	124,720	7.37	4.49	na	19.49
		10:30	94	1007.68	20.85	126,130	7.38	4.51	na	19.21
Off	1	10:45	94.67	1007.73	20.9	127,550	7.38	4.53	na	19.18
On	1	11:00	n/a	986.83	0	127,590	n/a	n/a	n/a	n/a
		11:15	86.67	1006.58	19.75	128,890	7.41	4.39	0.75	19.21
		11:30	95.33	1006.73	19.9	130,320	7.39	4.79	na	19.22
		11:45	96.67	1006.83	20	131,770	7.4	4.83	na	19.5
		12:00	97.33	1006.83	20	133,230	7.4	4.87	na	19.64
		12:15	96.67	1006.83	20	134,680	7.44	4.83	na	19.4
		12:31	95	1006.83	20	136,200	7.46	4.75	na	19.55
Off	1	13:00	100	1006.83	20	137,600	7.44	5.00	na	19.53

Table 8.1-1 (continued)

Status	Screen	Time	Pumping Rate (gpm)	Depth to Water (ft bgs)	Draw Down (ft)	Cumulative Purge Volume (gal.)	pH	Specific Capacity (gpm/ft)	Turbidity (NTU)	Temp (°C)
On	1	13:30	n/a	986.83	0	137,720	n/a	n/a	n/a	n/a
		13:45	76	986.83	0	138,860	na	na	3.35	na
		14:00	86	986.83	0	140,160	na	na	0.85	na
		14:15	73	986.83	0	141,260	na	na	na	na
		14:30	66	997.73	10.9	142,250	na	6.06	na	na
		14:45	65	997.73	10.9	143,230	na	5.96	na	na
		15:00	64	997.63	10.8	144,200	na	5.93	na	na
		15:15	64	997.73	10.9	145,170	na	5.87	na	na
		15:30	65	997.73	10.9	146,150	na	5.96	na	na
		15:45	64	997.73	10.9	147,120	na	5.87	na	na
		16:00	65	997.73	10.9	148,100	na	5.96	na	na
		16:15	64	997.73	10.9	149,070	na	5.87	na	na
Off	1	16:30	65	997.73	10.9	150,050	na	5.96	na	na
9/29/14										
On	1	9:30	n/a	986.8	0	150,080	n/a	n/a	n/a	n/a
		9:45	80	1003.8	17	151,280	na	4.71	na	na
		10:00	95	1004.1	17.3	152,710	na	5.49	na	na
		10:15	95	1004.3	17.5	154,140	na	5.43	na	na
		10:30	95	1004.3	17.5	155,570	na	5.43	na	na
		10:45	95	1004.3	17.5	157,000	na	5.43	na	na
		11:00	95	1004.3	17.5	158,430	na	5.43	na	na
		11:15	95	1004.3	17.5	159,860	na	5.43	na	na
		11:30	95	1004.4	17.6	161,290	na	5.40	na	na
		12:00	95	1004.5	17.7	164,160	na	5.37	na	na
		12:30	95	1004.5	17.7	167,030	na	5.37	na	na
		13:00	95	1004.5	17.7	169,900	na	5.37	na	na

Table 8.1-1 (continued)

Status	Screen	Time	Pumping Rate (gpm)	Depth to Water (ft bgs)	Draw Down (ft)	Cumulative Purge Volume (gal.)	pH	Specific Capacity (gpm/ft)	Turbidity (NTU)	Temp (°C)
Off	1	13:30	95	1004.4	17.6	172,750	na	5.40	na	na
Off	1	15:30	0	985.8	0	174,410	na	na	na	na
On	1	15:40	82	1016.8	31	175,230	na	2.65	na	na
		15:50	143	1017	31.2	176,660	na	4.58	na	na
Off	1	16:00	n/a	n/a	n/a	178,090	na	na	na	na

Note: Cumulative purge volumes on September 19 are biased low because of clogging of the flow meter from high initial sediment load in water.

[a] n/a = Not applicable.

[b] na = Not available.

Table 8.2-1
Aquifer Pumping Test Results for Well CrEX-1

Status	Screen	Time	Pumping Rate (gpm)	Depth to Water (ft bgs)	Draw Down (ft)	Purge Volume (gal.)	Cumulative Purge Volume (gal.)	Specific Capacity (gpm/ft)
Step Test								
10/1/14								
On at 20% max	1	8:15	19	997.08	0	0	0	na[a]
		8:20	19	1003.33	6.25	20	20	3.04
		8:25	16	1002.33	5.25	80	100	3.05
		8:30	20	1000.53	3.45	100	200	5.80
		8:35	18	1000.73	3.65	90	290	4.93
		8:40	20	1000.73	3.65	100	390	5.48
		8:45	26	1000.73	3.65	130	520	7.12
		8:50	16	1000.73	3.65	80	600	4.38
		8:55	22	1000.73	3.65	110	710	6.03
		9:00	20	1000.63	3.55	100	810	5.63
		9:05	22	1000.73	3.65	110	920	6.03
		9:10	22	1000.73	3.65	110	1030	6.03
		9:15	22	1000.73	3.65	110	1140	6.03
		9:25	22	1000.63	3.55	220	1360	6.20
		9:35	23	1000.63	3.55	230	1590	6.48
		9:45	21	1000.73	3.65	210	1800	5.75
		9:55	20	1000.73	3.65	200	2000	5.48
		10:05	21	1000.73	3.65	210	2210	5.75
		10:15	20	1000.73	3.65	200	2410	5.48

Table 8.2-1 (continued)

Status	Screen	Time	Pumping Rate (gpm)	Depth to Water (ft bgs)	Draw Down (ft)	Purge Volume (gal.)	Cumulative Purge Volume (gal.)	Specific Capacity (gpm/ft)
Change rate to 40% max	1	10:20	na	1003.03	5.95	190	2600	na
		10:25	36	1002.93	5.85	180	2780	6.15
		10:30	36	1002.93	5.85	180	2960	6.15
		10:35	38	1002.88	5.8	190	3150	6.55
		10:40	36	1002.83	5.75	180	3330	6.26
		10:45	36	1002.83	5.75	180	3510	6.26
		10:50	38	1002.83	5.75	190	3700	6.61
		10:55	36	1002.78	5.7	180	3880	6.32
		11:00	36	1002.78	5.7	180	4060	6.32
		11:05	36	1002.78	5.7	180	4240	6.32
		11:10	38	1002.78	5.7	190	4430	6.67
		11:15	36	1002.83	5.75	180	4610	6.26
		11:20	36	1002.78	5.7	180	4790	6.32
		11:30	37	1002.78	5.7	370	5160	6.49
		11:40	36	1002.78	5.7	360	5520	6.32
		11:50	37	1002.78	5.7	370	5890	6.49
		12:00	37	1002.78	5.7	370	6260	6.49
		12:10	36	1002.78	5.7	360	6620	6.32
		12:20	37	1002.78	5.7	370	6990	6.49

Table 8.2-1 (continued)

Status	Screen	Time	Pumping Rate (gpm)	Depth to Water (ft bgs)	Draw Down (ft)	Purge Volume (gal.)	Cumulative Purge Volume (gal.)	Specific Capacity (gpm/ft)
Change rate to 60% max	1	12:25	57	1007.33	10.25	290	7280	5.56
		12:30	62	1007.33	10.25	310	7590	6.05
		12:35	60	1007.33	10.25	300	7890	5.85
		12:40	60	1007.33	10.25	300	8190	5.85
		12:45	60	1007.33	10.25	300	8490	5.85
		12:50	60	1007.38	10.3	300	8790	5.83
		12:55	60	1007.38	10.3	300	9090	5.83
		13:00	62	1007.43	10.35	310	9400	5.99
		13:05	62	1007.43	10.35	310	9710	5.99
		13:10	58	1007.43	10.35	290	10,000	5.60
		13:15	60	1007.43	10.35	300	10,300	5.80
		13:20	60	1007.43	10.35	300	10,600	5.80
		13:25	62	1007.43	10.35	310	10,910	5.99
		13:35	60	1007.43	10.35	600	11,510	5.80
		13:45	60	1007.43	10.35	600	12,110	5.80
		13:55	61	1007.43	10.35	610	12,720	5.89
		14:05	60	1007.43	10.35	600	13,320	5.80
		14:15	67	1007.43	10.35	670	13,990	6.47
		14:25	55	1007.43	10.35	550	14,540	5.31

Table 8.2-1 (continued)

Status	Screen	Time	Pumping Rate (gpm)	Depth to Water (ft bgs)	Draw Down (ft)	Purge Volume (gal.)	Cumulative Purge Volume (gal.)	Specific Capacity (gpm/ft)
Change rate to 80% max	1	14:30	na[a]	1008.13	11.05	360	14,900	na
		14:35	74	1008.23	11.15	370	15,270	6.64
		14:40	74	1008.23	11.15	370	15,640	6.64
		14:45	74	1008.33	11.25	370	16,010	6.58
		14:50	74	1008.33	11.25	370	16,380	6.58
		14:55	74	1008.33	11.25	370	16,750	6.58
		15:00	74	1008.33	11.25	370	17,120	6.58
		15:05	76	1008.33	11.25	380	17,500	6.76
		15:10	74	1008.38	11.3	370	17,870	6.55
		15:20	74	1008.38	11.3	380	18,250	6.55
		15:25	76	1008.38	11.3	750	19,000	6.73
		15:30	74	1008.38	11.3	370	19,370	6.55
		15:40	76	1008.38	11.3	760	20,130	6.73
		15:50	75	1008.38	11.3	750	20,880	6.64
		16:00	75	1008.43	11.35	750	21,630	6.61
		16:10	76	1008.43	11.35	760	22,390	6.70
		16:20	75	1008.43	11.35	750	23,140	6.61
		16:30	76	1008.43	11.35	760	23,900	6.70

Table 8.2-1 (continued)

Status	Screen	Time	Pumping Rate (gpm)	Depth to Water (ft bgs)	Draw Down (ft)	Purge Volume (gal.)	Cumulative Purge Volume (gal.)	Specific Capacity (gpm/ft)
Change rate to 100% max	1	16:35	na	1013.23	16.15	470	24,370	na
		16:40	96	1013.23	16.15	480	24,850	5.94
		16:45	96	1013.23	16.15	480	25,330	5.94
		16:50	94	1013.23	16.15	470	25,800	5.82
		16:55	98	1013.23	16.15	490	26,290	6.07
		17:00	96	1013.23	16.15	480	26,770	5.94
		17:05	96	1013.23	16.15	480	27,250	5.94
		17:10	96	1013.23	16.15	480	27,730	5.94
		17:15	98	1013.23	16.15	490	28,220	6.07
		17:20	96	1013.23	16.15	480	28,700	5.94
		17:25	98	1013.23	16.15	490	29,190	6.07
		17:30	94	1013.23	16.15	470	29,660	5.82
		17:35	96	1013.23	16.15	480	30,140	5.94
		17:45	96	1013.23	16.15	960	31,100	5.94
		17:55	96	1013.23	16.15	960	32,060	5.94
		18:05	96	1013.23	16.15	960	33,020	5.94
		18:15	96	1013.23	16.15	960	33,980	5.94
		18:25	96	1013.23	16.15	960	34,940	5.94
Off	1	18:35	97	1013.23	16.15	970	35,910	6.01

Table 8.2-1 (continued)

Status	Screen	Time	Pumping Rate (gpm)	Depth to Water (ft bgs)	Draw Down (ft)	Purge Volume (gal.)	Cumulative Purge Volume (gal.)	Specific Capacity (gpm/ft)
24-h Constant Rate Test								
10/3/14								
On	1	8:05	0	997.33	0	10	35,920	na
		8:08	Water to surface	n/a[b]	n/a	n/a	n/a	n/a
		8:10	40	1016.9	19.57	200	36,120	2.04
		8:15	100	1016.65	19.32	500	36,620	5.18
		8:20	96	1016.65	19.32	480	37,100	4.97
		8:25	92	1016.8	19.47	460	37,560	4.73
		8:30	108	1016.9	19.57	540	38,100	5.52
		8:35	80	1016.9	19.57	400	38,500	4.09
		8:50	102	1017	19.67	1530	40,030	5.19
		9:05	89.33	1017.1	19.77	1340	41,370	4.52
		9:20	100	1017.15	19.82	1500	42,870	5.05
		9:35	96.67	1017.2	19.87	1450	44,320	4.87
		10:05	95	1017.25	19.92	2850	47,170	4.77
		10:35	96.33	1017.3	19.97	2890	50,060	4.82
		11:05	96.33	1017.35	20.02	3180	53,240	4.81
		11:30	96.52	1017.37	20.04	2220	55,460	4.82
		12:00	95.33	1017.37	20.04	2860	58,320	4.76
		12:30	96.33	1017.38	20.05	2890	61,210	4.80
		13:00	97	1017.38	20.05	2910	64,120	4.84
		13:30	96.67	1017.38	20.05	2900	67,020	4.82
		14:00	97	1017.38	20.05	2910	69,930	4.84
		14:30	96.86	1017.39	20.06	3390	73,320	4.83
		15:00	94.8	1017.39	20.06	2370	75,690	4.73

Table 8.2-1 (continued)

Status	Screen	Time	Pumping Rate (gpm)	Depth to Water (ft bgs)	Draw Down (ft)	Purge Volume (gal.)	Cumulative Purge Volume (gal.)	Specific Capacity (gpm/ft)
	1	15:30	95.15	1017.42	20.09	3140	78,830	4.74
		16:00	99.26	1017.42	20.09	2680	81,510	4.94
		16:30	96.33	1017.42	20.09	2890	84,400	4.79
		17:00	96.33	1017.45	20.12	2890	87,290	4.79
		17:30	96.33	1017.46	20.13	2890	90,180	4.79
		18:00	96.33	1017.48	20.15	2890	93,070	4.78
		18:30	96	1017.49	20.16	2880	95,950	4.76
		19:00	97.77	1017.49	20.16	2640	98,590	4.85
		19:30	95.66	1017.49	20.16	2870	101,460	4.75
		20:00	95.66	1017.51	20.18	2870	104,330	4.74
		20:30	95.66	1017.51	20.18	2870	107,200	4.74
		21:00	96	1017.51	20.18	2880	110,080	4.76
		21:30	95.66	1017.51	20.18	2870	112,950	4.74
		22:00	95.66	1017.55	20.22	2870	115,820	4.73
		22:30	95.66	1017.53	20.2	2870	118,690	4.74
		23:00	95.66	1017.55	20.22	2870	121,560	4.73
		23:30	95.66	1017.57	20.24	2870	124,430	4.73
		24:00	95.66	1017.6	20.27	2870	127,300	4.72
		0:30	96	1017.63	20.3	2880	130,180	4.73
		1:00	95.33	1017.63	20.3	2860	133,040	4.70
		1:30	95.66	1017.65	20.32	2870	135,910	4.71
		2:00	96	1017.65	20.32	2880	138,790	4.72
		2:30	95.33	1017.65	20.32	2860	141,650	4.69
		3:00	95.66	1017.63	20.3	2870	144,520	4.71
		3:30	95.66	1017.65	20.32	2870	147,390	4.71

Table 8.2-1 (continued)

Status	Screen	Time	Pumping Rate (gpm)	Depth to Water (ft bgs)	Draw Down (ft)	Purge Volume (gal.)	Cumulative Purge Volume (gal.)	Specific Capacity (gpm/ft)
	1	4:00	95.33	1017.66	20.33	2860	150,250	4.69
		4:30	95.66	1017.65	20.32	2870	153,120	4.71
		5:00	95.33	1017.65	20.32	2860	155,980	4.69
		5:30	95.66	1017.65	20.32	2870	158,850	4.71
		6:00	95.66	1017.65	20.32	2870	161,720	4.71
		6:30	96.66	1017.69	20.36	2900	164,620	4.75
		7:00	94.66	1017.7	20.37	2840	167,460	4.65
		7:30	95.33	1017.7	20.37	2860	170,320	4.68
Off	1	8:05	na	1017.7	20.37	3350	173,670	na

[a] na = Not available.

[b] n/a = Not applicable.

Table 8.6-1
Summary of Waste Characterization Samples Collected during Drilling, Construction, and Development of CrEX-1

Event ID	Sample ID	Date Collected	Description	Sample Matrix
5765	WST05-14-84406	07/08/14	CrEx-1 drill cuttings (top)	Solid
5765	WST05-14-84409	07/08/14	CrEx-1 drill cuttings trip blank	Solid
5765	WST05-14-84407	07/21/14	CrEx-1 drill cuttings(middle)	Solid
5765	WST05-14-84411	07/21/14	CrEx-1 drill cuttings trip blank	Solid
5765	WST05-14-85767	08/04/14	CrEx-1 drill cuttings (bottom)	Solid
5765	WST05-14-85765	08/04/14	CrEx-1 drill cuttings trip blank	Solid
5764	WST05-14-84405	09/03/14	CrEX-1 drill cuttings	Solid
5766	WST05-14-84414	07/08/14	CrEx-1drilling fluids (top)	Liquid
5766	WST05-14-84418	07/08/14	CrEx-1drilling fluids trip blank	Liquid
5766	WST05-14-84415	07/08/14	CrEx-1 drilling field dup	Liquid
5766	WST05-14-84413	07/21/14	CrEx-1 drilling fluid	Liquid
5766	WST05-14-84419	07/21/14	CrEx-1 drilling fluid trip blank	Liquid
5766	WST05-14-84417	07/21/14	CrEx-1 drilling fluid dup	Liquid
5766	WST05-14-84414	08/04/14	CrEx-1 drilling fluid	Liquid
5766	WST05-14-84420	08/04/14	CrEx-1 drilling fluid trip blank	Liquid
5766	WST05-14-84416	08/04/14	CrEx-1 drilling fluid dup	Liquid
5761	WST05-14-84269	10/27/14	CrEx-1 drilling fluid	Liquid
5761	WST05-14-84270	10/27/14	CrEx-1 drilling fluid dup	Liquid
5761	WST05-14-84403	10/27/14	CrEx-1 drilling fluid	Liquid
6869	WST05-14-86626	TBD*	CrEx-1 decon water	Liquid

*TBD = To be determined.

Appendix A

Final Well Design and New Mexico Environmental Department Approval

From: Everett, Mark Capen
Sent: Friday, August 08, 2014 12:39 PM
To: Jerzy Kulis (jerzy.kulis@state.nm.us); Wear, Benjamin, NMENV (Benjamin.Wear@state.nm.us); Michael Dale (Michael.Dale@state.nm.us)
Cc: Shen, Hai; Rodriguez, Cheryl L; Woodworth, Woody; Swickley, Stephani Fuller; Katzman, Danny; Ball, Ted; Douglass, Craig R
Subject: CrEX-1 proposed well design

Jerzy,

Here is the CrEX-1 proposed well design which includes a narrative, two diagrams depicting the proposed design, and a Schlumberger geophysical log montage for discussion. We will be in touch around 1:15.

Thanks,

Mark Everett, PG
CAP-ES LANL
(505) 667-5931 (o)
(505) 231-6002 (c)

From: Kulis, Jerzy, NMENV [mailto:jerzy.kulis@state.nm.us]
Sent: Friday, August 08, 2014 2:48 PM
To: Katzman, Danny; Wear, Benjamin, NMENV
Cc: Ball, Ted; Everett, Mark Capen; Shen, Hai; Cobrain, Dave, NMENV; Dale, Michael, NMENV
Subject: RE: CrEX-1 well design narrative (2)

Danny,

NMED hereby approves the installation of the chromium extraction well CrEX-1 as proposed in your e-mail below and in the e-mail sent by Mark Everett on August 8, 2014 at 12:39 PM. This approval is based on information available to NMED at the time of the approval. LANL must provide the results of groundwater sampling, any modifications to the well design proposed in the above-mentioned e-mails, and any additional information relevant to the installation of CrEX-1 as soon as such data or information becomes available. LANL must perform installation of CrEX-1 and its subsequent development in the manner the minimizes communication between the upper and lower screens and possible cross-contamination.

Please let me know if you have any questions.

Jerzy Kulis
Environmental Scientist
Hazardous Waste Bureau
New Mexico Environment Department
2905 Rodeo Park Drive East, Bldg 1
Santa Fe, NM 87505-6303
Phone: 505-476-6039
Fax: 505-476-6030

From: Katzman, Danny [mailto:katzman@lanl.gov]
Sent: Friday, August 08, 2014 2:15 PM
To: Kulis, Jerzy, NMENV; Wear, Benjamin, NMENV
Cc: Ball, Ted; Everett, Mark Capen; Shen, Hai
Subject: CrEX-1 well design narrative (2)

Jerzy, Ben- following on our discussion, here's an updated well-design rationale sheet for CrEX-1. Please review and provide a response at your earliest convenience.
Thanks again for facilitating such an efficient review.
Danny

CrEX-1

Key objectives that guide design:

- Establish capture zone within the plume which is in the upper 70-100 ft of aquifer
- Optimize removal of only chromium contaminated water
- Reach downgradient towards R-50 if possible
- Avoid drawing chromium contamination downward

Key observations from geophysics:

- Water table is at approximately 990’ bgs
- Contact between Puye formation and Miocene Pumiceous Unit is at ~1052’ bgs
- Good probability of production from water table to ~1050’ bgs
- Very high conductivity/free water/production zone between 1050 – 1150 (appears to correlate with Miocene pumiceous unit)

Recommendation:

- Build a two-screen well with a 50’ screen starting at water table (990’ – 1040’ bgs), a 30’ blank section, and a 20’ lower screen set from 1070 – 1090’ bgs
- The “water table” screen has a higher likelihood of reaching downgradient because it would be in a lower transmissivity zone than a deeper screen.
- A screen set exclusively in the deeper high production zone might not propagate capture towards the upper 75’ of the aquifer where the chromium is present.
- The lower screen would be packed off and only used if the upper screen does not produce the hydraulic response necessary for an optimized capture zone.
- Development would occur over the entire screen interval, then again in the upper screen after being packed off

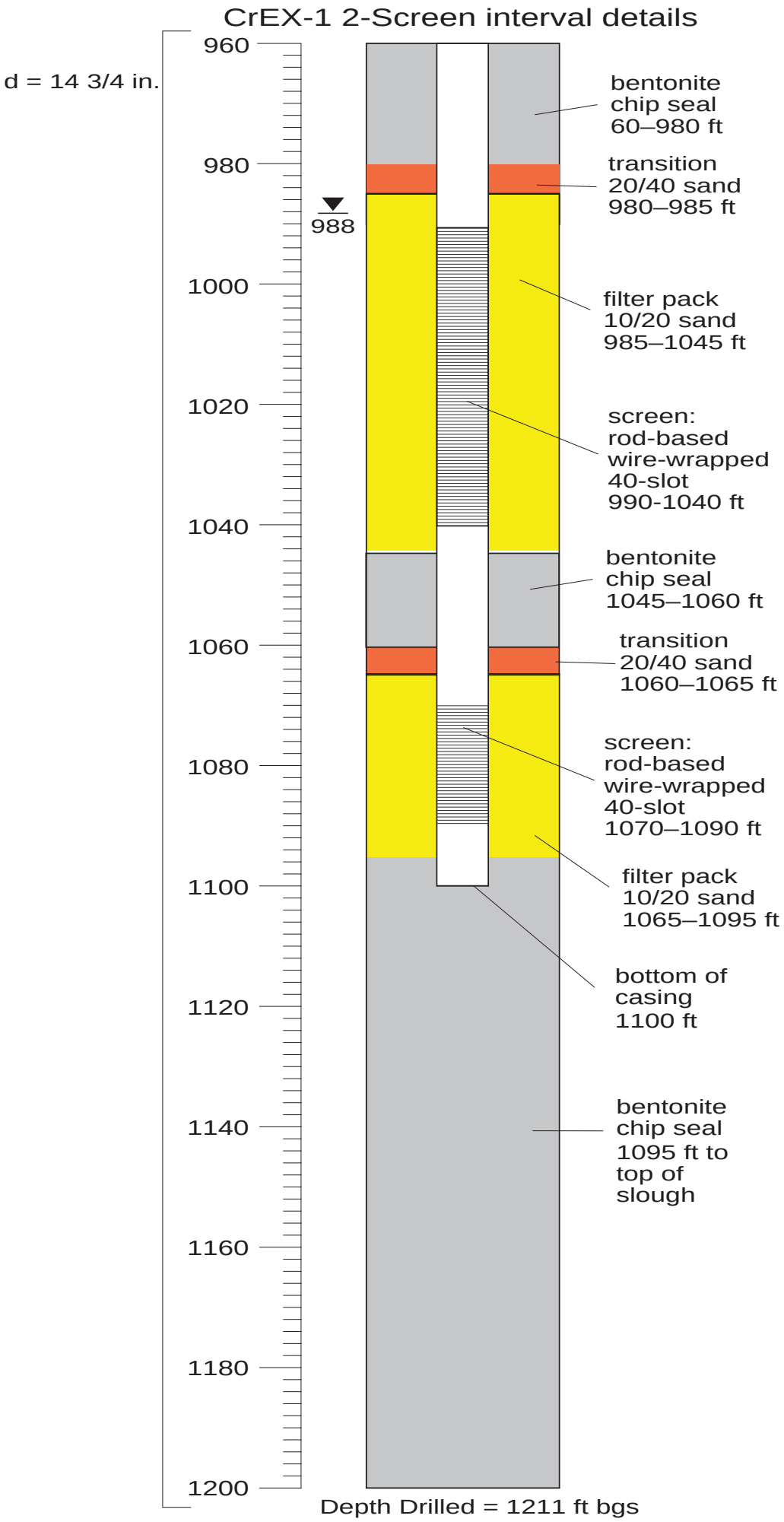
CrEX-1 2-Screen interval details
d = 14 3/4 in.
960
980
988
1000
1020
1040
1060
1080
1100
1120
1140
1160
1180
1200
bentonite chip seal 60–980 ft
transition 20/40 sand 980–985 ft
filter pack 10/20 sand 985–1045 ft
screen: rod-based wire-wrapped 40-slot 990-1040 ft
bentonite chip seal 1045–1060 ft
transition 20/40 sand 1060–1065 ft
screen: rod-based wire-wrapped 40-slot 1070–1090 ft
filter pack 10/20 sand 1065–1095 ft
bottom of casing 1100 ft
bentonite chip seal 1095 ft to top of slough
Depth Drilled = 1211 ft bgs

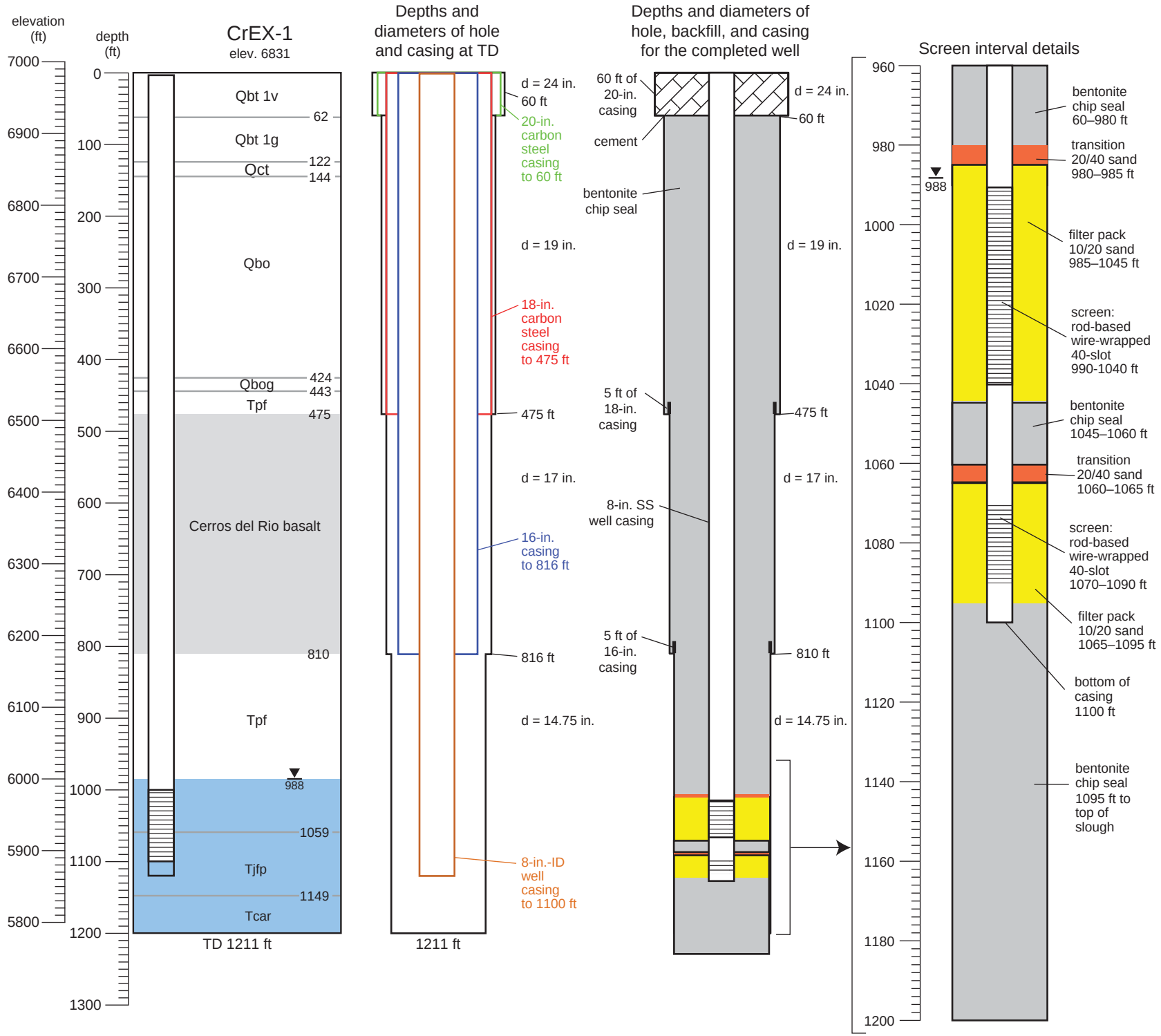
elevation (ft)
depth (ft)
CrEX-1
elev. 6831
7000
6900
6800
6700
6600
6500
6400
6300
6200
6100
6000
5900
5800
0
100
200
300
400
500
600
700
800
900
1000
1100
1200
1300
Qbt 1v
62
Qbt 1g
122
Qct
144
Qbo
424
Qbog
443
Tpf
475
Cerros del Rio basalt
810
Tpf
988
1059
Tjfp
1149
Tcar
TD 1211 ft
Depths and diameters of hole and casing at TD
d = 24 in.
60 ft
20-in. carbon steel casing to 60 ft
d = 19 in.
18-in. carbon steel casing to 475 ft
475 ft
d = 17 in.
16-in. casing to 816 ft
816 ft
d = 14.75 in.
8-in.-ID well casing to 1100 ft
1211 ft
Depths and diameters of hole, backfill, and casing for the completed well
60 ft of 20-in. casing
cement
bentonite chip seal
d = 24 in.
60 ft
d = 19 in.
5 ft of 18-in. casing
475 ft
d = 17 in.
8-in. SS well casing
5 ft of 16-in. casing
810 ft
d = 14.75 in.
Screen interval details
960
980
1000
1020
1040
1060
1080
1100
1120
1140
1160
1180
1200
988
bentonite chip seal 60–980 ft
transition 20/40 sand 980–985 ft
filter pack 10/20 sand 985–1045 ft
screen: rod-based wire-wrapped 40-slot 990-1040 ft
bentonite chip seal 1045–1060 ft
transition 20/40 sand 1060–1065 ft
screen: rod-based wire-wrapped 40-slot 1070–1090 ft
filter pack 10/20 sand 1065–1095 ft
bottom of casing 1100 ft
bentonite chip seal 1095 ft to top of slough

Schlumberger

MR Scanner
Pc / Sw Evaluation
Composite Log

COMPANY:	Los Alamos National Laboratory		
WELL:	CrEX-1		
FIELD:	LANL		
State:	New Mexico		
COUNTRY:	USA		
Date Processed:	07-Aug-2014	Date Logged:	07-Aug-2014
Job Number:		Processed at:	
Well Location:	Mortandad Canyon		
Latitude:	35deg 51' 28" N	Longitude:	106deg 15' 23" W
Elevations:	KB:	DF:	GL:

MRX advanced processing

FOLD HERE The well name, location and borehole reference data were furnished by the customer.

Mud Invasion

RXO_HRLT RXO_HRL
0 (ohm.m) 1000

RLA5 RLA5@ConPr_
0 (ohm.m) 1000

RLA4 RLA4@ConPr_
0 (ohm.m) 1000

RLA3 RLA3@ConPr_
0 (ohm.m) 1000

ConPr_R3L8Up_S02
Horizontal Scale: 1 : 28.134
Straight Image
0 120 240 360

T1 (0.7 in)

T1 (1 in)

	Bit Size 10 (in) 20	RLA1 RLA1@ConPr_ 0 (ohm.m) 1000		Resistive MR Image Conductive						T1 (2.7 in) 0 ( ) 63	T1 (4 in) 0 ( ) 63
	Hole Diameter 10 (in) 20	T-C Perm. (2.7" 1 (mD) 10000	APS N/F Vol. Wat 0.5 (ft3/ft3) 0	Free Water						T1PC 1 (ms) 9000	T1PC 1 (ms) 9000
	Washout	T-C Perm. (4 in) 1 (mD) 10000	MR Water (2.7 in 0.5 (ft3/ft3) 0	FFV (4 in) 0.4 (ft3/ft3) 0	Pc Dist 0 ( ) 49		Pc Dist 0 ( ) 49			T1LM 1 (ms) 9000	T1LM 1 (ms) 9000
MD 1 : 240 ft	SP -50 (mV) 50	True Form. Resi. 0 (ohm.m) 1000	MR Water (4 in) 0.5 (ft3/ft3) 0	FFV (2.7 in) 0.4 (ft3/ft3) 0	Pc Sw 1 (ft3/ft3) 0	Pc Dist 0 ( ) 49	Pc Sw 1 (ft3/ft3) 0	Pc Dist 0 ( ) 49	T1 Cutoff 1 (ms) 9000	T1 Cutoff 1 (ms) 9000	
800											
850											
900											
950											

1000

1050

1100

1150

1200

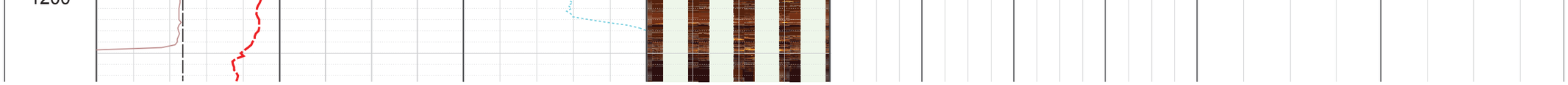
1200

Appendix B

Borehole Video Logging
(on DVD included with this document)

TO VIEW THE VIDEO THAT ACCOMPANIES THIS DOCUMENT, PLEASE CALL THE HAZARDOUS WASTE BUREAU AT 505-476-6000 TO MAKE AN APPOINTMENT

Appendix C

Geophysical Logs and Schlumberger Geophysical Logging Report (on CD included with this document)

Schlumberger

6
C
Carbon

13
Al
Aluminium

16
S
Sulfur

14
Si
Silicon

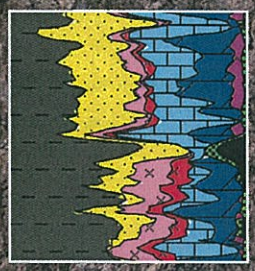

20
Ca
Calcium

26
Fe
Iron

1
H
Hydrogen

19
K
Potassium

11
Na
Sodium

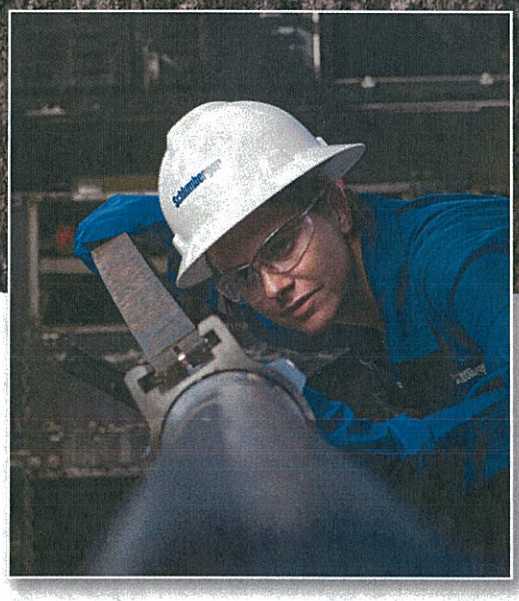

25
Mn
Manganese

17
Cl
Chlorine

12
Mg
Magnesium

Litho Scanner

High-definition
spectroscopy service

Applications

- Detailed quantitative mineralogy in complex lithologies
- Real-time element measurements and robust quantitative lithology
  - Ca, Fe, Mg, and S for carbonate lithology
  - Al, Fe, and Si for siliciclastic lithology
  - Al, Ca, Fe, K, and Si for unconventional reservoirs
- Total organic carbon (TOC) log for lithology and salinity-independent hydrocarbon saturation
  - Kerogen volume in unconventional reservoirs
  - Weight-percent oil in heavy oil reservoirs and oil sands
  - Oil volume from TOC
- Matrix properties for petrophysical evaluation
  - Accurate density porosity
  - Gas identification through matrix-corrected neutron and density
  - Accurate formation fluid sigma
- Element logs for well-to-well correlation and sequence stratigraphy
- Metals for mining exploration: Cu, Gd, Ni, and Ti
- Quick, accurate bulk mineralogy and TOC inputs to sCore* lithofacies classification to target intervals with superior reservoir and completion quality

Features and Benefits

- Enhanced suite of elements measured, including Al, Ba, C, Ca, Cl, Fe, Gd, K, Mg, Mn, Na, S, Si, Ti, and metals such as Cu and Ni
- Stand-alone TOC output
- Large cerium-doped lanthanum bromide ($LaBr_3$:Ce) gamma ray detector exclusive to Litho Scanner service for the most accurate and precise mineralogy in the industry
  - Excellent spectral resolution
  - Unmatched temperature performance
  - Industry's highest count-rate capabilities
- High-speed electronics to support high count rates
- High-performance pulsed neutron generator (PNG)
  - Elimination of AmBe source
  - High-neutron-flux output for greater precision
  - Simultaneous inelastic and capture spectra
  - 350 degF [177 degC] rating
- Combinable with most openhole services and compatible with main conveyance modes (wireline, TLC* tough logging conditions drillpipe-assisted, and tractor)
- Improved elemental precision with high-quality data at faster logging speeds
- Unlimited acquisition time at high temperatures for deep or horizontal wells

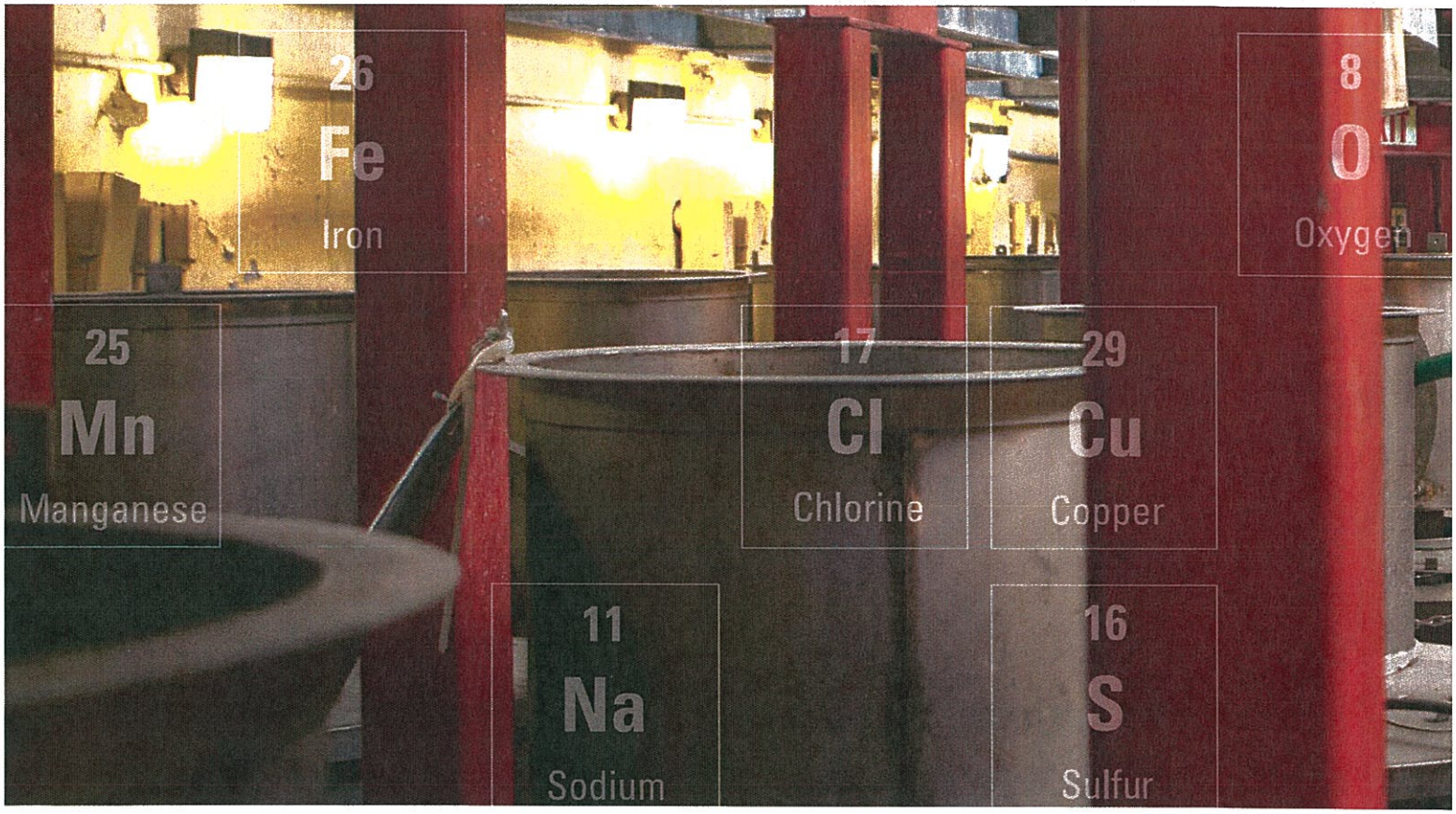

6
C
Carbon

12
Mg
Magnesium

Unlocking the key elements of your reservoir

Litho Scanner* high-definition spectroscopy service revolutionizes gamma ray spectroscopy to enable detailed description of complex reservoirs. In addition to measuring key elements in a wide variety of rock formations with higher precision and accuracy than previously possible, Litho Scanner service provides a stand-alone quantitative determination of total organic carbon (TOC).

13
Al
Aluminium

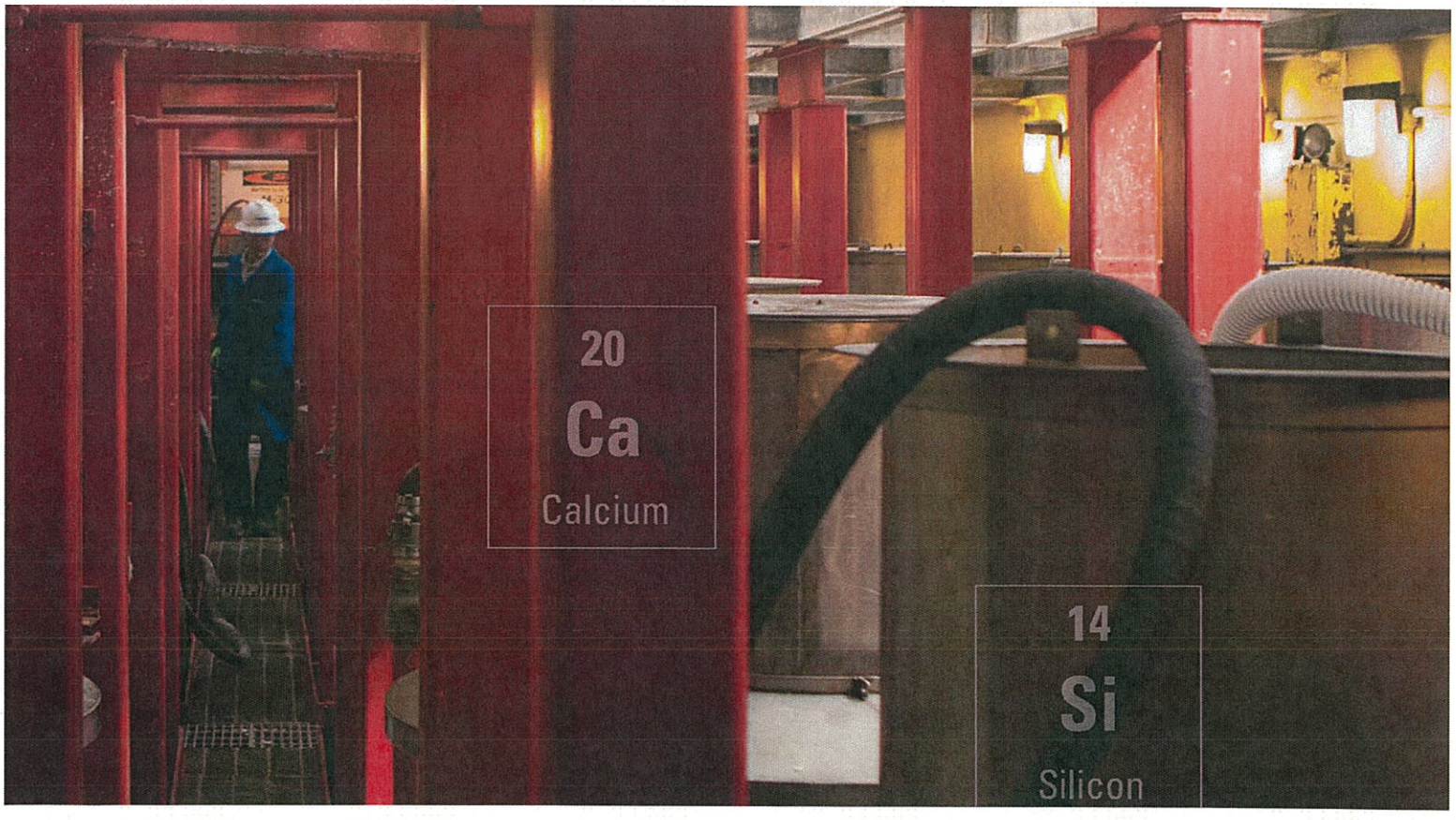

Unlocking the elements of your reservoir

The increasing complexity of today's reservoirs demands an accurate understanding of formation composition and mineralogy. This is particularly the case for unconventional reservoirs, for which the quantification of both mineralogy and organic carbon is critical for resource evaluation with confidence.

Litho Scanner high-definition spectroscopy service provides the key quantitative measurements of elements and mineralogy, delivered with previously unavailable accuracy and speed. The high neutron output, high count-rate capability, and outstanding spectral resolution make it possible to log at higher speeds without a loss of precision or accuracy. The pulsed neutron generator's (PNG's) intricate pulsing scheme and sharp neutron bursts enable unambiguous separation of inelastic and capture gamma rays to improve the quality of both measurements. Elimination of reliance on a ^{241}AmBe logging source improves radiation safety and environmental protection for operations in any reservoir environment.

16
S
Sulfur

26
Fe
Iron

Slim diameter, high performance

With an outside diameter of 4.5 in [11.4 cm], the compact Litho Scanner tool is the slimmest openhole spectroscopy tool in the industry. The tungsten-shielded PNG emits 14.1-MeV neutrons at a high output of about 3×10^8 neutrons per second, which is approximately 8 times higher than that of current industry tools using chemical sources. The clear separation of inelastic and capture data enables measuring more elements—including carbon—than previous-generation tools.

The very fast $LaBr_3$:Ce scintillator provides high light output and excellent spectral resolution. Its integration with a state-of-the-art photomultiplier and dedicated high-performance electronics means that counting rates in excess of 2,500,000 counts per second can be handled without sacrificing spectral resolution, unlike the detectors in previous-generation spectroscopy tools. The outstanding high-temperature performance of the $LaBr_3$:Ce scintillator eliminates the need for a detector cooling system and maintains spectral quality even during lengthy logging operations at the rated tool temperature of 350 degF [177 degC]. The housing near the detector is surrounded with a thermal neutron shield containing boron to reduce the number of capture gamma rays produced from the tool.

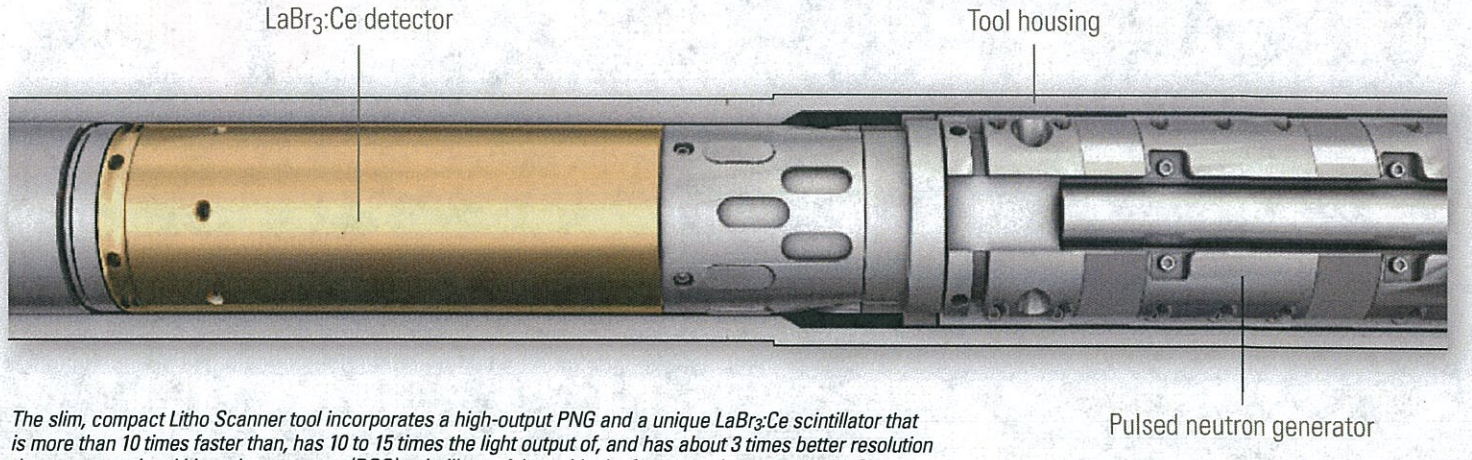

The slim, compact Litho Scanner tool incorporates a high-output PNG and a unique $LaBr_3$:Ce scintillator that is more than 10 times faster than, has 10 to 15 times the light output of, and has about 3 times better resolution than a conventional bismuth germanate (BGO) scintillator. A large block of tungsten between the PNG and the detector prevents the direct passage of fast neutrons.

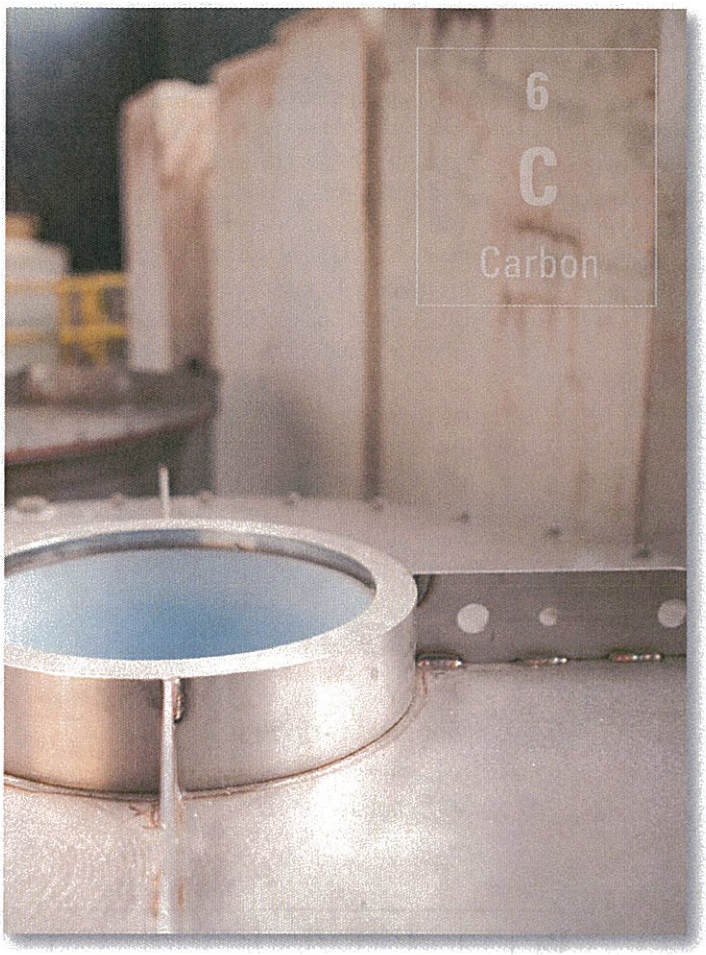

20
Ca
Calcium

12
Mg
Magnesium

14
Si
Silicon

To ensure accuracy, the tool response is calibrated at the Schlumberger Environmental Effects Calibration Facility over a wide range of lithologies, porosities, and environmental conditions in laboratory formations with known properties.

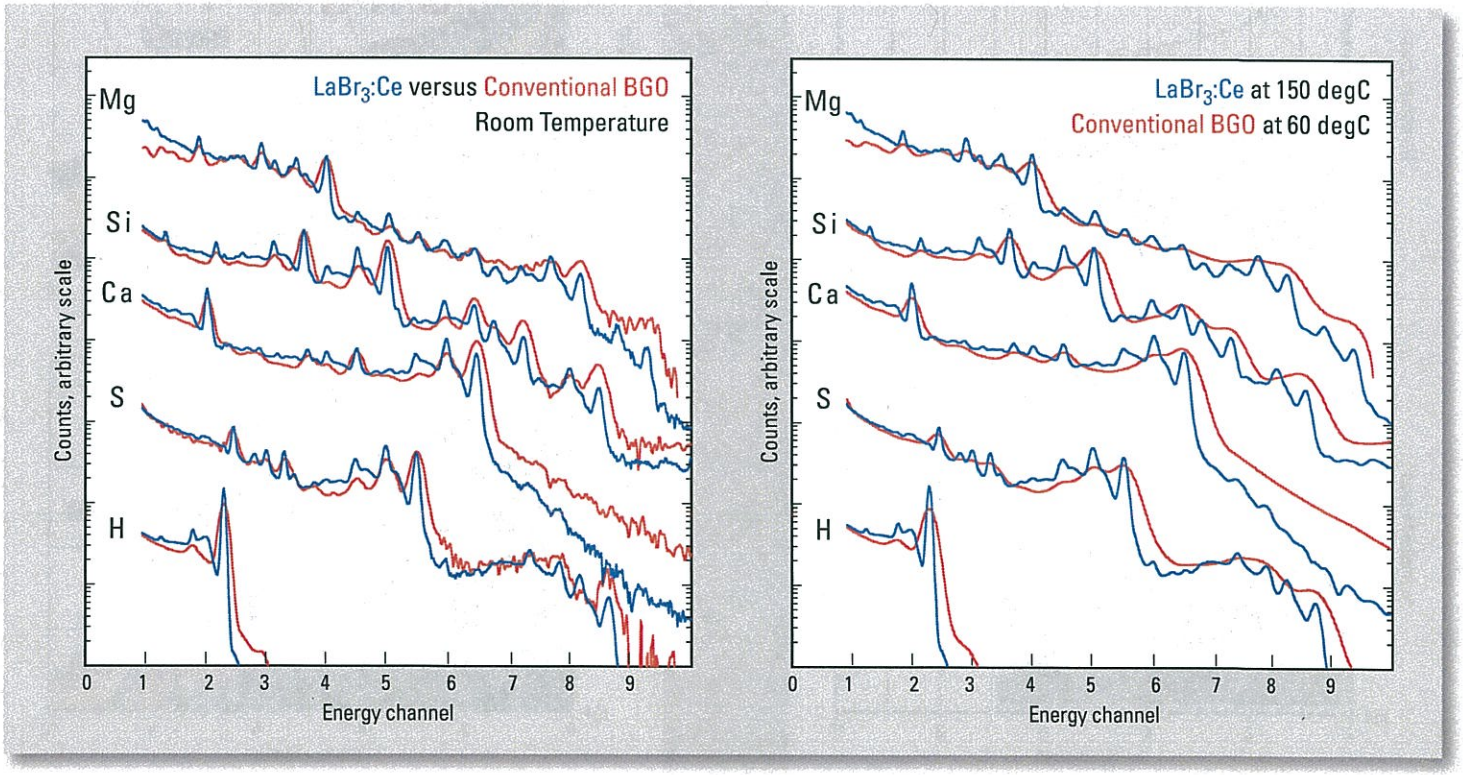

Elemental standard spectra measured with the Litho Scanner $LaBr_3$:Ce gamma ray detector (blue) on the left panel have better resolution, with sharper, better defined features that improve the accuracy of deconstructing each measured spectrum into its components in comparison with the spectra from conventional BGO detectors (red). The right panel compares performance at elevated temperatures. At 300 degF [150 degC] $LaBr_3$:Ce (blue) maintains its high light output, whereas the BGO (red) decrease in light output significantly degrades the elemental standard spectra at only 150 degF [60 degC].

How it works

The science of spectroscopy

The neutrons emitted by the PNG of the Litho Scanner tool induce the emission of gamma rays from the formation via two primary interactions: inelastic scattering and thermal neutron capture. Each of these interactions produces gamma rays with a specific set of characteristic energies.

The Litho Scanner tool's $LaBr_3$:Ce detector is coupled to a high-temperature spectroscopy photomultiplier, producing signals that are integrated, digitized, and processed by a high-performance pulse-height analyzer.

The analyzer determines the pulse height (proportional to energy) of each detected gamma ray and accumulates pulse-height histograms (spectra) that tally counts versus pulse height. Spectra are acquired during and after each neutron burst, which enables separation of the inelastic and capture gamma rays.

Each spectrum is decomposed into a linear combination of standard spectra from individual elements. This step involves correction for some environmental and electronic factors. The coefficients of the linear combination of the standard spectra are converted to elemental weight fractions via a modified geochemical oxides closure model or by using an inversion approach. Two methods are available to generate mineralogy and lithologic fractions from the elemental concentration logs. One is sequential SpectroLith* processing, which is based on the derivation of empirical relationships between elemental concentrations and mineral concentrations. The other is by using an iterative inversion technique, such as the Techlog* Quanti multicomponent inversion ELAN* module.

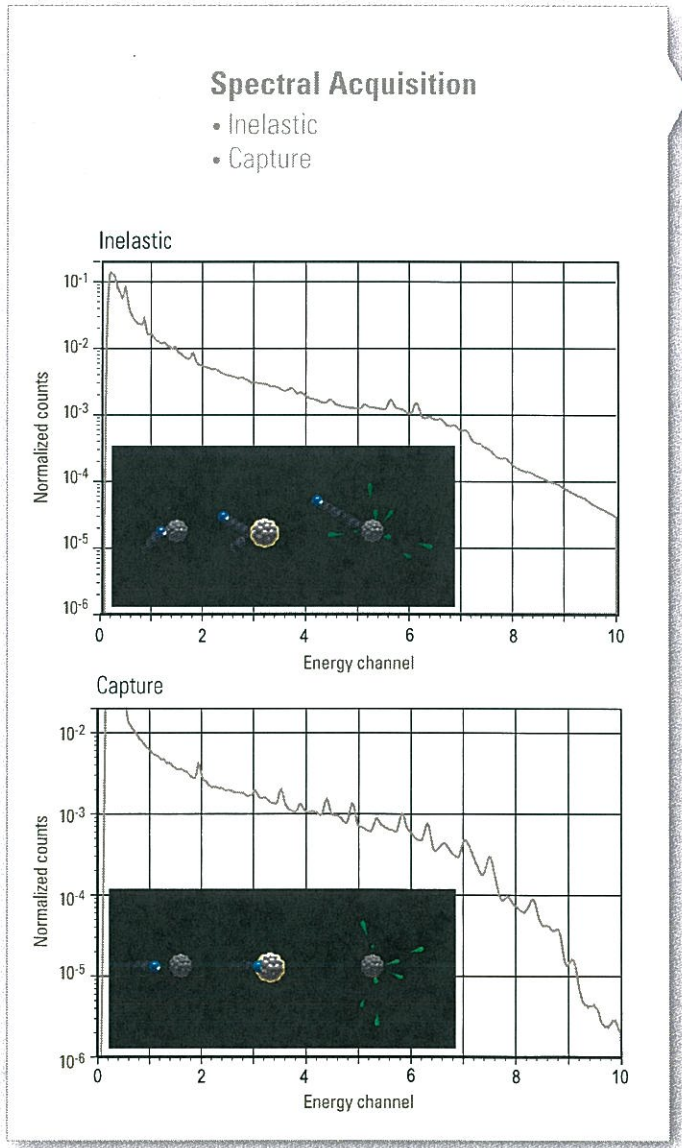

The spectroscopy workflow begins with measurement of the separated inelastic and capture gamma ray spectra.

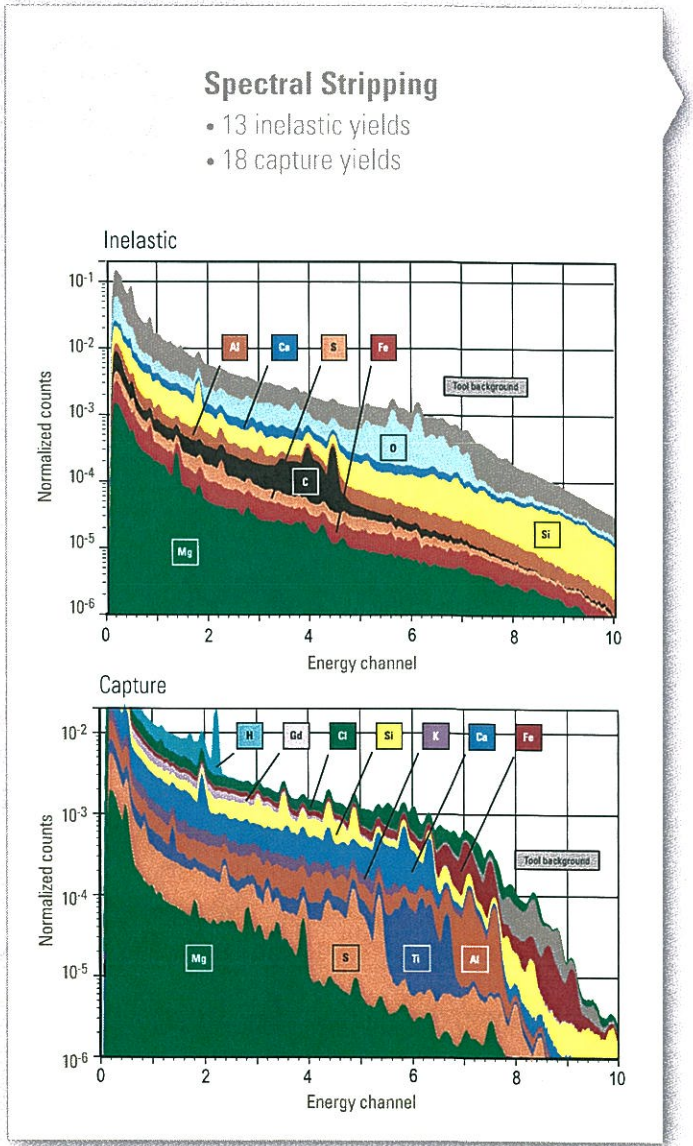

Each spectra is decomposed into the combination of spectra from the individual elements.

Inelastic

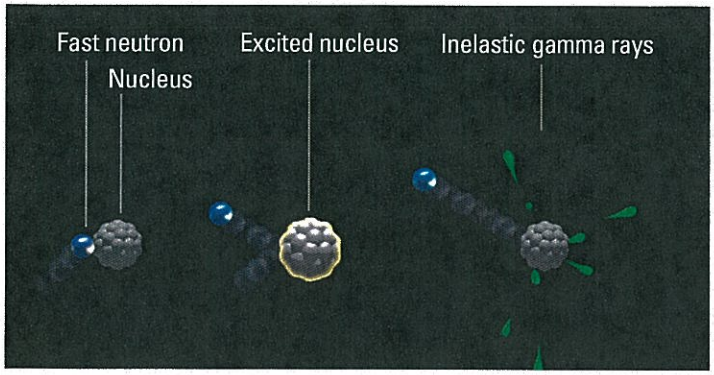

Capture

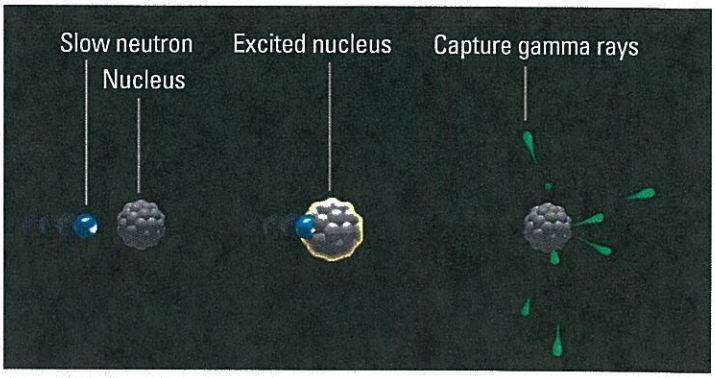

An inelastic collision (left) causes a fast neutron (energy > 1 MeV) to lose a large fraction of its energy. This energy is transferred to neutrons or protons in the nucleus and moves them into highly excited states, which decay rapidly while emitting one or more gamma rays with energies characteristic of the excited nucleus. Neutron capture (right) involves the capture of low-energy neutrons (energy < 0.4 eV) by certain nuclei, which turn into a heavier isotope of the same element. After capture, the nucleus is in a highly excited state and the excess energy is released rapidly by the emission of one or more characteristic gamma rays. Because the neutron burst emitted by the PNG is very well defined, the capture spectrum is not contaminated by inelastic gamma rays and an accurate inelastic spectrum can be obtained by subtracting capture background from the spectrum acquired during the neutron burst. The result is two sets of high-quality measurements, which are complementary for some elements.

Closure

- Elemental weight fractions

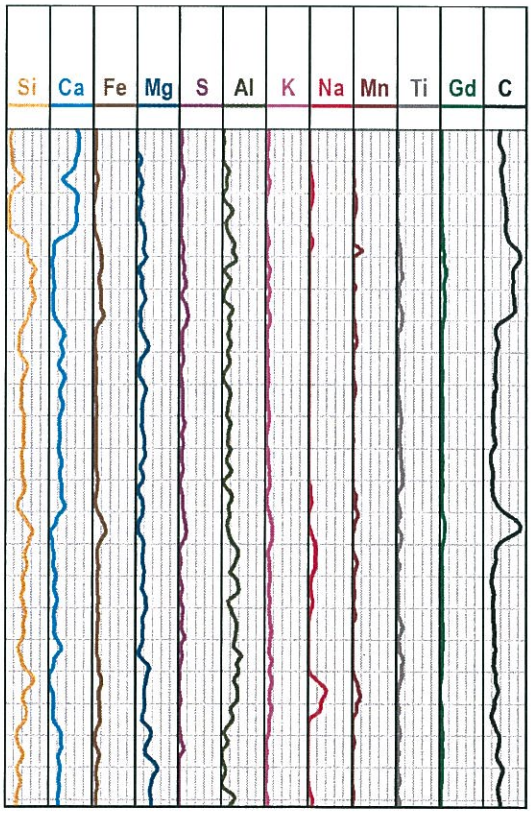

The individual spectral yields are then converted to elemental weight fractions presented as logs.

Interpretation

- Minerals
- Matrix properties
- TOC

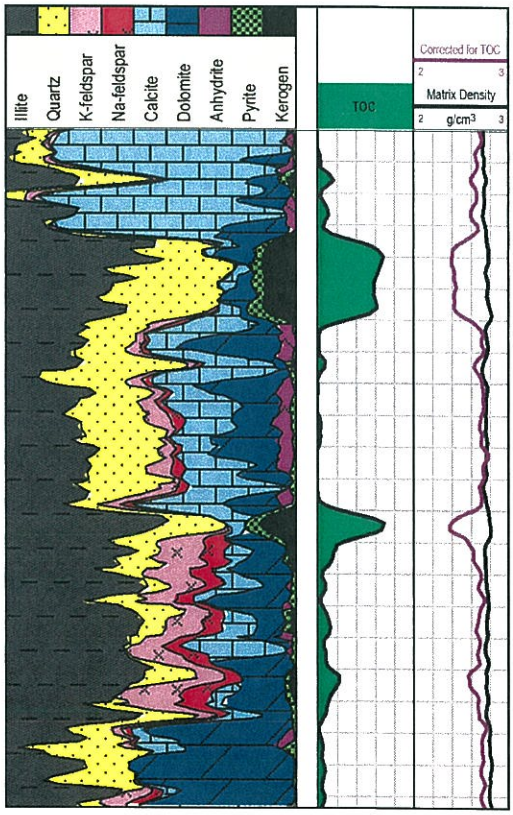

Interpretation of the elementary weight fractions determines mineralogy, matrix properties, and TOC.

The measure of minerals

Gamma ray spectroscopy has long been used in well logging to determine the concentration of elements in the formation surrounding the borehole. As shown in the table to the right, the Litho Scanner tool measures a greatly expanded suite of elements from previous spectroscopy services.

The two independent, high-quality sets of neutron capture and inelastic scattering spectra measured by the Litho Scanner tool contain information about the rock elements present in the formation. Some elements are exclusive of one type of interaction and some are present in both spectra, which provides confirmation of the measurements and helps improve precision.

The inelastic scattering measurement made with the Litho Scanner tool is of particular interest because of its sensitivity to C and Mg. Further insight is provided by the measurement of S.

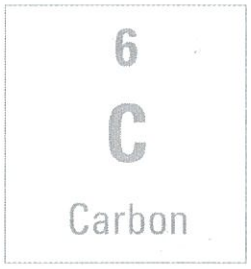

- Magnesium: Comparison of the inelastic and capture yields of Mg for mutual consistency increases the precision and accuracy of the measurement by determining the weighted average of the dry-weight Mg obtained from both spectra.
- In carbonates, Mg can be used to accurately differentiate calcite from dolomite at standard wireline logging speeds. The improved S measurement also supports the quantification of anhydrite from calcite.
- Carbon: From common association factors for carbonate minerals, the amount of inorganic carbon present can be quantified and subtracted from the total inelastic measurement of C to compute TOC and kerogen contents for shale gas plays. The S measurement is also of use in organic-rich shales to determine pyrite content.

Two other elemental measurements of significance are K and Al. The direct measurement of Al is used to quantify clay volume. The Litho Scanner direct measurement of K compares well with spectral gamma ray measurements of K with less sensitivity to KCl mud.

The acquired spectra are deconstructed into the fractions, or yields, of the constituent elemental spectra. The elemental sensitivities are then used to convert the yields to concentrations (weight fractions), which are further analyzed to determine mineralogy, as listed in the table below. Matrix density calculated from the common rock-forming minerals present is combined with the conventional bulk density measurements to accurately derive total porosity. Similarly, elemental concentrations are used to correct the neutron log for rock matrix effects.

Relation of Litho Scanner Elemental Weight Fractions to Mineralogy

Mineral Group	Mineral	Composition	Key Elements	Al	C	Ca	Fe	K	Mg	Mn	Na	S	Si
Quartz	Quartz	SiO_2	Si										0.467
Feldspars	Orthoclase	$KAlSi_3O_8$	Al, Ca, K, Na, Si	0.097				0.141					0.303
	Albite	$NaAlSi_3O_8$		0.103							0.088		0.321
	Anorthite	$CaAl_2Si_2O_8$		0.194		0.144							0.202
Micas	Muscovite	$KAl_2(Si_3Al)O_{10}(OH, F)_2$	Al, K, Si	0.191			0.013	0.078	0.001	0.001	0.005		0.212
	Biotite	$K(Mg, Fe)_3(AlSi_3O_{10})(OH, F)_2$		0.060		0.002	0.136	0.072	0.077	0.003	0.004		0.182
Calcite	Calcite	$CaCO_3$	C, Ca		0.120	0.400							
Dolomite	Dolomite	$CaMg(CO_3)_2$	C, Ca, Mg		0.130	0.217			0.132				
Clays	Kaolinite	$Al_2Si_2O_5(OH)_4$	Al, Fe, K, Si	0.204		0.001	0.008	0.001	0.001		0.001		0.210
	Illite	$(K, H_3O)(Al, Mg, Fe)_2(Si, Al)_4O_{10}[(OH)_2, (H_2O)]$		0.132		0.005	0.048	0.045	0.012		0.004		0.249
	Smectite (wet)	$(Na, Ca)_{0.3}(Al, Mg)_2Si_4O_{10}(OH)_2 \cdot n(H_2O)$		0.070		0.007	0.015	0.006	0.015		0.008		0.205
	Smectite (dry)			0.091		0.013	0.020	0.006	0.020		0.007		0.264
	Chlorite	$(Ca, Na, K)(Mg, Fe, Al)_3(Si, Al)_4O_{20}(OH)_{10} \cdot n(H_2O)$		0.100		0.001	0.230		0.070	0.001			0.114
	Glauconite	$(K, Na)(Fe, Al, Mg)_2(Si, Al)_4O_{10}(OH)_2$		0.044		0.005	0.155	0.059	0.021		0.001		0.231
Fe-bearing minerals	Ankerite	$Ca(Fe, Mg, Mn)(CO_3)_2$	C, Ca, Fe		0.116	0.194	0.162		0.035	0.027			
	Siderite	$FeCO_3$	C, Fe		0.104		0.482						
	Pyrite	FeS_2	Fe, S				0.466					0.535	
	Hematite	Fe_2O_3	Fe				0.699						
Evaporites	Gypsum	$CaSO_4 \cdot 2(H_2O)$	Ca, S			0.233						0.190	
	Anhydrite	$CaSO_4$				0.294						0.240	

12
Mg
Magnesium

20
Ca
Calcium

14
Si
Silicon

Element Symbol	Element Name	Capture	Inelastic
Al	Aluminum	•	•
Ba	Barium	•	•
C	Carbon		•
Ca	Calcium	•	•
Cl	Chlorine	•	
Cu	Copper	•	
Fe	Iron	•	•
Gd	Gadolinium	•	
H	Hydrogen	•	
K	Potassium	•	
Mg	Magnesium	•	•
Mn	Manganese	•	
Na	Sodium	•	
Ni	Nickel	•	
O	Oxygen		•
S	Sulfur	•	•
Si	Silicon	•	•
Ti	Titanium	•	

The Litho Scanner tool measures an expanded suite of elements.

Elemental Weight Fractions from Spectroscopy

Al	C	Ca	Cu	Fe	Gd	K	Mg	Mn	Na	Ni	S	Si	Ti

Litho Scanner Outputs

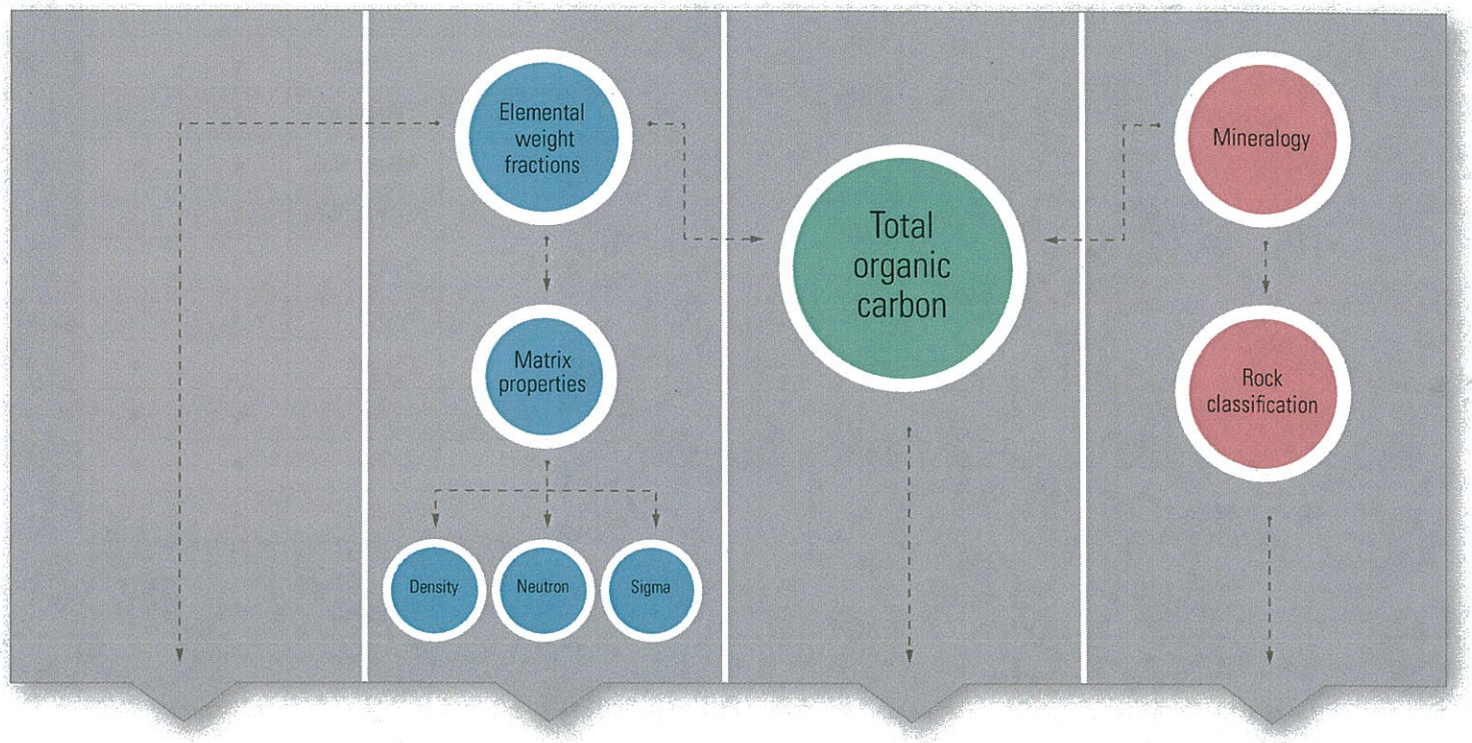

Petrophysical Interpretation

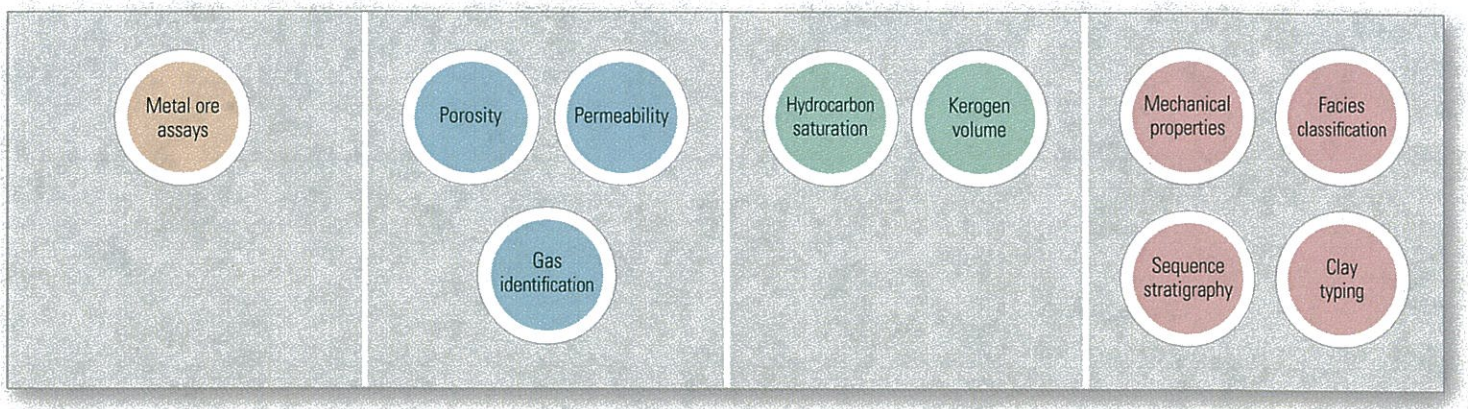

Accurate mineralogy and lithology determined from Litho Scanner spectrography measurements contribute extensively to petrophysical analysis for improved decision making.

Schlumberger Environmental Effects Calibration Facility

The Environmental Effects Calibration Facility (EECF) was constructed in 1985 in southeast Houston as a facility where nuclear tool response measurements could be made over a wide range of test formations and environmental conditions in a controlled, accurate, and efficient approach. It is at this state-of-the-art laboratory that the response of Schlumberger nuclear well logging tools is evaluated.

The facility houses a large number of well-characterized test formations for both neutron and density tools. This enables detailed experimental characterization and detailed benchmarking of modeling results over a wide range of lithologies, porosities, and environmental conditions such as borehole size, standoff, mud type, mud weight, mud salinity, and formation salinity. In addition, a variety of casings are used to characterize cased hole response.

Today, the EECF remains the industry's premier facility for testing and calibration of nuclear tools. From the creation of realistic formation simulations to the design of techniques to assure precise and reliable measurements, EECF capabilities are unmatched.

For Litho Scanner characterization, additional special formations were built to obtain accurate spectral response standards for the expanded set of elements determined by the tool. As for all predecessor tools, the spectral

response has been derived based on measured spectra to guarantee an accurate and unbiased answer. Nuclear modeling alone cannot provide a sufficiently accurate spectral response because of the limitations of the model and the underlying nuclear data. If inaccurate spectral response data are used, the result can be biases in the final response of the tool.

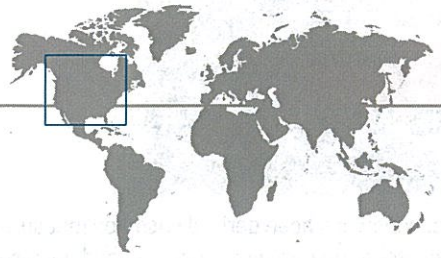

Litho Scanner accurate stand-alone TOC for unconventional formations

Until now TOC has been determined by using a complex model that requires multiple measurements from different logging and laboratory services. The variety of methodologies employed means that interpreters easily come up with different results. This uncontrolled variability in the interpreted results introduces significant ambiguity for one of the most important parameters in defining reservoir quality for unconventional plays.

The stand-alone TOC output is based on direct measurements solely by the Litho Scanner tool of both the carbon elemental concentration and accurate quantification of the carbonate minerals in the formation, which determines the carbon content associated with those minerals. The difference between the two is the TOC, independent of the environment and the reservoir, and presented as a continuous log available at the wellsite.

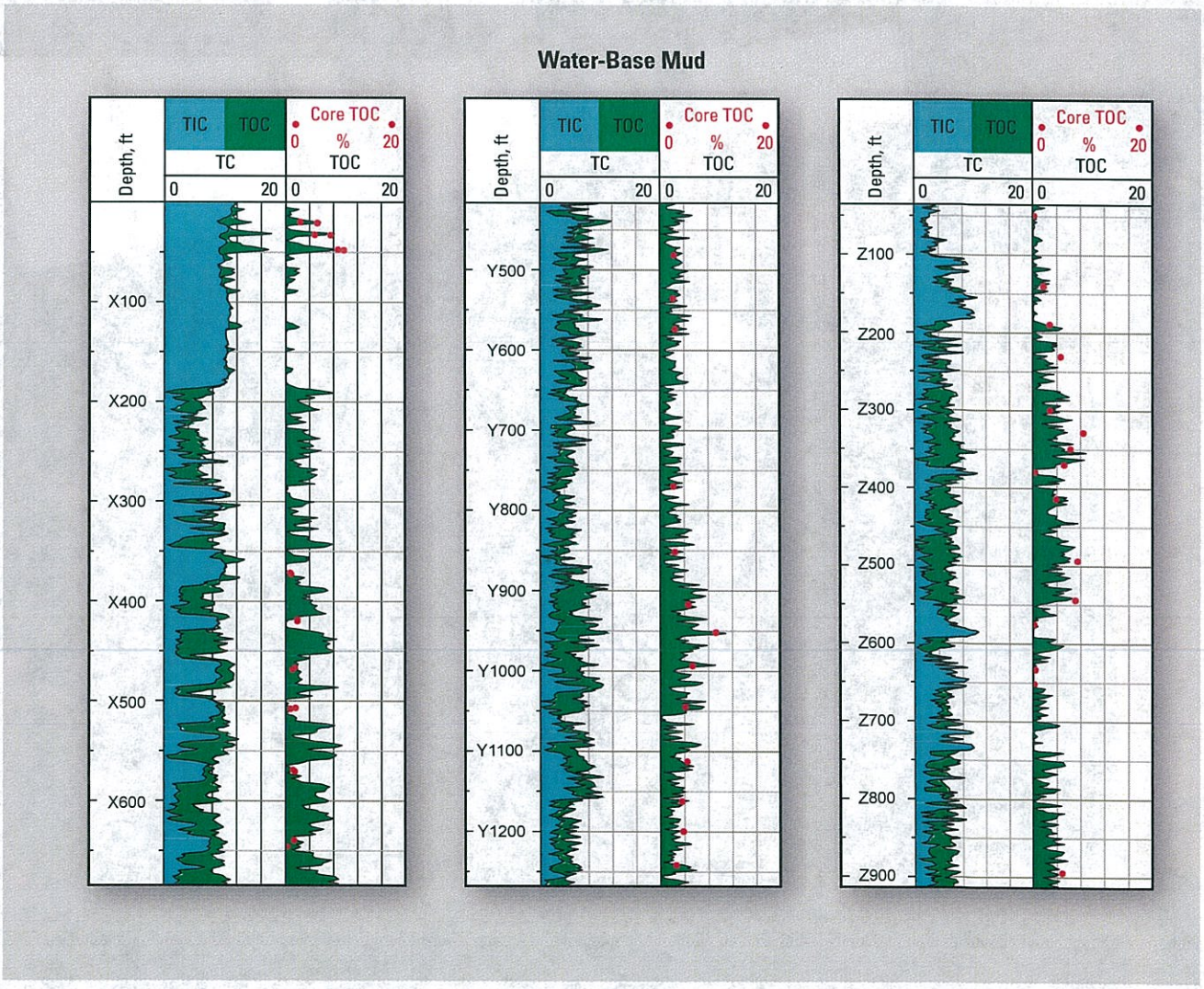

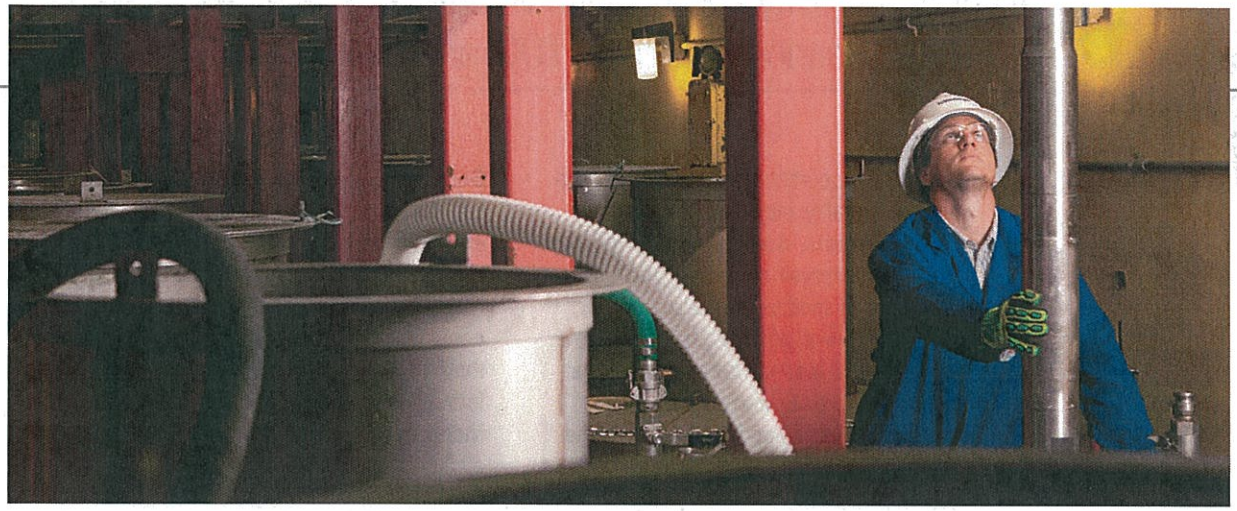

Oil-Base Mud

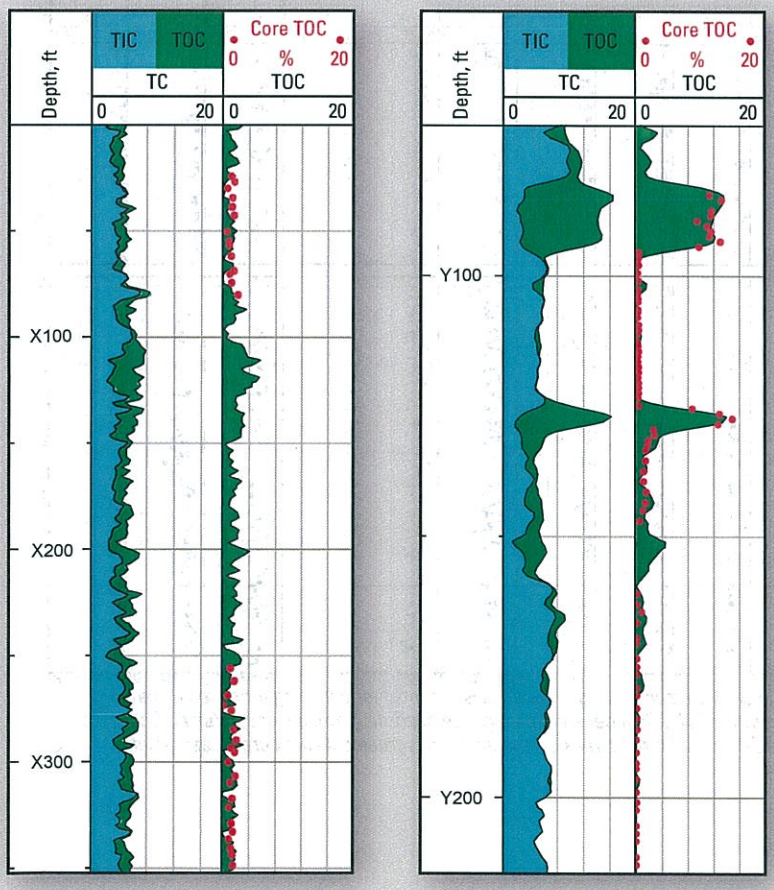

In both water- and oil-base mud, Litho Scanner TOC logs agree well with TOC measured from cores from different basins across North America. For each well, the first track shows the total carbon (TC, black curve) derived from the inelastic measurement and the total inorganic carbon (TIC, shaded blue) computed from carbonate minerals using capture spectroscopy elements. The separation between the two curves is the TOC (shaded green), which is repeated in the second track with core data (red) for validation.

Case Study 2

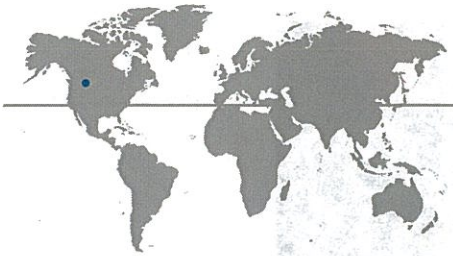

Accurate porosity and kerogen volume for shale gas reservoir from Litho Scanner lithology, TOC, and matrix density

A Canadian operator needed to determine reservoir quality, including porosity and kerogen volume, in a lithologically complex shale gas reservoir comprising multiple clay types in addition to quartz, feldspar, calcite, dolomite, ankerite, and pyrite. But petrophysical models using conventional resistivity, porosity, and acoustic logs are insufficient to accurately quantify the complex formation lithology and kerogen volume, which is a necessary step in accurately determining porosity.

Because correctly identifying the formation mineralogy requires extremely accurate elemental concentrations, the operator ran Litho Scanner service. The Litho Scanner inelastic carbon measurement is used in conjunction with the mineralogy to output the TOC weight fraction independent of the formation porosity, resistivity, and salinity. Matrix density is obtained from Litho Scanner elemental weight fractions and then corrected for TOC. The corrected matrix density in conjunction with the conventional bulk density measurement provides accurate porosity.

As shown in the log, the Litho Scanner elements and minerals are in very close agreement with results from core analysis.

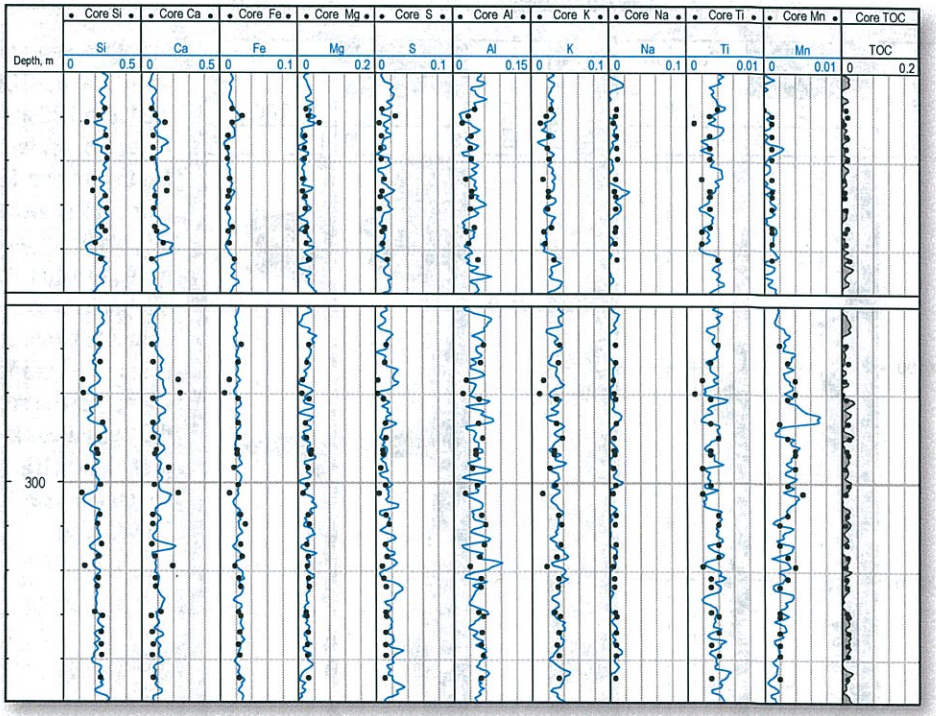

The accurate determination of elemental weight fractions is essential for obtaining formation mineralogy in this shale gas reservoir. The Litho Scanner element logs are confirmed by elements obtained from core analysis. Similarly, the TOC on the far right track shows excellent agreement with core measurements.

Accurate porosity and kerogen volume for shale gas reservoir from Litho Scanner lithology, TOC, and matrix density

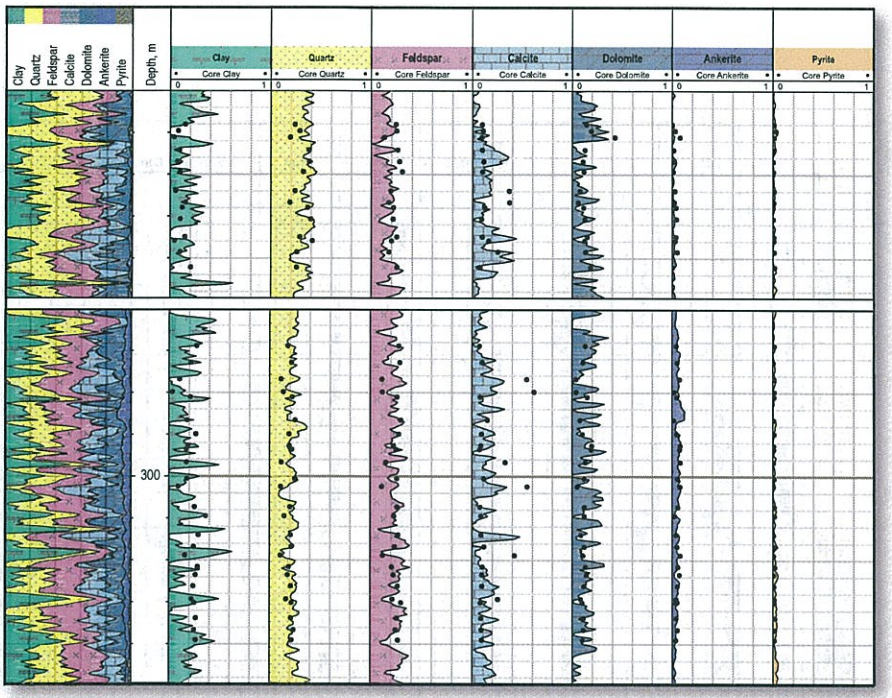

Mineralogy determined from Litho Scanner elemental weight fractions is confirmed by core mineralogy.

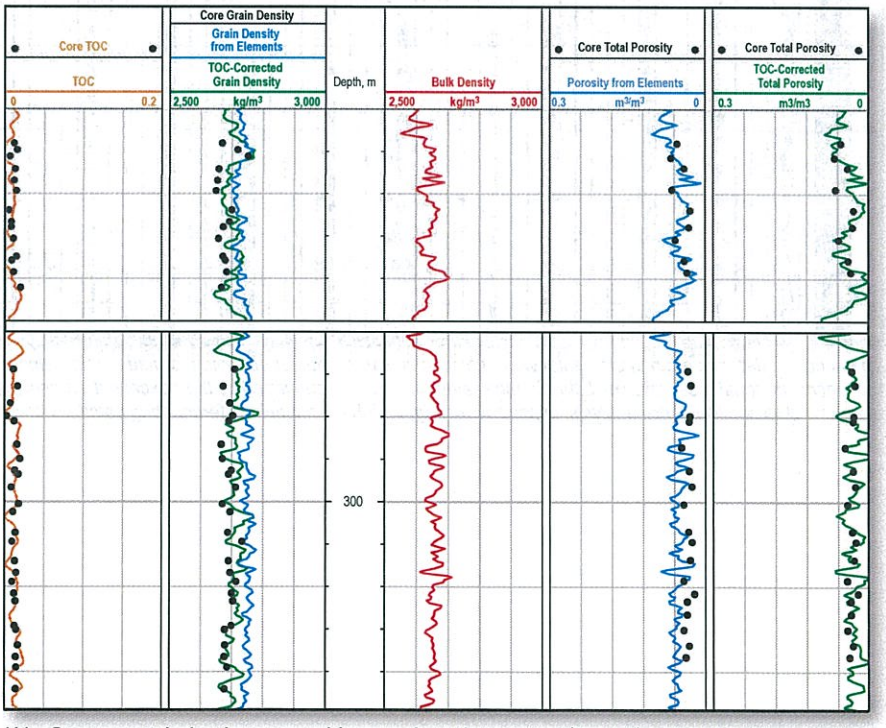

Litho Scanner matrix density corrected for organic carbon content (Track 2) and the resulting porosity (Track 5) are in much better agreement with core measurements than the uncorrected density (Track 2) and porosity (Track 4).

The Litho Scanner elemental weight fractions are used in the Techlog Quanti ELAN module to solve for formation lithology that includes shale, quartz, feldspars, calcite, dolomite, ankerite, and pyrite. As shown in the top log, there is very good agreement between the computed mineralogy and the mineralogy from core measurements.

An accurate matrix density is required to compute the correct porosity from a bulk density measurement. However, the grain density determined from the elements does not account for kerogen in the rock, which makes it heavier than the grain density obtained from core, as shown in Track 2 of the bottom log. The TOC (Track 1) was used to correct the grain density computed from the elements to provide significantly better agreement with the core-measured grain density (Track 2). The corrected grain density is based entirely on the Litho Scanner measurements, so it is obtained as a stand-alone, single-tool output.

Total porosity calculated using bulk density and the matrix density corrected for organic carbon shows much better agreement with the core porosity measurements (Track 5) compared with the uncorrected porosity in Track 4.

Case Study 3

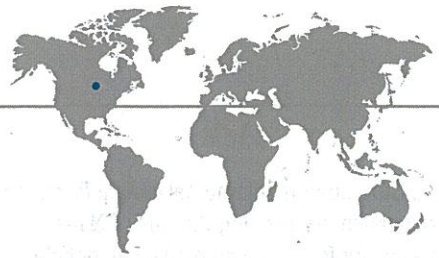

Accurate total porosity for Bakken and Three Forks formations from Litho Scanner mineralogy and TOC

Petrophysical evaluation of porosity and saturation in low-porosity and very low-permeability dolomitic limestones requires an accurate evaluation of matrix density, which is a function of formation mineralogy. The unprecedented accuracy of Litho Scanner elemental concentrations, particularly Mg, enables accurately evaluating mineralogy and matrix density even in complex reservoirs such as the Bakken and Three Forks.

Quantification of TOC is another key objective in the assessment of unconventional reservoirs. Litho Scanner service provides a direct measurement of formation carbon coupled with an assessment of inorganic carbon from mineralogy. The result is a robust, accurate TOC measurement that does not require core calibration, previous knowledge of the kerogen type or maturity, or optimization of empirical algorithms that rely on conventional core analysis.

The resulting mineralogy and matrix density corrected for organic content make it possible to correctly determine the porosity.

As shown on the logs for elements and mineralogy, the accuracy of the Litho Scanner element and mineral determinations is confirmed by their close agreement with core analysis results. A similar confirming relationship exists for matrix density corrected for organic content by using the Litho Scanner TOC output.

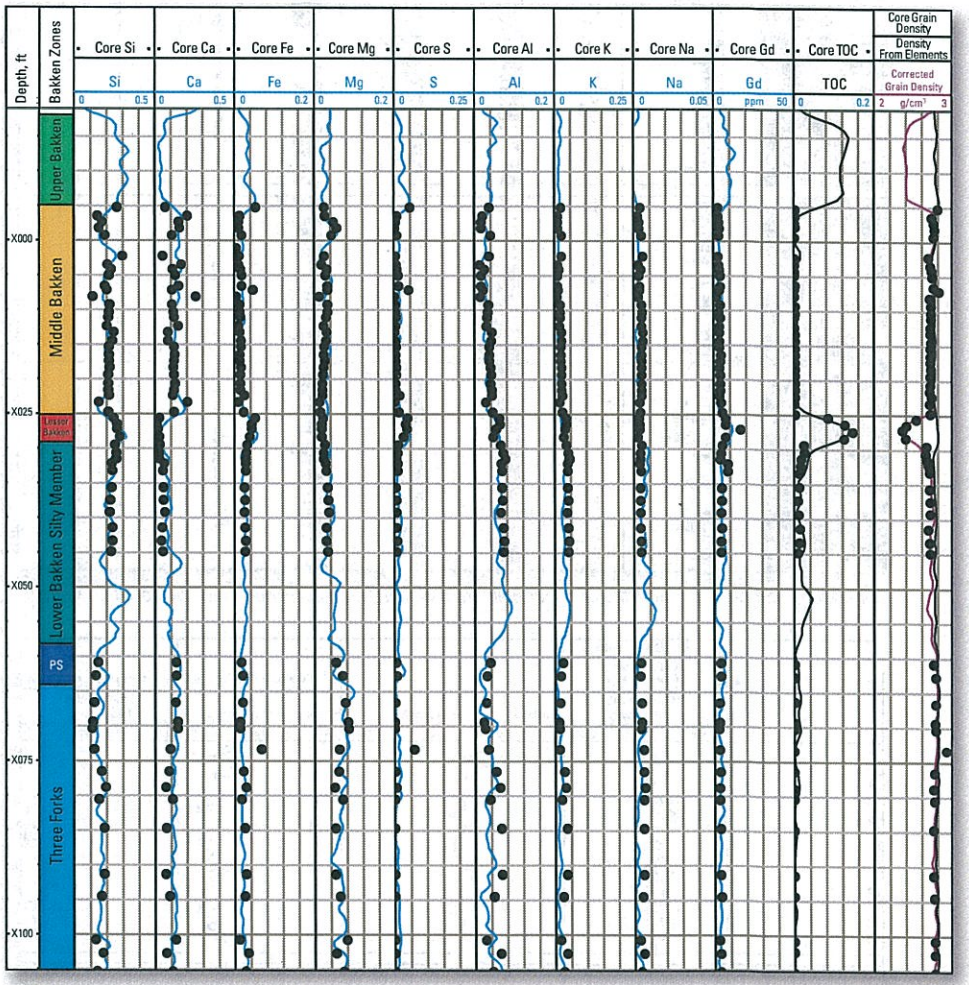

The accurate determination of elemental weight fractions is essential for obtaining formation mineralogy in this unconventional reservoir. The Litho Scanner element logs are confirmed by their excellent agreement with elements obtained from core analysis, especially for Mg, which is critical in differentiating calcite from dolomite.

Accurate total porosity for Bakken and Three Forks formations from Litho Scanner mineralogy and TOC

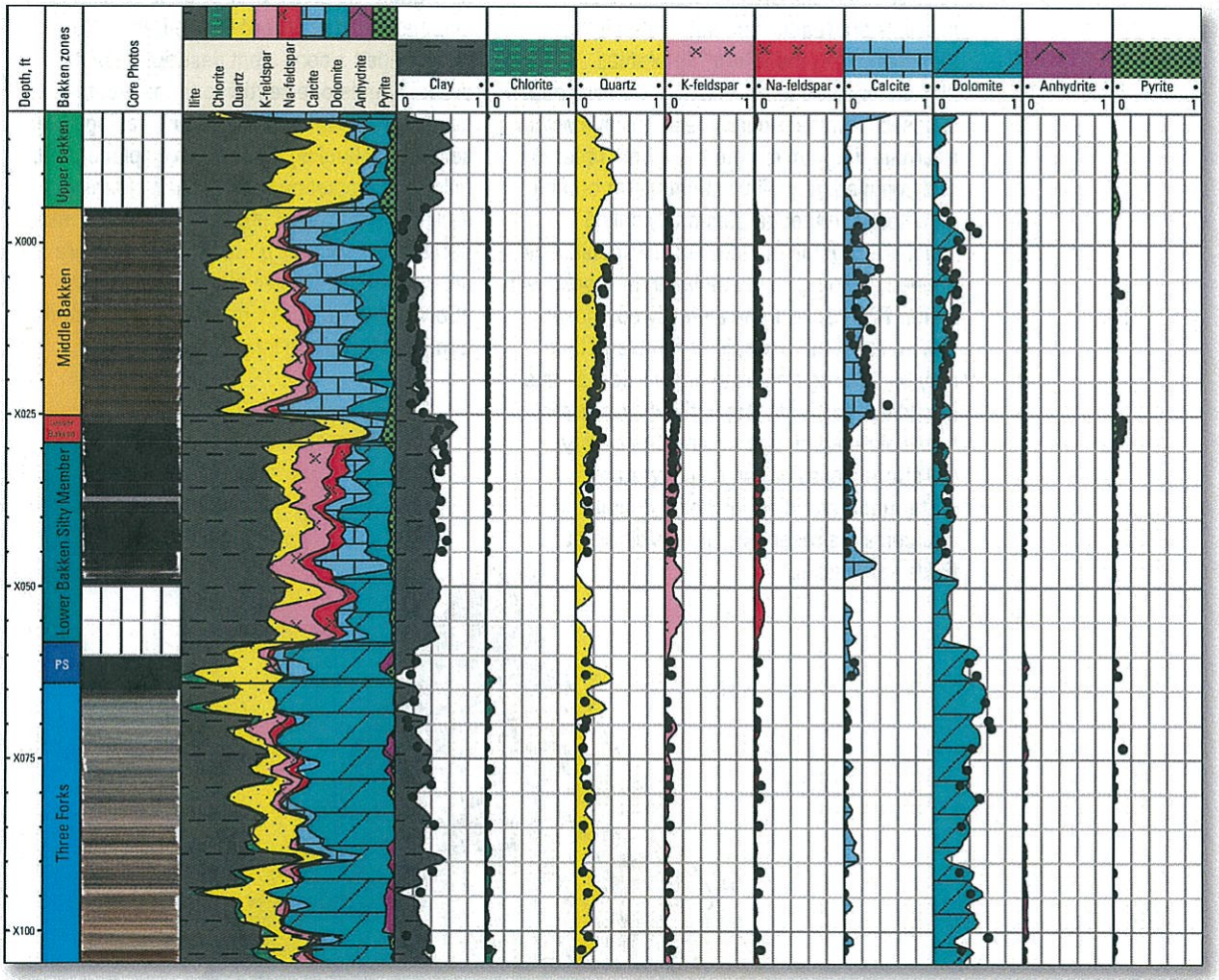

Mineralogy determined from Litho Scanner elemental weight fractions is confirmed by core mineralogy. The core photograph shows the highly laminated nature of the Three Forks formation, which can cause occasional scatter when comparing log data with standard core plug data.

Case Study 4

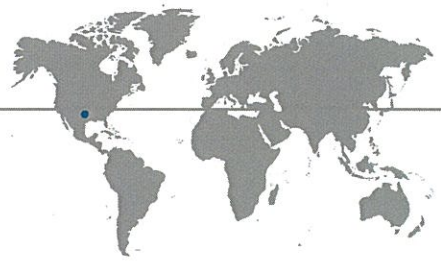

Accurate classification of organic mudstones based on Litho Scanner mineralogy

Key to successfully completing organic mudstone reservoirs for gas and liquids production is targeting intervals with superior reservoir and completion quality. These intervals are readily and automatically identified using the sCore* lithofacies classification scheme. The sCore classification is based on mineralogical relationships within a ternary diagram to determine both reservoir and completion quality indicators for organic mudstones. Although commonly called "shales," organic mudstones are specifically defined as fine-grained sedimentary rocks with a high TOC content and typically composed of a complex mineralogic assemblage that may be heterogeneous at fine vertical scales. In addition to identifying optimal intervals in terms of reservoir and completion quality, the sCore classification helps operators better understand depositional conditions and correlate reservoirs across different fields and basins.

The sCore log display is generated with minimal processing and no interpretation input required. Descriptive parameters such as organic carbon, pyrite, and the presence of expandable clays are flagged. The sCore log provides a consistent description of the organic mudstone section and the inputs necessary for effective decision making when selecting a landing points for well placement, tailoring completion designs, and planning a drilling development project. Quality indicator parameters such as porosity, TOC, fracture density, and stress are also overlaid on the sCore ternary diagram to relate the parameter quality to the sCore lithofacies types.

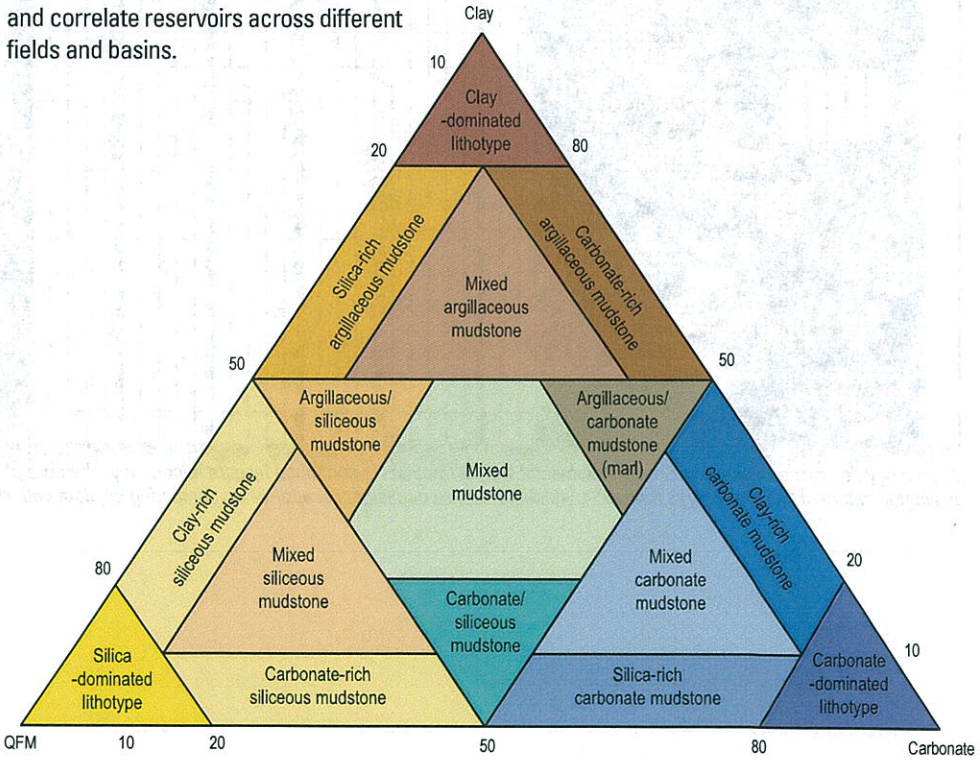

The sCore classification proposed for organic mudstones is defined by a ternary diagram, with the three apexes representing the dry-weight components clay, carbonate, and quartz, feldspar, and mica (QFM). The term "dominated" is used for a mudstone containing more than 80% of a particular component. When the primary component is 50% to 80% of the composition, the mudstone is described as siliceous (50% < dry-weight QFM < 80%), argillaceous (50% < dry-weight clay < 80%), or carbonate (50% < dry-weight carbonate < 80%). The term "rich" indicates a secondary component representing 20% to 50% of the total composition.

Accurate classification of organic mudstones based on Litho Scanner mineralogy

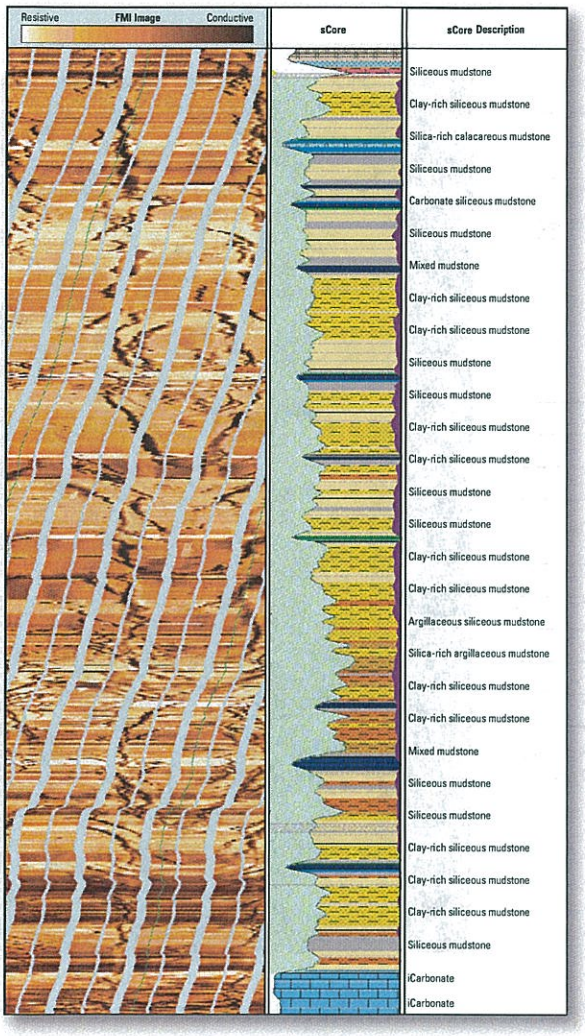

In this sCore log display for a 200-ft section of a vertical Barnett shale well, the FMI fullbore formation microimage in Track 1 reveals numerous drilling-induced features. The green area in Track 2 represents the organic mudstone interval to which the sCore classification was applied. The sCore lithofacies display in Track 2 was created with Litho Scanner inputs. The TOC flag, shown in purple along the right boundary of Track 2, represents TOC > 2%. The gray crosshatching pattern indicates zones affected by borehole rugosity. The left boundary of the lithofacies display represents the mineral-based brittleness index (MBI). Track 3 lists the sCore lithofacies in text format.*

In this Barnett shale well, Litho Scanner logging provided accurate inputs for bulk mineralogy and TOC that were combined with additional inputs from basic triple-combo logs to generate the sCore classification display. Using Litho Scanner mineralogy outputs saves significant time because they are quickly processed and available soon after logging. Laboratory XRD analysis requires collecting core samples for delivery to the laboratory for analysis. Reservoir quality and completion quality parameters are combined with the sCore ternary diagram, as shown below, for determining targets for both vertical and horizontal completions.

Reservoir Quality Indicator

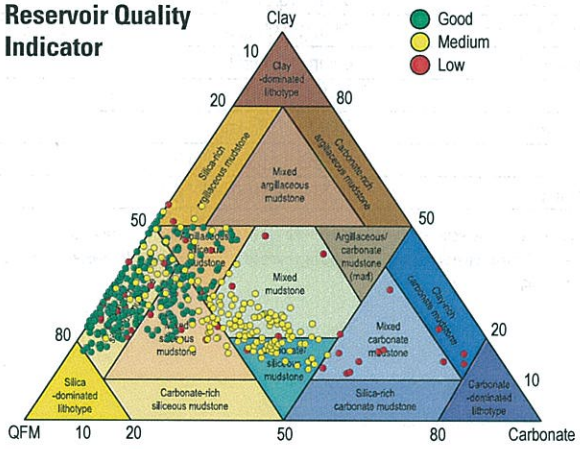

Completion Quality Indicator

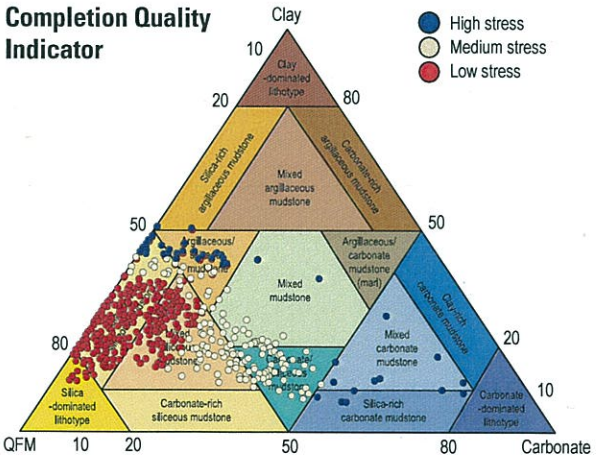

Gas-filled porosity (top) and in situ stress (bottom) measurements plotted on the sCore ternary diagram provide better understanding of reservoir quality and completion quality distribution within an organic mudstone interval.

Specifications	
	Litho Scanner Tool
Measurement	
Output	Elemental yields, elemental weight fractions, TOC, dry-weight mineral concentrations, matrix properties
Logging speed†	Max.: 3,600 ft/h [1,097 m/h]
Range of measurement	1 to 10 MeV
Vertical resolution	18 in [45.72 cm]
Mud type or weight limitations	None
Mechanical	
Temperature rating	350 degF [177 degC]
Pressure rating	20,000 psi [138 MPa]
Borehole size—min.	5.5 in [13.97 cm]
Borehole size—max.††	24 in [60.96 cm]
Outside diameter	4.5 in [11.4 cm]
Length	14 ft [4.27 m]
Weight (in air)	366 lbm [166 kg]
Tension	55,000 lbf [244,652 N]
Compression	22,500 lbf [100,085 N]

† A tool planner is used to estimate the precision of the elemental concentrations and interpreted properties such as matrix density for a given environment, with the recommended logging speed depending on the required precision.
†† With bow spring

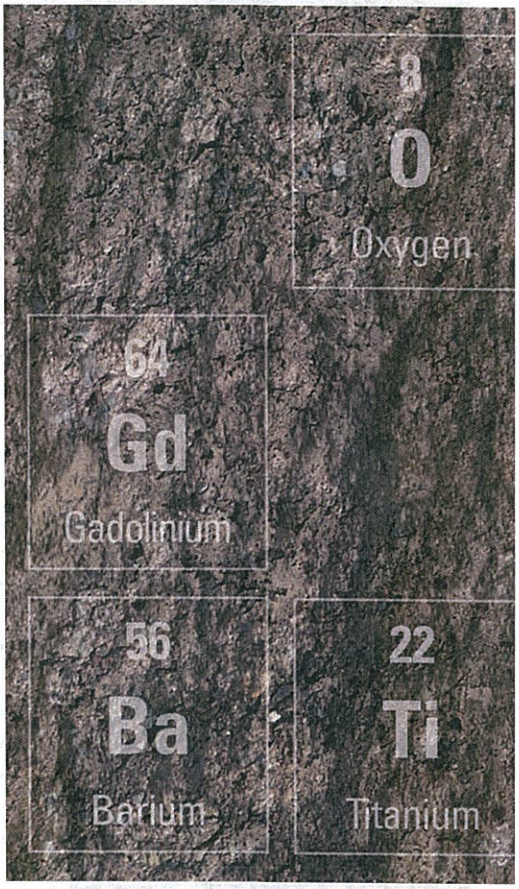

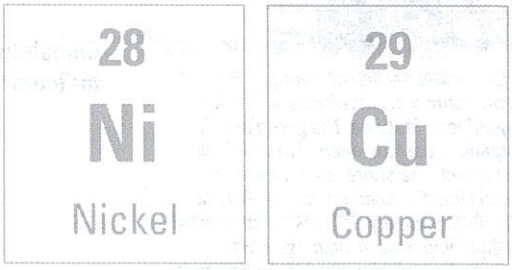

www.slb.com/ls

Schlumberger

Depth	Time	TCPU	EHT	COUNT	GR
ft	sec	'C	Volts		CPS
945.03	-999	23.3909	-999	-999	-999
945.19	0.664	23.3909	-923.914	61	91.8675
945.35	0.667	23.3909	-923.914	66	98.9505
945.52	0.666	23.3909	-919.999	63	94.5946
945.68	0.663	23.1737	-919.999	67	101.056
945.85	0.665	23.1737	-923.914	60	90.2256
946.01	0.673	23.3909	-916.084	65	96.5825
946.17	0.68	23.3909	-923.914	62	91.1765
946.34	0.68	23.3909	-919.999	59	86.7647
946.5	0.673	23.3909	-923.914	60	89.153
946.67	0.673	23.3909	-919.999	55	81.7236
946.83	0.674	23.3909	-919.999	61	90.5044
946.99	0.677	23.3909	-923.914	65	96.0118
947.16	0.675	23.3909	-923.914	56	82.963
947.32	0.671	23.3909	-916.084	52	77.4963
947.49	0.67	23.1737	-923.914	69	102.985
947.65	0.672	23.3909	-919.999	62	92.2619
947.81	0.681	23.3909	-923.914	52	76.3583
947.98	0.676	23.3909	-919.999	68	100.592
948.14	0.677	23.3909	-923.914	51	75.3324
948.31	0.676	23.3909	-916.084	60	88.7574
948.47	0.678	23.1737	-916.084	66	97.3451
948.63	0.681	23.3909	-916.084	59	86.6373
948.8	0.671	23.1737	-919.999	47	70.0447
948.96	0.668	23.3909	-916.084	52	77.8443
949.13	0.662	23.3909	-927.829	55	83.0816
949.29	0.665	23.1737	-916.084	58	87.218
949.45	0.666	23.3909	-919.999	52	78.0781
949.62	0.666	23.3909	-919.999	50	75.0751
949.78	0.667	23.3909	-919.999	53	79.4603
949.95	0.665	23.3909	-923.914	56	84.2105
950.11	0.669	23.3909	-923.914	46	68.7593
950.27	0.677	23.3909	-919.999	63	93.0576
950.44	0.677	23.3909	-916.084	54	79.7637
950.6	0.676	23.1737	-923.914	55	81.3609
950.77	0.673	23.3909	-916.084	52	77.266
950.93	0.672	23.3909	-923.914	61	90.7738

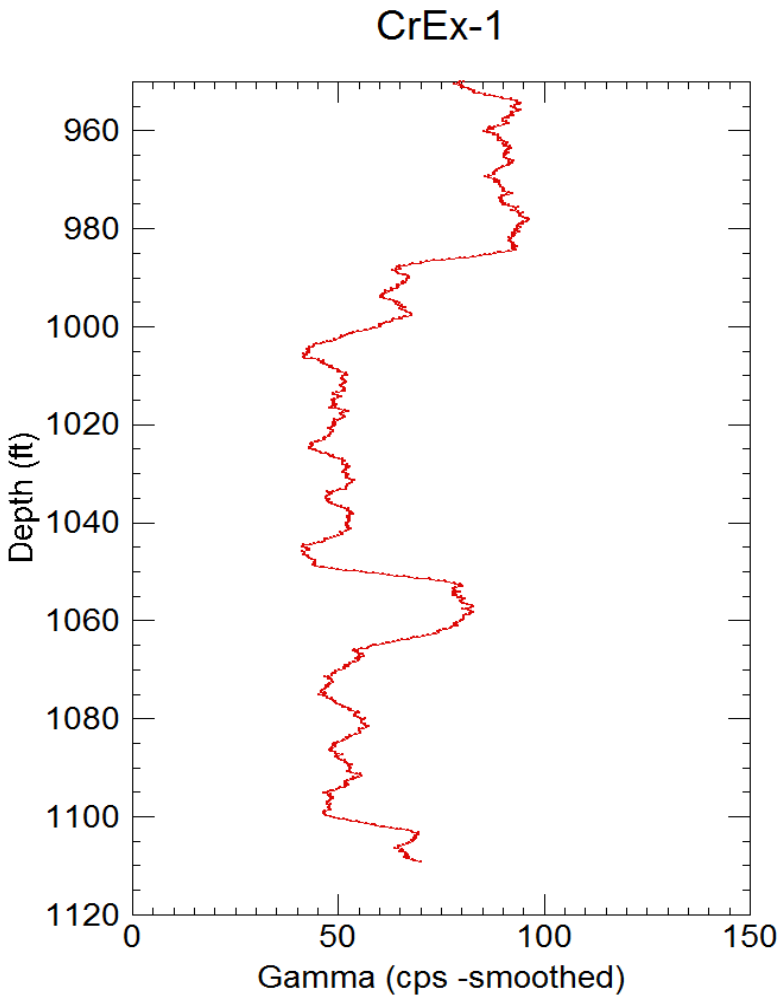

951.09	0.676	23.3909	-919.999	50	73.9645
951.26	0.677	23.1737	-919.999	55	81.2408
951.42	0.673	23.3909	-919.999	45	66.8648
951.59	0.675	23.3909	-919.999	46	68.1481
951.75	0.677	23.1737	-923.914	49	72.3781
951.91	0.683	23.3909	-916.084	62	90.776
952.08	0.679	23.3909	-916.084	42	61.8557
952.24	0.676	23.1737	-919.999	70	103.55
952.41	0.672	23.3909	-923.914	56	83.3333
952.57	0.678	23.3909	-919.999	58	85.5457
952.73	0.681	23.3909	-923.914	57	83.7004
952.9	0.679	23.3909	-919.999	59	86.8925
953.06	0.672	23.3909	-919.999	68	101.19
953.23	0.667	23.3909	-916.084	60	89.955
953.39	0.665	23.3909	-919.999	52	78.1955
953.55	0.668	23.3909	-923.914	63	94.3114
953.72	0.667	23.3909	-919.999	58	86.9565
953.88	0.664	23.3909	-919.999	59	88.8554
954.05	0.658	23.3909	-919.999	69	104.863
954.21	0.668	23.3909	-923.914	72	107.784
954.37	0.672	23.3909	-927.829	61	90.7738
954.54	0.672	23.3909	-923.914	65	96.7262
954.7	0.674	23.3909	-919.999	72	106.825
954.87	0.676	23.3909	-919.999	67	99.1124
955.03	0.68	23.1737	-919.999	54	79.4118
955.19	0.68	23.3909	-919.999	75	110.294
955.36	0.675	23.3909	-916.084	64	94.8148
955.52	0.671	23.3909	-916.084	61	90.9091
955.69	0.672	23.6081	-923.914	64	95.2381
955.85	0.676	23.1737	-919.999	63	93.1953
956.01	0.677	23.3909	-923.914	68	100.443
956.18	0.678	23.6081	-919.999	52	76.6962
956.34	0.676	23.3909	-916.084	53	78.4024
956.51	0.675	23.3909	-916.084	61	90.3704
956.67	0.681	23.1737	-923.914	47	69.0162
956.83	0.683	23.1737	-919.999	67	98.0966
957	0.682	23.1737	-919.999	59	86.5103
957.16	0.679	23.1737	-919.999	69	101.62
957.33	0.673	23.3909	-923.914	70	104.012
957.49	0.672	23.1737	-916.084	76	113.095
957.65	0.668	23.3909	-923.914	58	86.8263

957.82	0.663	23.6081	-923.914	42	63.3484
957.98	0.661	23.3909	-923.914	66	99.8487
958.15	0.664	23.3909	-923.914	67	100.904
958.31	0.669	23.1737	-923.914	72	107.623
958.47	0.67	23.1737	-919.999	57	85.0746
958.64	0.672	23.3909	-923.914	60	89.2857
958.8	0.672	23.3909	-916.084	55	81.8452
958.97	0.677	23.3909	-919.999	66	97.4889
959.13	0.673	23.3909	-919.999	55	81.7236
959.29	0.678	23.1737	-923.914	53	78.1711
959.46	0.677	23.1737	-919.999	69	101.92
959.62	0.671	23.3909	-916.084	51	76.006
959.79	0.672	23.3909	-923.914	65	96.7262
959.95	0.677	23.3909	-919.999	62	91.5805
960.11	0.68	23.1737	-919.999	55	80.8824
960.28	0.68	23.1737	-916.084	57	83.8235
960.44	0.679	23.3909	-916.084	51	75.1105
960.61	0.678	23.3909	-923.914	50	73.7463
960.77	0.678	23.1737	-923.914	57	84.0708
960.93	0.68	23.3909	-919.999	61	89.7059
961.1	0.677	23.1737	-923.914	52	76.8095
961.26	0.677	23.3909	-923.914	61	90.1034
961.43	0.68	23.3909	-923.914	52	76.4706
961.59	0.68	23.3909	-919.999	64	94.1176
961.75	0.673	23.3909	-919.999	61	90.6389
961.92	0.666	23.3909	-923.914	67	100.601
962.08	0.663	23.1737	-923.914	67	101.056
962.25	0.665	23.3909	-923.914	71	106.767
962.41	0.668	23.3909	-919.999	63	94.3114
962.57	0.666	23.3909	-919.999	70	105.105
962.74	0.669	23.3909	-919.999	53	79.2227
962.9	0.665	23.1737	-927.829	67	100.752
963.07	0.67	23.3909	-923.914	60	89.5522
963.23	0.68	23.3909	-923.914	55	80.8824
963.39	0.677	23.1737	-916.084	63	93.0576
963.56	0.675	23.1737	-919.999	55	81.4815
963.72	0.673	23.1737	-919.999	68	101.04
963.89	0.676	23.3909	-923.914	59	87.2781
964.05	0.678	23.3909	-919.999	63	92.9204
964.21	0.67	23.3909	-927.829	54	80.597
964.38	0.671	23.1737	-923.914	45	67.0641

964.54	0.673	23.3909	-919.999	66	98.0684
964.71	0.677	23.3909	-923.914	53	78.2866
964.87	0.681	23.3909	-919.999	69	101.322
965.03	0.679	23.3909	-919.999	63	92.7835
965.2	0.68	23.3909	-919.999	66	97.0588
965.36	0.677	23.3909	-923.914	70	103.397
965.53	0.679	23.3909	-923.914	59	86.8925
965.69	0.683	23.3909	-919.999	68	99.5608
965.85	0.678	23.3909	-919.999	64	94.3953
966.02	0.669	23.3909	-919.999	65	97.1599
966.18	0.662	23.3909	-923.914	63	95.1662
966.35	0.665	23.3909	-923.914	60	90.2256
966.51	0.669	23.3909	-923.914	54	80.7175
966.67	0.67	23.3909	-923.914	58	86.5672
966.84	0.666	23.3909	-923.914	56	84.0841
967	0.667	23.3909	-919.999	56	83.958
967.17	0.671	23.3909	-923.914	66	98.3607
967.33	0.68	23.3909	-919.999	69	101.471
967.49	0.679	23.3909	-923.914	71	104.566
967.66	0.675	23.3909	-919.999	57	84.4444
967.82	0.676	23.1737	-919.999	60	88.7574
967.99	0.675	23.3909	-923.914	47	69.6296
968.15	0.678	23.3909	-923.914	63	92.9204
968.31	0.676	23.3909	-919.999	71	105.03
968.48	0.669	23.3909	-923.914	52	77.728
968.64	0.671	23.1737	-919.999	64	95.38
968.81	0.68	23.3909	-919.999	65	95.5882
968.97	0.681	23.1737	-919.999	44	64.6109
969.13	0.682	23.3909	-923.914	62	90.9091
969.3	0.674	23.3909	-923.914	58	86.0534
969.46	0.673	23.1737	-919.999	64	95.0966
969.63	0.681	23.3909	-927.829	57	83.7004
969.79	0.682	23.3909	-919.999	62	90.9091
969.95	0.681	23.3909	-908.254	52	76.3583
970.12	0.674	23.3909	-923.914	51	75.6677
970.28	0.671	23.3909	-919.999	53	78.9866
970.45	0.67	23.3909	-919.999	63	94.0299
970.61	0.67	23.6081	-919.999	65	97.0149
970.77	0.668	23.3909	-919.999	48	71.8563
970.94	0.665	23.3909	-919.999	58	87.218
971.1	0.665	23.3909	-919.999	66	99.2481

971.27	0.669	23.3909	-923.914	60	89.6861
971.43	0.673	23.1737	-919.999	68	101.04
971.59	0.677	23.3909	-919.999	62	91.5805
971.76	0.676	23.6081	-919.999	79	116.864
971.92	0.677	23.3909	-923.914	61	90.1034
972.09	0.679	23.3909	-923.914	58	85.4197
972.25	0.68	23.3909	-919.999	55	80.8824
972.41	0.679	23.3909	-919.999	63	92.7835
972.58	0.674	23.3909	-919.999	60	89.0208
972.74	0.672	23.3909	-919.999	57	84.8214
972.91	0.677	23.3909	-916.084	67	98.966
973.07	0.676	23.3909	-919.999	60	88.7574
973.23	0.675	23.6081	-919.999	69	102.222
973.4	0.677	23.3909	-919.999	51	75.3324
973.56	0.675	23.1737	-919.999	56	82.963
973.73	0.683	23.3909	-919.999	54	79.063
973.89	0.682	23.6081	-923.914	58	85.044
974.05	0.681	23.3909	-919.999	67	98.3847
974.22	0.678	23.3909	-919.999	68	100.295
974.38	0.673	23.3909	-923.914	67	99.5542
974.55	0.666	23.3909	-923.914	71	106.607
974.71	0.669	23.3909	-919.999	41	61.2855
974.87	0.669	23.3909	-919.999	59	88.1913
975.04	0.663	23.3909	-916.084	52	78.4314
975.2	0.664	23.3909	-919.999	78	117.47
975.37	0.67	23.1737	-919.999	52	77.6119
975.53	0.674	23.3909	-919.999	61	90.5044
975.69	0.673	23.3909	-923.914	60	89.153
975.86	0.674	23.1737	-916.084	59	87.5371
976.02	0.676	23.3909	-923.914	58	85.7988
976.19	0.678	23.1737	-919.999	65	95.8702
976.35	0.677	23.3909	-916.084	64	94.5347
976.51	0.671	23.3909	-927.829	70	104.322
976.68	0.673	23.6081	-919.999	61	90.6389
976.84	0.678	23.1737	-919.999	71	104.72
977.01	0.678	23.3909	-919.999	60	88.4956
977.17	0.68	23.3909	-927.829	67	98.5294
977.33	0.675	23.3909	-919.999	76	112.593
977.5	0.675	23.3909	-919.999	57	84.4444
977.66	0.679	23.3909	-916.084	70	103.093
977.83	0.685	23.3909	-916.084	56	81.7518

977.99	0.68	23.3909	-923.914	67	98.5294
978.15	0.677	23.1737	-923.914	65	96.0118
978.32	0.674	23.3909	-923.914	62	91.9881
978.48	0.679	23.3909	-919.999	68	100.147
978.65	0.679	23.1737	-923.914	66	97.2018
978.81	0.671	23.3909	-919.999	53	78.9866
978.97	0.666	23.1737	-923.914	62	93.0931
979.14	0.666	23.3909	-916.084	61	91.5916
979.3	0.667	23.3909	-923.914	67	100.45
979.47	0.669	23.1737	-923.914	73	109.118
979.63	0.664	23.1737	-919.999	57	85.8434
979.79	0.668	23.1737	-923.914	74	110.778
979.96	0.671	23.3909	-919.999	65	96.8703
980.12	0.676	23.1737	-919.999	59	87.2781
980.29	0.68	23.3909	-923.914	58	85.2941
980.45	0.682	23.3909	-927.829	58	85.044
980.61	0.679	23.3909	-923.914	70	103.093
980.78	0.675	23.3909	-919.999	63	93.3333
980.94	0.678	23.3909	-923.914	55	81.1209
981.11	0.679	23.3909	-912.169	65	95.729
981.27	0.677	23.3909	-919.999	67	98.966
981.43	0.673	23.3909	-919.999	67	99.5542
981.6	0.672	23.3909	-923.914	54	80.3571
981.76	0.678	23.3909	-919.999	60	88.4956
981.93	0.685	23.3909	-923.914	63	91.9708
982.09	0.684	23.6081	-923.914	65	95.0292
982.25	0.678	23.3909	-923.914	68	100.295
982.42	0.679	23.3909	-923.914	50	73.6377
982.58	0.684	23.1737	-923.914	54	78.9474
982.75	0.685	23.3909	-919.999	72	105.109
982.91	0.677	23.3909	-919.999	68	100.443
983.07	0.67	23.3909	-919.999	67	100
983.24	0.665	23.3909	-923.914	69	103.759
983.4	0.666	23.3909	-923.914	49	73.5736
983.57	0.67	23.1737	-919.999	67	100
983.73	0.667	23.3909	-923.914	55	82.4588
983.89	0.666	23.3909	-923.914	55	82.5826
984.06	0.667	23.3909	-923.914	64	95.952
984.22	0.674	23.3909	-923.914	63	93.4718
984.39	0.681	23.1737	-923.914	64	93.9794
984.55	0.681	23.3909	-916.084	70	102.79

984.71	0.672	23.3909	-923.914	69	102.679
984.88	0.674	23.3909	-919.999	64	94.9555
985.04	0.677	23.6081	-919.999	62	91.5805
985.21	0.679	23.3909	-919.999	53	78.056
985.37	0.676	23.3909	-919.999	76	112.426
985.53	0.675	23.3909	-923.914	56	82.963
985.7	0.678	23.3909	-919.999	59	87.0207
985.86	0.68	23.6081	-919.999	60	88.2353
986.03	0.683	23.3909	-919.999	57	83.4553
986.19	0.681	23.3909	-923.914	48	70.4846
986.35	0.677	23.3909	-916.084	38	56.13
986.52	0.679	23.3909	-916.084	60	88.3652
986.68	0.681	23.1737	-919.999	61	89.5742
986.85	0.684	23.3909	-919.999	32	46.7836
987.01	0.684	23.3909	-923.914	52	76.0234
987.17	0.683	23.3909	-923.914	40	58.5652
987.34	0.693	23.3909	-919.999	31	44.733
987.5	0.691	23.3909	-923.914	39	56.4399
987.67	0.691	23.3909	-916.084	45	65.123
987.83	0.688	23.3909	-919.999	27	39.2442
987.99	0.683	23.3909	-923.914	45	65.8858
988.16	0.682	23.1737	-919.999	42	61.5836
988.32	0.692	23.3909	-927.829	43	62.1387
988.49	0.694	23.3909	-927.829	42	60.5187
988.65	0.694	23.3909	-923.914	53	76.3689
988.81	0.695	23.3909	-923.914	49	70.5036
988.98	0.698	23.3909	-923.914	51	73.0659
989.14	0.697	23.3909	-923.914	40	57.3888
989.31	0.698	23.3909	-927.829	44	63.0373
989.47	0.693	23.1737	-923.914	47	67.8211
989.63	0.692	23.1737	-923.914	59	85.2601
989.8	0.691	23.3909	-923.914	43	62.2287
989.96	0.697	23.3909	-919.999	45	64.5624
990.13	0.695	23.3909	-919.999	49	70.5036
990.29	0.695	23.1737	-927.829	43	61.8705
990.45	0.693	23.3909	-919.999	56	80.8081
990.62	0.702	23.3909	-919.999	43	61.2536
990.78	0.703	23.3909	-923.914	37	52.6316
990.95	0.701	23.3909	-919.999	63	89.8716
991.11	0.697	23.3909	-923.914	39	55.9541
991.27	0.696	23.3909	-916.084	43	61.7816

991.44	0.692	23.3909	-923.914	49	70.8092
991.6	0.684	23.3909	-919.999	40	58.4795
991.77	0.684	23.3909	-919.999	44	64.3275
991.93	0.682	23.3909	-919.999	37	54.2522
992.09	0.687	23.3909	-923.914	50	72.7802
992.26	0.69	23.3909	-923.914	50	72.4638
992.42	0.69	23.3909	-919.999	38	55.0725
992.59	0.69	23.3909	-919.999	36	52.1739
992.75	0.693	23.3909	-919.999	53	76.4791
992.91	0.699	23.3909	-919.999	39	55.794
993.08	0.7	23.3909	-923.914	40	57.1429
993.24	0.696	23.6081	-923.914	46	66.092
993.41	0.693	23.3909	-919.999	43	62.0491
993.57	0.687	23.3909	-919.999	52	75.6914
993.73	0.694	23.3909	-919.999	39	56.196
993.9	0.698	23.3909	-923.914	33	47.2779
994.06	0.696	23.3909	-916.084	43	61.7816
994.23	0.695	23.6081	-919.999	41	58.9928
994.39	0.697	23.3909	-919.999	40	57.3888
994.55	0.699	23.3909	-919.999	52	74.392
994.72	0.695	23.3909	-923.914	29	41.7266
994.88	0.7	23.3909	-923.914	44	62.8571
995.05	0.698	23.3909	-923.914	38	54.4413
995.21	0.697	23.3909	-923.914	39	55.9541
995.37	0.701	23.3909	-923.914	44	62.7675
995.54	0.694	23.3909	-923.914	41	59.0778
995.7	0.692	23.3909	-919.999	51	73.6994
995.87	0.685	23.3909	-923.914	49	71.5328
996.03	0.684	23.3909	-919.999	59	86.2573
996.19	0.687	23.6081	-919.999	50	72.7802
996.36	0.689	23.3909	-919.999	51	74.0203
996.52	0.688	23.1737	-923.914	46	66.8605
996.69	0.686	23.3909	-919.999	54	78.7172
996.85	0.694	23.3909	-919.999	48	69.1643
997.01	0.701	23.3909	-919.999	40	57.0613
997.18	0.702	23.1737	-923.914	50	71.2251
997.34	0.695	23.3909	-923.914	44	63.3094
997.51	0.694	23.3909	-919.999	41	59.0778
997.67	0.698	23.3909	-923.914	48	68.7679
997.83	0.698	23.3909	-923.914	47	67.3352
998	0.697	23.3909	-919.999	34	48.7805

998.16	0.693	23.3909	-923.914	35	50.5051
998.33	0.693	23.3909	-919.999	56	80.8081
998.49	0.694	23.3909	-919.999	38	54.755
998.65	0.701	23.3909	-916.084	46	65.6205
998.82	0.7	23.3909	-919.999	54	77.1429
998.98	0.699	23.3909	-919.999	41	58.6552
999.15	0.696	23.6081	-923.914	57	81.8966
999.31	0.701	23.3909	-919.999	52	74.1797
999.47	0.704	23.3909	-919.999	39	55.3977
999.64	0.693	23.3909	-927.829	44	63.4921
999.8	0.684	23.3909	-919.999	36	52.6316
999.97	0.686	23.3909	-923.914	51	74.344
1000.13	0.688	23.3909	-919.999	26	37.7907
1000.29	0.685	23.3909	-919.999	44	64.2336
1000.46	0.686	23.3909	-919.999	38	55.3936
1000.62	0.686	23.3909	-919.999	43	62.6822
1000.79	0.693	23.3909	-923.914	30	43.29
1000.95	0.701	23.3909	-916.084	35	49.9287
1001.11	0.699	23.6081	-919.999	39	55.794
1001.28	0.696	23.3909	-919.999	38	54.5977
1001.44	0.692	23.3909	-919.999	33	47.6879
1001.61	0.692	23.3909	-919.999	39	56.3584
1001.77	0.698	23.1737	-916.084	34	48.7106
1001.93	0.7	23.3909	-919.999	37	52.8571
1002.1	0.696	23.3909	-919.999	34	48.8506
1002.26	0.693	23.6081	-919.999	34	49.062
1002.43	0.696	23.3909	-919.999	43	61.7816
1002.59	0.702	23.3909	-923.914	30	42.735
1002.75	0.703	23.6081	-923.914	33	46.9417
1002.92	0.696	23.3909	-916.084	35	50.2874
1003.08	0.696	23.3909	-919.999	35	50.2874
1003.25	0.698	23.3909	-923.914	31	44.4126
1003.41	0.699	23.6081	-919.999	30	42.9185
1003.57	0.696	23.3909	-923.914	40	57.4713
1003.74	0.692	23.3909	-919.999	36	52.0231
1003.9	0.689	23.3909	-923.914	27	39.1872
1004.07	0.687	23.3909	-919.999	25	36.3901
1004.23	0.686	23.3909	-919.999	29	42.2741
1004.39	0.687	23.3909	-919.999	39	56.7686
1004.56	0.682	23.3909	-919.999	22	32.2581
1004.72	0.677	23.3909	-919.999	23	33.9734

1004.89	0.692	23.3909	-923.914	23	33.237
1005.05	0.695	23.3909	-923.914	27	38.8489
1005.21	0.696	23.3909	-919.999	20	28.7356
1005.38	0.694	23.3909	-919.999	28	40.3458
1005.54	0.696	23.3909	-923.914	33	47.4138
1005.71	0.702	23.3909	-919.999	31	44.1595
1005.87	0.698	23.3909	-923.914	29	41.5473
1006.03	0.694	23.6081	-919.999	30	43.2277
1006.2	0.691	23.1737	-923.914	25	36.1795
1006.36	0.696	23.3909	-919.999	35	50.2874
1006.53	0.699	23.6081	-923.914	41	58.6552
1006.69	0.695	23.6081	-916.084	30	43.1655
1006.85	0.696	23.3909	-919.999	31	44.5402
1007.02	0.699	23.3909	-919.999	32	45.7797
1007.18	0.702	23.3909	-923.914	26	37.037
1007.35	0.703	23.3909	-923.914	37	52.6316
1007.51	0.702	23.3909	-919.999	28	39.886
1007.67	0.699	23.3909	-919.999	22	31.4735
1007.84	0.697	23.3909	-927.829	34	48.7805
1008	0.693	23.6081	-919.999	27	38.961
1008.17	0.689	23.3909	-919.999	49	71.1176
1008.33	0.684	23.6081	-923.914	47	68.7134
1008.49	0.681	23.6081	-923.914	27	39.6476
1008.66	0.685	23.6081	-919.999	35	51.0949
1008.82	0.69	23.3909	-919.999	27	39.1304
1008.99	0.69	23.3909	-923.914	27	39.1304
1009.15	0.692	23.3909	-919.999	36	52.0231
1009.31	0.695	23.3909	-919.999	33	47.482
1009.48	0.7	23.3909	-919.999	39	55.7143
1009.64	0.696	23.6081	-919.999	43	61.7816
1009.81	0.696	23.3909	-923.914	30	43.1034
1009.97	0.694	23.6081	-919.999	38	54.755
1010.13	0.691	23.3909	-919.999	44	63.6758
1010.3	0.694	23.3909	-923.914	46	66.2824
1010.46	0.7	23.3909	-923.914	32	45.7143
1010.63	0.7	23.3909	-923.914	29	41.4286
1010.79	0.698	23.3909	-919.999	35	50.1433
1010.95	0.698	23.3909	-923.914	34	48.7106
1011.12	0.7	23.6081	-916.084	43	61.4286
1011.28	0.7	23.3909	-923.914	35	50
1011.45	0.7	23.3909	-919.999	33	47.1429

1011.61	0.695	23.3909	-919.999	42	60.4317
1011.77	0.699	23.3909	-919.999	39	55.794
1011.94	0.704	23.3909	-923.914	28	39.7727
1012.1	0.696	23.3909	-923.914	34	48.8506
1012.27	0.69	23.3909	-919.999	25	36.2319
1012.43	0.683	23.6081	-923.914	29	42.4597
1012.59	0.686	23.3909	-919.999	40	58.309
1012.76	0.69	23.6081	-923.914	37	53.6232
1012.92	0.689	23.3909	-923.914	42	60.9579
1013.09	0.688	23.6081	-919.999	34	49.4186
1013.25	0.688	23.3909	-919.999	33	47.9651
1013.41	0.69	23.3909	-919.999	31	44.9275
1013.58	0.701	23.6081	-919.999	36	51.3552
1013.74	0.699	23.6081	-916.084	46	65.8083
1013.91	0.695	23.3909	-916.084	35	50.3597
1014.07	0.693	23.3909	-919.999	37	53.3911
1014.23	0.696	23.3909	-916.084	35	50.2874
1014.4	0.699	23.3909	-923.914	39	55.794
1014.56	0.694	23.3909	-916.084	37	53.3141
1014.73	0.689	23.3909	-916.084	40	58.0552
1014.89	0.694	23.3909	-919.999	24	34.5821
1015.05	0.7	23.3909	-919.999	24	34.2857
1015.22	0.702	23.6081	-919.999	24	34.188
1015.38	0.7	23.3909	-923.914	30	42.8571
1015.55	0.699	23.6081	-923.914	37	52.9328
1015.71	0.698	23.6081	-916.084	39	55.8739
1015.87	0.703	23.3909	-916.084	40	56.899
1016.04	0.704	23.3909	-927.829	34	48.2955
1016.2	0.695	23.6081	-923.914	32	46.0432
1016.37	0.689	23.3909	-923.914	30	43.5414
1016.53	0.681	23.3909	-919.999	24	35.2423
1016.69	0.686	23.6081	-923.914	36	52.4781
1016.86	0.688	23.3909	-923.914	37	53.7791
1017.02	0.685	23.3909	-919.999	35	51.0949
1017.19	0.687	23.3909	-923.914	44	64.0466
1017.35	0.687	23.3909	-916.084	32	46.5793
1017.51	0.696	23.6081	-923.914	49	70.4023
1017.68	0.7	23.6081	-919.999	34	48.5714
1017.84	0.695	23.3909	-923.914	27	38.8489
1018.01	0.692	23.3909	-919.999	35	50.578
1018.17	0.695	23.3909	-919.999	32	46.0432

1018.33	0.694	23.3909	-923.914	44	63.4006
1018.5	0.693	23.6081	-919.999	37	53.3911
1018.66	0.694	23.6081	-916.084	45	64.8415
1018.83	0.688	23.6081	-923.914	40	58.1395
1018.99	0.696	23.3909	-927.829	30	43.1034
1019.15	0.701	23.3909	-919.999	26	37.0899
1019.32	0.702	23.3909	-923.914	32	45.584
1019.48	0.698	23.3909	-919.999	36	51.5759
1019.65	0.688	23.3909	-916.084	35	50.8721
1019.81	0.7	23.3909	-919.999	36	51.4286
1019.97	0.703	23.6081	-923.914	30	42.6743
1020.14	0.7	23.3909	-919.999	31	44.2857
1020.3	0.692	23.3909	-916.084	34	49.1329
1020.47	0.69	23.6081	-919.999	28	40.5797
1020.63	0.692	23.3909	-923.914	25	36.1272
1020.79	0.69	23.6081	-919.999	42	60.8696
1020.96	0.687	23.6081	-927.829	35	50.9461
1021.12	0.681	23.6081	-923.914	30	44.0529
1021.29	0.684	23.3909	-919.999	30	43.8596
1021.45	0.69	23.6081	-919.999	41	59.4203
1021.61	0.692	23.3909	-923.914	33	47.6879
1021.78	0.697	23.6081	-923.914	33	47.3458
1021.94	0.695	23.6081	-923.914	44	63.3094
1022.11	0.697	23.3909	-919.999	34	48.7805
1022.27	0.7	23.3909	-916.084	27	38.5714
1022.43	0.698	23.6081	-919.999	36	51.5759
1022.6	0.696	23.3909	-916.084	32	45.977
1022.76	0.693	23.3909	-919.999	37	53.3911
1022.93	0.696	23.3909	-912.169	38	54.5977
1023.09	0.7	23.3909	-923.914	34	48.5714
1023.25	0.694	23.6081	-919.999	26	37.464
1023.42	0.693	23.3909	-916.084	32	46.176
1023.58	0.698	23.6081	-919.999	30	42.9799
1023.75	0.701	23.3909	-919.999	30	42.796
1023.91	0.702	23.3909	-923.914	27	38.4615
1024.07	0.702	23.3909	-919.999	28	39.886
1024.24	0.696	23.3909	-919.999	25	35.9195
1024.4	0.695	23.6081	-919.999	32	46.0432
1024.57	0.691	23.6081	-919.999	28	40.521
1024.73	0.688	23.3909	-919.999	35	50.8721
1024.89	0.686	23.6081	-919.999	21	30.6122

1025.06	0.684	23.3909	-919.999	29	42.3977
1025.22	0.683	23.3909	-919.999	22	32.2108
1025.39	0.688	23.3909	-919.999	34	49.4186
1025.55	0.692	23.6081	-919.999	30	43.3526
1025.71	0.694	23.3909	-919.999	31	44.6686
1025.88	0.693	23.3909	-923.914	40	57.7201
1026.04	0.697	23.3909	-923.914	25	35.868
1026.21	0.7	23.3909	-919.999	35	50
1026.37	0.696	23.3909	-919.999	34	48.8506
1026.53	0.692	23.6081	-919.999	33	47.6879
1026.7	0.693	23.1737	-919.999	36	51.9481
1026.86	0.698	23.3909	-919.999	44	63.0373
1027.03	0.7	23.6081	-919.999	32	45.7143
1027.19	0.699	23.6081	-919.999	42	60.0858
1027.35	0.696	23.3909	-923.914	32	45.977
1027.52	0.696	23.3909	-919.999	44	63.2184
1027.68	0.703	23.3909	-919.999	35	49.7866
1027.85	0.704	23.6081	-916.084	37	52.5568
1028.01	0.699	23.3909	-919.999	40	57.2246
1028.17	0.697	23.6081	-923.914	29	41.6069
1028.34	0.695	23.6081	-916.084	34	48.9209
1028.5	0.701	23.3909	-919.999	45	64.194
1028.67	0.694	23.3909	-923.914	37	53.3141
1028.83	0.69	23.3909	-923.914	33	47.8261
1028.99	0.683	23.6081	-919.999	34	49.7804
1029.16	0.684	23.6081	-923.914	33	48.2456
1029.32	0.688	23.3909	-919.999	31	45.0581
1029.49	0.688	23.6081	-923.914	28	40.6977
1029.65	0.682	23.3909	-923.914	33	48.3871
1029.81	0.686	23.3909	-919.999	48	69.9708
1029.98	0.695	23.6081	-923.914	31	44.6043
1030.14	0.698	23.6081	-919.999	47	67.3352
1030.31	0.698	23.3909	-919.999	31	44.4126
1030.47	0.699	23.6081	-919.999	42	60.0858
1030.63	0.694	23.3909	-919.999	32	46.1095
1030.8	0.696	23.8254	-927.829	35	50.2874
1030.96	0.698	23.3909	-919.999	38	54.4413
1031.13	0.695	23.3909	-919.999	31	44.6043
1031.29	0.694	23.6081	-919.999	32	46.1095
1031.45	0.692	23.3909	-919.999	38	54.9133
1031.62	0.698	23.6081	-919.999	43	61.6046

1031.78	0.705	23.3909	-923.914	42	59.5745
1031.95	0.701	23.3909	-923.914	43	61.3409
1032.11	0.697	23.6081	-916.084	32	45.911
1032.27	0.698	23.6081	-923.914	32	45.8453
1032.44	0.703	23.3909	-919.999	39	55.4765
1032.6	0.705	23.8254	-919.999	31	43.9716
1032.77	0.698	23.3909	-923.914	45	64.4699
1032.93	0.686	23.3909	-916.084	37	53.9359
1033.09	0.681	23.6081	-919.999	40	58.7372
1033.26	0.684	23.6081	-923.914	39	57.0175
1033.42	0.686	23.6081	-923.914	29	42.2741
1033.59	0.685	23.3909	-923.914	40	58.3942
1033.75	0.684	23.3909	-919.999	31	45.3216
1033.91	0.687	23.6081	-923.914	34	49.4905
1034.08	0.694	23.3909	-919.999	28	40.3458
1034.24	0.7	23.6081	-919.999	39	55.7143
1034.41	0.698	23.6081	-919.999	33	47.2779
1034.57	0.688	23.6081	-919.999	29	42.1512
1034.73	0.696	23.8254	-923.914	31	44.5402
1034.9	0.699	23.3909	-919.999	20	28.6123
1035.06	0.697	23.3909	-919.999	32	45.911
1035.23	0.695	23.3909	-919.999	26	37.4101
1035.39	0.694	23.6081	-923.914	23	33.1412
1035.55	0.699	23.8254	-919.999	37	52.9328
1035.72	0.705	23.8254	-919.999	43	60.9929
1035.88	0.703	23.3909	-919.999	30	42.6743
1036.05	0.699	23.3909	-923.914	30	42.9185
1036.21	0.698	23.6081	-923.914	39	55.8739
1036.37	0.7	23.6081	-923.914	31	44.2857
1036.54	0.7	23.3909	-923.914	42	60
1036.7	0.702	23.6081	-923.914	40	56.9801
1036.87	0.696	23.3909	-916.084	42	60.3448
1037.03	0.693	23.3909	-919.999	33	47.619
1037.19	0.692	23.6081	-919.999	31	44.7977
1037.36	0.688	23.3909	-919.999	37	53.7791
1037.52	0.687	23.3909	-923.914	40	58.2242
1037.69	0.685	23.6081	-923.914	33	48.1752
1037.85	0.684	23.3909	-923.914	39	57.0175
1038.01	0.689	23.6081	-923.914	41	59.5065
1038.18	0.693	23.6081	-919.999	39	56.2771
1038.34	0.692	23.6081	-919.999	34	49.1329

1038.51	0.694	23.3909	-919.999	30	43.2277
1038.67	0.694	23.6081	-923.914	38	54.755
1038.83	0.701	23.3909	-923.914	37	52.7817
1039	0.697	23.6081	-919.999	38	54.5194
1039.16	0.697	23.6081	-923.914	38	54.5194
1039.33	0.694	23.6081	-919.999	39	56.196
1039.49	0.693	23.6081	-919.999	33	47.619
1039.65	0.696	23.3909	-923.914	42	60.3448
1039.82	0.701	23.6081	-923.914	36	51.3552
1039.98	0.698	23.6081	-923.914	31	44.4126
1040.15	0.696	23.6081	-923.914	40	57.4713
1040.31	0.703	23.6081	-919.999	31	44.0967
1040.47	0.706	23.3909	-919.999	33	46.7422
1040.64	0.704	23.8254	-923.914	40	56.8182
1040.8	0.698	23.6081	-919.999	39	55.8739
1040.97	0.695	23.3909	-919.999	39	56.1151
1041.13	0.695	23.6081	-923.914	30	43.1655
1041.29	0.694	23.6081	-923.914	44	63.4006
1041.46	0.683	23.3909	-919.999	38	55.6369
1041.62	0.682	23.6081	-923.914	34	49.8534
1041.79	0.686	23.6081	-919.999	28	40.8163
1041.95	0.69	23.6081	-923.914	29	42.029
1042.11	0.689	23.6081	-919.999	39	56.6038
1042.28	0.694	23.6081	-919.999	43	61.9597
1042.44	0.694	23.6081	-919.999	39	56.196
1042.61	0.698	23.6081	-919.999	36	51.5759
1042.77	0.701	23.3909	-923.914	49	69.9001
1042.93	0.697	23.6081	-919.999	34	48.7805
1043.1	0.693	23.6081	-923.914	35	50.5051
1043.26	0.691	23.3909	-919.999	26	37.6266
1043.43	0.696	23.6081	-923.914	33	47.4138
1043.59	0.699	23.6081	-919.999	19	27.1817
1043.75	0.701	23.6081	-923.914	38	54.2083
1043.92	0.695	23.3909	-916.084	28	40.2878
1044.08	0.695	23.6081	-919.999	43	61.8705
1044.25	0.704	23.3909	-923.914	25	35.5114
1044.41	0.704	23.3909	-923.914	26	36.9318
1044.57	0.695	23.6081	-919.999	30	43.1655
1044.74	0.699	23.6081	-923.914	33	47.2103
1044.9	0.699	23.3909	-919.999	22	31.4735
1045.07	0.699	23.6081	-919.999	30	42.9185

1045.23	0.697	23.3909	-919.999	29	41.6069
1045.39	0.694	23.6081	-919.999	28	40.3458
1045.56	0.684	23.6081	-919.999	31	45.3216
1045.72	0.686	23.3909	-919.999	30	43.7318
1045.89	0.689	23.6081	-923.914	20	29.0276
1046.05	0.686	23.3909	-923.914	24	34.9854
1046.21	0.686	23.6081	-923.914	24	34.9854
1046.38	0.684	23.6081	-923.914	31	45.3216
1046.54	0.69	23.3909	-916.084	31	44.9275
1046.71	0.7	23.8254	-923.914	42	60
1046.87	0.702	23.6081	-923.914	31	44.1595
1047.03	0.696	23.3909	-919.999	30	43.1034
1047.2	0.693	23.6081	-919.999	31	44.733
1047.36	0.697	23.3909	-927.829	35	50.2152
1047.53	0.703	23.6081	-919.999	21	29.872
1047.69	0.696	23.6081	-919.999	33	47.4138
1047.85	0.697	23.6081	-919.999	26	37.3027
1048.02	0.693	23.6081	-919.999	30	43.29
1048.18	0.697	23.6081	-923.914	27	38.7374
1048.35	0.7	23.6081	-923.914	36	51.4286
1048.51	0.7	23.8254	-923.914	31	44.2857
1048.67	0.698	23.6081	-919.999	31	44.4126
1048.84	0.696	23.6081	-923.914	33	47.4138
1049	0.703	23.6081	-919.999	41	58.3215
1049.17	0.704	23.6081	-919.999	28	39.7727
1049.33	0.697	23.6081	-916.084	34	48.7805
1049.49	0.684	23.6081	-919.999	23	33.6257
1049.66	0.683	23.6081	-919.999	23	33.675
1049.82	0.688	23.6081	-916.084	29	42.1512
1049.99	0.688	23.6081	-923.914	37	53.7791
1050.15	0.685	23.6081	-923.914	32	46.7153
1050.31	0.685	23.8254	-923.914	38	55.4745
1050.48	0.687	23.3909	-919.999	29	42.2125
1050.64	0.697	23.3909	-923.914	54	77.4749
1050.81	0.698	23.6081	-923.914	40	57.3066
1050.97	0.697	24.0426	-916.084	50	71.736
1051.13	0.695	23.6081	-919.999	54	77.6978
1051.3	0.697	23.6081	-923.914	59	84.6485
1051.46	0.696	23.6081	-919.999	58	83.3333
1051.63	0.697	23.6081	-923.914	54	77.4749
1051.79	0.699	23.6081	-919.999	53	75.8226

1051.95	0.694	23.3909	-923.914	54	77.8098
1052.12	0.7	23.6081	-923.914	65	92.8571
1052.28	0.706	23.6081	-919.999	56	79.3201
1052.45	0.704	23.6081	-916.084	70	99.4318
1052.61	0.703	23.8254	-916.084	52	73.9687
1052.77	0.697	23.8254	-923.914	51	73.1707
1052.94	0.699	23.6081	-923.914	53	75.8226
1053.1	0.702	23.8254	-919.999	66	94.0171
1053.27	0.699	23.6081	-919.999	37	52.9328
1053.43	0.694	23.8254	-923.914	64	92.219
1053.59	0.691	23.6081	-919.999	54	78.1476
1053.76	0.691	23.6081	-919.999	45	65.123
1053.92	0.685	23.3909	-923.914	57	83.2117
1054.09	0.685	23.6081	-923.914	56	81.7518
1054.25	0.685	23.6081	-919.999	57	83.2117
1054.41	0.684	23.8254	-919.999	52	76.0234
1054.58	0.684	23.6081	-919.999	58	84.7953
1054.74	0.693	23.6081	-919.999	46	66.3781
1054.91	0.696	23.8254	-919.999	43	61.7816
1055.07	0.692	23.8254	-919.999	49	70.8092
1055.23	0.697	23.6081	-923.914	54	77.4749
1055.4	0.703	23.8254	-919.999	55	78.2361
1055.56	0.703	23.6081	-919.999	71	100.996
1055.73	0.697	23.8254	-919.999	71	101.865
1055.89	0.693	23.6081	-919.999	45	64.9351
1056.05	0.696	23.6081	-927.829	53	76.1494
1056.22	0.701	23.3909	-923.914	59	84.1655
1056.38	0.7	23.6081	-919.999	54	77.1429
1056.55	0.698	23.6081	-919.999	55	78.7966
1056.71	0.701	23.6081	-919.999	67	95.5777
1056.87	0.705	23.6081	-923.914	54	76.5957
1057.04	0.704	23.6081	-916.084	64	90.9091
1057.2	0.704	23.8254	-923.914	60	85.2273
1057.37	0.7	23.6081	-919.999	50	71.4286
1057.53	0.702	23.3909	-919.999	54	76.9231
1057.69	0.698	23.6081	-919.999	54	77.3639
1057.86	0.693	23.3909	-923.914	58	83.6941
1058.02	0.685	23.6081	-919.999	59	86.1314
1058.19	0.68	23.6081	-919.999	51	75
1058.35	0.682	23.6081	-923.914	56	82.1114
1058.51	0.688	23.6081	-919.999	62	90.1163

1058.68	0.689	23.6081	-927.829	57	82.7286
1058.84	0.691	23.6081	-919.999	58	83.9363
1059.01	0.693	23.6081	-923.914	60	86.5801
1059.17	0.695	23.8254	-923.914	40	57.554
1059.33	0.7	23.6081	-916.084	59	84.2857
1059.5	0.691	23.6081	-923.914	63	91.1722
1059.66	0.696	23.8254	-919.999	64	91.954
1059.83	0.694	23.6081	-916.084	59	85.0144
1059.99	0.696	23.6081	-923.914	60	86.2069
1060.15	0.697	23.8254	-923.914	51	73.1707
1060.32	0.7	23.3909	-923.914	56	80
1060.48	0.699	23.6081	-919.999	50	71.5308
1060.65	0.698	23.6081	-927.829	53	75.9312
1060.81	0.704	23.6081	-919.999	48	68.1818
1060.97	0.705	23.6081	-923.914	53	75.1773
1061.14	0.701	23.8254	-923.914	57	81.3124
1061.3	0.696	23.6081	-923.914	56	80.4598
1061.47	0.696	23.6081	-923.914	52	74.7126
1061.63	0.703	23.6081	-923.914	57	81.0811
1061.79	0.7	23.6081	-919.999	49	70
1061.96	0.693	23.6081	-916.084	50	72.1501
1062.12	0.684	23.6081	-919.999	48	70.1754
1062.29	0.686	23.6081	-916.084	68	99.1254
1062.45	0.689	23.6081	-923.914	54	78.3745
1062.61	0.687	23.3909	-919.999	48	69.869
1062.78	0.687	23.6081	-923.914	44	64.0466
1062.94	0.685	23.8254	-919.999	55	80.292
1063.11	0.691	23.6081	-916.084	62	89.725
1063.27	0.696	23.8254	-919.999	41	58.908
1063.43	0.699	23.6081	-919.999	50	71.5308
1063.6	0.695	23.8254	-919.999	39	56.1151
1063.76	0.694	23.6081	-919.999	49	70.6052
1063.93	0.697	23.6081	-919.999	52	74.6055
1064.09	0.7	23.8254	-923.914	55	78.5714
1064.25	0.7	23.6081	-919.999	36	51.4286
1064.42	0.693	23.8254	-919.999	45	64.9351
1064.58	0.693	23.6081	-923.914	35	50.5051
1064.75	0.701	23.6081	-919.999	39	55.6348
1064.91	0.703	23.6081	-919.999	33	46.9417
1065.07	0.7	23.6081	-919.999	46	65.7143
1065.24	0.7	23.6081	-919.999	40	57.1429

1065.4	0.7	23.6081	-923.914	35	50
1065.57	0.706	23.8254	-923.914	28	39.6601
1065.73	0.704	23.6081	-923.914	59	83.8068
1065.89	0.698	23.8254	-923.914	38	54.4413
1066.06	0.689	23.6081	-919.999	29	42.09
1066.22	0.686	23.6081	-919.999	38	55.3936
1066.39	0.685	23.8254	-919.999	41	59.854
1066.55	0.688	23.8254	-919.999	38	55.2326
1066.71	0.688	23.8254	-923.914	32	46.5116
1066.88	0.683	23.8254	-923.914	39	57.101
1067.04	0.688	23.8254	-919.999	33	47.9651
1067.21	0.695	23.6081	-912.169	42	60.4317
1067.37	0.701	23.6081	-919.999	33	47.0756
1067.53	0.7	23.8254	-923.914	31	44.2857
1067.7	0.697	23.6081	-923.914	45	64.5624
1067.86	0.697	23.8254	-919.999	30	43.0416
1068.03	0.699	24.0426	-923.914	43	61.5165
1068.19	0.694	23.8254	-923.914	47	67.7233
1068.35	0.699	23.8254	-923.914	52	74.392
1068.52	0.692	23.6081	-919.999	35	50.578
1068.68	0.698	23.6081	-919.999	37	53.0086
1068.85	0.705	23.8254	-923.914	34	48.227
1069.01	0.702	23.6081	-919.999	46	65.5271
1069.17	0.699	24.0426	-923.914	37	52.9328
1069.34	0.699	23.6081	-919.999	30	42.9185
1069.5	0.696	23.6081	-923.914	41	58.908
1069.67	0.704	23.8254	-923.914	40	56.8182
1069.83	0.702	24.0426	-919.999	35	49.8576
1069.99	0.695	23.6081	-923.914	28	40.2878
1070.16	0.691	23.8254	-923.914	27	39.0738
1070.32	0.693	23.8254	-923.914	28	40.404
1070.49	0.69	23.8254	-919.999	33	47.8261
1070.65	0.688	23.6081	-919.999	24	34.8837
1070.81	0.683	23.8254	-923.914	35	51.2445
1070.98	0.686	23.8254	-923.914	39	56.8513
1071.14	0.689	23.6081	-919.999	31	44.9927
1071.31	0.69	23.8254	-923.914	34	49.2754
1071.47	0.694	23.8254	-923.914	39	56.196
1071.63	0.697	23.8254	-919.999	30	43.0416
1071.8	0.701	23.6081	-919.999	38	54.2083
1071.96	0.702	23.6081	-919.999	36	51.2821

1072.13	0.702	23.6081	-919.999	37	52.7066
1072.29	0.698	23.6081	-919.999	35	50.1433
1072.45	0.694	23.6081	-923.914	35	50.4323
1072.62	0.695	23.8254	-923.914	34	48.9209
1072.78	0.702	23.8254	-919.999	27	38.4615
1072.95	0.7	23.8254	-923.914	29	41.4286
1073.11	0.696	23.8254	-916.084	30	43.1034
1073.27	0.695	23.6081	-919.999	45	64.7482
1073.44	0.702	23.8254	-916.084	28	39.886
1073.6	0.702	23.6081	-923.914	35	49.8576
1073.77	0.701	23.8254	-919.999	34	48.5021
1073.93	0.698	23.6081	-923.914	33	47.2779
1074.09	0.698	23.6081	-923.914	26	37.2493
1074.26	0.699	23.6081	-923.914	41	58.6552
1074.42	0.688	23.6081	-916.084	26	37.7907
1074.59	0.682	23.6081	-923.914	28	41.0557
1074.75	0.685	23.8254	-916.084	33	48.1752
1074.91	0.684	23.8254	-919.999	29	42.3977
1075.08	0.686	23.8254	-919.999	35	51.0204
1075.24	0.689	23.6081	-919.999	41	59.5065
1075.41	0.693	23.6081	-916.084	26	37.518
1075.57	0.692	23.8254	-919.999	31	44.7977
1075.73	0.698	24.0426	-919.999	27	38.6819
1075.9	0.703	23.8254	-923.914	37	52.6316
1076.06	0.699	23.6081	-919.999	29	41.4878
1076.23	0.697	23.8254	-919.999	28	40.1722
1076.39	0.693	23.6081	-919.999	41	59.1631
1076.55	0.7	23.8254	-923.914	33	47.1429
1076.72	0.703	23.8254	-919.999	20	28.4495
1076.88	0.702	23.8254	-919.999	45	64.1026
1077.05	0.7	23.8254	-923.914	41	58.5714
1077.21	0.699	23.6081	-919.999	39	55.794
1077.37	0.705	23.8254	-916.084	36	51.0638
1077.54	0.705	23.8254	-923.914	41	58.156
1077.7	0.701	23.8254	-923.914	40	57.0613
1077.87	0.699	23.8254	-923.914	32	45.7797
1078.03	0.696	23.8254	-923.914	34	48.8506
1078.19	0.7	23.8254	-919.999	37	52.8571
1078.36	0.7	23.8254	-919.999	30	42.8571
1078.52	0.692	23.8254	-923.914	39	56.3584
1078.69	0.684	23.8254	-916.084	42	61.4035

1078.85	0.685	23.8254	-916.084	39	56.9343
1079.01	0.687	23.8254	-923.914	38	55.313
1079.18	0.688	23.8254	-923.914	27	39.2442
1079.34	0.684	23.8254	-919.999	43	62.8655
1079.51	0.683	23.6081	-919.999	41	60.0293
1079.67	0.693	23.8254	-919.999	36	51.9481
1079.83	0.701	23.8254	-919.999	32	45.6491
1080	0.699	23.8254	-923.914	39	55.794
1080.16	0.701	23.8254	-919.999	48	68.4736
1080.33	0.695	23.8254	-919.999	51	73.3813
1080.49	0.7	23.8254	-923.914	30	42.8571
1080.65	0.703	23.8254	-923.914	37	52.6316
1080.82	0.703	23.8254	-919.999	36	51.2091
1080.98	0.697	23.8254	-923.914	38	54.5194
1081.15	0.696	23.8254	-919.999	36	51.7241
1081.31	0.699	23.8254	-916.084	46	65.8083
1081.47	0.704	23.6081	-919.999	43	61.0795
1081.64	0.705	23.8254	-919.999	53	75.1773
1081.8	0.702	23.6081	-916.084	27	38.4615
1081.97	0.701	23.8254	-919.999	31	44.2225
1082.13	0.703	23.8254	-919.999	45	64.0114
1082.29	0.705	23.8254	-923.914	40	56.7376
1082.46	0.702	24.0426	-923.914	39	55.5556
1082.62	0.692	23.8254	-923.914	39	56.3584
1082.79	0.69	23.8254	-923.914	39	56.5217
1082.95	0.688	23.8254	-919.999	46	66.8605
1083.11	0.686	23.8254	-923.914	40	58.309
1083.28	0.684	23.8254	-919.999	37	54.0936
1083.44	0.682	23.8254	-923.914	33	48.3871
1083.61	0.686	23.8254	-919.999	31	45.1895
1083.77	0.694	23.8254	-919.999	40	57.6369
1083.93	0.702	23.6081	-916.084	32	45.584
1084.1	0.702	23.8254	-919.999	37	52.7066
1084.26	0.697	24.0426	-923.914	39	55.9541
1084.43	0.69	23.8254	-919.999	35	50.7246
1084.59	0.702	23.8254	-916.084	39	55.5556
1084.75	0.701	23.8254	-919.999	30	42.796
1084.92	0.696	23.8254	-923.914	39	56.0345
1085.08	0.697	23.8254	-923.914	33	47.3458
1085.25	0.702	23.8254	-916.084	33	47.0085
1085.41	0.708	23.8254	-923.914	20	28.2486

1085.57	0.704	23.8254	-923.914	37	52.5568
1085.74	0.698	23.8254	-919.999	45	64.4699
1085.9	0.698	23.8254	-919.999	25	35.8166
1086.07	0.701	24.0426	-923.914	40	57.0613
1086.23	0.703	24.0426	-919.999	35	49.7866
1086.39	0.696	23.8254	-923.914	30	43.1034
1086.56	0.698	23.6081	-919.999	36	51.5759
1086.72	0.692	24.0426	-916.084	28	40.4624
1086.89	0.691	23.8254	-923.914	32	46.3097
1087.05	0.692	24.0426	-919.999	40	57.8035
1087.21	0.686	23.8254	-916.084	31	45.1895
1087.38	0.686	24.0426	-923.914	38	55.3936
1087.54	0.684	23.8254	-923.914	22	32.1637
1087.71	0.685	23.8254	-919.999	40	58.3942
1087.87	0.692	24.2598	-923.914	33	47.6879
1088.03	0.697	23.8254	-919.999	32	45.911
1088.2	0.694	23.8254	-923.914	34	48.9914
1088.36	0.699	24.0426	-919.999	44	62.9471
1088.53	0.702	23.8254	-923.914	45	64.1026
1088.69	0.7	24.0426	-919.999	36	51.4286
1088.85	0.698	23.8254	-916.084	45	64.4699
1089.02	0.697	23.8254	-919.999	34	48.7805
1089.18	0.701	23.8254	-919.999	25	35.6633
1089.35	0.701	24.0426	-919.999	30	42.796
1089.51	0.701	23.8254	-919.999	29	41.3695
1089.67	0.699	23.8254	-923.914	44	62.9471
1089.84	0.697	23.8254	-919.999	34	48.7805
1090	0.701	24.0426	-923.914	46	65.6205
1090.17	0.703	24.0426	-923.914	43	61.1664
1090.33	0.706	23.8254	-923.914	30	42.4929
1090.49	0.7	23.8254	-919.999	39	55.7143
1090.66	0.699	23.8254	-923.914	39	55.794
1090.82	0.696	23.8254	-919.999	42	60.3448
1090.99	0.693	23.8254	-923.914	37	53.3911
1091.15	0.687	23.8254	-919.999	30	43.6681
1091.31	0.681	24.0426	-923.914	37	54.3319
1091.48	0.685	23.8254	-923.914	31	45.2555
1091.64	0.691	23.8254	-919.999	39	56.4399
1091.81	0.69	24.0426	-919.999	41	59.4203
1091.97	0.691	23.8254	-916.084	39	56.4399
1092.13	0.694	24.0426	-919.999	37	53.3141

1092.3	0.699	23.8254	-919.999	39	55.794
1092.46	0.705	24.0426	-923.914	39	55.3191
1092.63	0.702	23.8254	-927.829	33	47.0085
1092.79	0.698	23.8254	-919.999	50	71.6332
1092.95	0.695	23.8254	-923.914	42	60.4317
1093.12	0.696	24.0426	-923.914	42	60.3448
1093.28	0.702	23.8254	-919.999	40	56.9801
1093.45	0.7	23.8254	-919.999	33	47.1429
1093.61	0.699	23.8254	-919.999	24	34.3348
1093.77	0.699	24.0426	-923.914	39	55.794
1093.94	0.704	24.0426	-919.999	30	42.6136
1094.1	0.705	23.8254	-919.999	34	48.227
1094.27	0.698	24.0426	-923.914	26	37.2493
1094.43	0.694	24.0426	-923.914	31	44.6686
1094.59	0.699	23.8254	-919.999	35	50.0715
1094.76	0.703	23.8254	-923.914	32	45.5192
1094.92	0.699	23.8254	-919.999	42	60.0858
1095.09	0.693	23.8254	-919.999	43	62.0491
1095.25	0.686	24.0426	-919.999	29	42.2741
1095.41	0.688	24.0426	-923.914	43	62.5
1095.58	0.69	24.0426	-923.914	31	44.9275
1095.74	0.688	23.8254	-923.914	22	31.9767
1095.91	0.686	24.0426	-919.999	32	46.6472
1096.07	0.687	24.0426	-919.999	24	34.9345
1096.23	0.691	23.8254	-916.084	38	54.9928
1096.4	0.7	23.8254	-919.999	33	47.1429
1096.56	0.703	23.8254	-919.999	35	49.7866
1096.73	0.701	23.8254	-919.999	25	35.6633
1096.89	0.696	23.8254	-916.084	34	48.8506
1097.05	0.699	23.8254	-919.999	45	64.3777
1097.22	0.703	23.8254	-927.829	33	46.9417
1097.38	0.703	24.0426	-919.999	34	48.3642
1097.55	0.7	23.8254	-923.914	39	55.7143
1097.71	0.695	24.0426	-923.914	34	48.9209
1097.87	0.701	23.8254	-919.999	29	41.3695
1098.04	0.703	23.8254	-919.999	27	38.4068
1098.2	0.701	23.8254	-916.084	33	47.0756
1098.37	0.7	23.8254	-916.084	39	55.7143
1098.53	0.698	23.8254	-916.084	35	50.1433
1098.69	0.7	24.0426	-923.914	34	48.5714
1098.86	0.703	23.8254	-919.999	36	51.2091

1099.02	0.701	24.0426	-919.999	35	49.9287
1099.19	0.69	24.0426	-916.084	31	44.9275
1099.35	0.682	24.0426	-919.999	31	45.4545
1099.51	0.688	23.8254	-919.999	23	33.4302
1099.68	0.687	24.0426	-916.084	32	46.5793
1099.84	0.683	23.8254	-919.999	34	49.7804
1100.01	0.681	23.8254	-923.914	36	52.8634
1100.17	0.687	24.0426	-919.999	28	40.7569
1100.33	0.698	24.0426	-923.914	33	47.2779
1100.5	0.703	24.0426	-919.999	26	36.9844
1100.66	0.699	24.0426	-919.999	31	44.3491
1100.83	0.695	23.8254	-919.999	37	53.2374
1100.99	0.696	24.0426	-919.999	34	48.8506
1101.15	0.699	24.0426	-919.999	38	54.3634
1101.32	0.698	24.0426	-919.999	32	45.8453
1101.48	0.7	24.0426	-919.999	29	41.4286
1101.65	0.699	24.0426	-919.999	49	70.1001
1101.81	0.701	24.0426	-916.084	51	72.7532
1101.97	0.704	23.8254	-919.999	53	75.2841
1102.14	0.704	24.0426	-923.914	52	73.8636
1102.3	0.703	24.0426	-919.999	48	68.2788
1102.47	0.7	24.0426	-919.999	49	70
1102.63	0.701	24.0426	-927.829	53	75.6063
1102.79	0.704	23.8254	-923.914	39	55.3977
1102.96	0.697	23.8254	-923.914	50	71.736
1103.12	0.693	24.0426	-923.914	51	73.5931
1103.29	0.692	24.0426	-919.999	44	63.5838
1103.45	0.693	24.0426	-923.914	39	56.2771
1103.61	0.689	23.8254	-919.999	52	75.4717
1103.78	0.689	23.8254	-919.999	41	59.5065
1103.94	0.685	24.0426	-919.999	48	70.073
1104.11	0.684	23.8254	-919.999	54	78.9474
1104.27	0.684	24.0426	-919.999	48	70.1754
1104.43	0.694	23.8254	-927.829	56	80.6916
1104.6	0.699	24.0426	-919.999	54	77.2532
1104.76	0.696	24.0426	-923.914	34	48.8506
1104.93	0.698	23.8254	-923.914	50	71.6332
1105.09	0.701	24.0426	-919.999	48	68.4736
1105.25	0.703	24.2598	-919.999	55	78.2361
1105.42	0.706	24.2598	-931.744	48	67.9887
1105.58	0.706	24.0426	-916.084	44	62.3229

1105.75	0.72	24.0426	-923.914	51	70.8333
1105.91	0.748	24.0426	-919.999	46	61.4973
1106.07	0.747	24.0426	-919.999	62	82.9987
1106.24	0.747	24.0426	-916.084	40	53.5475
1106.4	0.76	24.0426	-923.914	48	63.1579
1106.57	0.779	24.0426	-923.914	47	60.3338
1106.73	0.788	24.0426	-916.084	58	73.6041
1106.89	0.8	24.0426	-919.999	30	37.5
1107.06	0.802	24.0426	-916.084	48	59.8504
1107.22	0.81	24.0426	-919.999	55	67.9012
1107.39	0.819	23.8254	-923.914	37	45.177
1107.55	0.825	24.0426	-919.999	49	59.3939
1107.71	0.823	23.8254	-919.999	54	65.6136
1107.88	0.824	23.8254	-919.999	68	82.5243
1108.04	0.834	24.0426	-919.999	50	59.952
1108.21	0.859	24.0426	-923.914	69	80.326
1108.37	0.894	24.0426	-919.999	68	76.0626
1108.53	0.917	24.0426	-919.999	67	73.0643
1108.7	0.926	24.0426	-923.914	57	61.5551
1108.86	0.953	24.0426	-919.999	71	74.5016
1109.03	1.001	24.0426	-919.999	83	82.9171
1109.19	1.032	24.2598	-927.829	80	77.5194
1109.35	1.067	24.0426	-919.999	72	67.4789
1109.52	1.074	24.0426	-919.999	74	68.9013
1109.68	1.099	23.8254	-919.999	68	61.8744
1109.85	1.134	24.0426	-919.999	60	52.9101
1110.01	1.187	24.0426	-923.914	98	82.5611
1110.17	1.209	24.0426	-919.999	77	63.689
1110.34	1.287	24.0426	-919.999	83	64.4911
1110.5	1.392	24.0426	-919.999	98	70.4023
1110.67	1.569	24.0426	-919.999	115	73.2951
1110.83	1.912	24.0426	-923.914	142	74.2678

October 20, 2014

Advanced Borehole Geophysical Logging of LANL Extraction Well CrEX-1

Summary Report

Schlumberger
Water Services

October 20, 2014

Advanced Borehole Geophysical Logging of LANL Extraction Well CrEX-1

Summary Report

DRAFT: 054361.R

Prepared for:

Yellow Jacket Drilling Services. LLC.
PO Box 801
Gilbert, AZ 85299-0801

Prepared by:

Schlumberger Water Services
2045 N. Forbes Blvd.
Suite 103
Tucson, AZ 85745, USA

Schlumberger
Water Services

CONTENTS

TABLES

FIGURES

APPENDICES

ATTACHMENTS

EXECUTIVE SUMMARY

Geophysical logging was performed by Schlumberger in the Los Alamos National Laboratory (LANL) chromium extraction well CrEX-1 in August 2014 before well completion. The logging measurements were acquired from 200 to 1,211 feet (ft) below ground surface (bgs), when the borehole was open (uncased) from 816 to 1,211 ft (bottom of hole, as measured by the logs), drilled with an approximately 14.75 inch (in.) diameter bit size, and contained temporary 16 in. diameter freestanding steel casing from ground surface to 816 ft. A second 18 in. diameter temporary casing string resided behind the 16 in. casing from surface to 460 ft.

The primary purpose of the geophysical logging was to characterize the geology and hydrogeology across the depth section where well screens were being considered, with emphasis on determining regional aquifer groundwater level; depths and hydrogeologic properties of aquifer zones, vadose zone moisture content and relative water saturation, and the stratigraphy and lithology of geologic units. The logs provided valuable near real-time in-situ measurements to assist with well completion decision-making. A secondary purpose of the geophysical logging was to evaluate the borehole conditions such as borehole diameter versus depth, deviation versus depth, and degree of drilling fluid invasion. These objectives were accomplished by measuring, nearly continuously, along the length of the well (1) total and effective water-filled porosity and pore-size distribution from which a continuous estimate of hydraulic conductivity is made; (2) bulk electrical resistivity at multiple radial depths of investigation, sensitive to drilling fluid invasion and formation water saturation; (3) volumetric water/moisture content and neutron capture cross-section from epithermal neutron porosity; (4) spectral natural gamma ray, including potassium, thorium, and uranium concentrations; (5) neutron induced gamma ray spectroscopy for bulk concentrations of mineral-forming elements; (6) borehole electrical imaging for geologic texture, bedding and fracture orientation, and fracture aperture; (7) borehole inclination and azimuth; and (8) borehole diameter.

The following Schlumberger geophysical logging tools were used in the project (Table 1):

- Magnetic Resonance (MR) Scanner (MRX*)
- Accelerator Porosity Sonde (APS*)
- High Resolution Laterolog Array (HRLA*) and Array Induction Tool (AIT*)
- Formation Micro-Imager (FMI*) tool
- Hostile Natural Gamma Spectroscopy (HNGS*) and gamma ray (GR)
- Litho Scanner* (NEXT*)

* Mark of Schlumberger

Table 1: Geophysical Logging Tool, Technology, Corresponding Measured Properties

Tool	Technology	Properties Measured
Magnetic Resonance Scanner (MRX)	Magnetic resonance proton precession	Effective (moveable) versus bound water-filled porosity, estimated hydraulic conductivity and relative flow capacity versus depth
Accelerator Porosity Sonde (APS)	Epithermal neutron porosity and neutron capture cross-section	Water/moisture content, lithologic variations
Array Induction Tool (AIT) and High Resolution Laterolog Array (HRLA)	Bulk electrical resistivity at multiple radial depths of investigation; spontaneous potential and borehole fluid resistivity	Stratigraphic delineation, relative permeability and water saturation from the borehole fluid invasion profile, clay content
Fullbore Formation Micro-Imager (FMI)	Fully-oriented electrical resistivity imaging	Bedding, geologic texture and structure, discrete fracture characterization; borehole diameter
Hostile Natural Gamma Spectroscopy (HNGS) and gross gamma ray (GR)	Gross and spectral natural gamma ray, including potassium, thorium, and uranium concentrations; log to log depth correlation	Rock matrix geochemistry, lithology and mineralogy
Litho Scanner (NEXT)	Neutron induced gamma ray spectroscopy	Weight fractions of rock forming elements; rock matrix geochemistry, lithology and mineralogy; pore fluid bulk chemistry

Once the Yellow Jacket Drilling Services well drilling project team provided Schlumberger final notification that CrEX-1 was ready for geophysical well logging, the Schlumberger Wireline district in Roswell, NM, mobilized a wireline logging truck, the appropriate wireline logging tools and associated equipment, and crew to the job site. Table 2 summarizes the geophysical logging runs performed in CrEX-1.

Table 2: Geophysical logging services, their combined tool runs and intervals logged, as performed by Schlumberger in well CrEX-1

Date of Logging	Run #	Tool 1 (bottom)	Tool 2	Tool 3 (top)	Depth Interval (ft bgs)
7-August-2014	1	APS	HNGS		200 – 1208
	2	AIT	NEXT	GR	200 – 1180
	3	FMI	GR		840 – 1210
	4	MRX	GR		858 – 1196
	5	AIT	HRLT	HNGS	200–1211 (HRLT top depth 816)

Preliminary results of these measurements were generated in the logging truck at the time the geophysical services were performed and are documented in field logs provided on site. However, the measurements presented in the field results are not fully corrected for borehole conditions (particularly air-filled casing), some require additional processing for full results (such as the FMI oriented electrical image), and are provided as separate, individual logs. The field results were reprocessed by Schlumberger Water Services to (1) correct/improve the measurements, as best as possible, for borehole/formation environmental conditions; (2) generate additional outputs through more refined workstation processing; (3) perform an integrated analysis of the log measurements so that they are all coherent and provide consistent hydrogeologic and geologic results; and (4) combine the logs in a single presentation, enabling integrated interpretation. Preliminary processing and analysis was performed during and

immediately after the logging to assist the LANL project team with design and completion of the extraction well. Comprehensive processing and analysis was performed afterwards. The reprocessed log results provide better quantitative property estimates that are consistent for all applicable measurements, as well as estimates of properties that otherwise could not be reliably estimated from the single measurements alone (e.g., hydraulic conductivity and transmissivity, moisture content and water saturation, lithology and mineralogy).

The geophysical log measurements from well CrEX-1 provide, overall, very good quality results, especially in the uncased section of the well (816–1210 ft, the zone of primary interest), that are consistent with each other across the logged interval. The cased hole section (0–816 ft at the time of logging) presented challenges for the geophysical measurements, primarily due to the existence, extent, and effect on the geophysical logs of a water or air-filled annulus between the casing and the borehole wall (voids behind the casing). Such voids are difficult to determine, especially without a bulk density log (not run because it requires a radioactive source) and, thus, there is uncertainty about how well some of the log measurements represent true geologic formation conditions (unaffected by drilling). The distance between the logging tool sensor and formation is unknown and, thus, difficult to account or correct for. The greatest impact on the log processing of the casing annulus was likely erroneously high water content in sections of the cased hole below the standing water level, particularly in the 580–794 ft interval of the basalt section and 794–807 ft top section of the alluvium/fanglomerate clastics, where water content is significantly higher than below and above (20 to 30% of total rock volume).

Additionally, without the bulk density measurement, total porosity in the vadose zone (which includes both water and air-filled porosity) is difficult to assess in open hole and impossible to evaluate in cased hole. Thus, in the cased hole section (above 816 ft), total porosity was set to a constant value for the integrated log analysis, as deemed appropriate for each major geologic unit and the geophysical measurement response.

Through the integrated analysis and interpretation of all the logs, the individual shortcomings of the specific measurements are reduced. Thus, the results derived from integrated log analysis (e.g., the optimized water-filled porosity log) are the most robust single representation of the geophysical log measurements—providing a wealth of valuable high-resolution information on the geologic and hydrogeologic environment of the CrEX-1 locale.

Important results from the processed geophysical logs in CrEX-1 include the following (also see well section in Figure 1):

1. The well standing water level in CrEX-1 was 611–616 ft bgs at the time of logging, dropping slightly between the first and the last logging runs.
2. The integrated log processing analysis indicates that the intersected geologic section is fully saturated with water from the bottom of the borehole (1211 ft bgs) to 974 ft bgs, which lies within alluvium/fanglomerate (Puye Formation). The volumetric water content log from the epithermal neutron porosity, as well as the relative hydrogen yield from the Litho Scanner, measure a significant decrease in water content at 974 ft. However, the estimates of water saturation from the magnetic resonance logs indicate water saturation doesn't decrease significantly until 940 ft and above. The spontaneous potential (SP) log sometimes is sensitive to water saturation, which shows an SP shift at 974 ft, but a bigger shift at 93 ft.

   Below 1032 ft the log estimated water content mostly matches the total porosity computed from integrated log analysis, resulting in an estimated water saturation of 100% or close to it (relative to pore space volume) – although without the bulk density log, there is limited information on total porosity. Between 985 and 1032 ft there are zones where the estimated water saturation drops below 75% (985–1005 ft, 1022–1032 ft), but it increases back to 100% from 974 to 985 ft, suggesting the decrease in

water saturation in these lower zones could be due to the difficulty in estimating total porosity without a bulk density log.

Based on these processed log results, the depth of the Regional Aquifer water level (depth at which there is full water saturation) is most likely 974 ft, but possibly as high as 940 ft.

3. Above 974 ft bgs, the estimated water content ranges 7–15% of total rock volume up to 807 ft. Water/moisture content is elevated in the overall interval 580–807 ft, reaching as high as 30% at 586 ft and 743 ft and greater than 20% in the zones 584–595 ft, 616–700 ft, 743–755 ft, and 788–805 ft. This zone is mostly in the lower two thirds of the basalt volcanics section in the well and at the bottom of the temporary casing emplaced in the borehole at the time to prevent borehole collapse and seal off water inflow from perched water zones. Thus, it is quite likely the water measured by the geophysical logs is trapped water behind this casing and/or bentonite grout. The top part of the basalt section (462–580 ft) has much lower measured moisture content, less than 10% (mostly less than 5%).

   Above 460 ft there were two strings of temporary casing in the hole at the time of geophysical logging, a very challenging well environment for quantitative borehole geophysical measurements. However, the processed geophysical logs provide reasonable rock property estimates, including moisture content, in this section, which is comprised of the Bandelier Tuff with the Guaje Pumice Bed at bottom. The results indicate the highest moisture content in the bottom of the Guaje (13%) with uniform or slightly decreasing moisture above (5 to 9%). This corresponds closely with the log results in other LANL wells.

4. The hydraulic conductivity estimate and relative flow profile generated from the processed magnetic resonance logs and integrated log analysis indicate that almost all of the well productive potential is in the lower Puye Formation fanglomerate, extending from 1054 ft to 1150 ft bgs, where the estimated hydraulic conductivity is mostly in the range 1 to 50 ft/day and the total and effective porosity ranges 32–40% and 20–33%, respectively. The most productive zone is 1054–1074 ft (50% of estimated total well production potential), followed by 1125–1140 ft (25% of well production potential) and 1074–1125 ft (20%). Between 974 ft and 1054 ft (top of the Regional Aquifer) the estimated hydraulic conductivity is one to two orders of magnitude lower (0.01 to 0.1 ft/day) and total and effective porosity ranges 20–25% and 0–10%, respectively. From 1150 ft to 1195 ft (bottom of the logged interval) the estimated hydraulic conductivity ranges 0.1 to 1 ft/day and total and effective porosity ranges 15–30% and 10–15%, respectively.

5. The geophysical log results clearly delineate that the bottom saturated/water-filled section of the borehole consists of clastic sediments (alluvium/fanglomerate) that extend up to 794 ft, likely comprising the Puye Formation. The integrated log analysis provides a quantitative mineral and pore space evaluation that clearly distinguishes subunits of the alluvium/fanglomerate – (1) an upper unit (794–1053 ft) with a grain density of 2.55 to 2.6 grams per cubic centimeter (g/cc), that is highly heterogeneous, poorly sorted, and not well bedded (as seen on the high resolution electrical resistivity borehole image); (2) a slightly more silica and silica glass rich and iron-deficient middle unit (1053–1143 ft) with a grain density of 2.47 to 2.52 g/cc, that is significantly more finely bedded/laminated, likely comprising the pumiceous unit of the Puye; (3) a more iron and clay-rich bottom section (1143–1185 ft, bottom of logged interval) with a grain density of 2.55 to 2.6 g/cc.

   At the top of the alluvium/fanglomerate (794 ft) there is a very distinct rock matrix geochemical change with high iron and titanium, consistent higher calcium, and low thorium and potassium, dry weight concentrations. This geochemical change translates to high augite and plagioclase feldspar, the

presence of magnetite, and negligible quartz, mineral content from the integrated log analysis with a grain density of 2.85 to 3.05 g/cc – likely corresponding to basalt lava that extends up to 462 ft. The top of this lava sequence (462–616 ft) has a different geochemical signature, with even higher iron content that translates to an increase in magnetite content and higher grain density (2.9–3.05 g/cc compared to 2.85–2.95 g/cc for the lower lava section).

Overlying the lava sequence is the characteristic geochemical signature of the Guaje Pumice Bed unit of the Bandelier Tuff (430–462 ft), with high uranium, thorium and silicon, and low iron, weight concentrations. This results in very high estimated silica glass mineral content. Above 430 ft to the top of the logged section (200 ft) the geochemical signature is characteristic of volcanic tuff (likely Bandelier Tuff) with high thorium, potassium, and silicon, and low iron that translates to high silica glass (inclusive of cristobalite and tridymite) and potassium/plagioclase feldspar.

6. The interpreted planar bedding features across the electrically imaged interval 840–1207 ft bgs have fairly widely varying dip azimuths (direction beds are dipping towards), especially in the upper fanglomerate (upper Puye) interval above 1053 ft that is not well bedded, compared to the fanglomerate interval below (lower pumiceous Puye) that is finely bedded/laminated in many sections. The lower interval has predominant bedding dip azimuths to the south and southeast, with all bedding dip angles (angle relative horizontal) less than 20 degrees (mostly less than 10 degrees). The bedding in the upper interval is much more scattered, with dip azimuths mostly varying northeast to southwest and bedding dip angles mostly less than 20 degrees (higher angles likely cross bedding).

   No fractures were identified across the imaged interval.

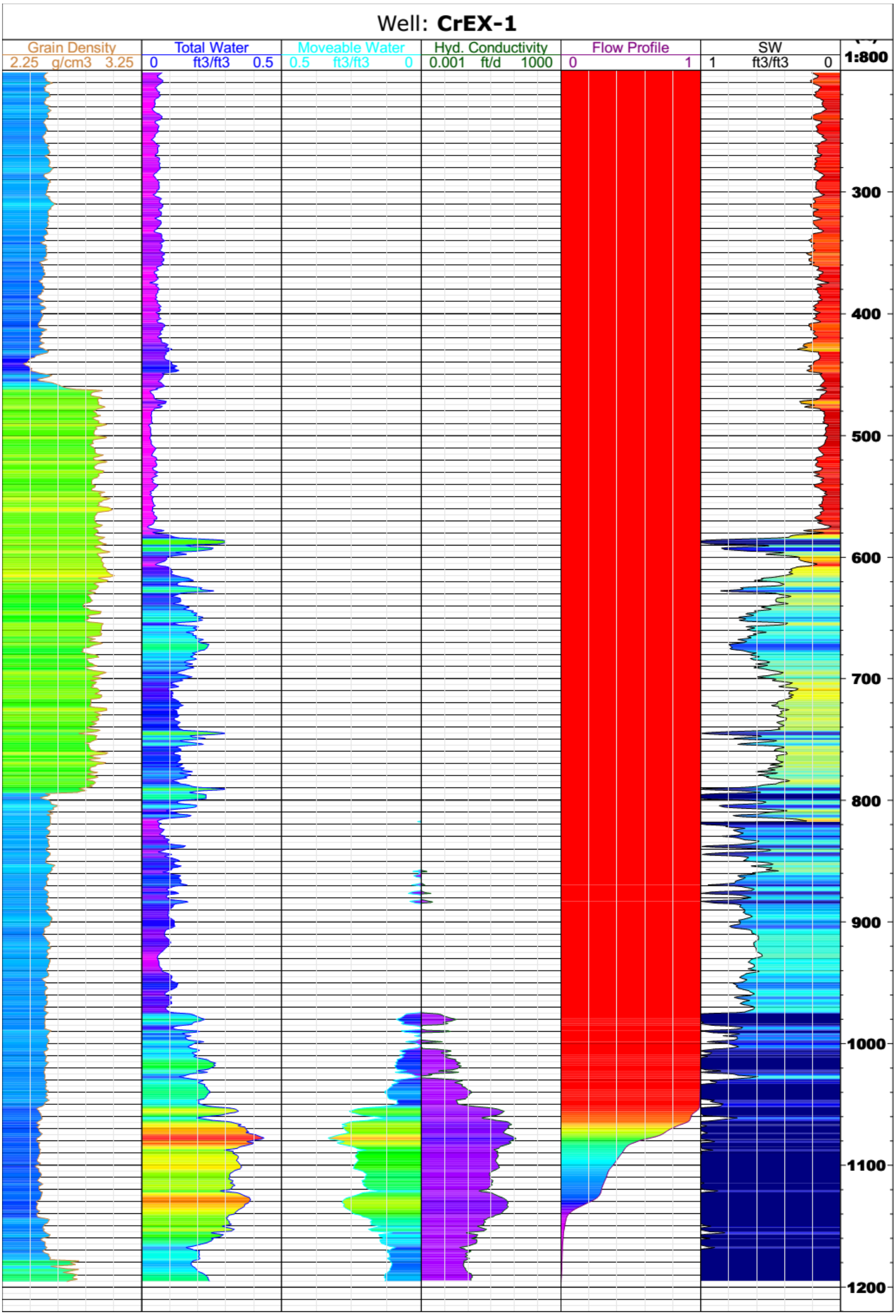

Figure 1: Well section of CrEX-1 displaying key processed hydrogeologic property logs (from left to right – grain density, total water-filled porosity, effective water-filled porosity, hydraulic conductivity [on log scale of 10^{-3} to 10^{3} feet per day], relative flow potential profile, and water saturation

1 INTRODUCTION

Geophysical logging services were performed in extraction well CrEX-1 by Schlumberger in August 2014 before initial well completion. The purpose of these services was to acquire in-situ measurements to help characterize the near-borehole geologic formation environment. The primary objective of the geophysical logging was to provide in-situ evaluation of formation properties (hydrogeology and geology) intersected by the well. This information was used by scientists, engineers, and project managers in the LANL environmental program to help design the well completion, to better understand subsurface site conditions, and assist in overall decision-making.

The primary geophysical logging tools used by Schlumberger in well CrEX-1 were the following:

- Magnetic Resonance (MR) Scanner (MRX) tool, which measures, in water or air-filled uncased hole, the nuclear magnetic resonance response of the formation to evaluate water volumes and moveability at multiple radial depths of investigation – used to estimate in-situ pore size distribution, total and effective water-filled porosity, and hydraulic conductivity;
- Array Porosity Sonde (APS), which measures, through casing and in water or air-filled hole, volumetric water content of the formation at several depths of investigation to evaluate moist/porous zones using a pulsed epithermal neutron measurement, as well as neutron capture cross section, which is sensitive to water and lithology;
- Array Induction Tool (AIT) and High Resolution Laterolog Array (HRLA), which measure formation electrical resistivity at five depths of investigation and borehole fluid resistivity to evaluate drilling fluid invasion into the formation (a qualitative indicator of permeability, also valuable for determining water saturation), presence of moist zones far from the borehole wall, and presence of clay-rich zones;
- Formation Micro-Imager (FMI) tool, which measures electrical conductivity images of the borehole wall in fluid-filled open-hole and borehole diameter with a two-axis caliper to evaluate geologic bedding and fracturing, including strike and dip of these features and fracture apertures, and rock/sediment texture;
- Hostile Natural Gamma Spectroscopy (HNGS) tool, which measures gross natural gamma and spectral natural gamma ray activity, including potassium, thorium, and uranium concentrations, to evaluate geology/lithology, particularly the amount of thorium and potassium-bearing minerals;
- Litho Scanner (NEXT) tool, which measures neutron induced gamma ray spectroscopy providing quantitative relative yields and weight fractions of a large suite of rock forming elements; rock matrix geochemistry, lithology and mineralogy;

Calibrated gross gamma ray (GR) was recorded with every service for the purpose of correlating depths between the different logging runs. Table 3 summarizes the geophysical logging runs performed in CrEX-1.

Table 3: Geophysical logging services, their combined tool runs and intervals logged, as performed by Schlumberger in borehole CrEX-1

Date of Logging	Borehole Status	Run #	Tool 1 (bottom)	Tool 2	Tool 3 (top)	Depth Interval (ft bgs)
7-August-2014	Uncased hole below 816 ft drillied with a bit size of 14.75 in. 16 in. steel casing from surface to 816 ft and 18 in. from surface to 460 ft	1	APS	HNGS	GR	200 – 1208
		2	AIT	NEXT		200 – 1180
		3	FMI	GR		840 – 1210
		4	MRX	GR		858 – 1196
		5	AIT	HRLT	GR	200–1211 (HRLT top depth 816)

A more detailed description of these geophysical logging tools can be found on the Schlumberger website (http://www.slb.com/content/services/evaluation/index.asp).

2 METHODOLOGY

This section describes the methods Schlumberger employed for geophysical logging of Well CrEX-1, including the following stages/tasks:

- Measurement acquisition at the well site
- Quality assessment of logs
- Reprocessing of field data

2.1 Acquisition Procedure

Once the well drilling project team notified Schlumberger that CrEX-1 was ready for geophysical well logging, the Schlumberger district in Roswell, NM, mobilized a wireline logging truck, the appropriate wireline logging tools and associated equipment, and crew to the job site. Upon arriving at the LANL site, the crew completed site-entry paperwork and received a site-specific safety briefing.

After arriving at the well site, the crew proceeded to rig up the wireline logging system, including:

1. Parking and stabilizing the logging truck in a position relative to the borehole that was best for performing the surveys
2. Setting up a lower and an upper sheave wheel (the latter attached to, and hanging above, the borehole from the drilling rig)
3. Threading the wireline cable through the sheaves
4. Attaching to the end of the cable the appropriate sonde(s) for the first run

Next, pre-logging checks and any required calibrations were performed on the logging sondes, and the tool string was lowered into the borehole. The tool string was lowered to the bottom of the borehole and brought up at the appropriate logging speed as measurements were made.

Upon reaching the surface, post-logging measurement checks were performed as part of log quality control and assurance. The tool string was cleaned as it was pulled out of the hole, separated, and disconnected.

The second tool string was attached to the cable for another logging run, followed by subsequent tool strings and logging runs. After the final logging run was completed, the cable and sheave wheels were rigged down.

Before departure, the logging engineer printed field logs and created a compact disc containing the field log data for on-site distribution and sent the data via satellite to the Schlumberger data storage center. The Schlumberger Water Services data processing center was alerted that the data were ready for post-acquisition processing.

2.2 Log Quality Control and Assessment

Schlumberger has a thorough set of procedures and protocols for ensuring that the geophysical logging measurements are of very high quality. This includes full calibration of tools when they are first built, regular recalibrations and tool measurement/maintenance checks, and real-time monitoring of log quality as measurements are made. Indeed one of the primary responsibilities of the logging engineer is to ensure, before and during acquisition, that the log measurements meet prescribed quality criteria.

A tool-specific base calibration that directly relates the tool response to the physical measurement using the designed measurement principle is performed on all Schlumberger logging tools when first assembled in the engineering production centers. This is accomplished through a combination of computer modeling and controlled measurements in calibration models with known chemical and physical properties.

The base calibration for most Schlumberger tools is augmented through regular "master calibrations" typically performed every one to six months in local Schlumberger shops (such as Farmington, NM), depending on tool design. Master calibrations consist of controlled measurements using specially designed calibration tanks/jigs and internal calibration devices that are built into the tools, both with known physical properties. The measurements are used to fine-tune the tool's calibration parameters and to verify that the measurements are valid.

In addition, on every logging job, before and after on-site "calibrations" are executed for most Schlumberger tools directly before/after lowering/removing the tool string from the borehole. For most tools, these represent a measurement verification instead of an actual calibration used to confirm the validity of the measurements directly before acquisition and to ensure that they have not drifted or been corrupted during the logging job.

All Schlumberger logging measurements have a number of associated depth-dependent quality control (QC) logs and flags to assist with identifying and determining the magnitude of log quality problems. These QC logs are monitored in real-time by the logging engineer during acquisition and are used in the post-acquisition processing of the logs to determine the best processing approach for optimizing the overall validity of the property estimates derived from the logs.

Additional information on specific tool calibration procedures can be found on the Schlumberger web page (http http://www.slb.com/content/services/evaluation/index.asp).

The geophysical log measurements from well CrEX-1 provide, overall, very good quality results, especially in the uncased section of the well (816–1210 ft, the zone of primary interest), that are consistent with each other across the logged interval. The cased hole section (0–816 ft at the time of logging) presented challenges for the geophysical measurements, primarily due to the existence, extent, and effect on the geophysical logs of a water or air-filled annulus between the casing and the borehole wall (voids behind the casing). Such voids are difficult to determine, especially without a bulk density log (not run because it requires a radioactive source) and, thus, there is uncertainty about how well some of the log measurements represent true geologic formation conditions (unaffected by drilling). The distance between the logging tool sensor and formation is unknown and, thus, difficult to account or correct for. The greatest impact on the log processing of the casing annulus was likely erroneously high water content in sections of the cased hole below the standing water level, particularly in the 580–794 ft interval of the basalt section and 794–807 ft top section of the alluvium/fanglomerate clastics, where water content is significantly higher than below and above (20 to 30% of total rock volume).

Additionally, without the bulk density measurement, total porosity in the vadose zone (which includes both water and air-filled porosity) is difficult to assess in open hole and impossible to evaluate in cased hole. Thus, in the cased hole section (above 816 ft), total porosity was set to a constant value for the integrated log analysis, as deemed appropriate for each major geologic unit and the geophysical measurement response.

Through the integrated analysis and interpretation of all the logs, the individual shortcomings of the specific measurements are reduced. Thus, the results derived from integrated log analysis (e.g., the optimized water-filled porosity log) are the most robust single representation of the geophysical log measurements—providing a wealth of valuable high-resolution information on the geologic and hydrogeologic environment of the CrEX-1 locale.

2.3 Processing Procedure

After the geophysical logging job was completed in the field and the data was archived, the data was downloaded to the Schlumberger processing center. There, the data were processed in the following sequence: (1) the measurements were corrected for near-wellbore environmental conditions and the measurement field processing for certain tools (in this case the CMR) was redone or refined using better processing algorithms and parameters, (2) the log curves from different logging runs were depth matched and spliced, and (3) the near-wellbore substrate lithology/mineralogy and pore fluids were modeled through integrated log analysis. Separately, the FMI electrical image was processed to produce scaled and normalized high-resolution images that were interpreted to identify geologic features and compute fracture apertures. Afterwards, an integrated log montage was built to combine and compile all the processed log results.

2.3.1 Environmental Corrections and Raw Measurement Reprocessing

If required, the field log measurements were processed to correct for conditions in the well, including fluid type (water or air), presence of steel casing, and (to a much lesser extent) pressure, temperature, and fluid salinity. Basically, these environmental corrections entail subtracting from the measurement response the known influences of the set of prescribed borehole conditions. In CrEX-1, the log measurements requiring these corrections are the APS porosities and neutron capture cross section, HNGS spectral gamma ray logs, and Litho Scanner elemental relative yields and dry weights.

Two neutron porosity measurements are available – one that measures thermal ("slow") neutrons, and one that measures epithermal ("fast") neutrons. Measurement of epithermal neutrons is required to make neutron porosity measurements in air-filled holes. In water/mud-filled holes, both the epithermal and thermal neutron measurements are valid. The APS makes epithermal porosity measurements. In CrEX-1 the borehole was partly water-filled (below ~611 ft during the logging) and partly air-filled (above 611 ft), as well as cased above 816 ft. The APS measurements were reprocessed for casing, borehole fluid type (air versus water), and other environmental conditions. The APS also makes a measurement of neutron capture cross section; this measurement was also corrected for well environmental conditions at the time of logging.

The HNGS spectral gamma ray is affected by the material (fluid, air, and casing) in the borehole because different types and amounts of these materials have different gamma ray shielding properties; the HNGS measures incoming gamma rays emitted by radioactive elements in the formation surrounding the borehole. The processing algorithms try to correct for the damping influence of the borehole material. The HNGS logs from CrEX-1 were reprocessed to fully account for the environmental effects of the borehole fluid (water below ~611 ft and air above), casing (above 816 ft), and hole size.

The raw Litho Scanner elemental yield measurements include the contribution of iron from steel casing. The processing consists of subtracting this unwanted contribution from the raw normalized iron yield, then performing the normal elemental yields-to-weight fraction processing. The contribution to subtract is a constant baseline amount (or zoned constant values if there are bit/casing size changes), usually determined by comparing the normalized raw yields in zones directly below/above the borehole casing/fluid change. Casing corrections were applied to the Litho Scanner logs across the entire log interval, attempting to account for one string of steel casing below 460 ft and above 816 ft, and two strings above 460 ft. A similar approach was used to correct the hydrogen yield for standing water in the well so that the corrected hydrogen yield is primarily sensitive to water in the formation.

The measurements cannot be fully corrected for borehole washouts or casing annulus since the specific characteristics (e.g., geometry) of these features are unknown and their effects on the measurements are often too significant to account for. Thus, the compromising effects of these conditions on the measurements should be accounted for in the interpretation of the log results.

2.3.2 Depth-Matching

Once the logs were environmentally corrected for the conditions in the borehole and the raw measurement reprocessing was completed, the logs from different tool runs were depth-matched to each other, as needed, using the gross gamma ray log, acquired in all the logging runs, for depth correlation, or other logs that are well correlated (e.g., porosity). The depth reference for all field prints and processed logs, including those presented in this report, is ground surface.

2.3.3 Integrated Log Analysis

An integrated log analysis, using as many of the processed logs as possible, was performed to model the near-wellbore substrate lithology/mineralogy and pore fluids. This analysis was performed using the Elemental Log Analysis (ELAN*) program (Juneer and Sibbit, 1980; Quieren et al, 1986) – a petrophysical interpretation program designed for depth-by-depth quantitative formation evaluation from borehole geophysical logs. ELAN estimates the volumetric fractions of user-defined rock matrix and pore constituents at each depth based on the known log measurement responses to each individual constituent by itself. ELAN requires an a priori specification of the volume components present within the formation, i.e., fluids, minerals, and rocks. For each component, the relevant response parameters for each measurement are also required. For example, if one assumes that quartz is a volume component within the formation and the bulk density tool is used, then the bulk density parameter for this mineral is well known to be 2.65 grams per cubic centimeter (g/cc).

As many processed logging tool measurements as possible were used in the ELAN analysis, including the Litho Scanner re-normalized elemental yields for Fe, Si, Ca, S, Al, Na, Mg, Ti, Mn and H, which, along with the HNGS concentrations, providing strong support for quantitative mineral evaluation using a comprehensive mineral suite appropriate for the geology. In the uncased interval (below 816 ft) an invasion model was used that distinguishes between the log response in the near borehole where drilling fluid invasion occurs and the univaded formation, enabling characterization of the total porosity where air has been replaced by water/fluid in the invased zone. The MR Scanner free fluid volume was used to evaluate water-filled effective porosity, while the APS volumetric water content and the Litho Scanner hydrogen yield.

The final results of the analysis – an optimized mineral-fluid volume model – are shown on the integrated log montage (see Attachment 1), 6th track from the right (inclusive of the depth track). In addition, the ELAN program provides a direct comparison of the modeled versus the actual measured geophysical logs, as well as a composite log of all of the key ELAN-derived results, including geologic/hydrogeologic properties computed from the mineral-fluid volume model (see Attachment 2). To make best use of all the measurement data and to perform the analysis across as much of the well interval as possible (200 to 1,195 ft bgs), as many as possible of the processed logs were included in the analysis, with less weighting applied to less robust logs. Not all of the tool measurements are used for the entire interval analyzed, as not all the measurements are available, or of good quality, across certain sections of the borehole. To accommodate fewer tool measurements, certain model constituents are removed from the analysis in some intervals. Most notably, above 858 ft bgs moveable/free water had to be removed from the analysis because no MRX measurement is available (MRX has the only measurement that is independently sensitive to

moveable and bound water independently) and above 816 ft total porosity had to be set since not enough information is available from the measurements to infer (in particular bulk density is not available).

The ELAN analysis was performed with as few constraints or prior assumptions as possible. A considerable effort was made to choose a set of minerals or mineral types for the model that is representative of Los Alamos area geology and its volcanic origins. For the ELAN analysis, the log interval from 200 to 462 ft bgs was assumed to be tuff or pumice, and a mineral suite considered representative of this volcanic tuff, based on LANL cuttings mineral analysis, was used (primary "minerals" silica glass/cristobalite/tridymite [indistinguishable from the log measurements], quartz, potassium feldspar, plagioclase feldspar; secondary minerals hematite and augite). The results of laboratory analyses of Bandelier Tuff and Puye Formation samples from around the LANL site were also used to constrain the proportion of quartz versus the combination of glass/cristobalite/tridymite in the ELAN analysis. The log interval 794–1195 ft bgs were assumed to be Puye fanglomerate and a mineral suite considered as representative of this geology as possible, based on LANL cuttings mineral analysis of the Puye, was used (primary "minerals" silica glass/cristobalite/tridymite [indistinguishable from the log measurements], potassium feldspar, plagioclase feldspar; quartz at a defined small fraction of the silica glass content; possible secondary minerals montmorillinite clay and augite; and constrained small amounts of biotite and hematite).

No prior assumption is made about water saturation—where the boundary between saturated and unsaturated zones lies (e.g., the depth to the top of the regional aquifer or perched zones). There were no measurements in the open-hole logging suite specifically sensitive to air-filled or total porosity (bulk density which could not be acquired in uncased potable aquifer because the tool requires a radioactive source). However, the deep-reading bulk resistivity measurement from the HRLA tool was found to be sensitive to total porosity and water content, especially when combined and contrasted with shallow-reading resistivity measurements affected by drilling/borehole fluids. Above 816 ft there was not enough measurement sensitivity to total porosity – thus an arbitrary, albeit realistic, total porosity was chosen. In addition, water was not included in the analysis above 206 ft bgs, as mentioned above, because there are no log measurements sensitive to water above that depth. There is no way to objectively correct for the adverse effect on the log measurements from casing annulus; therefore the decision was made to perform the ELAN analysis so as to primarily honor the log measurements (other than the porosity constraints). Accordingly, interpretations should be made from the ELAN results with the understanding that the mineral-fluid model represents a mathematically optimized solution that is not necessarily a physically accurate representation of the native geologic formation. Within this context, the ELAN model is a robust estimate of the bulk mineral-fluid composition that accounts for the combined response from all the geophysical measurements.

3 RESULTS

Preliminary results from the wireline geophysical logging measurements acquired by Schlumberger in CrEX-1 were generated in the logging truck at the time the geophysical services were performed and were documented in the field logs provided on site. However, the measurements presented in the field results are not fully corrected for undesirable influence (from a measurement standpoint) of borehole and geologic conditions and are provided as separate, individual logs. The field log results have been processed (1) to correct/improve the measurements, as best as possible, for borehole/formation environmental conditions, and (2) to ensure that all the logs from different tool runs are on depth. Additional logs were generated from integrated analysis of processed measured logs, providing valuable estimates of key geologic and hydrologic properties.

The processed log results are presented as continuous curves of the processed measurement versus depth and are displayed as (1) a one-page, compressed summary log display for selected directly related sets of measurements (see Figures 3.1 and 3.2); (2) an integrated log montage that contains all the key processed log curves, on depth and side by side (see Attachment 1); and (3) an expanded scale composite log of the processed and interpreted FMI electrical resistivity image log, also containing other useful log results for high resolution interpretation (see Attachment 3). The summary log displays address specific characterization needs, such as porosity, production capacity, moisture content, water saturation, and lithologic changes. The purpose of the integrated log montage is to present, side by side, all the most salient processed logs and log-derived models, depth-matched to each other, so that correlations and relationships between the logs can be identified. The electrical image composite log provides a very high resolution visual representation of the geologic section, including characterization of rock/sediment texture and fracturing.

Important results from the processed geophysical logs in CrEX-1 are described below.

3.1 Well Fluid Level

The well standing water level in CrEX-1 was 611–616 ft bgs at the time of logging, dropping slightly between the first and the last logging runs.

3.2 Regional Aquifer

The integrated log processing analysis indicates that the intersected geologic section is fully saturated with water from the bottom of the borehole (1211 ft bgs) to 974 ft bgs, which lies within alluvium/fanglomerate (Puye Formation). The volumetric water content log from the epithermal neutron porosity, as well as the relative hydrogen yield from the Litho Scanner, measure a significant decrease in water content at 974 ft. However, the estimates of water saturation from the magnetic resonance logs indicate water saturation doesn't decrease significantly until 940 ft and above. The spontaneous potential (SP) log sometimes is sensitive to water saturation, which shows an SP shift at 974 ft, but a bigger shift at 93 ft.

Below 1032 ft the log estimated water content mostly matches the total porosity computed from integrated log analysis, resulting in an estimated water saturation of 100% or close to it (relative to pore space volume) – although without the bulk density log, there is limited information on total porosity. Between 985 and 1032 ft there are zones where the estimated water saturation drops below 75% (985–1005 ft, 1022–1032 ft), but it increases back to 100% from 974 to 985 ft, suggesting the decrease in water saturation in these lower zones could be due to the difficulty in estimating total porosity without a bulk density log.

Based on these processed log results, the depth of the Regional Aquifer water level (depth at which there is full water saturation) is most likely 974 ft, but possibly as high as 940 ft.

The hydraulic conductivity estimate and relative flow profile generated from the processed magnetic resonance logs and integrated log analysis indicate that almost all of the well productive potential is in the lower Puye Formation fanglomerate, extending from 1054 ft to 1150 ft bgs, where the estimated hydraulic conductivity is mostly in the range 1 to 50 ft/day and the total and effective porosity ranges 32–40% and 20–33%, respectively. The most productive zone is 1054–1074 ft (50% of estimated total well production potential), followed by 1125–1140 ft (25% of well production potential) and 1074–1125 ft (20%). Between 974 ft and 1054 ft (top of the Regional Aquifer) the estimated hydraulic conductivity is one to two orders of magnitude lower (0.01 to 0.1 ft/day) and total and effective porosity ranges 20–25% and 0–10%, respectively. From 1150 ft to 1195 ft (bottom of the logged interval) the estimated hydraulic conductivity ranges 0.1 to 1 ft/day and total and effective porosity ranges 15–30% and 10–15%, respectively.

3.3 Vadose Zone Perched Water

As mentioned above, the depth to the top of the Regional Aquifer and, thus, the extent of the vadose zone most likely extends from 974 ft bgs to ground surface. Above 974 ft bgs, the estimated water content ranges 7–15% of total rock volume up to 807 ft. Water/moisture content is elevated in the overall interval 580–807 ft, reaching as high as 30% at 586 ft and 743 ft and greater than 20% in the zones 584–595 ft, 616–700 ft, 743–755 ft, and 788–805 ft. This zone is mostly in the lower two thirds of the basalt volcanics section in the well and at the bottom of the temporary casing emplaced in the borehole at the time to prevent borehole collapse and seal off water inflow from perched water zones. Thus, it is quite likely the water measured by the geophysical logs is trapped water behind this casing and/or bentonite grout. The top part of the basalt section (462–580 ft) has much lower measured moisture content, less than 10% (mostly less than 5%).

Above 460 ft there were two strings of temporary casing in the hole at the time of geophysical logging, a very challenging well environment for quantitative borehole geophysical measurements. However, the processed geophysical logs provide reasonable rock property estimates, including moisture content, in this section, which is comprised of the Bandelier Tuff with the Guaje Pumice Bed at bottom. The results indicate the highest moisture content in the bottom of the Guaje (13%) with uniform or slightly decreasing moisture above (5 to 9%). This corresponds closely with the log results in other LANL wells.

3.4 Geology

The geophysical log results clearly delineate that the saturated/water-filled section of the borehole consists of clastic sediments (alluvium/fanglomerate) that extends up to 794 ft bgs, likely comprising the Puye Formation. The integrated log analysis provides a quantitative mineral and pore space evaluation that clearly distinguishes subunits of the alluvium/fanglomerate:

- an upper unit (794–1053 ft) with a grain density of 2.55 to 2.6 grams per cubic centimeter (g/cc), that is highly heterogeneous, poorly sorted, and not well bedded (as seen on the high resolution electrical resistivity borehole image);
- a slightly more silica and silica glass rich and iron-deficient middle unit (1053–1143 ft) with a grain density of 2.47 to 2.52 g/cc, that is significantly more finely bedded/laminated, likely comprising the pumiceous unit of the Puye;

- a more iron and clay-rich bottom section (1143–1185 ft, bottom of logged interval) with a grain density of 2.55 to 2.6 g/cc.

At the top of the alluvium/fanglomerate (794 ft) there is a very distinct rock matrix geochemical change with high iron and titanium, consistent higher calcium, and low thorium and potassium, dry weight concentrations. This geochemical change translates to high augite and plagioclase feldspar, the presence of magnetite, and negligible quartz, mineral content from the integrated log analysis with a grain density of 2.85 to 3.05 g/cc – likely corresponding to basalt lava that extends up to 462 ft. The top of this lava sequence (462–616 ft) has a different geochemical signature, with even higher iron content that translates to an increase in magnetite content and higher grain density (2.9–3.05 g/cc compared to 2.85–2.95 g/cc for the lower lava section).

Overlying the lava sequence is the characteristic geochemical signature of the Guaje Pumice Bed unit of the Bandelier Tuff (430–462 ft), with high uranium, thorium and silicon, and low iron, weight concentrations. This results in very high estimated silica glass mineral content. Above 430 ft to the top of the logged section (200 ft) the geochemical signature is characteristic of volcanic tuff (likely Bandelier Tuff) with high thorium, potassium, and silicon, and low iron that translates to high silica glass (inclusive of cristobalite and tridymite) and potassium/plagioclase feldspar.

The interpreted planar bedding features across the electrically imaged interval 840–1207 ft bgs have fairly widely varying dip azimuths (direction beds are dipping towards), especially in the upper fanglomerate (upper Puye) interval above 1053 ft that is not well bedded, compared to the fanglomerate interval below (lower pumiceous Puye) that is finely bedded/laminated in many sections. The lower interval has predominant bedding dip azimuths to the south and southeast, with all bedding dip angles (angle relative horizontal) less than 20 degrees (mostly less than 10 degrees). The bedding in the upper interval is much more scattered, with dip azimuths mostly varying northeast to southwest and bedding dip angles mostly less than 20 degrees (higher angles likely cross bedding). No fractures were identified across the imaged interval.

3.5 Summary Logs

Two summary log displays have been generated for CrEX-1 to highlight the key hydrogeologic and geologic information provided by the processed geophysical log results:

- Hydrogeology summary log showing continuous hydrogeologic property logs, including total porosity (water and air), water-filled porosity, moveable water content, water saturation, estimated hydraulic conductivity, transmissivity, and relative producibility (flow capacity); highlights key hydrologic information obtained from the integrated log results (Figure 2, also displayed on an expanded scale in Attachment 2)
- Geochemical and lithology/mineralogy summary showing a high vertical resolution, continuous volumetric analysis of formation elemental geochemistry and mineral composition (based on an integrated analysis of the logs), and lithologic/stratigraphic correlation logs from the spectral gamma ray measurement (concentrations of gamma-emitting elements); highlights the geologic lithology, stratigraphy, and correlation information obtained from the log results (Figure 3, also displayed on an expanded scale in Attachment 2)

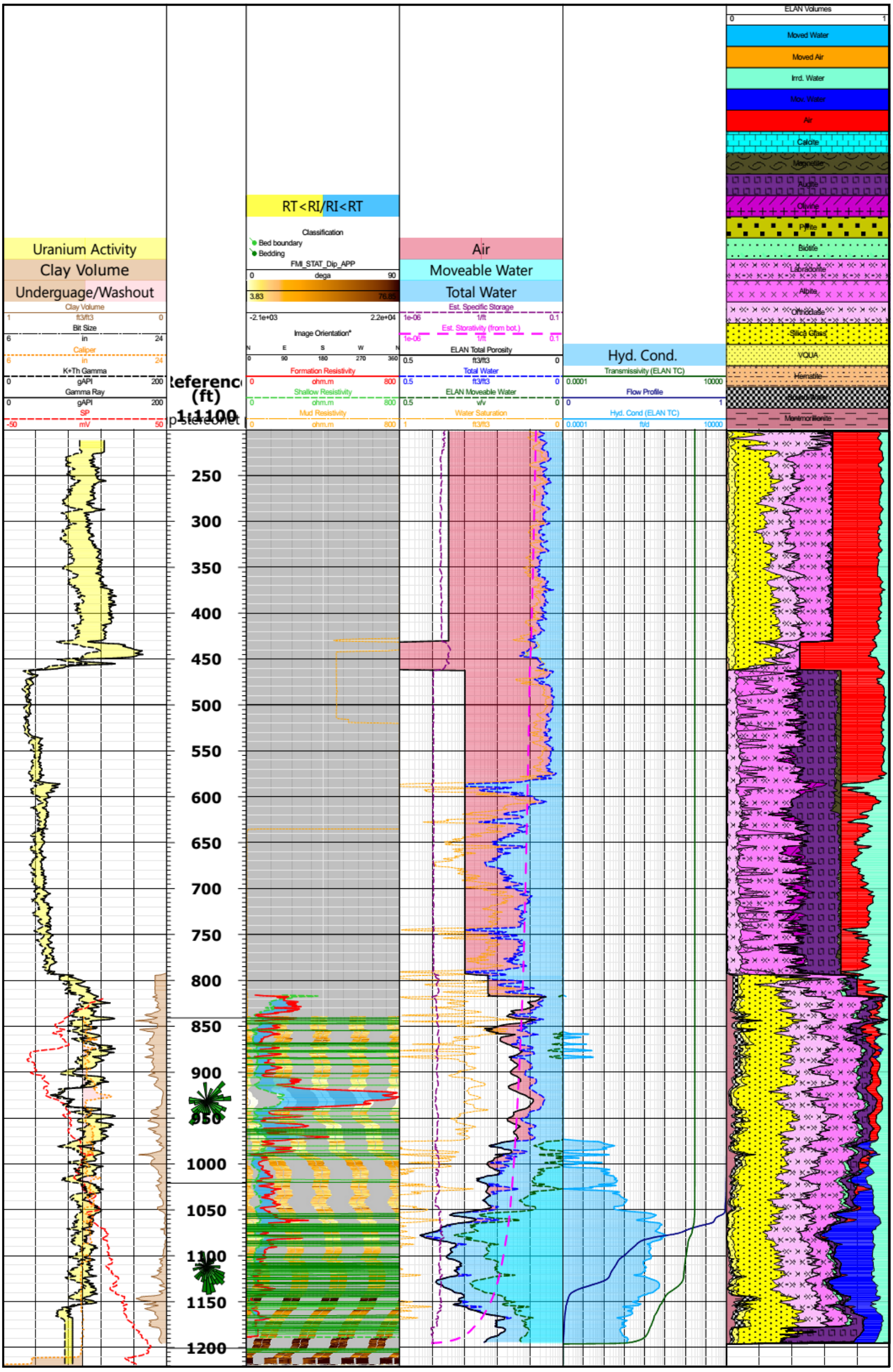

Figure 2: CrEX-1 hydrogeology summary log composite from processed advanced geophysical logging results. Displayed logs are described in detail in following section.

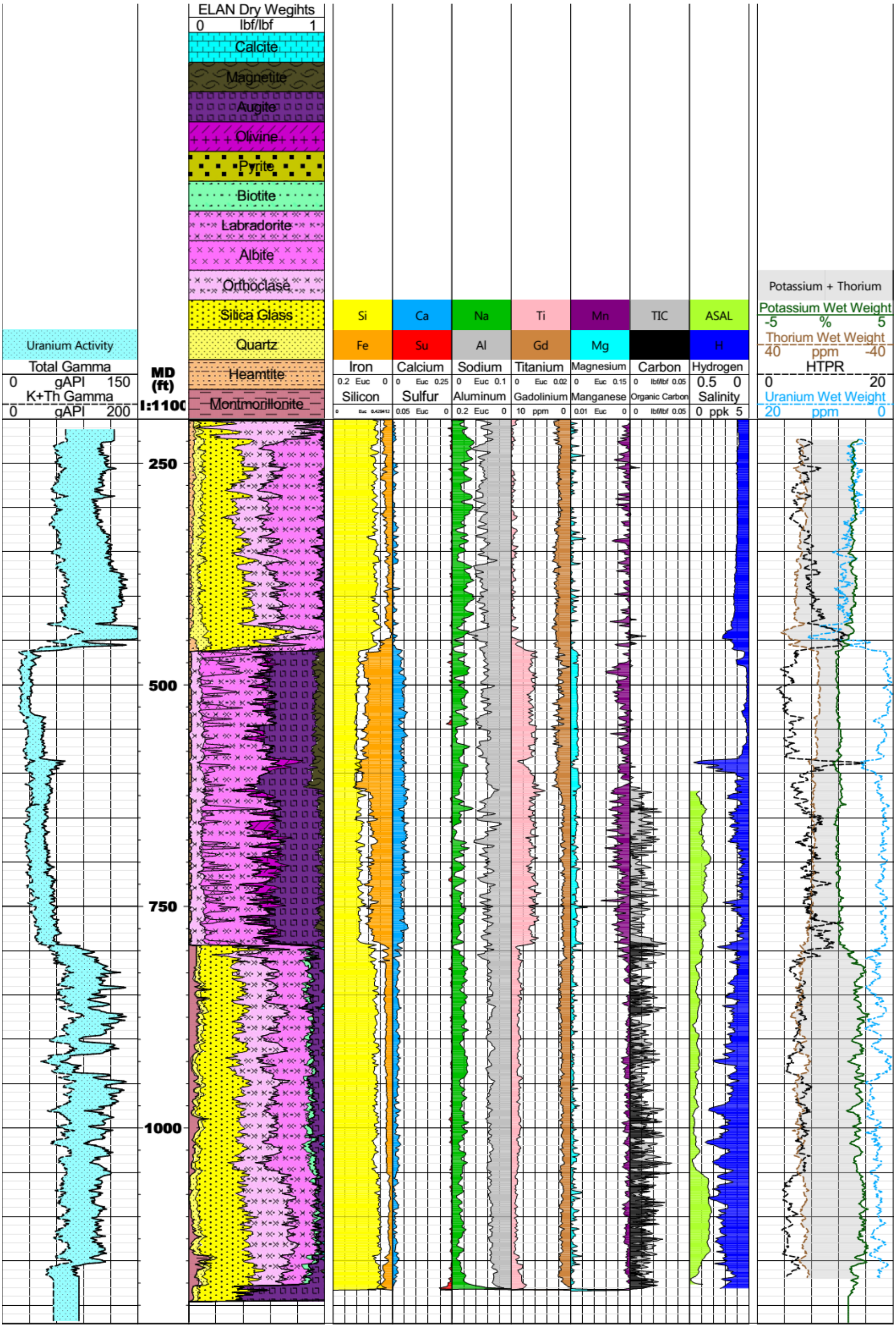

Figure 3: CrEX-1 geochemistry summary log composite from processed advanced geophysical logging results. Displayed logs include HNGS gamma ray spectroscopy (1st track on the left and last on the right), ELAN mineral dry weights model (right of depth track), and Litho Scanner elemental dry weights and hydrogen and chlorine wet concentrations.

3.6 Description of Hydrogeology Summary Log Composite

Specific processed geophysical log results displayed in the hydrogeology summary log composite for the CrEX-1 well shown in Figure 2 are described below.

Track 1 – Basic and Correlation Logs

The first track on the left presents a number of basic and correlation log curves:

- spectroscopy gross gamma ray (thick solid black curve), total gamma ray response from the natural gamma ray spectroscopy tool, recorded in American Petroleum Institute gamma ray standard units (gAPI) and displayed on a scale of 0 to 125 gAPI units;
- spectroscopy thorium and potassium gamma ray (dashed black curve), thorium plus potassium gamma ray response from the natural gamma ray spectroscopy tool with uranium contribution highlighted (yellow shading between this and the total gamma ray curves), recorded in American Petroleum Institute gamma ray standard units (gAPI) and displayed on a scale of 0 to 125 gAPI units;
- caliper from the FMI micro-resistivity tool (dotted orange curve) with borehole washout (pink shading) and borehole undergauge (brown shading) highlighted, recorded as hole diameter in inches and displayed on a scale of 6 to 16 in.;
- spontaneous potential or SP from the AIT tool (long-dashed red curve), recorded in units of millivolts (mV) and displayed on a relative wrapping scale spanning 100 mV (increasing from left to right);
- total clay volume estimate from the ELAN integrated log analysis (thin solid brown curve with brown shading), recorded in units of volumetric fraction (ratio of cubic feet per cubic feet [ft^3/ft^3]) and displayed on a scale of 1 to 0 ft^3/ft^3 (left to right)

Track 2 – Depth

The second track from the left contains the depth below ground surface in units of feet, as measured by the geophysical logging system during the FMI logging run. Also displayed are fanplots of the bedding dip azimuth (direction beds/laminations are dipping towards).

Track 3 – Electrical Resistivity Borehole Image and Resistivity Logs

The third track from the left displays electrical resistivity-based log measurements:

- high resolution formation electrical resistivity image from the FMI electrical imaging tool (underlying brown toned image), scaled to the bulk formation resistivity measurement from the AIT induction resistivity tool with lighter tones corresponding to higher resistivity and darker tones to lower resistivity;
- bulk formation resistivity from HRLA resistivity tool for the invaded zone (RXO) and univaded zone beyond drilling fluids invasion green (RT, “true” formation reesistivity), recorded in units of ohm-meters (ohm.m) and displayed on a linear scale of 0 to 800 ohm-m, with the area between RXO and RT resistivity curves shaded yellow when RT is greater than RXO (labeled “RI<RT”) and blue when RXO is greater than RT (labeled “RT<RI”).
- wellbore fluid resistivity from the HRLA, displayed on a linear scale of 0 to 800 ohm.m

Track 4 – Porosity and Storage Property Logs

The fourth track from the left displays key groundwater storage related log curves derived from the processed geophysical measurements:

- total porosity estimate from the ELAN integrated log analysis (solid dark grey curve with red shading representing air volume), recorded in units of volumetric fraction (ratio of cubic feet per cubic feet [ft^3/ft^3]) and displayed on a scale of 0.5 to 0 ft^3/ft^3 (left to right);
- total water estimate from the ELAN integrated log analysis (dashed blue curve with blue shading), recorded in units of volumetric fraction (ratio of cubic feet per cubic feet [ft^3/ft^3]) and displayed on a scale of 0.5 to 0 ft^3/ft^3 (left to right);
- effective water-filled porosity (moveable/free water content) estimate from the ELAN integrated log analysis (light blue solid curve with cyan shading), recorded in units of volumetric fraction (ratio of cubic feet per cubic feet [ft^3/ft^3]) and displayed on a scale of 0.5 to 0 ft^3/ft^3 (left to right);
- specific storage estimate (long-dashed maroon curve), computed from total porosity and mineralogy results from the ELAN integrated log analysis, as well as Sonic Scanner compressional and shear velocity analysis, the latter used to estimate bulk compressibility of the formation, recorded in units of inverse feet (1/ft) and displayed on a logarithmic scale of 1e-06 to 0.1 1/ft (left to right);
- cumulative storativity estimate from the bottom to the top of the main aquifer zone (long-dashed violet curve) computed by integrating the specific storage log, depth-by-depth, from bottom to top (i.e., the reported value at each depth is the storativity of the interval extending from the bottom to that depth, albeit it is also computed in the unconfined sections of the well), recorded in non-dimensional units of (ft/ft) and displayed on a logarithmic scale of 1e-06 to 0.1 (left to right);
- water saturation estimate from the ELAN integrated log analysis (thin solid orange curve), recorded in units of volumetric pore fraction (ratio of cubic feet per cubic feet [ft^3/ft^3]) and displayed on a scale of 1 to 0 ft^3/ft^3 (left to right).

Track 5 – Flow Capacity and Water Salinity Logs

The fifth track from the left displays key groundwater flow capacity and water quality related log curves derived from the processed geophysical measurements:

- hydraulic conductivity estimate (solid light blue curve with light blue shading) computed using the Timur-Coates equation with the inputs total and effective water-filled porosity (free water content) logs from the ELAN integrated log analysis, recorded in units of feet per day (ft/day) and displayed on a logarithmic scale of 0.0001 to 10,000 ft/day;
- cumulative relative water flow (flow profile) estimate from the bottom to the top of the log interval, normalized to 1, that mimic a flow meter (spinner) acquired under flowing conditions (blue line coming from left-hand side at bottom of log interval), computed by integrating the ELAN Timur-Coates estimate of hydraulic conductivity, recorded in non-dimensional units of fraction of total flow and displayed on a linear scale of 0 to 1;
- cumulative transmissivity estimate from the bottom to the top of the log interval (solid maroon curve) computed by integrating the ELAN Timur-Coates estimate estimate of hydraulic conductivity, depth-by-depth, from bottom to top (i.e., the reported value at each depth is the transmissivity of the interval

extending from the bottom to that depth), recorded in units of feet squared per day (ft^2/day) and displayed on a logarithmic scale of 0.0001 to 10,000 ft^2/day;

Track 6 – ELAN Integrated Log Analysis Lithology and Pore Volumes

The track furthest to the right displays matrix mineralogy/lithology and pore fluid results from the ELAN integrated log analysis – presented as wet mineral and pore fluid volume fractions and recorded in units of volume of mineral/pore fluid per volume of total formation volume (V/V):

- Montmorillinite clay (brown with black hatches)
- Clay-bound water (stippled checkboard pattern)
- Hematite (orange with small black dots)
- Quartz (yellow with closely spaced small black dots)
- Combined silica glass, tridymite, and cristobalite (yellow with widely spaced large black dots)
- Orthoclase or other potassium feldspar (lavender with black xx)
- Albite (dark pink with black xx)
- Labradorite (pink with black xx)
- Biotite (light green with small black dots)
- Pyrite (yellow-green with black squares)
- Olivine (maroon with hash and plus marks)
- Augite (purple with outlined squares)
- Magnetite (dark olive with arcs)
- Calcite (blue with outlined rectangles)
- Air (red)
- Moveable Water (dark blue)
- Capillary-bound (irreducible) water (light blue)
- Moved air (orange)
- Moved water (light blue)

4 REFERENCES

Juneer, C. and A. Sibbit, 1980. “GLOBAL, A New Approach to Computer-Processed Log Interpretation.” Paper SPE 9341 presented at the 1980 SPE Annual Technical Conference and Exhibition.

Quirein, J., S. Kimminau, J. LaVigne, J. Singer, and F. Wendel. 1986. “A Coherent Framework for Developing and Applying Multiple Formation Evaluation Models.” Paper DD in 27th Annual Logging Symposium Transactions: Society of Professional Well Log Analysts.

5 REPORT LIMITATIONS

This report has been prepared for the specific purpose identified herein at the request of and for the use of the Client. Observations, conclusions, and recommendations contained herein are opinions based upon the scope of services, information obtained through observations and measurements taken by Schlumberger Water Services (Schlumberger) at certain points and certain times, and interpretation and extrapolation of secondary information from published and unpublished material. The report may infer the configuration of strata, ground and groundwater conditions both between data points and below the maximum depth of investigation. The report also may deduce temporal trends and averages for climatic, hydrological and water quality parameters. Such interpretations and extrapolations are only indicative and no liability is accepted for variations between the opinions expressed herein and conditions which may be identified at a later date through direct measurement and observation.

Unless otherwise agreed in writing by Schlumberger, Schlumberger accepts no responsibility for any use of, or reliance on any contents of this report by any person other than Client and shall not be liable to any person other than Client, on any ground, for any loss, damage or expense arising from such use or reliance.

Should any information contained in this report be used by any unauthorized third party, it is done so at their own risk.

APPENDIX A: DESCRIPTION OF INTEGRATED LOG MONTAGE PRESENTATION

INTEGRATED LOG MONTAGE

The following section provides a detailed description of the specific log results displayed in the integrated log montage for well CrEX-1 (color print of the montage is provided in Attachment 1). The log presentation is divided into vertical tracks containing grids, with the vertical axis corresponding to depth below ground surface and the horizontal axis corresponding to the scale for displayed log properties – independent for each log curve. The following descriptions are organized according to the tracks in the log presentations, characterizing the individual log curves displayed in each track – starting from the furthest left track and continuing track by track to the right.

Track 1–Depth

The first track on the left displays the depth below ground surface in units of feet, as measured by the geophysical logging system during the FMI-GR logging run. All the geophysical logs are depth-matched to the gross gamma log acquired with this logging run.

Track 2–Borehole Geometry and Correlation Logs

The second track from the left presents a number of measured borehole geometry and basic correlation log curves:

- spectroscopy total gamma ray (bold solid black curve), total gamma ray response from the natural gamma ray spectroscopy tool, recorded in American Petroleum Institute gamma ray standard units (gAPI) and displayed on a scale of 0 to 200 gAPI;
- gross gamma ray minus the contribution from uranium thorium plus potassium gamma ray response from the natural gamma ray spectroscopy tool (dotted black curve), with uranium contribution to total gross gamma highlighted (yellow shading between this and the total gamma ray curves), recorded in American Petroleum Institute gamma ray standard units (gAPI) and displayed on a scale of 0 to 200 gAPI;
- spontaneous potential or SP (bold long-dashed red curve), measured with the AIT resistivity tool, recorded in millivolts and displayed on a relative scale (increasing from left to right);
- single arm caliper from the MCFL micro-resistivity tool (dotted orange curve) with borehole washout/rugosity (pink shading) highlighted, recorded as hole diameter in inches and displayed on a scale of 14 to 19 in;
- two orthogonal calipers from the FMI electrical imaging tool (thin dotted black curves) with drilling bit size as a reference (thin short-dashed black line) to show borehole washout/rugosity (pink shading) and orange shading between the two caliper curves to show borehole ovality, recorded as hole diameter in inches and displayed on a scale of 14 to 19 in.;
- neutron capture cross section from the APS (green), recorded in standard capture units (cu) and displayed on a scale of 0 to 50 cu (left to right). in.

Track 3–Electrical Resistivity Measurements

The third track from the left displays the electrical resistivity measurements from the HRLT high resolution laterolog array resistivity tool. All the resistivity logs are recorded in units of ohmmeters (ohm.m) and are displayed on a linear scale of 0 to 800 ohm.m. The eight resistivity logs from that are displayed are:

- formation resistivity (bold red line);
- flushed zone resistivity (dashed green) with shading between flushed zone resistivity and formation resistivity representing radial variations in bulk resistivity (potentially from invasion of drilling fluids)- yellow shading where flushed zone resistivity is less than formation resistivity (labeled "RI<RT") and blue shading where formation resistivity is less than flushed zone resistivity (labeled "RT<RI");
- formation resistivity at five median radial depths of investigation(RLA1 as the shallowest reading to RLAS 5 as the deepest reading) - RLA1 (blue), RLA2 (light blue), RLA3 (green), RLA4 (orange), RLA5 (thin red) ; –
- borehole fluid resistivity (dashed orange).

Track 4–Pore Volume Evaluation Logs

The fourth track from the left displays the processed pore volume logs, all recorded in units of volumetric fraction (ratio of cubic feet per cubic feet [ft^3/ft^3]) and displayed on a scale of 0.6 to 0 ft^3/ft^3 (left to right):

- APS slowing down time porosity derived from pulsed neutron time series in the array detectors (orange curve) – shallowest reading and highest vertical resolution epithermal neutron porosity from APS tool, processed for zoned air-filled and water-filled open/cased hole;
- APS epithermal neutron porosity derived from near-far detector pairing in water-filled hole and array-far detector pairing in air-filled hole (solid dark green curve);
- total porosity from the ELAN integrated log analysis (black dotted curve), includes all pore water, clay-bound water, and air- yellow shading indicates air filled porosity;
- total water-filled porosity estimate from the ELAN integrated log analysis (dashed dark pink);
- clay bound water-filled porosity (immoveable water) estimate from the ELAN integrated log analysis, delineated as the difference between the total water-filled porosity and non-clay bound porosity estimates (dark blue shading between the total water-filled porosity and non-clay bound porosity logs);
- non-clay bound water-filled porosity estimate from the ELAN integrated log analysis, delineated as the difference between the non-clay bound water-filled porosity and moveable water-filled porosity estimates (light blue shading between the non-clay bound water-filled porosity and moveable water-filled porosity logs);
- effective water-filled porosity (moveable water) estimate from the ELAN integrated log analysis (dark green dashed curve with light green shading);
- magnetic resonance total water-filled porosity (water content) from the MRX magnetic resonance tool (light pink curve), derived from the 4.0" DOI reading from both MRX runs (first run is the solid curve, second run is the dashed curve);

- magnetic resonance moveable water content (effective water-filled porosity) from the MRX magnetic resonance tool (light green), derived from the 4.0" DOI reading from both MRX runs (first run is the solid curve, second run is the dashed curve).

Track 5–Magnetic Resonance Primary Porosity Measurements

The fifth track from the left displays the primary processed porosity logs from the MRX magnetic resonance scanner tool, all recorded in units of volumetric fraction (ratio of cubic feet per cubic feet [ft^3/ft^3]) and displayed on a scale of 0.5 to 0 ft^3/ft^3 (left to right):

- magnetic resonance mid total water-filled porosity (grey curves- long dash for run 1, short dash for run 2) – representing the total water volume fraction measured by the magnetic resonance tool, derived from the 4" DOI, T1 relaxation distribution;
- magnetic resonance deepest total water-filled porosity (black curves- solid for run 1, dash for run 2) – representing the total water volume fraction measured by the magnetic resonance tool, derived from the 4.0" DOI, T1 relaxation distribution;
- magnetic resonance deep 3 millisecond (ms) porosity (brown curves- long dash for run 1, short dash for run 2) – representing the water volume fraction corresponding to the portion of the magnetic resonance tool measured T1 distribution, derived from the 2.7" DOI, that is above 3 ms, a cutoff that is considered to be generally representative of the break between clay-bound water (less than 3 ms) and all other types of water (greater than 3 ms);
- effective water-filled, or free-fluid, porosity (pink curves- solid for run 1, dash for run 2) – representing the water volume fraction that is moveable (can flow), derived from the 4.0" DOI and based on a 50 ms T1 distribution cutoff that is considered representative of the break between bound water (less than defined cutoff value) and moveable water (greater than defined cutoff), displayed on the same scale as the total water-filled porosity log;
- clay-bound water (brown area shading between deep total and 3 ms porosity logs) – representing the magnetic resonance tool apparent water volume fraction that is bound within clays;
- capillary-bound water (tan area shading between 3 ms and effective porosity logs) – representing the magnetic resonance tool apparent water volume fraction that is bound within matrix pores by capillary forces.

Track 6–Magnetic Resonance, Deep Pore Size Distribution

The sixth track from the left displays the water-filled pore size distribution as determined by the MRX magnetic resonance tool T1 distribution, 4.0" DOI, measurement – shown as cumulative binned water-filled porosities. The binned porosity logs are presented on a volume fraction scale of 0.5 to 0 cubic feet per cubic feet [ft^3/ft^3] with colored area shading corresponding to the different bins:

- apparent clay-bound water (brown area shading);
- apparent "silt"-bound water, micro-pore and small-pore water, the sum comprising capillary-bound water (tan, gray and blue area shading, respectively);
- apparent medium-pore, large-pore, and late-decay, the sum comprising effective water-filled porosity (yellow, red, green, and cyan area shading, respectively).

Track 7–Magnetic Resonance, Deep Relaxation Distribution (Waveforms)

The seventh track from the left displays the MRX magnetic resonance tool T1 distribution, 4.0" DOI, as green waveform traces at discrete depths. The T1 distribution corresponds to the measured bulk water hydrogen proton relaxation time series response, recorded as normalized amplitude of response (higher waveform peaks [green shading] corresponding to higher amplitude) versus relaxation time. The latter is displayed on a logarithmic scale from 1 to 9000 milliseconds (ms), with fast (short) relaxation time on the left (corresponding to small pores/bound water) and slow (long) relaxation time on the right (corresponding to large pores/moveable water). Also plotted on the same time scale are the:

- T1 distribution logarithmic mean (blue curves- solid for run 1, dash for run 2);
- T1 distribution cutoff time used for differentiating between bound and moveable/free water (dashed red line) – chosen based on the character of the T1 distribution (location of peaks and troughs) and the standard cutoff used for sand-silt-clay clastic environments, based on field/core measurements from around the world.

Track 8–Magnetic Resonance, Deep Relaxation Distribution (Heated Amplitude Image)

The eighth track from the left displays the MRX magnetic resonance tool T1 distribution, 4.0" DOI, as a heated color image. The T1 distribution corresponds to the measured bulk water hydrogen proton relaxation time series response, recorded as normalized amplitude of response (hotter colors corresponding to higher amplitude) versus relaxation time. The latter is displayed on a logarithmic scale from 1 to 9000 milliseconds (ms), with fast (short) relaxation time on the left (corresponding to small pores/bound water) and slow (long) relaxation time on the right (corresponding to large pores/moveable water). Also plotted on the same time scale are the:

- T1 distribution logarithmic mean (black curves- solid for run 1, dash for run 2);
- T1 distribution cutoff time used for differentiating between bound and moveable/free water (dashed red line) – chosen based on the character of the T1 distribution (location of peaks and troughs) and the standard cutoff used for sand-silt-clay clastic environments, based on field/core measurements from around the world.

Track 9–Magnetic Resonance, Mid-range Relaxation Distribution (Waveforms)

The ninth track from the left displays the MRX magnetic resonance tool T1 distribution, 2.7" DOI, as green waveform traces at discrete depths. The T1 distribution corresponds to the measured bulk water hydrogen proton relaxation time series response, recorded as normalized amplitude of response (higher waveform peaks [green shading] corresponding to higher amplitude) versus relaxation time. The latter is displayed on a logarithmic scale from 1 to 9000 milliseconds (ms), with fast (short) relaxation time on the left (corresponding to small pores/bound water) and slow (long) relaxation time on the right (corresponding to large pores/moveable water). Also plotted on the same time scale are the:

- T1 distribution logarithmic mean (blue curves- solid for run 1, dash for run 2);
- T1 distribution cutoff time used for differentiating between bound and moveable/free water (solid red line) – chosen based on the character of the T1 distribution (location of peaks and troughs) and the standard cutoff used for sand-silt-clay clastic environments, based on field/core measurements from around the world.

Track 10–Magnetic Resonance, Mid-range Relaxation Distribution (Heated Amplitude Image)

The tenth track from the left displays the MRX magnetic resonance tool T1distribution, 1.5" DOI, as a heated color image. The T1 distribution corresponds to the measured bulk water hydrogen proton relaxation time series response, recorded as normalized amplitude of response (hotter colors corresponding to higher amplitude) versus relaxation time. The latter is displayed on a logarithmic scale from 1 to 9000 milliseconds (ms), with fast (short) relaxation time on the left (corresponding to small pores/bound water) and slow (long) relaxation time on the right (corresponding to large pores/moveable water). Also plotted on the same time scale are the:

- T1 distribution logarithmic mean (black curves- solid for run 1, dash for run 2);
- T1 distribution cutoff time used for differentiating between bound and moveable/free water (solid black line) – chosen based on the character of the T1distribution (location of peaks and troughs) and the standard cutoff used for sand-silt-clay clastic environments, based on field/core measurements from around the world.

Track 11–Magnetic Resonance, Mid-range Pore Size Distribution

The eleventh track from the left displays the water-filled pore size distribution as determined by the MRX magnetic resonance tool T1 distribution, 2.7" DOI, measurement – shown as cumulative binned water-filled porosities. The binned porosity logs are presented on a volume fraction scale of 0.5 to 0 cubic feet per cubic feet [ft^3/ft^3] with colored area shading corresponding to the different bins:

- apparent clay-bound water (brown area shading);
- apparent "silt"-bound water, micro-pore and small-pore water, the sum comprising capillary-bound water (tan, gray and blue area shading, respectively);
- apparent medium-pore, large-pore, and late-decay, the sum comprising effective water-filled porosity (yellow, red, green, and cyan area shading, respectively).

Track 12–Magnetic Resonance Mean Grain Size Indicator

The twelfth track from the left displays apparent mean grain size derived empirically from the MRX magnetic resonance tool measurement of the relaxation distribution T1 and T2 logarithmic mean. First, mean pore size is computed using a surface-to-volume ratio petrophysical model that assumes spherical grains and employs empirical coefficients. Then the mean pore size estimate is converted to a mean grain size estimate using a least squares regression fit from a petroleum reservoir-based core database. The coefficients in the pore size estimator are qualitatively scaled to produce a range of mean grain sizes that seemed reasonable across the depth section of the well. Thus, at best, the presented mean grain size indicator log depicts relative mean grain size variations. A quantitative magnetic resonance grain size estimator could be established by locally calibrating the empirical equations by statistically comparing magnetic resonance log results with (ideally) collocated sample grain size analyses.

Two mean grain size indicator logs are displayed:

- mean grain size from T2 logarithmic mean (solid curves- light tan run 1, dark tan run 2- with gold area shading containing regularly spaced black crosses) derived from the MR Scanner logarithmic mean of the measured T2 longitudinal relaxation distribution, recorded in millimeters (mm) and displayed on a logarithmic scale of 0.005 to 5 mm;

- mean grain size from T1 logarithmic mean (dashed curves- light tan run 1, dark tan run 2) derived from the MR Scanner logarithmic mean of the measured T1 transverse relaxation distribution, recorded in millimeters (mm) and displayed on a logarithmic scale of 0.005 to 5 mm.

Track 13– Magnetic Resonance Capillary Pressure Estimate

Track 13 displays a continuous-in-depth estimate of capillary pressure versus water saturation distribution derived from the MR Scanner magnetic resonance tool deep measurement (4.0 inch) of the T1 longitudinal relaxation distribution. The computation is based on a petrophysical model relating the magnetic resonance relaxation time to pore radius, in turn related to capillary pressure using the capillary tube model. In addition, a scaling factor is required to account for interfacial tension between the phases and the magnetic resonance surface relaxivity. A quantitative magnetic resonance capillary pressure distribution estimator could be established by locally calibrating the semi-empirical equation thru statistically comparison of the magnetic resonance log results with (ideally) collocated core/sample capillary pressure analyses. The following capillary pressure related logs are displayed:

- capillary pressure versus water saturation distribution from magnetic resonance T1 distribution (heated color image) with cooler colors corresponding to higher capillary pressure;
- entry capillary pressure from magnetic resonance T1 distribution (violet curve, solid for run 1 and dashed for run 2) corresponding to the entry (threshold) pressure from the estimated capillary pressure versus water saturation distribution and displayed on a linear scale of 1 to 0 ft3/ft3 (left to right).

Track 14– Hydraulic Conductivity and Transmissivity Log Estimates

Track 14 displays hydraulic conductivity and transmissivity estimates derived from the processed geophysical measurements, for the saturated zone and unsaturated zone (the latter corresponding to the hypothetical condition of fully-water saturated conditions from surface):

- Intrinsic hydraulic conductivity estimate (bold brown curve) computed using the Timur-Coates equation with the inputs total porosity and effective water-filled porosity (free water content) logs from the ELAN integrated log analysis, recorded in units of feet per day (ft/day) and displayed on a logarithmic scale of 1e-05 to 100,000 ft/day;
- ELAN Timur-Coates hydraulic conductivity estimate (bold solid dark blue curve with multi-color shading) computed using the Timur-Coates equation with the inputs total porosity and effective water-filled porosity (free water content) logs from the ELAN integrated log analysis, recorded in units of feet per day (ft/day) and displayed on a logarithmic scale of 1e-05 to 100,000 ft/day;
- ELAN mineral hydraulic conductivity estimate (dashed light blue curve) computed using ELAN results recorded in units of feet per day (ft/day) and displayed on a logarithmic scale of 1e-05 to 100,000 ft/day;
- K-Lambda magnetic resonance hydraulic conductivity estimate (short-dashed blue curve) computed using the magnetic resonance version of the K-Lambda equation with the inputs ELAN total water-filled porosity and T1 logarithmic mean logs from the MR Scanner tool, broadly calibrated for near-surface unconsolidated sediments, displayed on a logarithmic scale of 1e-05 to 100,000 ft/day;
- K-Lambda saturated/intrinsic hydraulic conductivity estimate (thin dotted-dashed purple curve) computed using the mineral version of the K-Lambda equation with the inputs ELAN mineral dry weights and total porosity, displayed on a logarithmic scale of 1e-05 to 100,000 ft/day;

- ELAN Timur-Coates cumulative transmissivity estimate from the bottom to the top of the log interval (bold solid dark green curve) computed by integrating the ELAN Timur-Coates equation estimate of hydraulic conductivity, depth-by-depth, from bottom to top (i.e., the reported value at each depth is the transmissivity of the interval extending from the bottom to that depth), recorded in units of squared feet per day (ft^2/day) and displayed on a logarithmic scale of 1e-05 to 100,000 ft^2/day;
- ELAN mineral cumulative transmissivity estimate from the bottom to the top of the log interval (short dashed light green curve) computed by integrating the ELAN mineral estimate of hydraulic conductivity, depth-by-depth, from bottom to top (i.e., the reported value at each depth is the transmissivity of the interval extending from the bottom to that depth), recorded in units of squared feet per day (ft^2/day) and displayed on a logarithmic scale of 1e-05 to 100,000 ft^2/day;
- K-Lambda cumulative saturated/intrinsic estimate from the bottom to the top of the log interval (thin dotted lime green curve) computed by integrating the K-Lambda mineral-based permeability estimate of saturated hydraulic conductivity, depth-by-depth, from bottom to top (i.e., the reported value at each depth is the saturated transmissivity of the interval extending from the bottom to that depth), displayed on a logarithmic scale of 1e-05 to 100,000 ft^2/day.

Area color shading has been applied from the left side of the track up to the ELAN Timur-Coates hydraulic conductivity estimate (considered the most reliable hydraulic conductivity estimate from the geophysical log measurements), with different colors corresponding to ranges of hydraulic conductivity with representative clastic grain sizes:

- Grey – clay hydraulic conductivity range (less than 1e-03 ft/day);
- Brown – silt hydraulic conductivity range (1e-03 to 0.1 ft/day);
- Orange – silty-sand hydraulic conductivity range (0.1 to 10 ft/day);
- Yellow – clean sand hydraulic conductivity range (10 to 1,000 ft/day);
- Blue – gravel hydraulic conductivity range (greater than 1,000 ft/day).

Track 15–Oriented Borehole Electrical Image (Dynamic Normalization) With Interpreted Features Overlain

Track 15 displays the fully processed and oriented FMI image, processed with dynamic normalization to amplify small-scale electrical resistivity features (e.g., geologic texture, bedding) for interpretation. (With dynamic normalization, the range of electrical resistivity amplitudes – colors in the image – is normalized across a small moving depth window.) The image is fully oriented and corresponds to an unwrapped cylindrical section of the formation just beyond the borehole wall, such that the left-hand side represents true north, half-way across the image is south, and the right-hand side is north again. The four color tracks in the image correspond to portions of the borehole wall contacted by the four FMI caliper pads; the blank space in between is the portion of the borehole wall not covered by the pads.

Track 16–Interpreted Features from the Borehole Electrical Image

Track 16 displays the interpreted planar features picked from the FMI image, shown in two ways:

- Individually, as tadpoles at the depths the bedding plane or fracture plane crosses the midpoint of the borehole – where the horizontal position of the "heads" (circles/triangles) represent the dip angle (true angle between a flat horizontal reference plane and the plane of the interpreted feature) on a tangential

scale of 0 to 90 degrees, and the angles of the "tails" (line segments) represent the true dip azimuth (direction the bed is dipping towards) where true north is to the top of the plot, south is to bottom, east to the right and west to the left. Interpreted bedding planes/laminations are shown as circular-headed dark green tadpoles and interpreted bed boundaries as circular-headed bright green tadpoles.

- Summed, as dip azimuth fan plot histograms (dark green diagonal hashed fan plots for bedding/laminations) – where the number of interpreted geologic features having a dip direction within a particular sector are summed and normalized, thus highlighting the predominant dip directions (true north is to the top of the plot, south is to bottom, east to the right and west to the left).

Track 17–Straightened Borehole Electrical Image (Static Normalization)

Track 17 displays the fully processed FMI image, processed with static normalization to highlight larger scale features (e.g., geologic beds) and trends. (With static normalization, the range of electrical resistivity amplitudes – colors in the image – is normalized across the entire length of the log interval.) The image corresponds to an unwrapped cylindrical section of the formation just beyond the borehole wall and is displayed as a straight image (no georeferenced orientation) to provide better visualization of overall structure. The four color tracks in the image correspond to portions of the borehole wall contacted by the four FMI caliper pads; the blank space in between is the portion of the borehole wall not covered by the pads.

Track 18–Natural Gamma Ray Spectroscopy Logs

Track 18 displays the key processed spectral results from the HNGS natural gamma ray spectroscopy tool:

- potassium wet weight concentration (solid green curve) recorded in units of percent (%) and displayed on a linear scale of -5 to 5% (left to right);
- thorium wet weight concentration (long-dashed brown curve) recorded in units of parts per million (ppm) and displayed on a scale of 40 to -40 ppm (left to right);
- uranium wet weight concentration (dashed-dotted blue curve) recorded in units of parts per million (ppm) and displayed on a scale of 20 to 0 ppm (left to right);
- thorium / potassium ratio (dashed black curve) reported in non-dimensional units and displayed on a linear scale of 0 to 20.

The area between the potassium and thorium logs is shaded grey to emphasize the relative changes in the overall concentration of both elements.

Tracks 19 to 25–Litho Scanner Elemental Weight Fractions

Tracks 19 to 25 display the elemental weight fractions estimated using the Litho Scanner elemental yields:

Track 19 displays the processed silicon and iron dry weights:

- silicon dry weight (yellow shading)
- iron dry weight (orange shading).

Track 20 displays the processed calcium and sulfur dry weights:

- calcium (blue shading)
- sulfur (red shading).

Track 21 displays the processed sodium and aluminum dry weights:

- sodium dry weight (green shading)
- aluminum dry weight (grey shading).

Track 22 displays the processed titanium and gadolinium dry weights:

- titanium dry weight (pink shading)
- gadolinium dry weight (brown shading).

Track 23 displays the processed magnesium and manganese dry weights:

- magnesium dry weight (purple shading)
- manganese dry weight (bright blue shading).

Track 24 displays the processed carbon and organic carbon dry weights:

- carbon dry weight (black shading)
- organic carbon dry weight (grey shading).

Track 25 displays the processed hydrogen and chlorine:

- hydrogen dry weight (dark blue shading)
- salinity (light green shading).

Track 26–ELAN Mineralogy Model Results (Dry Weight Fraction)

Track 26 displays the mineralogical results from the ELAN integrated log analysis (the matrix portion) – presented as dry-weight fraction of mineral types chosen in the model and recorded in units of pound of mineral per pound of total dry rock/sediment (lbf/lbf):

- Hematite (orange with small black dots)
- Quartz (yellow with closely spaced small black dots)
- Combined silica glass, tridymite, and cristobalite (yellow with widely spaced large black dots)
- Orthoclase or other potassium feldspar (lavender with black xx)
- Albite (dark pink with black xx)
- Labradorite (pink with black xx)
- Biotite (light green with small black dots)
- Pyrite (yellow-green with black squares)
- Olivine (maroon with hash and plus marks)
- Augite (purple with outlined squares)
- Magnetite (dark olive with arcs)
- Calcite (blue with outlined rectangles)

Track 27–ELAN Mineralogy and Pore Space Model Results (Wet Volume Fraction)

Track 27 displays the mineralogical results from the ELAN integrated log analysis – presented as wet mineral and pore fluid volume fractions and recorded in units of volume of mineral/pore fluid per volume of total formation volume (V/V):

- Montmorillinite clay (brown with black hatches)
- Clay-bound water (stippled checkboard pattern)
- Hematite (orange with small black dots)
- Quartz (yellow with closely spaced small black dots)
- Combined silica glass, tridymite, and cristobalite (yellow with widely spaced large black dots)
- Orthoclase or other potassium feldspar (lavender with black xx)
- Albite (dark pink with black xx)
- Labradorite (pink with black xx)
- Biotite (light green with small black dots)
- Pyrite (yellow-green with black squares)
- Olivine (maroon with hash and plus marks)
- Augite (purple with outlined squares)
- Magnetite (dark olive with arcs)
- Calcite (blue with outlined rectangles)
- Air (red)
- Moveable Water (dark blue)
- Capillary-bound (irreducible) water (light blue)
- Moved air (orange)
- Moved water (light blue)

Track 28–Estimated Geomechanical and Storage Property Logs

Track 28 displays a number of emulated formation geomechanical property logs, as well as continuous log estimates of groundwater storage capacity properties:

- bulk density estimate (dashed violet curve) computed from the ELAN integrated log analysis resultant mineral-pore fluid model, recorded in units of grams per cubic centimeter (g/cm^3) and displayed on a scale of 1.5 to 2.5 g/cm^3;
- synthetic formation bulk compressibility estimate (dashed red curve) computed from the ELAN integrated log analysis resultant mineral-pore fluid model using the Hill average moduli estimator with reference values for individual mineral compressibilities (Mavko et al, 1998), reported in units of inverse millions of pounds per square inch (1 E-06 1/psi) and displayed on a linear scale of 0 to 10 x 1 E-06 1/psi;
- specific storage estimate (bold solid green curve) computed from total porosity and mineralogy results from the ELAN integrated log analysis, the latter used to estimate bulk compressibility of the formation, recorded in units of inverse feet (1/ft) and displayed on a logarithmic scale of 1e-06 to 0.1 1/ft;

- cumulative storativity estimate from the bottom to the top of the log interval (short-dashed dark green curve) computed by integrating the specific storage log, depth-by-depth, from bottom to top (i.e., the reported value at each depth is the storativity of the interval extending from the bottom to that depth, albeit it is also computed in the unconfined and unsaturated sections of the well), recorded in non-dimensional units of (ft/ft) and displayed on a logarithmic scale of 1e-06 to 0.1.

Track 29–Predicted Relative Flow Profile

Track 29 displays an estimate of relative flow versus depth profile for the entire log interval:

- cumulative relative water flow estimate from the bottom to the top of the log interval, normalized to 1, that mimics a flow meter (spinner) log acquired under flowing conditions, computed by integrating the ELAN Timur-Coates estimate (bold solid blue curve coming from left-hand side at bottom of log interval with light blue background shading), ELAN mineral estimate (thin blue curve), ELAN K-Lambda estimate (dashed-dotted purple curve), and K-Lambda magnetic resonance estimate (solid light blue); recorded in non-dimensional units of fraction of total flow and displayed on a linear scale of 0 to 1.

Track 30–Water Saturation

Track 30 displays the continuous-in-depth water saturation logs estimated from the processed logs, recorded in units of volumetric fraction of pore space filled with water (ratio of cubic feet per cubic feet [ft3/ft3]) and presented on a scale of 0 to 1 ft3/ft3 (left to right).

- optimized estimate of water saturation (volumetric fraction of pore space filled with water) from the ELAN analysis (bold dashed-dotted purple curve with blue shading to the right and red shading to the left, corresponding to water-filled and air-filled pore space, respectively);
- entry capillary pressure from magnetic resonance T1 distribution (violet curve 4" DOI, pink curves 2.7" DOI, solid curves for run 1 and dashed curves for run 2) corresponding to the entry (threshold) pressure from the estimated capillary pressure versus water saturation distribution and displayed on a linear scale of 1 to 0 ft3/ft3 (left to right).

Track 31–Summary Logs Track

Track 31, the second track from the right, displays several summary logs that describe the fluid and air-filled volume measured by the geophysical tools:

- total volume fraction water estimate from the ELAN analysis (solid blue curve and blue plus green area shading);
- volume fraction moveable water (non-clay bound moveable water-filled porosity) estimate from the ELAN analysis (dashed cyan curve and green area shading);
- total volume fraction of air-filled porosity estimate from the ELAN analysis (black curve and red area shading);

The porosity and volumetric water content scales are from 0 to 0.5 total volume fraction, left to right.

Track 32–Depth

The furthest track to the right, the same as the first track on the left, displays the depth below ground surface in units of feet, as measured by the geophysical logging system during the FMI-GR logging run.

APPENDIX B: TECHNOLOGY DESCRIPTION OF SCHLUMBERGER GEOPHYSICAL LOGGING TOOLS USED IN CREX-1

Additional documentation for this Appendix:
LithoScanner_Brochure.PDF

MAGNETIC RESONANCE SCANNER (MR SCANNER*)

The MR-Scanner (MR Scanner) tool uses the nuclear magnetic resonance (NMR) technique to log subsurface porous formations and predict their producibility (Allen et al., 1997). The unique advantage that NMR provides is a measure of pore size distribution independent of lithology, without the requirement of radioactive source. In the water industry, NMR logging is focused on delineating "producing" from "non-producing" zones and further quantifying formation total versus effective porosity and hydraulic conductivity. In turn, this information can be used to determine proper well screen locations and optimal well yield for production or monitoring wells.

The MR-Scanner tool measures the total fluid-filled porosity and pore size distribution of the formation from which the bound and moveable water distribution and hydraulic conductivity are estimated. This is achieved by utilizing large permanent magnets (Figure B-1) that align the non-lattice bound hydrogen nuclei along a magnetic field. This process, called polarization, increases exponentially in time with a constant T1, which can be measured as a continuous log with the MR Scanner tool. A magnetic pulse from a radio frequency antenna in the MR Scanner tool rotates, or tips, the aligned protons into a plane perpendicular to the polarization. The protons, now aligned in a plane transverse to the polarization field, will start to precess around the direction of the field. The precessing protons sweep out oscillating magnetic fields like a radio antenna. Unique to the MR-Scanner is the multi antenna and multi frequency design (Figure B-1). The main antenna (18" vertical resolution) operates at multiple frequencies, enabling multiple depths of investigation of 1.5", 2.7", or 4" in a single logging pass. Also available are two high resolution antennas (7.5" vertical resolution) that operate at one single frequency, enabling one depth of investigation of 1.25". The main antenna operates at a frequency range of 1,000 to 500 kHz while the high resolution antenna range is near 1,100 kHz. The multiple depths of investigation are often referred to as shells, which correspond to independent measurement volumes that form concentric arcs in front of the antenna.

The MR Scanner tool employs a receiver connected to the same antennae used to induce the spin-flipping pulse to measure these magnetic fields. Ideally, the spinning protons continue to precess around the direction of the external magnetic field until they encounter an interaction that would change their spin orientation out of phase with others in the transverse direction—a transverse relaxation process. The time constant for the transverse relaxation process is called T2.

* Mark of Schlumberger

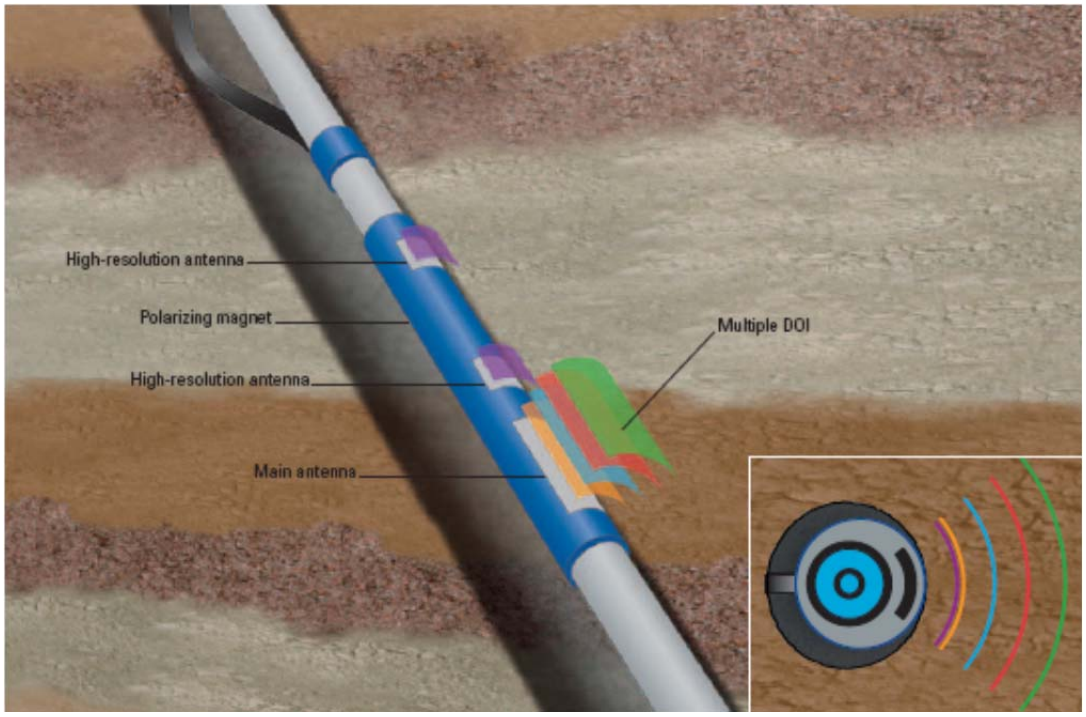

Figure B-1 MR-Scanner tool schematic with enlarged cross-section of the sensor.

The decay of the precessing signal is the heart of the NMR measurement and is a function of 1) the intrinsic bulk relaxation rate within the borehole fluid, 2) the grain surface relaxation rate, and 3) diffusion (Kenyon et al, 1995). Intrinsic bulk relaxation and diffusion are predominantly related to fluid viscosity and rock grain magnetic properties, while surface relaxation time is predominantly related to pore size.

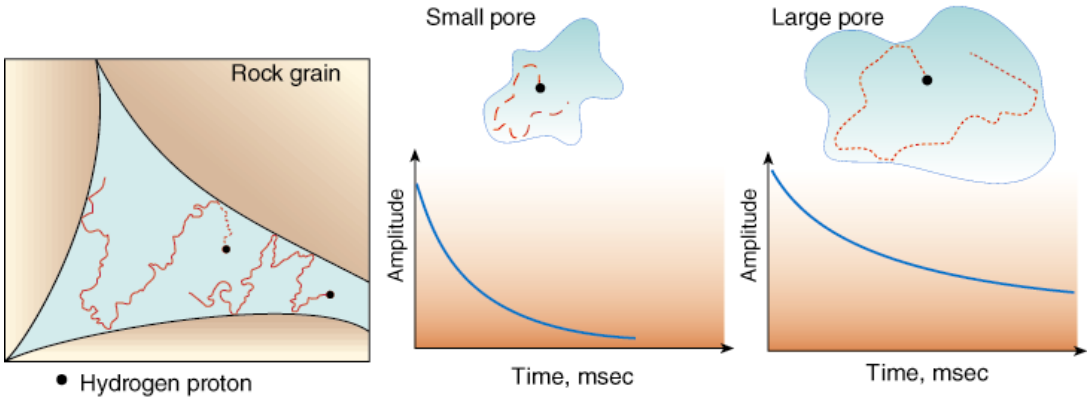

Figure B-2 MR-Scanner Grain surface relaxation as function of pore size.

In most porous formations, overall relaxation times depend on pore sizes (Figure B-2). Small pores shorten relaxation times—the shortest times corresponding to clay-bound and capillary-bound water. Large pores allow long relaxation times. Therefore, the distribution of relaxation times is a measure of the distribution of pore sizes (Figure

B-3). The total water-filled porosity is determined from the total area under the T2 distribution and particular pore size volumes are represented by fractions of the total area.

The relaxation time cutoffs in the T2 distribution between different pore size bins (e.g. producible versus bound water, capillary bound versus clay bound water) are determined empirically from laboratory NMR measurements of core, which have shown the cutoffs to be sharp and consistent. For example, the producible-bound water cutoff is determined by measuring the T2 distribution of a water saturated core, then removing producible water from the core using a centrifuge and re-measuring the T2 distribution (Figure B-4). The two T2 distributions are compared and the cutoff identified. Based on thousands of core measurements from geologic formations around the world, it has been determined that there are consistent cutoffs for different general geologic formation types. However, at least a few core analyses should be performed in a new area to verify the T2 distribution cutoffs – particularly the producible-bound fluid cutoff.

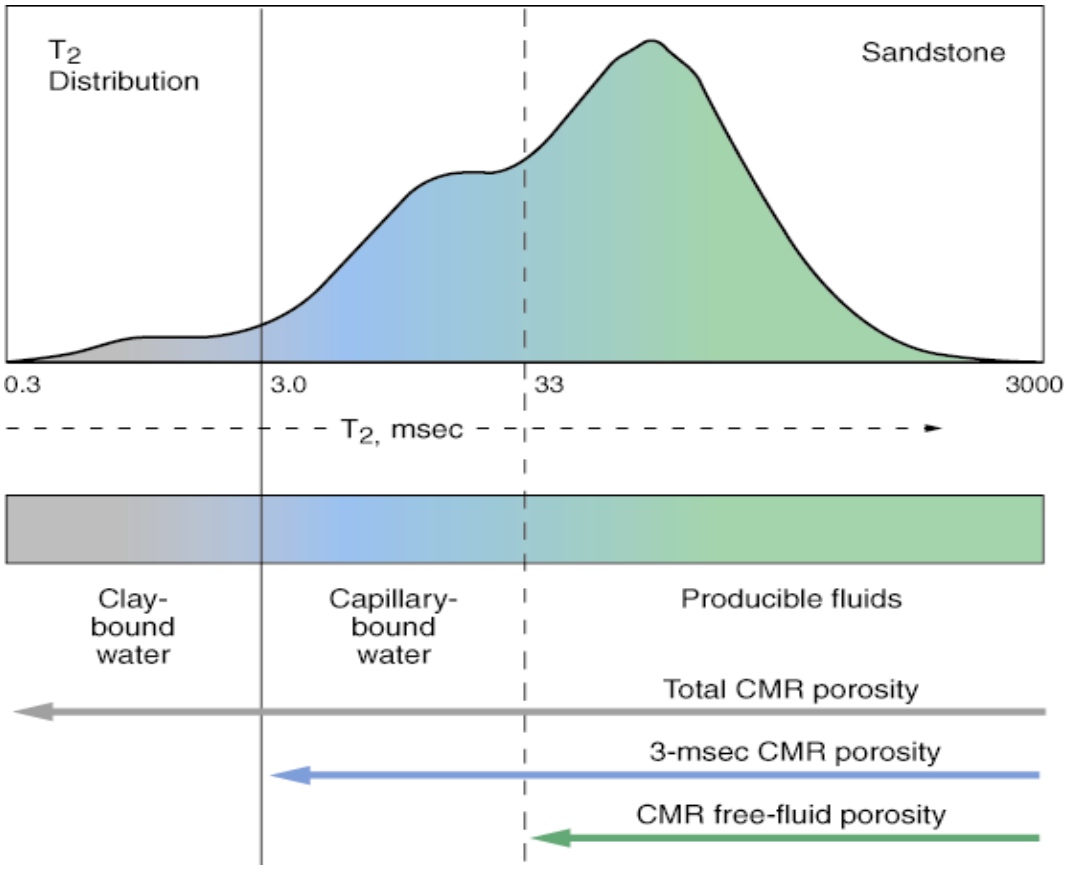

Figure B-3 Pore size as function of NMR relaxation time.

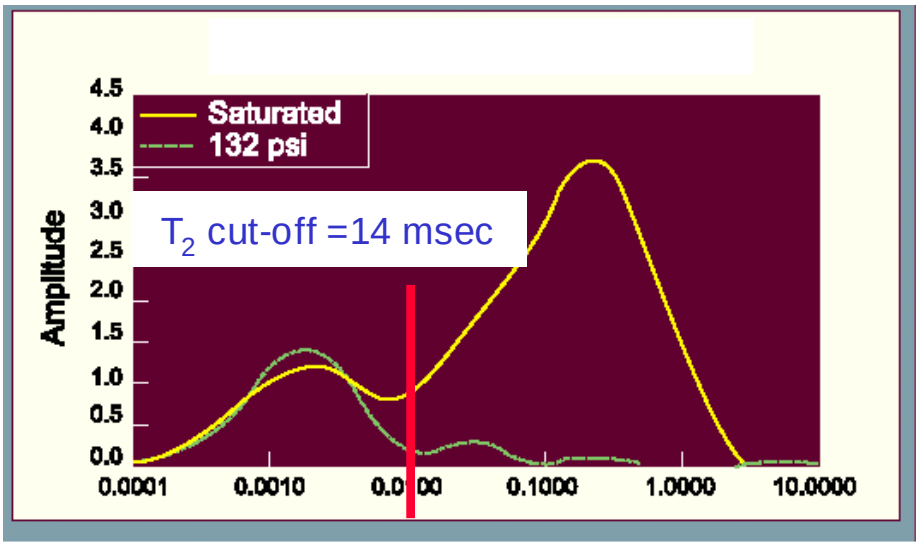

Figure B-4 Example of standard lab NMR analysis of core sample (lithic sandstone in this example) for determination of producible versus bound water T2 distribution cutoff. The yellow curve is the measured T2 distribution of the saturated core (amplitude versus relaxation time in seconds), the green curve is the measured T2 distribution after centrifuging in air at the equivalent of 132 psi pressure, and the red line is the determined T2 cutoff based on the difference between the two T2 distributions.

T2 relaxation times and their distributions may be interpreted to give other parameters such as hydraulic conductivity, capillary pressure versus water saturation relationships and water saturation. The following equations are commonly used to estimate permeability or hydraulic conductivity:

$$k_{SDR} = A(\phi_{NMR})^m (T_{2,\log})^n$$

$$k_{TIM} = B(\phi_{NMR})^m (FFV / BFV)^n$$

k_{SDR} estimated permeability (The Schlumberger Doll Research (SDR) equation)

k_{TIM} estimated permeability (Timur-Coates equation)

ϕ_{NMR} MR Scanner porosity

$T_{2,\log}$ logarithmic mean of the T2 distribution

FFV free (producible) fluid volume (as fraction of total volume)

BFV bound fluid volume (as fraction of total volume)

A, B scaling constants

m, n exponent constants

As these equations indicate, an accurate estimation of hydraulic conductivity requires the correct determination of the constants *A* and *B*, and secondarily the exponents *m* and *n*. While there are standard values for these constants that have been determined to work fairly well universally for different general geologic formation types, it is best to calibrate the constants for a local region by matching the log-derived results to another reliable measurement of hydraulic conductivity, preferably several core analyses. Once calibrated, the MRX permeability estimators usually provide a robust, high vertical resolution estimation of hydraulic conductivity – probably the most accurate and repeatable of any geophysical log derived estimate – reported every 18 inches along the logged depth interval.

Processing of the MRX measurements is typically performed at the wellsite, although additional enhancements and outputs can be generated with office processing. This logging tool operates in an open-hole that is either water- or air-filled. The standard vertical resolution is 18 inches and high resolution is 7.5 inches; Depth of investigation ranges from 1.5", 2.3", 2.7", & 4" at standard resolution and 1.25" using the high resolution antenna. MRX measurement precision (repeatability) is 1% for total porosity and 0.5% for effective (producible) porosity.

Since the MRX makes can measure up to 4" into the formation, it can overcome problems such as borehole wall-to-pad contact, disruption of contact between the skid and the wall because of borehole washout or hole rugosity affects data quality, resulting in erroneously high/low total and producible water content in water/air-filled hole. Similarly, the measurement can be affected by whole invasion of drilling mud or air, where the fine particles in the drilling mud penetrate more than an inch into the formation or where air drilling dessicates the near borehole formation. Whole mud invasion usually does not occur if a mudcake forms on the borehole wall during drilling, but can occur if clay is used in the mud and the formation is highly porous. The dessication effect of air-drilling can be avoided by letting the near borehole resaturate before logging. The measurement also can be significantly affected by a sizeable presence of iron-rich minerals, such as magnetite, but the effect on the T2 distribution is usually identifiable, consistent and well-known and, thus, can be effectively corrected for.

ARRAY INDUCTION TOOL (AIT*)

The AIT is a focused electrical induction probe that measures electrical conductivity/resistivity at multiple radial depths of investigation and vertical resolutions. The measurement is made by generating a highly focused electromagnetic field around the tool that induces a current in the formation, subsequently creating a secondary electromagnetic field that is measured by the tool. The tool measures direct and induced signals from eight coil arrays, six of which operate at two frequencies simultaneously. The surface acquisition unit processes these raw measurements into five resistivity logs in real-time, each with matched vertical resolution and with median radial depths of investigation ranging from 10 to 90 in. These depths of investigation change minimally over the entire range of formation conductivities. Each set of five logs is available in vertical resolution widths of 4, 2, and 1 ft. The AIT also measures borehole fluid resistivity and spontaneous potential.

From these measurements the AIT provides quantitative estimates of the following:

- True bulk formation resistivity – Formation resistivity is a function of water content, water salinity, and conductive mineral content.
- Drilling fluid invasion – In instances where the borehole fluid and formation fluid possess contrasting electrical conductivity values, the depth of invasion of filtrate can be mapped and zones with higher permeability can be identified.

The results are also useful for stratigraphic correlation. Vertical resolutions down to 1 ft show laminations and other formation structures with minimal influence on the measurements from environmental effects.

In concert with other porosity and lithology logs, quantitative estimates of water saturation and true formation water salinity can be obtained using the deep-reading resistivity measurement. The following equations (particularly Archie's equation) are commonly used to estimate formation water electrical conductivity or water saturation:

$$R_t = \frac{aR_w}{\phi^m S_w^n}$$, Archie's Equation

$$\frac{1}{R_t} = \frac{\phi^m S_w^n}{aR_w(1-V_{sh})} + \frac{V_{sh}S_w}{R_{sh}}$$, Total Shale Equation

$R_{xo} / R_t = R_{mf} / R_w$, Resistivity Ratio Method

R_t true bulk resistivity of uninvaded formation

R_w resistivity of water in the uninvaded formation

R_{sh} resistivity of the shale/clay beds

R_{xo} bulk resistivity of the near borehole invaded formation

* Mark of Schlumberger

R_{mf} resistivity of water (drilling mud filtrate) in the invaded formation

ϕ total porosity (exclusive of shale/clay-bound water)

V_{sh} fraction of total formation volume occupied by shale/clay

S_w water saturation

a constant

m constant (cementation factor)

n constant (saturation exponent)

When estimating formation water electrical resistivity in fully saturated conditions the saturation terms are set to 1. Archie's equation assumes the matrix (sediments) is not electrical conductive, whereas the total shale equation, a variation of Archie's equation, accounts for the fact that clay minerals in shales are electrical conductive. There are a number of other equations that account for clay minerals using different approaches. These equations do not directly account for other minerals that are electrically conductive, such as iron-bearing minerals (e.g. magnetite and pyrite).

As these equations indicate, an accurate estimation of formation water resistivity requires the correct determination of the constants *a* and *m* (and *n* if water saturation is being estimated). While there are standard values for these constants that have been determined to work fairly well universally for different general geologic formation types, it is best to calibrate the constants for a local region by matching the log-derived results to another reliable measurement of true formation water resistivity, preferably from discrete depths. Once calibrated, these log-based estimators can provide a robust high vertical resolution estimation of formation water resistivity/conductivity – reported every three inches along the logged depth interval.

Since a current is not directly emitted into the formation, the measurement does not require water in the borehole and is accurate in the sub-saturated zone above the water table. For the same reason the AIT can be run in PVC or fiberglass casing, albeit not steel casing. The AIT is largely insensitive to borehole environmental conditions since it has a deep depth of investigation.

Basic measurement specifications for the AIT are shown below and a schematic diagram of the basic tool setup in Figure B-5.

Range of measurement:	0.2–2000 Ohm.m (best below 1000 Ohm.m)
Total measurement error:	2% of measurement
Min/Max. hole size:	4.75 in. / 20 in.
Vertical Resolution:	1 ft, 2 ft, 4 ft
Depth of Investigation:	10, 20, 30, 60 and 90 in. (median response)

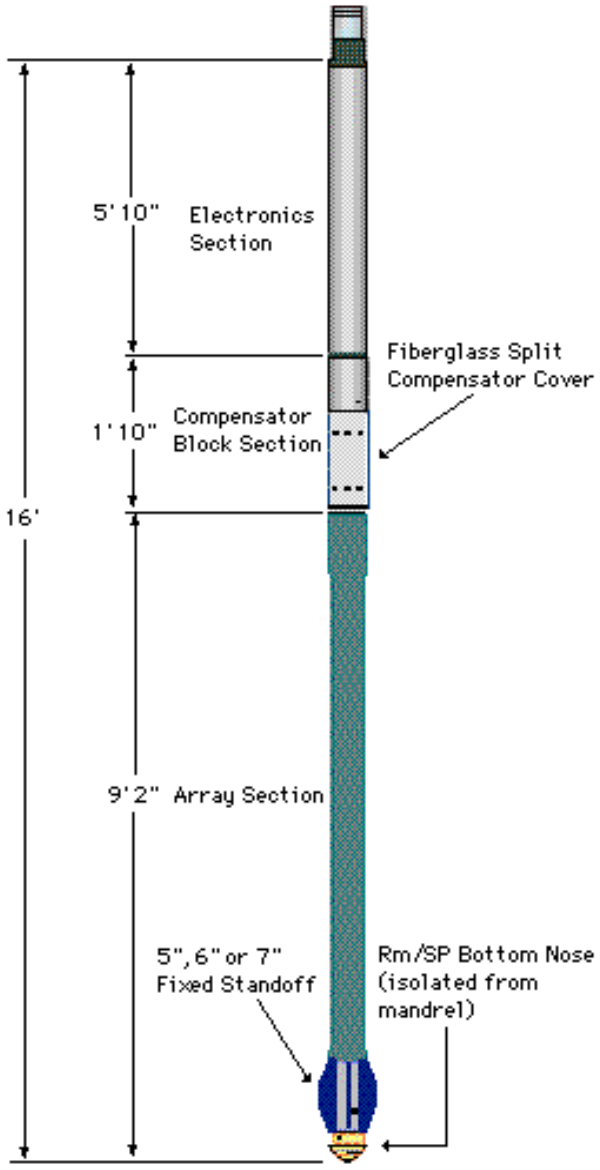

Figure B-5: Schematic diagram of AIT tool, showing component lengths and standard logging setup

HOSTILE NATURAL GAMMA RAY SPECTROSCOPY TOOL (HNGS*)

The HNGS tool is a passive gamma ray measuring sonde that measures the natural gamma activity energy spectrum of incoming gamma rays emitted by the formation. The tool differs from standard gamma ray tools in that it measures the energy, in addition to the number, of gamma rays – enabling the distinction between different gamma ray sources. The tool measures the natural gamma activity energy spectrum with two bismuth germanate (BGO) crystal detectors and uses an advanced spectral weighted-least squares processing algorithm to quantitatively resolve the three most common components of naturally occurring radiation—potassium, thorium, and uranium. In addition, special adaptations have been made to the processing to enable highly accurate activity/concentration measurements of particular man-made radionuclides, such as cesium and cobalt isotopes.

The tool is designed for continuous logging and provides a depth/time averaged continuous log of measured elemental components in relative wt% (usually potassium, thorium, and uranium). In addition, the standard gross gamma ray and gamma ray minus uranium are computed. The spectral gamma measurements are useful for evaluating clay content and clay type, as well as overall lithology and mineralogy – especially when integrated with other types of log measurements. In addition, the measurements are very useful for stratigraphic correlation between wells and can be used for evaluation cation exchange capacity and REDOX conditions.

The HNGS can be used in water- or air-filled, open or cased boreholes. Basic specifications for the HNGS and a schematic diagram of the measurement sensor are shown below and in Figure B-6, respectively.

Range of measurement:

GR	0 to >750 API units;
Potassium	0 to ~50%;
Thorium	0 to ~10,000 ppm;
Uranium	0 to ~10,000 ppm

Statistical precision (1 std):	Th – 0.7 ppm; U – 0.4 ppm; K – 0.14%
Min./Max. hole size:	4.5 in / 24 in
Depth of Investigation:	9.5 in

* Mark of Schlumberger

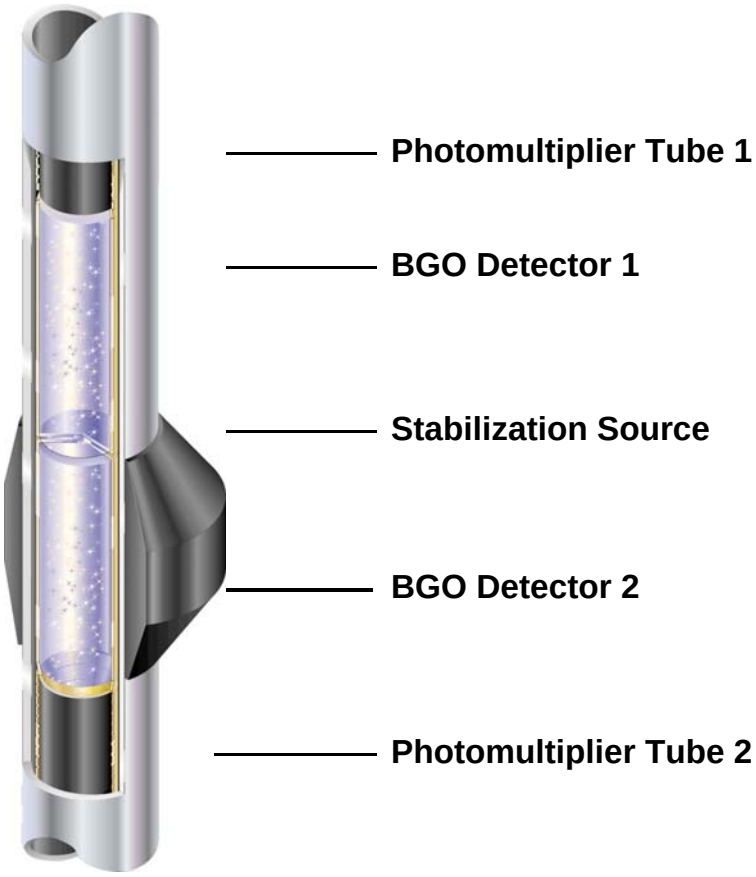

Figure B-6: Schematic diagram of HNGS sensor. BGO is bismuth germanate crystal – a high efficiency scintillation gamma ray detector. The stabilization source is a very low activity ^{22}Na stabilization source sandwiched in between the detectors.

FULLBORE FORMATION MICRO IMAGER (FMI*)

The Fullbore Formation Micro-Imager (FMI*) tool creates a picture of the borehole wall by mapping its electrical resistivity using an array of 192 small, pad-mounted button electrodes to provide an electrical image of the borehole with a resolution of ≈ 0.2 in (5 mm).

The tool (Figure B-7) contains arrays of microresistivity sensors set upon four orthogonal pads and attached flaps. During logging, the lower section of the tool emits current into the formation. The current is recorded as a series of curves that represent relative changes

in microresistivity caused by varying electrolytic conduction as a function of pore geometry, fracture geometry, or by cation exchange on the surfaces of clays and other conductive minerals. These effects produce variations on the images in response to porosity, fracture aperture, grain size, mineralogy, cementation and fluid type.

The current intensity measurements recorded in each button electrode, which reflect the microresistivity variations, are converted to variable-intensity color images. The lightest tone representing the most resistive samples, and the darkest the most electrically conductive (Figure B-8). The color is synthetic and does not indicate lithology or the true color of the formation.

A planar surface cutting the borehole describes an ellipse on the cylindrical borehole boundary surface. If the cylinder representing the borehole side is cut open and unrolled to become a flat surface, the ellipse becomes a sine wave. The amplitude of this sinusoid is proportional to the apparent dip of the intersecting plane, and the orientation of the trough indicates its apparent azimuth.

A triaxial accelerometer permits determination of tool position, and three magnetometers allow determination of tool orientation. With these inputs, the orientation of all planar features that intersect the borehole wall (e.g., bedding and fractures) is calculated. This information also provides a measurement of borehole deviation. Dip is represented on a log by a small circle with a tail. The position of the circle along the horizontal axis portrays dip magnitude, ranging from 0 to 90° on the right. Tail direction is analogous to dip direction, with north at the top of the log.

Features than can be identified and measured include:

- Bedding planes that permit the determination of structural strike and dip plus the orientation of stratigraphic features such as foresets.
- Structural features such as faults, folds, or soft-sediment deformation.
- Non-bedding features such as fractures, burrowing, vugs, pebbles, concretions, fissures, stylolites, etc. Fracture orientation and aperture can also be determined, the latter requires scaling of the image an appropriate resistivity log.

* Mark of Schlumberger

Figure B-7: Photo of FMI sensor section, showing the four caliper arms, each containing a main pad and extender pad with electrode buttons (located on copper colored plates).

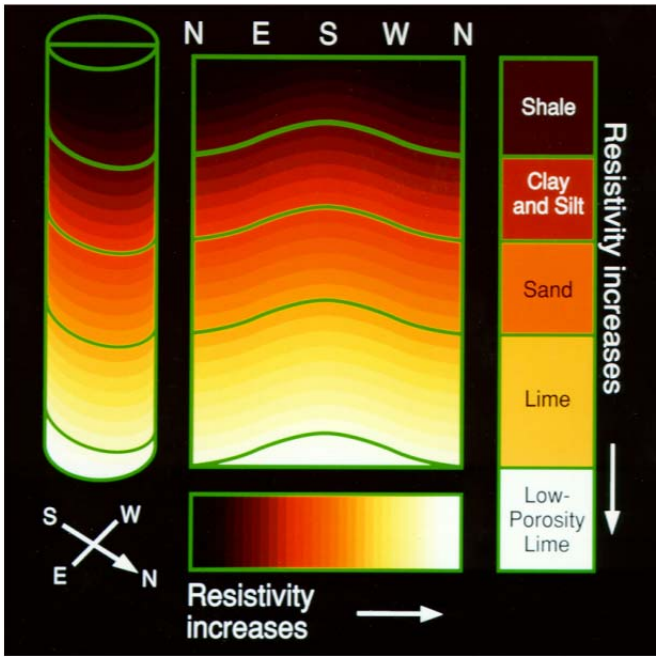

Figure B-8: FMI image generation

Fractures form a fairly unambiguous feature on this type of log. Dark (electrically conductive) lines that typically cut across bedding, and sometimes parallel it, are usually considered open, water-filled fractures. Healed fractures typically appear light instead of dark. The image does not tell whether a fracture contributes to aquifer production; it tells only that the fracture is present at the wellbore. Determining whether the fracture will produce water, or act as a hydraulic conductivity path or barrier requires the calculation of fracture aperture.

Once fractures are mapped and their orientation is calculated, then fracture density and spacing can be computed. Fracture aperture can be estimated through additional data processing.

Forward modeling of the electrical field present around a fracture using a finite-element code was used to determine the relationship between fracture aperture, formation resistivity, mud resistivity, and additional current flow caused by the presence of the fracture. The resulting equation is:

$$A = \frac{W}{R_m \bullet c}\left(\frac{R_{xo}}{R_m}\right)^{1-b}$$

W fracture width (mm)

R_{xo} formation resistivity

R_m water resistivity

A integrated excess current caused by presence of fracture

c coefficient obtained numerically from forward modeling

b exponent obtained numerically from forward modeling

Note that formation resistivity cannot be determined with the imaging tool; it requires the integration of a conventional resistivity or induction log data.

A three-step process to detect, trace, and quantify fractures is used. The fractures are typically mapped as part of the interpretation process; the trace for each fracture is determined by mapping where electrical conductivity significantly exceeds local matrix conductivity followed by line sharpening; and apertures are computed for all fracture locations. This method allows the detection of fractures of 10μm aperture and may resolve fractures about 1 cm apart.

The FMI passes an electrical current into the formation and, thus, requires water or drilling mud in the borehole and cannot be operated in cased hole. However, unlike borehole video, borehole fluid opacity has no effect on the measurement. The measurement is best when the four pads are in physical contact with the borehole wall, but is still obtainable when the pad(s) lose contact. The tool generally handles washouts quite well.

Basic measurement specifications for the FMI are shown below and an FMI log collected in a fractured basalt aquifer is shown in Figure B-9.

Statistical precision (1 std):Inclination – ±0.2°; Orientation – ±2°

Vertical Resolution: 0.2 in (5 mm)

Min/Max. hole size: 6.25 in. / 21 in.

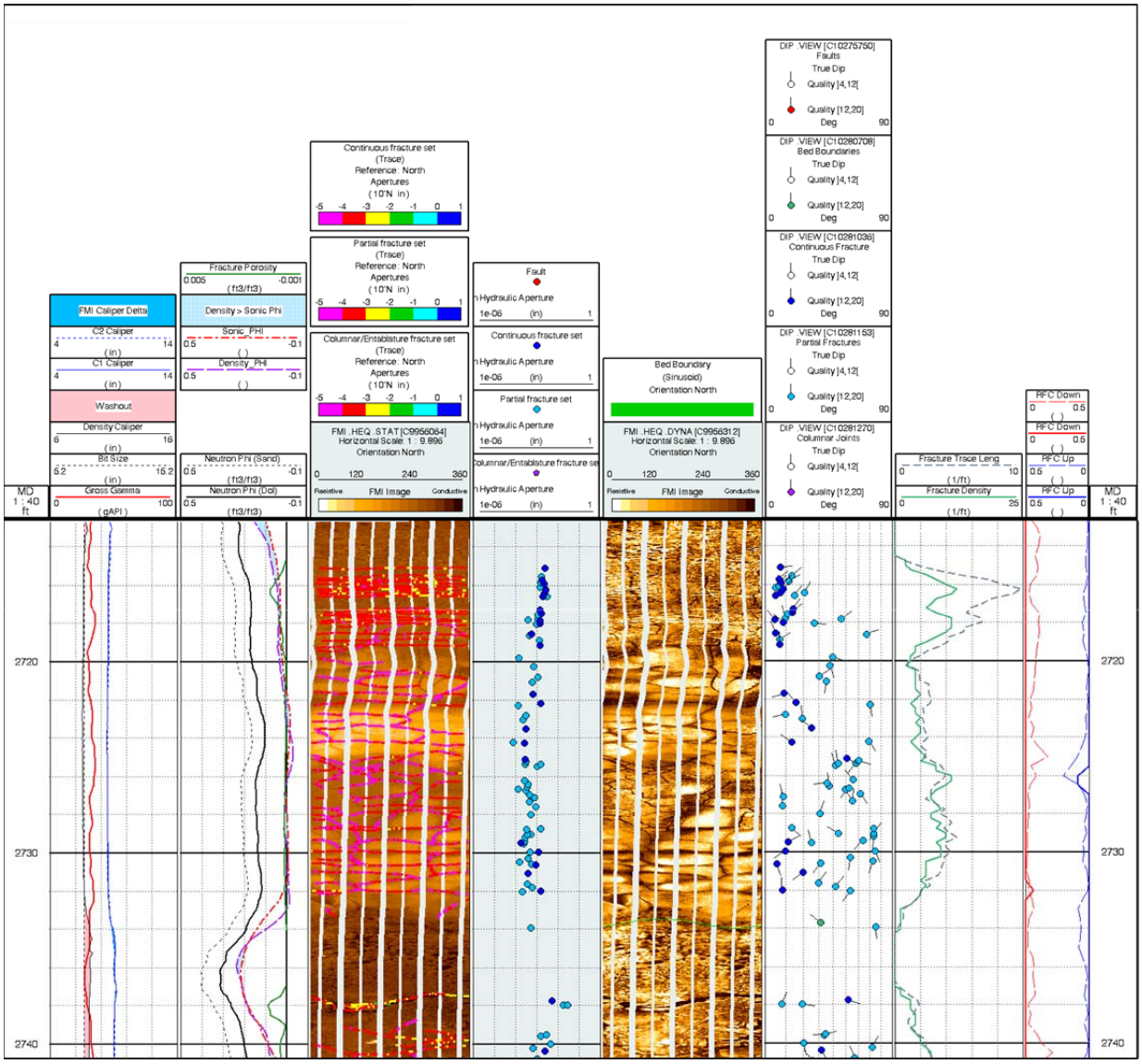

Figure B-9: Electrical imager log of basaltic aquifer. A portion of a log collected in a fractured aquifer, the Miocene Columbia River Basalt of Washington, US. This log depicts primarily the FMI results that include: images (tracks 3 and 5), calculated apertures in logarithmic scale (track 4), fracture orientation (track 6), fracture trace length and density (track 7). Each fracture trace with aperture is superimposed on the image in track 3. Track 2 depicts different porosity logs, and it includes the fracture porosity. Each horizontal division is equivalent to 2 feet (60 cm) in depth.

APPENDIX C: DESCRIPTION OF PROCESSING PERFORMED ON SCHLUMBERGER GEOPHYSICAL LOGS ACQUIRED IN WELL CREX–1

MAGNETIC RESONANCE LOG

The MR Scanner porosity and pore size distribution measurements are based on pulsed directional magnetic polarization of the hydrogen nuclei in formation pore fluids – induced using magnetic fields generated by the tool with a set of large permanent magnets and an antenna. The signal created by the precession, and resulting oscillating magnetic field, of the fluid hydrogen nuclei between polarizations is the magnetic resonance response measured by the tool's antenna. The total signal amplitude from all the precessing hydrogen nuclei is a measure of the total fluid hydrogen content, or porosity, of the formation, whereas the rate at which the precession decays is related to pore size distribution. Since only the hydrogen protons of fluids can be polarized, the magnetic resonance total porosity measurement is lithology-independent – unlike all other porosity measurements from geophysical logs (e.g., sonic porosity is derived from the measured acoustic velocity of the bulk formation, matrix plus pore fluids, usually by assuming a matrix velocity and mixing model such as the Wyllie Equation).

The relationship between the formation magnetic resonance response and pore size distribution (including effective porosity) is dependent on the geologic environment. In particular, the distinction between effective and bound porosity (moveable/free versus immoveable/bound water) in the measured magnetic resonance signal amplitude versus alignment and precession time (referred to as the T1 and T2 distributions, respectively) is empirical and varies for different formation characteristics. However, the distinction, typically defined as a cutoff in the T1/T2 distribution, is usually consistent for a particular geologic formation and lithology. The effective/bound porosity T1/T2 cutoff is ideally determined by performing laboratory magnetic resonance measurements of core samples that are representative of the geologic formations in the area of investigation – comparing, for each sample, the measured T1/T2 distribution when it is fully saturated to that when it has been centrifuged to drain all moveable water. In lieu of such laboratory core analysis, the T1/T2 cutoff can be determined from visual inspection of the log-measured T2 distribution along with knowledge of typical cutoff values for different geology/lithology types – developed from extensive experience of running magnetic resonance logs in different geologic environments around the world. For example it has been determined that the T1/T2 cutoff is typically 50/33 milliseconds (ms) in quartz rich clastic sand-shale environments and 100 ms in carbonates. The T2 cutoff is known to vary from as low as 9 ms in iron rich sands to as high as 230 ms in some cherts.

No known laboratory magnetic resonance analyses have been performed on core from the geologic formations encountered in the Los Angeles Groundwater Basin; such physical sample analyses would assist with determining T1/T2 cutoffs. Instead, knowledge of the local geology and visual inspection of the measured T1/T2 distribution from the MR Scanner logs were paired with globally determined T1/T2 cutoff values for similar geologic environments to choose zoned cutoff values for each of the four monitoring wells that were logged. The standard T1/T2 cutoff for clastic sediments/rocks, 50/33 ms, was used as a starting point. From visual inspection of the T1/T2 distribution this cutoff appears appropriate (when there is bimodal distribution with a distinct low amplitude "trough" that occurs around 50/33 ms).

Once the T1/T2 cutoff was zoned the raw MR Scanner field measurements were reprocessed using the new cutoffs and processing settings that are optimized for the specific acquisition scenario in each well to obtain new effective porosity results.

If the MR Scanner sensor pad is not in contact with the formation the magnetic resonance measurement may be sensitive to the borehole fluid between the pad and the formation. Similarly, if drilling mud solids (e.g., bentonite clay) directly enter into the formation (referred to as whole mud invasion), the measurement may be sensitive to the

introduced mud solids – elevating the clay bound water signal, and often the total porosity. In these situations there is no systematic way to eliminate the component of the magnetic resonance measurement originating from the borehole fluid/mud instead of the formation. The MR Scanner Scanner log results were not adversely affected by poor sensor pad contact with the formation or drilling mud solids penetration into the formation.

GROUND WATER FLOW AND STORAGE CAPACITY COMPUTATIONS

Robust quantitative estimates of a number of key physical hydrogeological properties, including hydraulic conductivity and specific storage, were computed in each of the four monitoring wells using the considerable amount of discrete-depth information about the rock/sediment matrix and fluid composition provided by the processed geophysical logs. In particular, information about the pore size distribution provided by the magnetic resonance measurement – incorporated in the ELAN integrated log analysis to delineate between bound versus moveable water fractions of total porosity – was central to the estimation of hydraulic conductivity. Logs of total porosity and lithologic/mineralogic composition, also from the ELAN analysis optimized mineral-pore volume model, were used to compute specific storage – the latter providing information about matrix compressibility.

The analysis of ground water flow capacity from the processed geophysical logs was performed using two well-established empirical relationships for estimating permeability from oil and gas reservoir evaluation – the Timur-Coates equation and the SDR equation (see Appendix B under the MR Scanner section for a complete description of the equations). These empirical relationships were developed for magnetic resonance measurements – based on laboratory analysis of core from petroleum reservoirs of different geologic composition around the world – but the Timur-Coates equation is valid for any measurement/analysis that provides both total and effective porosity. In this study the optimized total and effective porosity from the ELAN integrated analysis results were used in the Timur-Coates equation as the primary estimate of permeability/hydraulic conductivity. The SDR equation was implemented as a secondary estimate of permeability/hydraulic conductivity, utilizing as log inputs the ELAN total porosity and the reprocessed logarithmic mean of the magnetic resonance T2 distribution.

As these equations indicate, an accurate estimation of hydraulic conductivity requires the correct determination of the scaling and exponent constants. While there are standard values for these constants that have been determined to work fairly well universally for different general geologic formation types, it is best to calibrate the constants for a local region by matching the log-derived results to another reliable measurement of hydraulic conductivity, preferably several core analyses or small scale zonal testing results. Once calibrated, these permeability estimators, incorporating magnetic resonance log results, usually provide a robust high vertical resolution estimation of permeability/hydraulic conductivity – probably the most accurate and repeatable of any geophysical log derived estimate. For this project standard values were used.

The permeability estimators were used to generate discrete-depth permeability logs across the logged depth intervals in each of the four monitoring wells. These nearly continuous high resolution logs were used to derive a number of other valuable results related to formation flow capacity including:

- hydraulic conductivity (computed using a simple conversion that incorporates fluid viscosity and density computed based on estimated groundwater salinity and temperature)
- relative flow capacity versus depth profile, emulating continuous flowmeter results (computed by mathematically integrating the permeability log from bottom to top, then normalizing the resulting log to range between 0 at bottom and 1 at top)
- transmissivity (computed by mathematically integrating the hydraulic conductivity log from bottom to top or across selected intervals)
- produced water salinity (computed by taking a weighted depth average, from bottom to top or across selected intervals, of the estimated ground water salinity log, with the weights determined from the estimated normalized inflow capacity [proportional to hydraulic conductivity] at each depth).

Storage properties, including effective porosity/specific yield, specific storage, and storativity, were estimated from the log results across most of the well depth section. Effective porosity, interpreted to be equivalent to specific yield, is derived from the integrated log analysis – largely guided by the magnetic resonance and neutron-gamma spectroscopy free fluid and air-filled porosity measurements, respectively. In the saturated zone the magnetic resonance tool distinguishes between free (moveable/producible) water and bound water volumes – the effective porosity estimate is essentially derived from the free water porosity. In the unsaturated zone the magnetic resonance measurement is only sensitive to the water present in the pore space (bound or free water porosity), not to the air-filled porosity. However, the AIT tool, based on the difference in the measurement responses between shallow and deep reading bulk resistivity measurements, is sensitive to air content and can be used to estimate the air-filled porosity in combination with other logs. In addition the sonic compressional velocity measurement is very sensitive to the presence of air n the pore space. Effective porosity is estimated as the sum of air-filled porosity and free water porosity, which assumes that the air-filled fraction of the pore space contains air because water can drain out of it (meaning such water would be free/moveable, as opposed to bound). This assumption is not true if evapotranspiration accounts for an appreciable amount of the air displacement of water.

The analysis of specific storage from the processed geophysical logs was performed using the rock mechanics determination of specific storage:

$$S_s = \rho g(\alpha + \phi\beta)$$

S_s estimated specific storage

ρ ground water density

g gravitational acceleration

α formation compressibility

ϕ total porosity (as fraction of total volume)

β ground water compressibility

The two unknowns on the right hand side of the equation are total porosity and formation compressibility; the other variables vary little across the range of possible conditions and were assigned values consistent with fresh ground water at typical shallow aquifer conditions. The optimized total porosity log computed from the ELAN integrated log analysis was used as the total porosity input. None of the geophysical logs acquired was directly related to formation compressibility, but the mineralogical/lithologic information provided by the comprehensive matrix plus pore volume model generated from the ELAN analysis was used to derive an indirect estimate of formation compressibility. This was accomplished by computing a synthetic bulk compressibility log from the ELAN mineral and pore volumes using the Hill average moduli estimator and published individual mineral compressibilities (Mavko et al. 1998). The derived synthetic formation bulk compressibility log was used with the ELAN total porosity log to produce a continuous log of specific storage. Subsequently, storativity was computed by mathematically integrating the specific storage log from bottom to top or across selected intervals.

The derived synthetic formation bulk compressibility log was used with the ELAN total porosity log to produce a continuous log of specific storage. Subsequently, storativity was computed by mathematically integrating the specific storage log from bottom to top or across selected intervals.

ATTACHMENT 1: COLOR PRINT OF INTEGRATED LOG WELL MONTAGE FOR WELL CREX-1

Schlumberger

CrEX-1

Processsed Montage

Scale: 1:500

COMPANY: Los Alamos National Laboratory
WELL: CrEX-1
FIELD: LANL
RIG:
COUNTRY: New Mexico USA

Date Logged: 07-Aug-2014 Date Processed: 21 October
Surface Longitude: 106° 15' Latitude: 35° 51' 28"
Elevations: KB: 6831 ft DF: 6836 ft GL: 6831 ft

FOLD HERE: The well name, location and borehole reference data were furnished by the customer.

Svc. Order #:	Interpretation Center:	Analyst: HANSARD	Process Date: 21

Remarks:

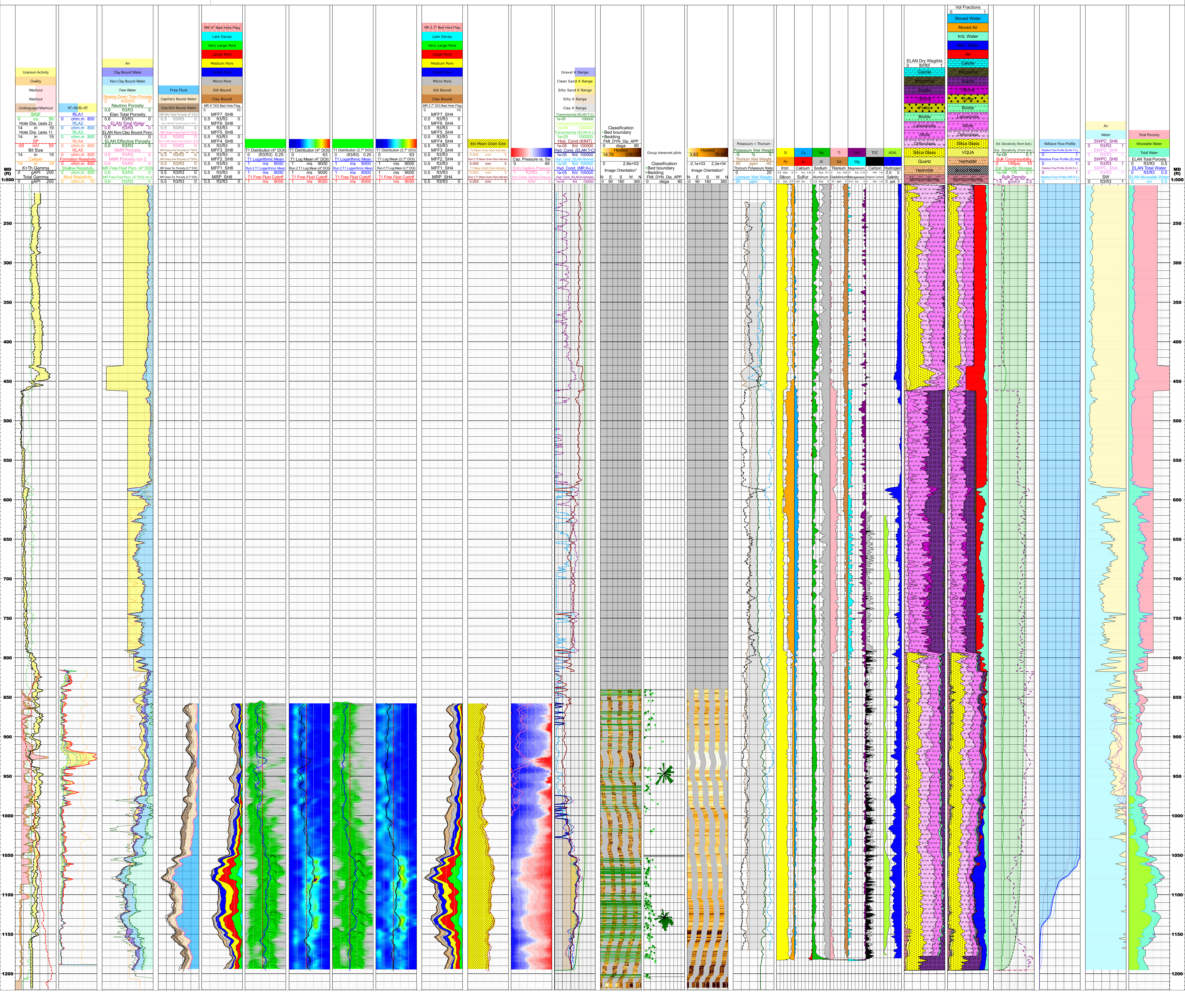

ATTACHMENT 2: COLOR PRINTS OF HYDROGEOLOGY SUMMARY COMPOSITE AND GEOCHEMICAL SUMMARY COMPOSITE OF ELAN OPTIMIZED MINERAL AND PORE VOLUME MODEL RESULTS FOR WELL CREX-1

Uranium Activity

Total Gamma
0 gAPI 150

K+Th Gamma
0 gAPI 200

MD (ft)
1:500

ELAN Dry Weights
0 lbf/lbf 1

Calcite
Magnetite
Augite
Olivine
Pyrite
Biotite
Labradorite
Albite
Orthoclase
Silica Glass
Quartz
Heamtite
Montmorillonite

Si | Ca | Na | Ti | Mn | TIC | ASAL
Fe | Su | Al | Gd | Mg | | H
Iron | Calcium | Sodium | Titanium | Magnesium | Carbon | Hydrogen
0.2 Euc 0 | 0 Euc 0.25 | 0 Euc 0.1 | 0 Euc 0.02 | 0 Euc 0.15 | 0 lbf/lbf 0.05 | 0.5 0
Silicon | Sulfur | Aluminum | Gadolinium | Manganese | Organic Carbon | Salinity
0 Euc 0.429412 | 0.05 Euc 0 | 0.2 Euc 0 | 10 ppm 0 | 0.01 Euc 0 | 0 lbf/lbf 0.05 | 0 ppk 5

Potassium + Thorium
Potassium Wet Weight
-5 % 5
Thorium Wet Weight
40 ppm -40
HTPR
0 20
Uranium Wet Weight
20 ppm 0

300
400
500
600
700
800
900
1000
1100
1200

Uranium Activity

Clay Volume

Underguage/Washout

Clay Volume
1 ft3/ft3 0
Bit Size
6 in 24
Caliper
6 in 24
K+Th Gamma
0 gAPI 200
Gamma Ray
0 gAPI 200
SP
-50 mV 50

Reference (ft)
1:500

RT < RI/RI < RT

Classification
Bed boundary
Bedding
FMI_STAT_Dip_APP
0 dega 90
3.83 76.85
-2.1e+03 2.2e+04
Image Orientation°
N E S W N
0 90 180 270 360
Formation Resistivity
0 ohm.m 800
Shallow Resistivity
0 ohm.m 800
Mud Resistivity
0 ohm.m 800

Air

Moveable Water

Total Water

Est. Specific Storage
1e-06 1/ft 0.1
Est. Storativity (from bot.)
1e-06 1/ft 0.1
ELAN Total Porosity
0.5 ft3/ft3 0
Total Water
0.5 ft3/ft3 0
ELAN Moveable Water
0.5 v/v 0
Water Saturation
1 ft3/ft3 0

Hyd. Cond.

Transmissivity (ELAN TC)
0.0001 10000
Flow Profile
0 1
Hyd. Cond (ELAN TC)
0.0001 ft/d 10000

ELAN Volumes
0 1
Moved Water
Moved Air
Irrd. Water
Mov. Water
Air
Calcite
Magnetite
Augite
Olivine
Pyrite
Biotite
Labradorite
Albite
Orthoclase
Silica Glass
VQUA
Hematite
Solid Hole
Montmorillonite

250
300
350
400
450
500
550
600
650
700
750
800
850
900
950
1000
1050
1100
1150
1200

ATTACHMENT 3: COLOR PRINT OF ELAN OPTIMIZED MINERAL AND PORE VOLUME MODEL RESULTS FOR WELL CREX-1

Schlumberger

ELAN* Geophysical Log Integrated Analysis

Optimized Mineral + Pore Volume Model

COMPANY: Los Alamos National Laboratory

WELL: CrEX-1

FIELD: LANL

State: New Mexico

COUNTRY: USA

*Elemental Log ANalysis, Mark of Schlumberger

Date Processed:	Oct-2014	Date Logged:	07-Aug-2014
Job Number:		Processed at:	SWS Tucson
Well Location:	Mortandad Canyon		
Latitude:	35deg 51' 28" N	Longitude:	106deg 15' 23" W
Elevations:	KB: 2082.09m	DF: 2083.61m	GL: 2082.09m

Depth ref. is ground surf. Total porosity constraints applied above 817 ft.

FOLD HERE

The well name, location and borehole reference data were furnished by the customer.

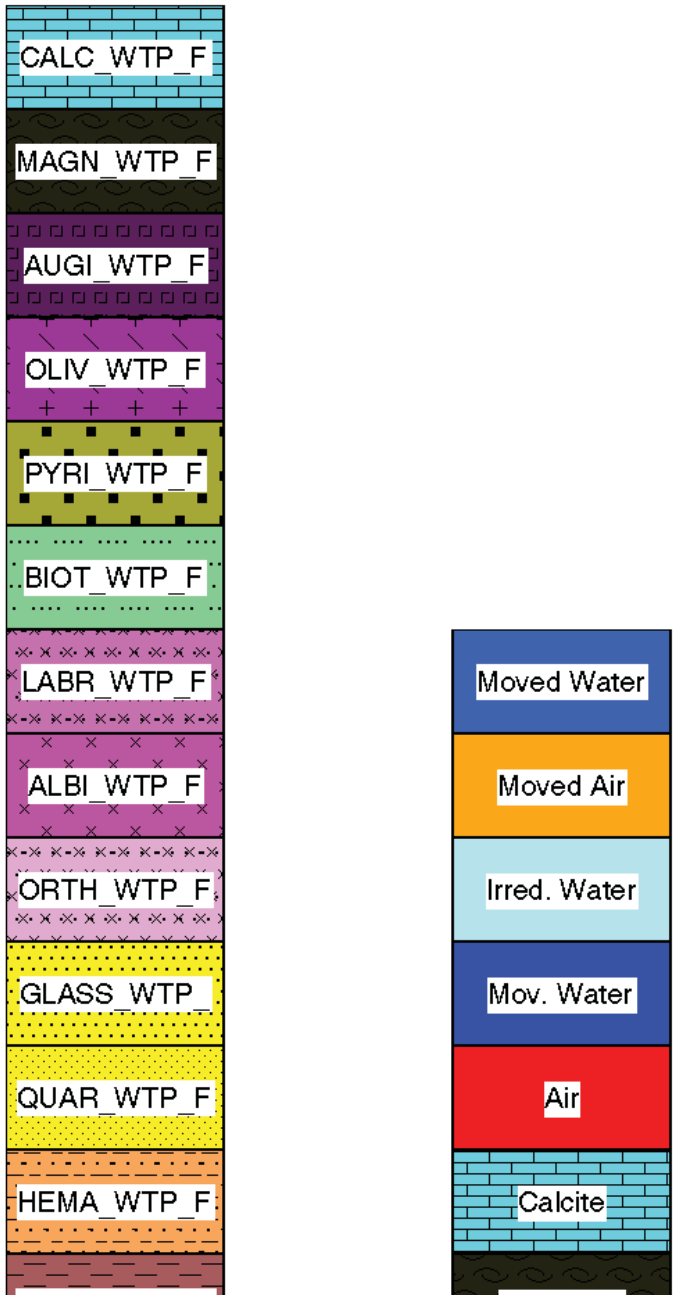

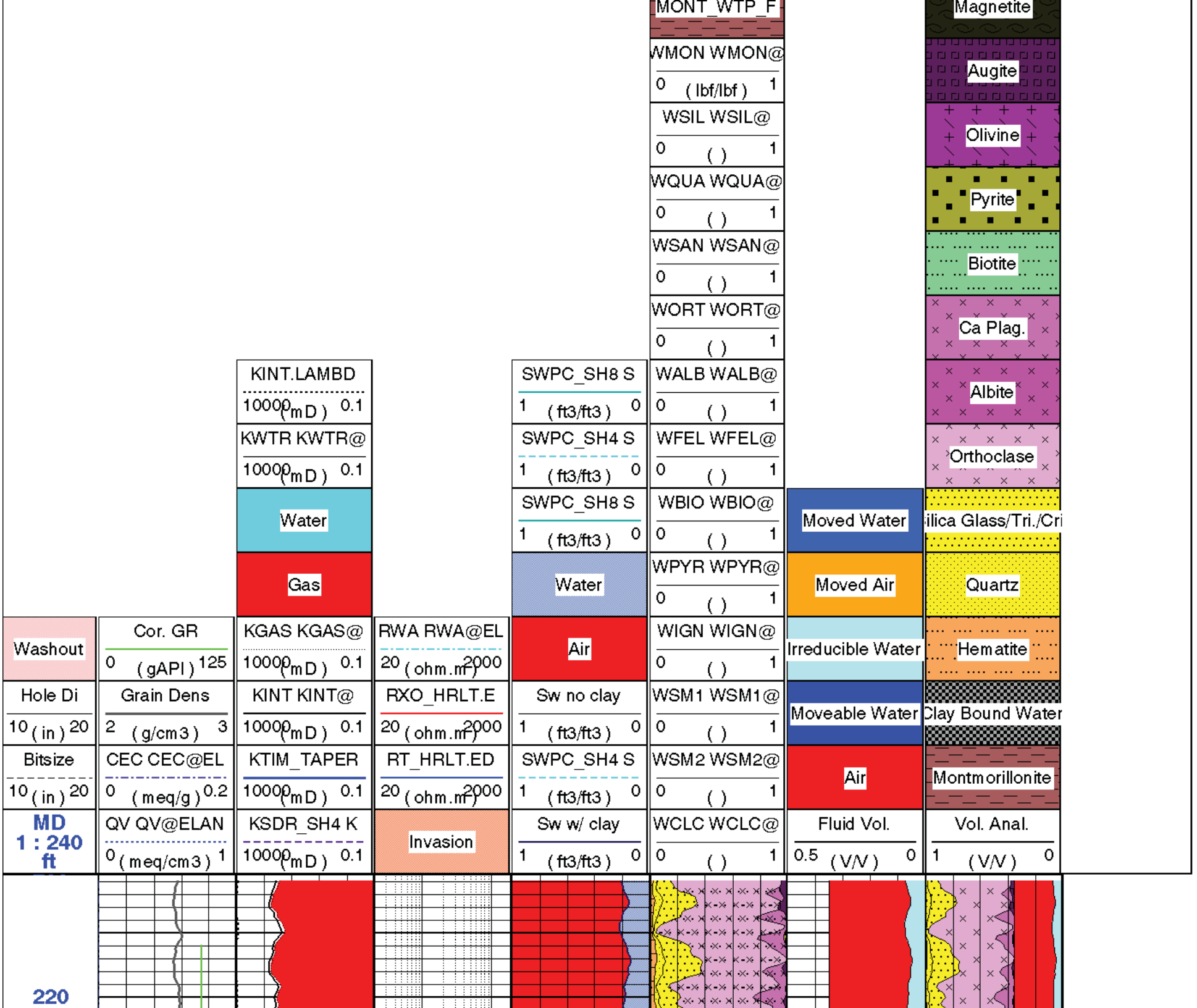
MONT_WTP_F
WMON WMON@
0 (lbf/lbf) 1
WSIL WSIL@
0 ( ) 1
WQUA WQUA@
0 ( ) 1
WSAN WSAN@
0 ( ) 1
WORT WORT@
0 ( ) 1
WALB WALB@
0 ( ) 1
WFEL WFEL@
0 ( ) 1
WBIO WBIO@
0 ( ) 1
WPYR WPYR@
0 ( ) 1
WIGN WIGN@
0 ( ) 1
WSM1 WSM1@
0 ( ) 1
WSM2 WSM2@
0 ( ) 1
WCLC WCLC@
0 ( ) 1
Magnetite
Augite
Olivine
Pyrite
Biotite
Ca Plag.
Albite
Orthoclase
ilica Glass/Tri./Cri
Quartz
Hematite
Clay Bound Water
Montmorillonite
Vol. Anal.
1 (V/V) 0
KINT.LAMBD
1000 (mD) 0.1
KWTR KWTR@
1000 (mD) 0.1
Water
Gas
KGAS KGAS@
1000 (mD) 0.1
KINT KINT@
1000 (mD) 0.1
KTIM_TAPER
1000 (mD) 0.1
KSDR_SH4 K
1000 (mD) 0.1
SWPC_SH8 S
1 (ft3/ft3) 0
SWPC_SH4 S
1 (ft3/ft3) 0
SWPC_SH8 S
1 (ft3/ft3) 0
Water
Air
Sw no clay
1 (ft3/ft3) 0
SWPC_SH4 S
1 (ft3/ft3) 0
Sw w/ clay
1 (ft3/ft3) 0
Moved Water
Moved Air
Irreducible Water
Moveable Water
Air
Fluid Vol.
0.5 (V/V) 0
RWA RWA@EL
20 (ohm.m) 2000
RXO_HRLT.E
20 (ohm.m) 2000
RT_HRLT.ED
20 (ohm.m) 2000
Invasion
Washout
Hole Di
10 (in) 20
Bitsize
10 (in) 20
Cor. GR
0 (gAPI) 125
Grain Dens
2 (g/cm3) 3
CEC CEC@EL
0 (meq/g) 0.2
QV QV@ELAN
0 (meq/cm3) 1
MD
1 : 240
ft
220

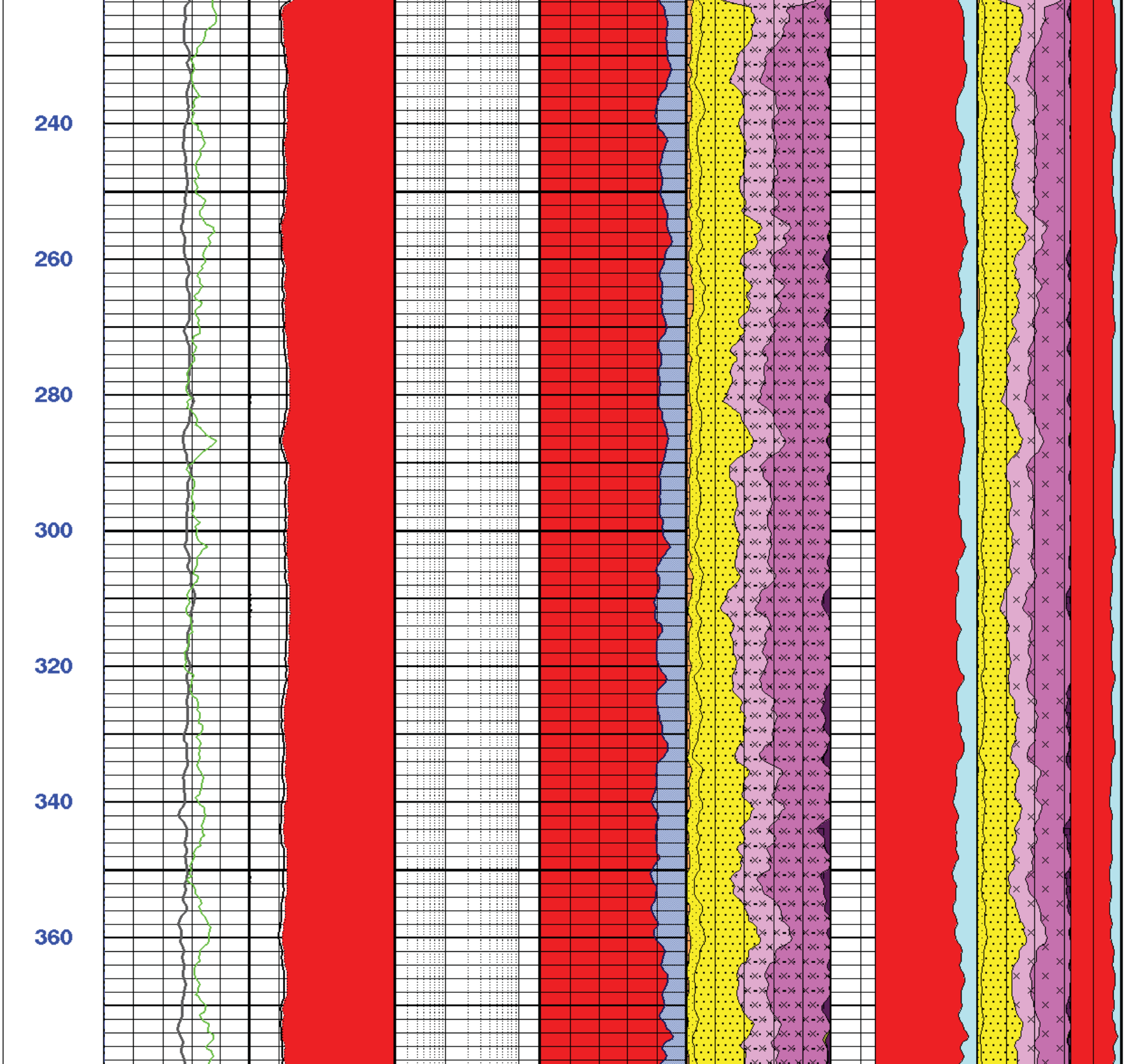
240
260
280
300
320
340
360

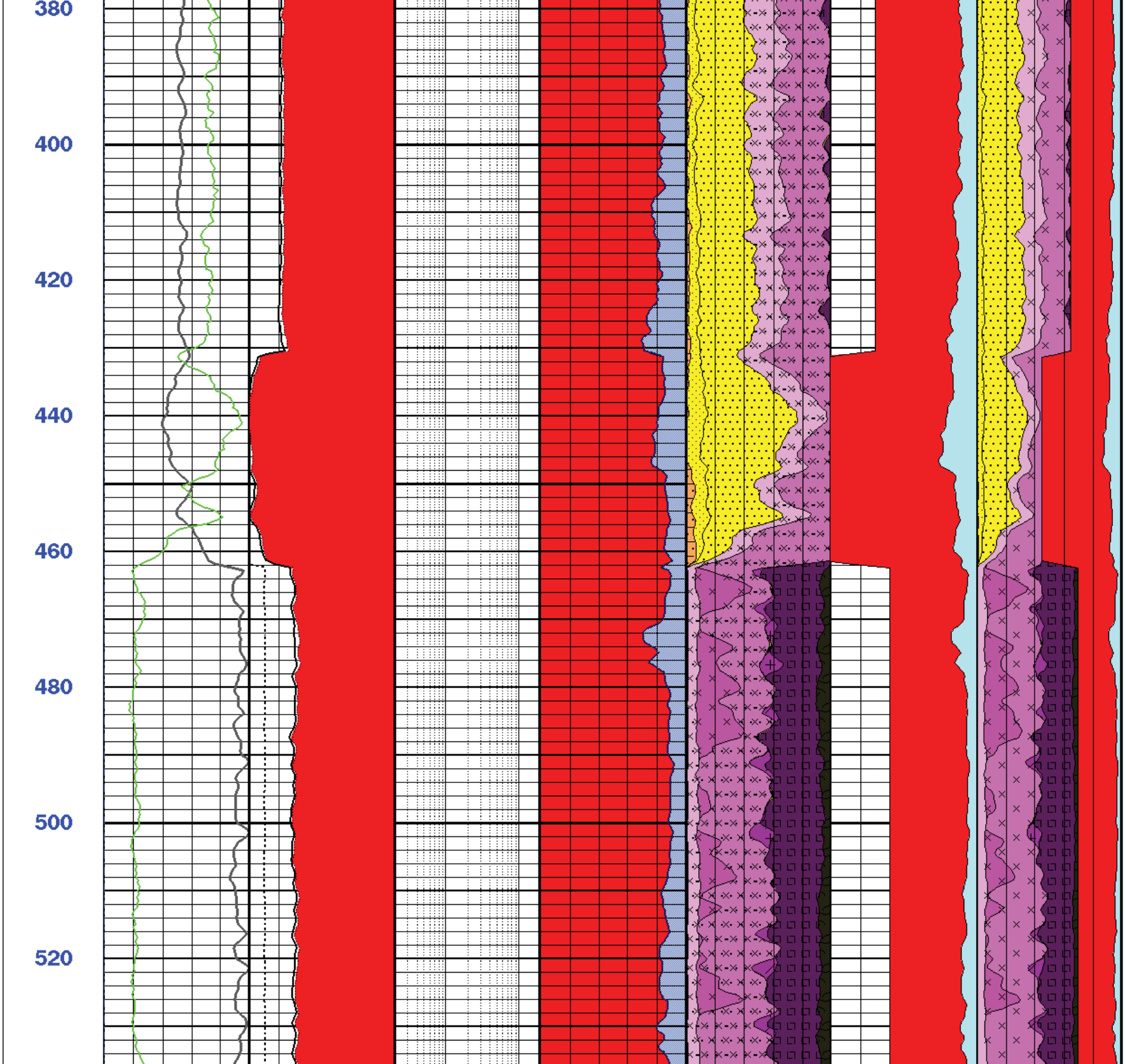
380
400
420
440
460
480
500
520

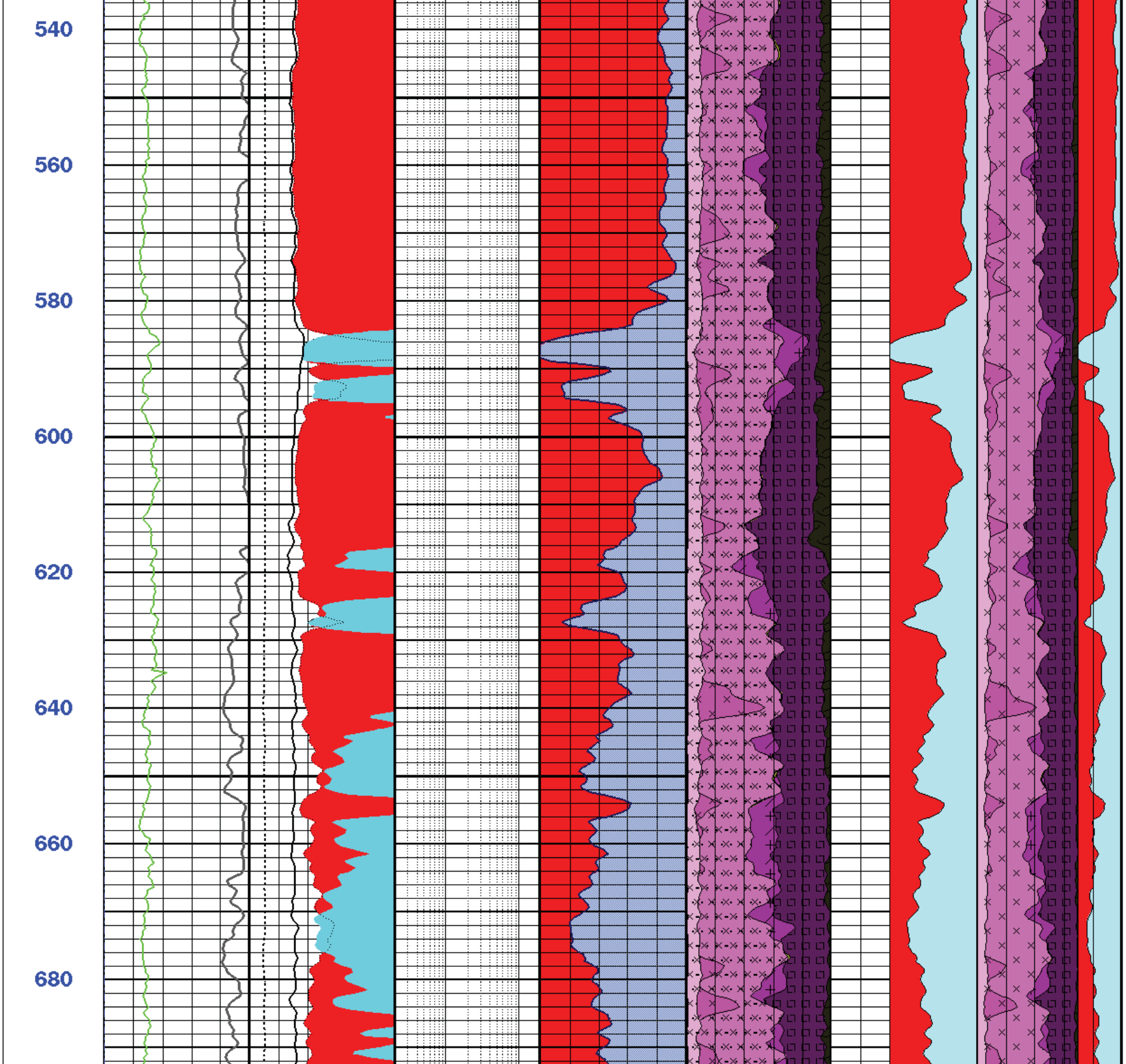
540
560
580
600
620
640
660
680

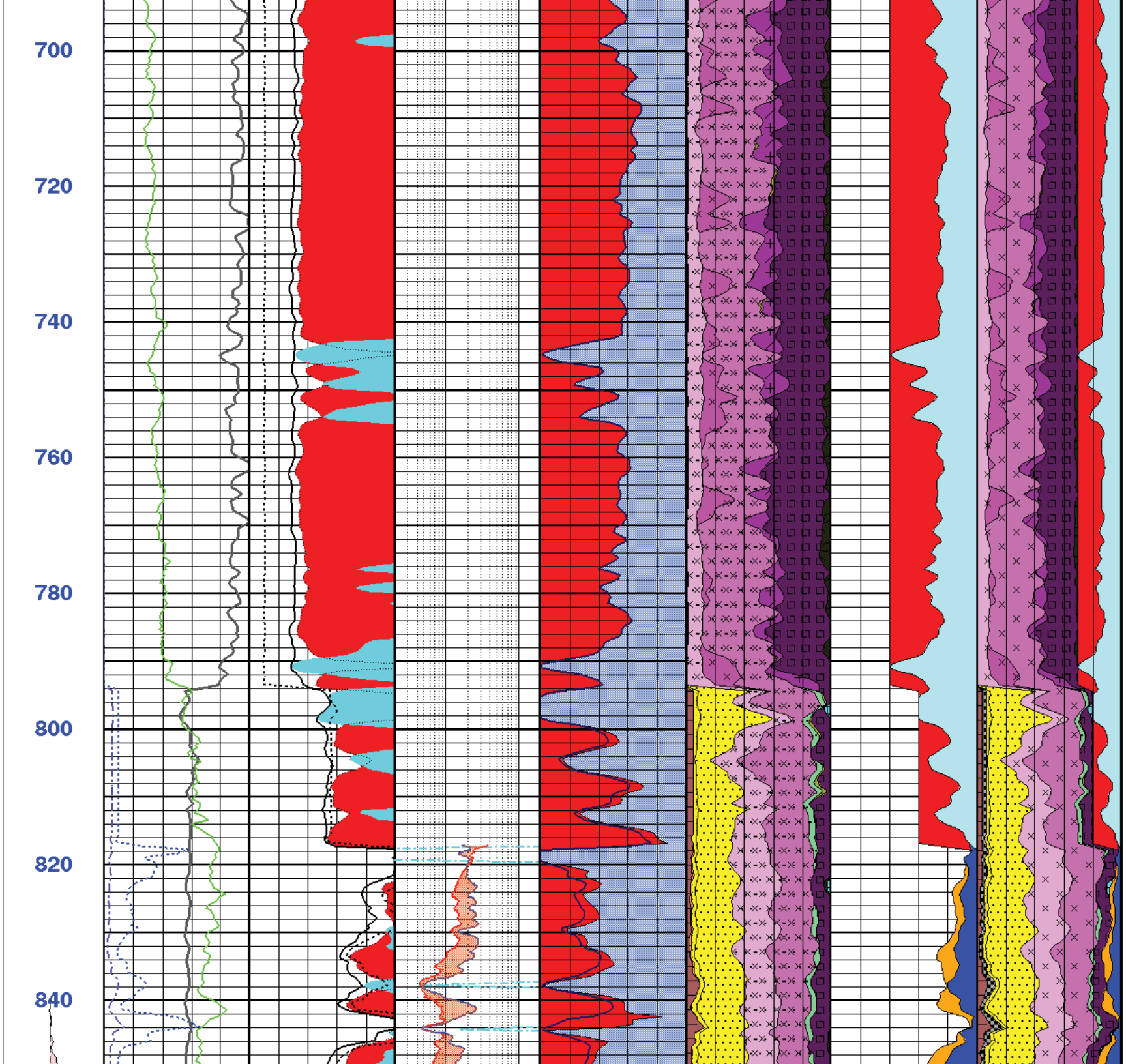
700
720
740
760
780
800
820
840

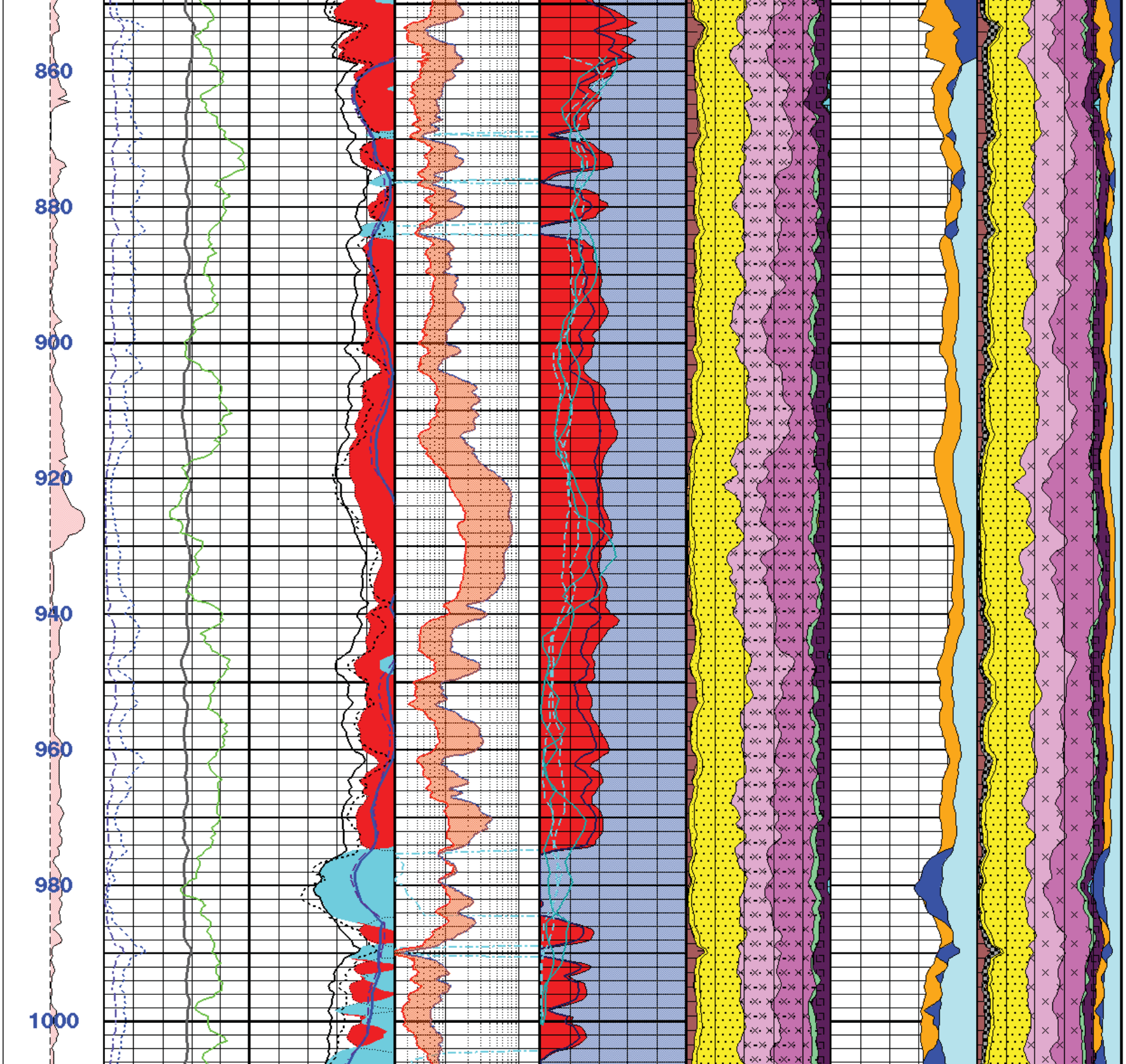
860
880
900
920
940
960
980
1000

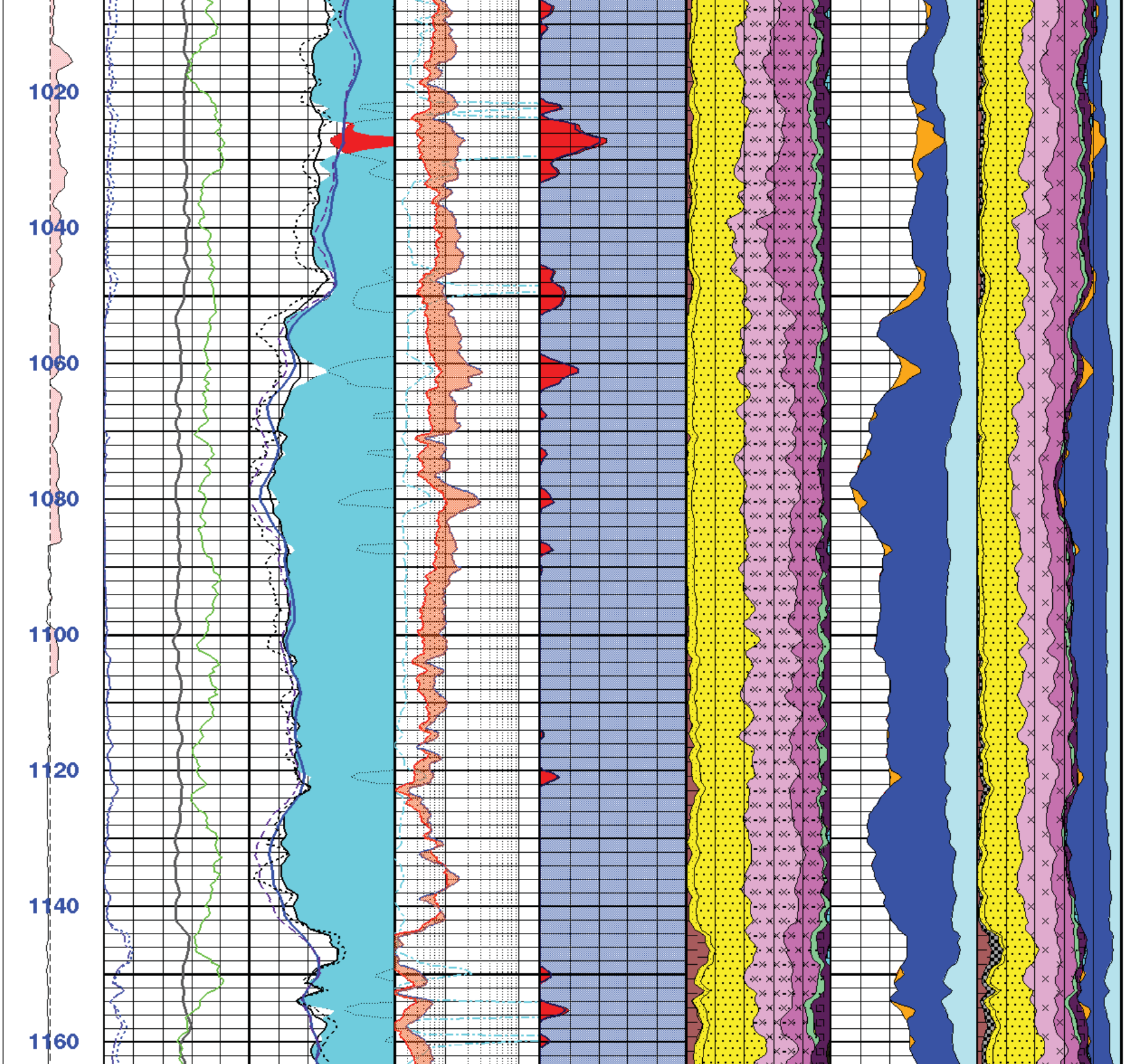
1020
1040
1060
1080
1100
1120
1140
1160

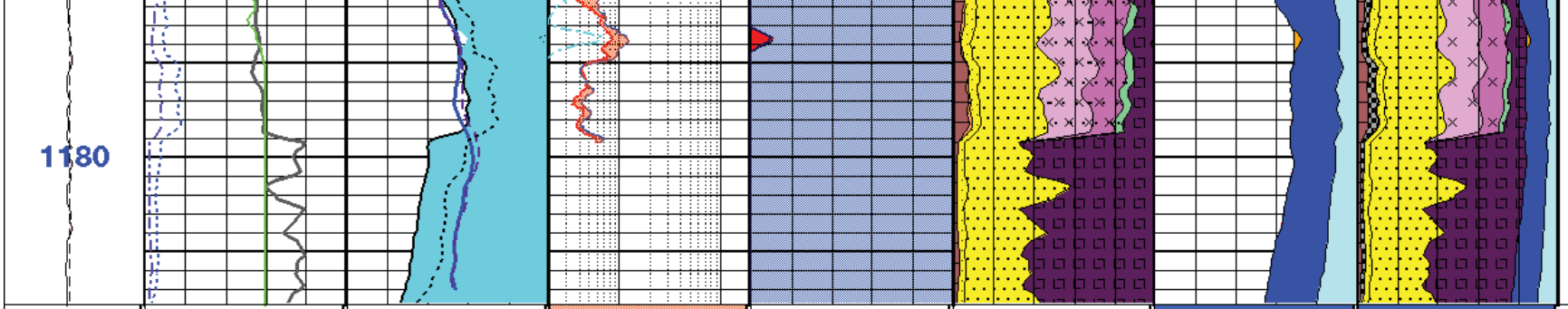

MD 1 : 240 ft	QV QV@ELAN	KSDR_SH4 K	Invasion	Sw w/ clay	WCLC WCLC@	Moved Water	Moved Water
	0 (meq/cm3) 1	10000 (mD) 0.1		1 (ft3/ft3) 0	0 ( ) 1		
Bitsize	CEC CEC@EL	KTIM_TAPER	RT_HRLT.ED	SWPC_SH4 S	WSM2 WSM2@	Moved Air	Moved Air
10 (in) 20	0 (meq/g) 0.2	10000 (mD) 0.1	20 (ohm.m) 2000	1 (ft3/ft3) 0	0 ( ) 1		
Hole Di	Grain Dens	KINT KINT@	RXO_HRLT.E	Sw no clay	WSM1 WSM1@	Irreducible Water	Irred. Water
10 (in) 20	2 (g/cm3) 3	10000 (mD) 0.1	20 (ohm.m) 2000	1 (ft3/ft3) 0	0 ( ) 1		
Washout	Cor. GR	KGAS KGAS@	RWA RWA@EL	Air	WIGN WIGN@	Moveable Water	Mov. Water
	0 (gAPI) 125	10000 (mD) 0.1	20 (ohm.m) 2000		0 ( ) 1		
		Gas		Water	WPYR WPYR@	Air	Air
					0 ( ) 1		
		Water		SWPC_SH8 S	WBIO WBIO@	Fluid Vol.	Calcite
				1 (ft3/ft3) 0	0 ( ) 1	0.5 (V/V) 0	
		KWTR KWTR@		SWPC_SH4 S	WFEL WFEL@		Magnetite
		10000 (mD) 0.1		1 (ft3/ft3) 0	0 ( ) 1		
		KINT.LAMBD		SWPC_SH8 S	WALB WALB@		Augite
		10000 (mD) 0.1		1 (ft3/ft3) 0	0 ( ) 1		
					WORT WORT@		Olivine
					0 ( ) 1		
					WSAN WSAN@		Pyrite
					0 ( ) 1		
					WQUA WQUA@		Biotite
					0 ( ) 1		
					WSIL WSIL@		Ca Plag.
					0 ( ) 1		
					WMON WMON@		Albite

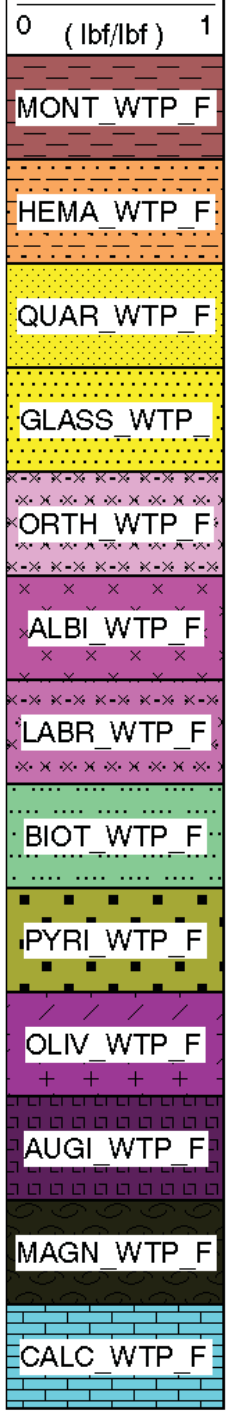
0
(lbf/lbf)
1
MONT_WTP_F
HEMA_WTP_F
QUAR_WTP_F
GLASS_WTP_
ORTH_WTP_F
ALBI_WTP_F
LABR_WTP_F
BIOT_WTP_F
PYRI_WTP_F
OLIV_WTP_F
AUGI_WTP_F
MAGN_WTP_F
CALC_WTP_F

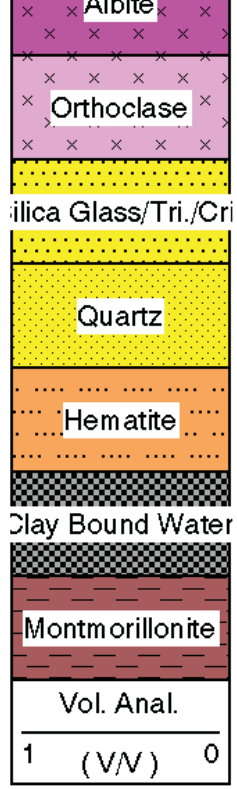
Albite
Orthoclase
ilica Glass/Tri./Cri
Quartz
Hematite
Clay Bound Water
Montmorillonite
Vol. Anal.
1
(V/V)
0

ATTACHMENT 4: COLOR PRINTS OF FMI COMPOSITE LOG FOR WELL CREX-1

See the following separate documents for this Attachment:
Attach4a-CrEX-1_processed_FMI_composite_log_1to20.PDF
Attach4b-CrEX-1_processed_FMI_composite_log_1to500.PDF

Schlumberger
Water Services

2045 N. Forbes Blvd., Suite 103, Tucson, AZ 85745, USA

Schlumberger

CrEX-1

Preliminary Processed FMI

COMPANY:	Los Alamos National Laboratory
WELL:	CrEX-1
FIELD:	LANL
RIG:	New Mexico
COUNTRY:	USA
Date Logged:	07-Aug-2014
Date Processed:	20 October
Surface Longitude:	106° 15'
Latitude:	35° 51' 28"
Elevations: KB:	6831 ft
DF:	6836 ft
GL:	6831 ft

FOLD HERE: The well name, location and borehole reference data were furnished by the customer.

Any interpretation, research, analysis, data, results, estimates, or recommendation furnished with the services or otherwise communicated by Schlumberger to the customer at any time in connection with the services are opinions based on inferences from measurements, empirical relationships, and/or assumptions; which, inferences, empirical relationships and/or assumptions are not infallible and with respect to which professionals in the industry may differ. Accordingly, Schlumberger cannot and does not warrant the accuracy, correctness, or completeness of any such interpretation, research, analysis, data, results, estimates, or recommendation. The customer acknowledges that it is accepting the services "as is," that Schlumberger makes no representation or warranty express

Svc. Order #:	Interpretation Center:	Analyst: HANSARD	Process Date: 20

Remarks:

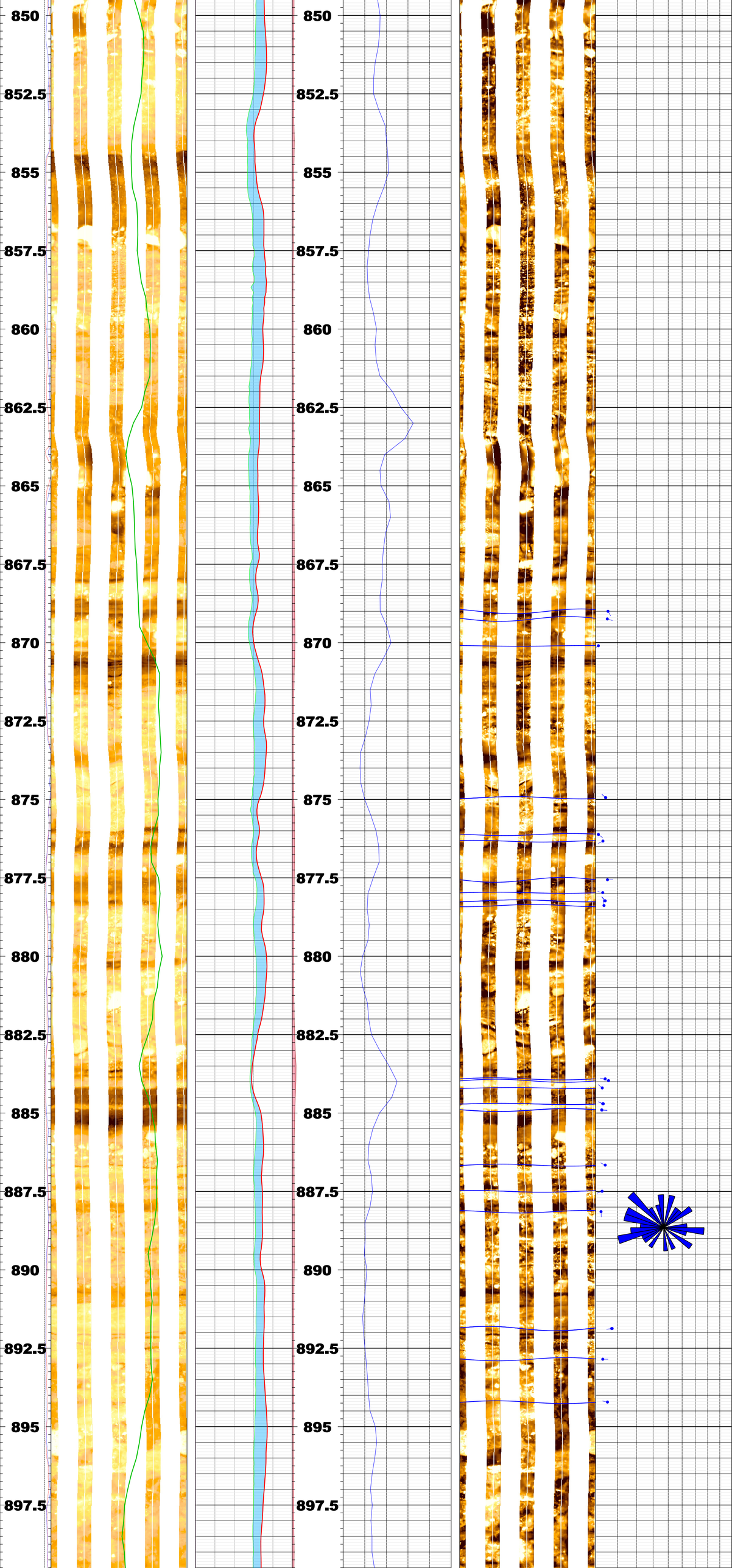
850
852.5
855
857.5
860
862.5
865
867.5
870
872.5
875
877.5
880
882.5
885
887.5
890
892.5
895
897.5

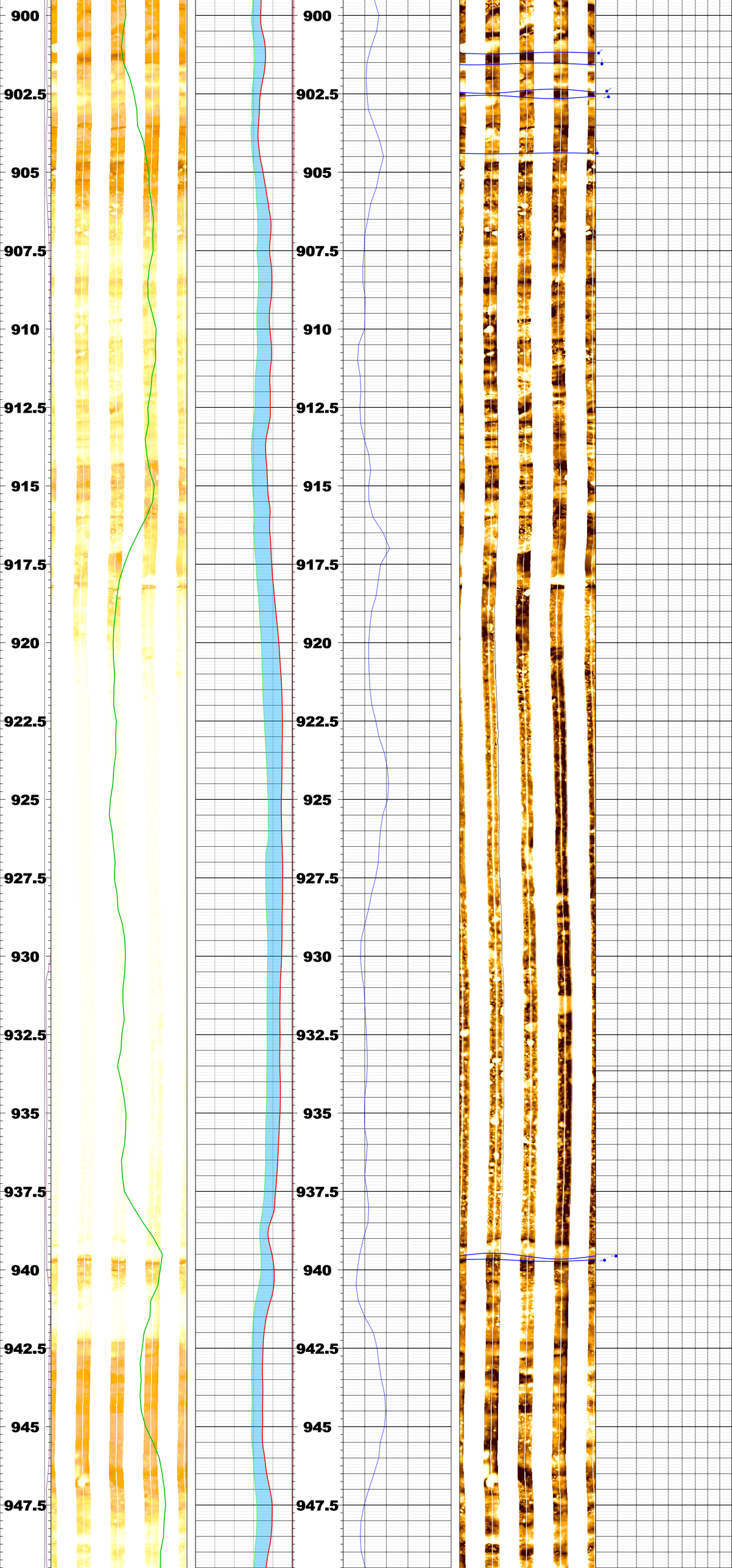
900
902.5
905
907.5
910
912.5
915
917.5
920
922.5
925
927.5
930
932.5
935
937.5
940
942.5
945
947.5

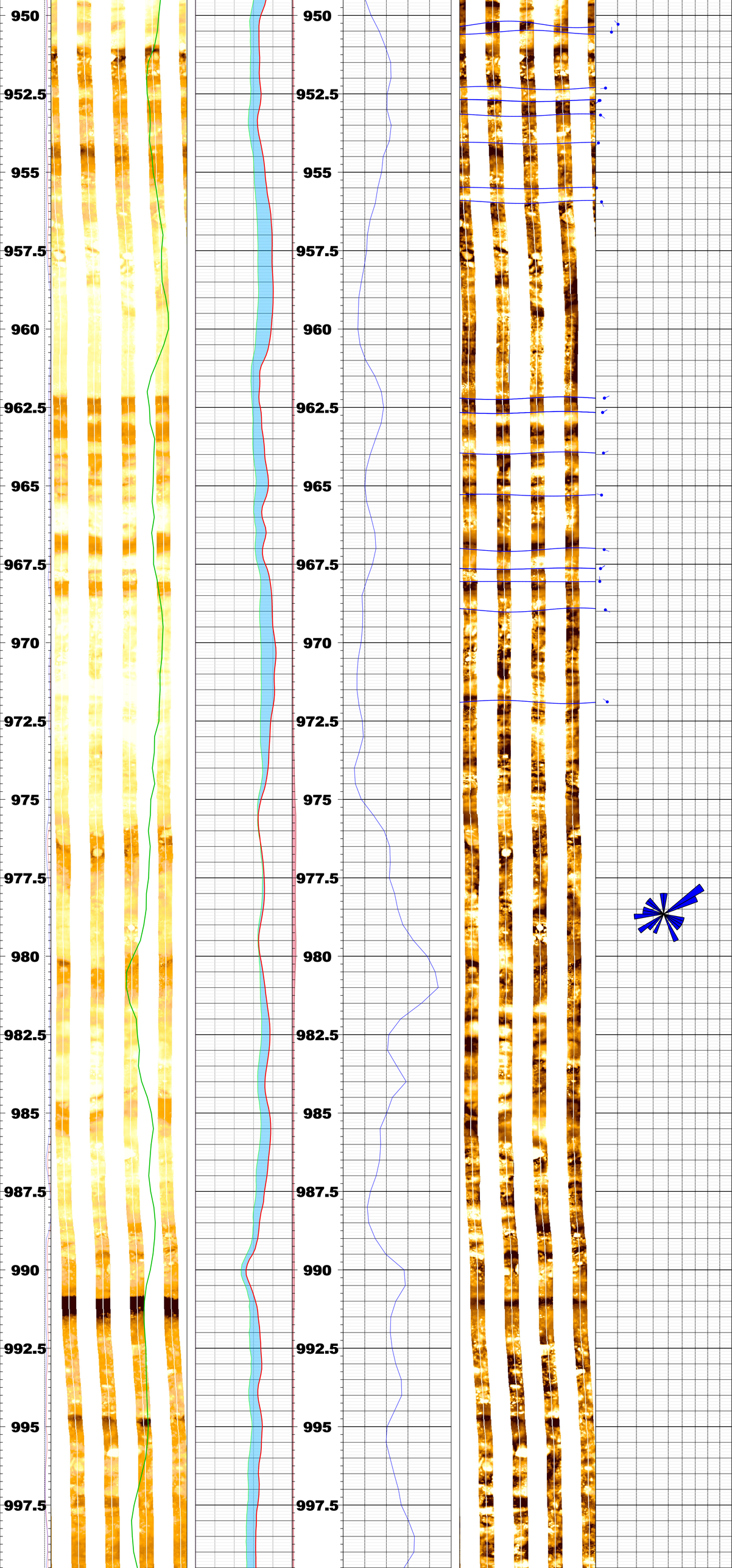
950
952.5
955
957.5
960
962.5
965
967.5
970
972.5
975
977.5
980
982.5
985
987.5
990
992.5
995
997.5

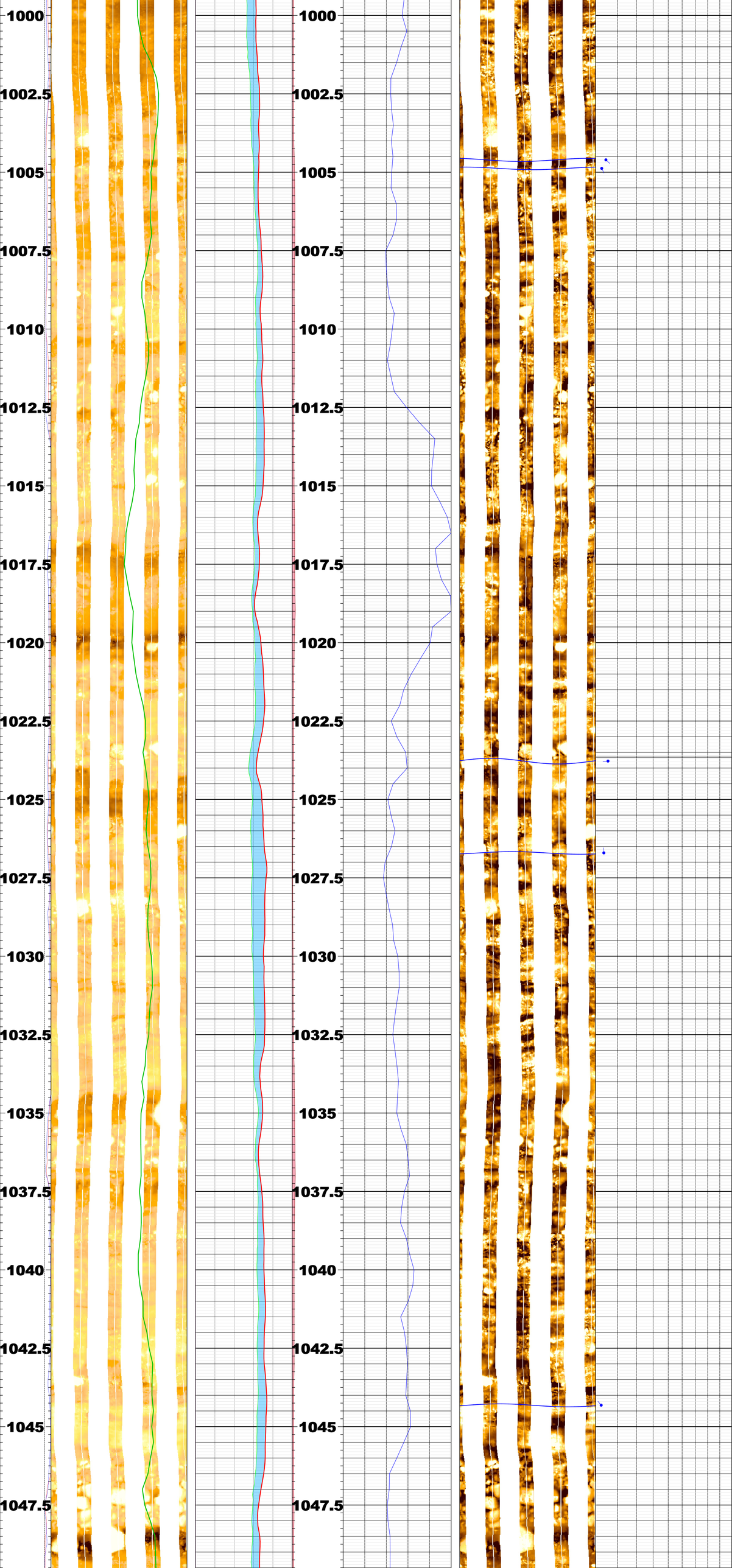
1000
1002.5
1005
1007.5
1010
1012.5
1015
1017.5
1020
1022.5
1025
1027.5
1030
1032.5
1035
1037.5
1040
1042.5
1045
1047.5

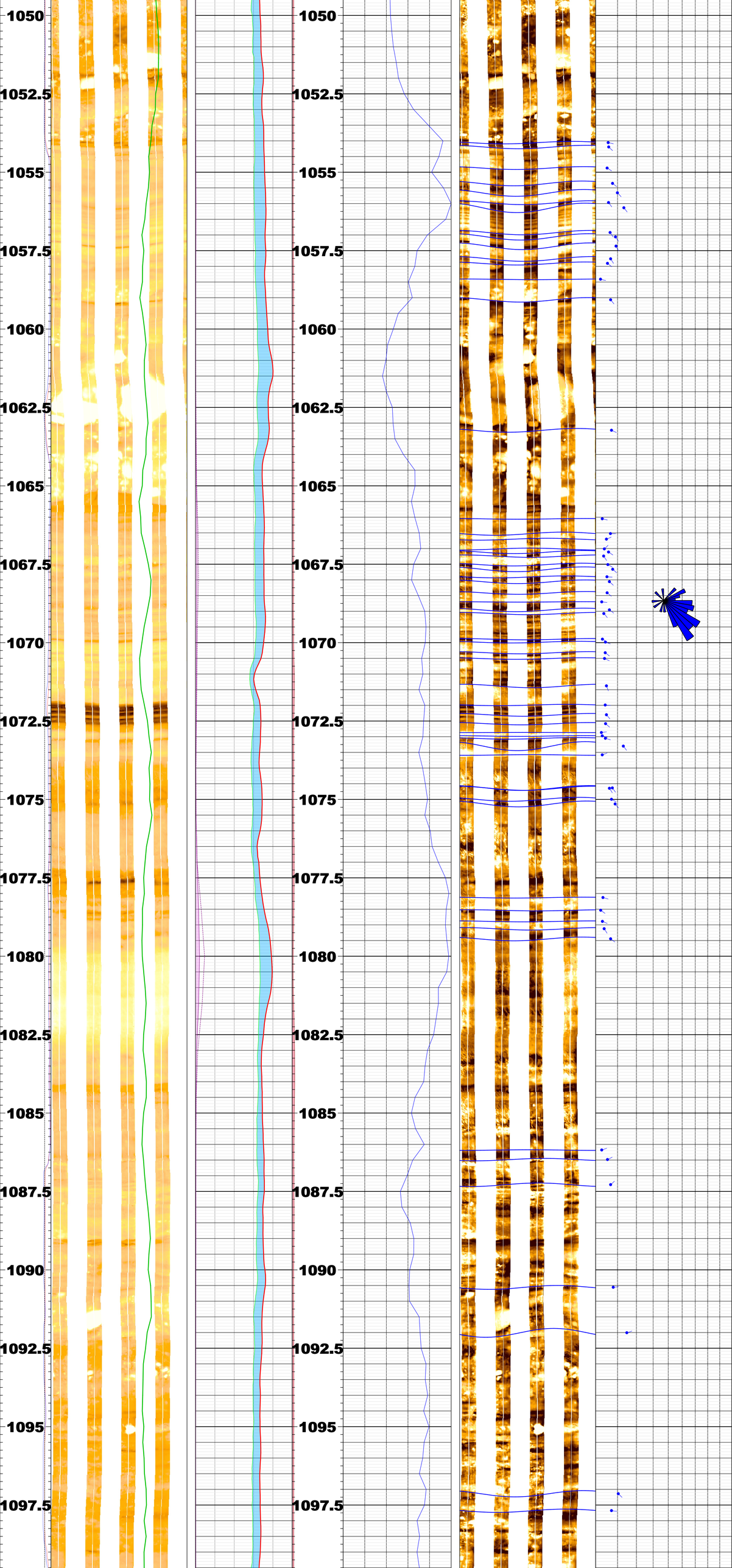
1050
1052.5
1055
1057.5
1060
1062.5
1065
1067.5
1070
1072.5
1075
1077.5
1080
1082.5
1085
1087.5
1090
1092.5
1095
1097.5

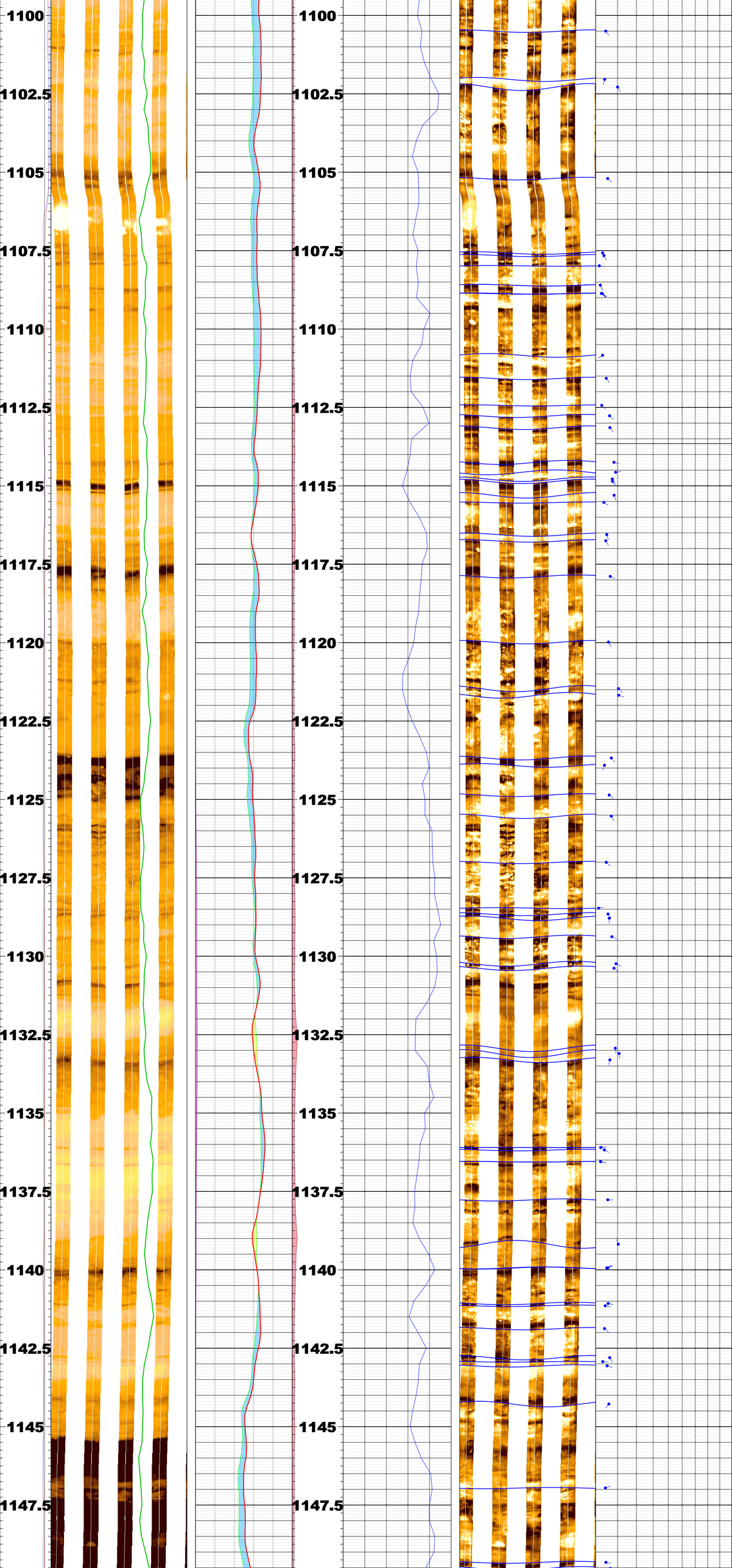
1100
1102.5
1105
1107.5
1110
1112.5
1115
1117.5
1120
1122.5
1125
1127.5
1130
1132.5
1135
1137.5
1140
1142.5
1145
1147.5

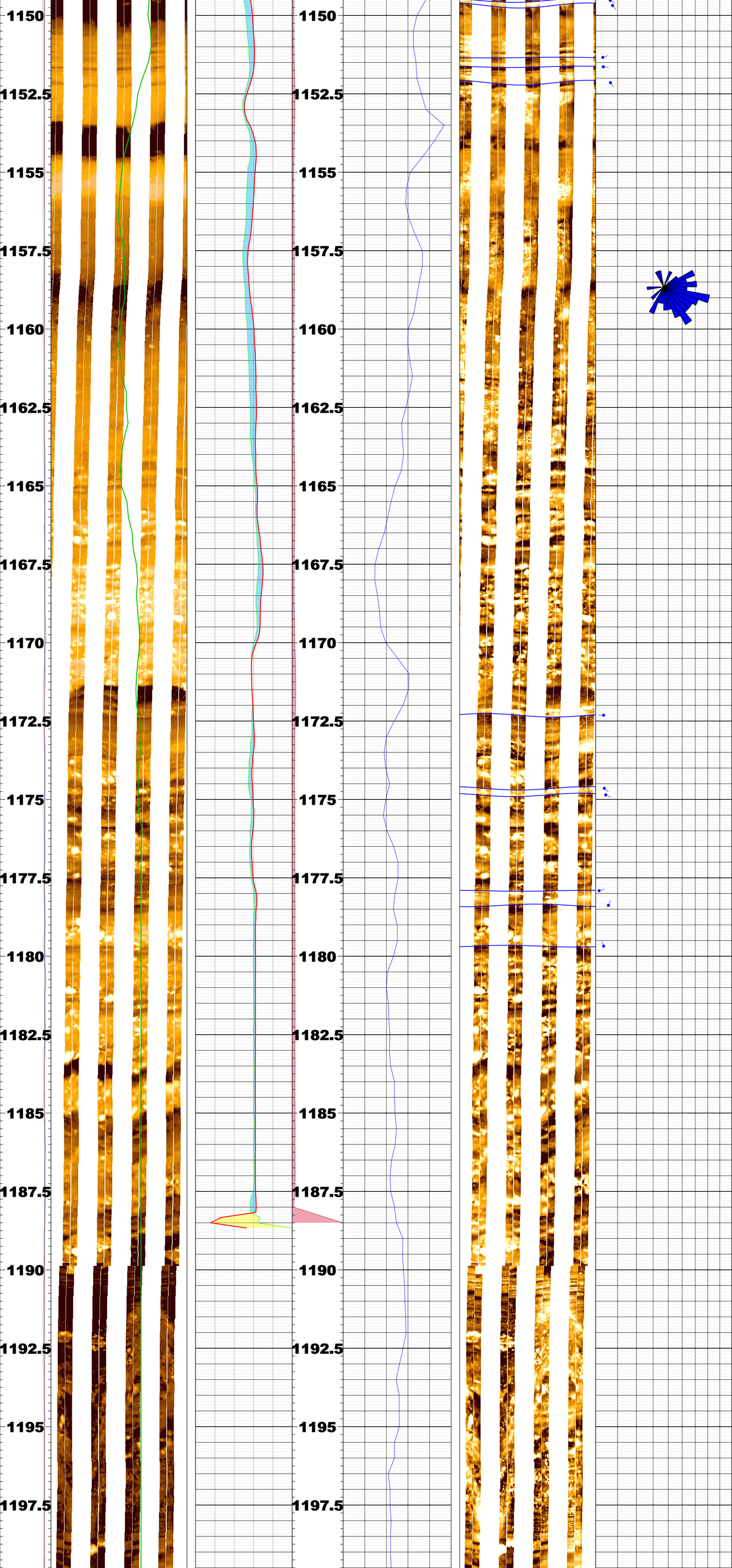
1150
1152.5
1155
1157.5
1160
1162.5
1165
1167.5
1170
1172.5
1175
1177.5
1180
1182.5
1185
1187.5
1190
1192.5
1195
1197.5

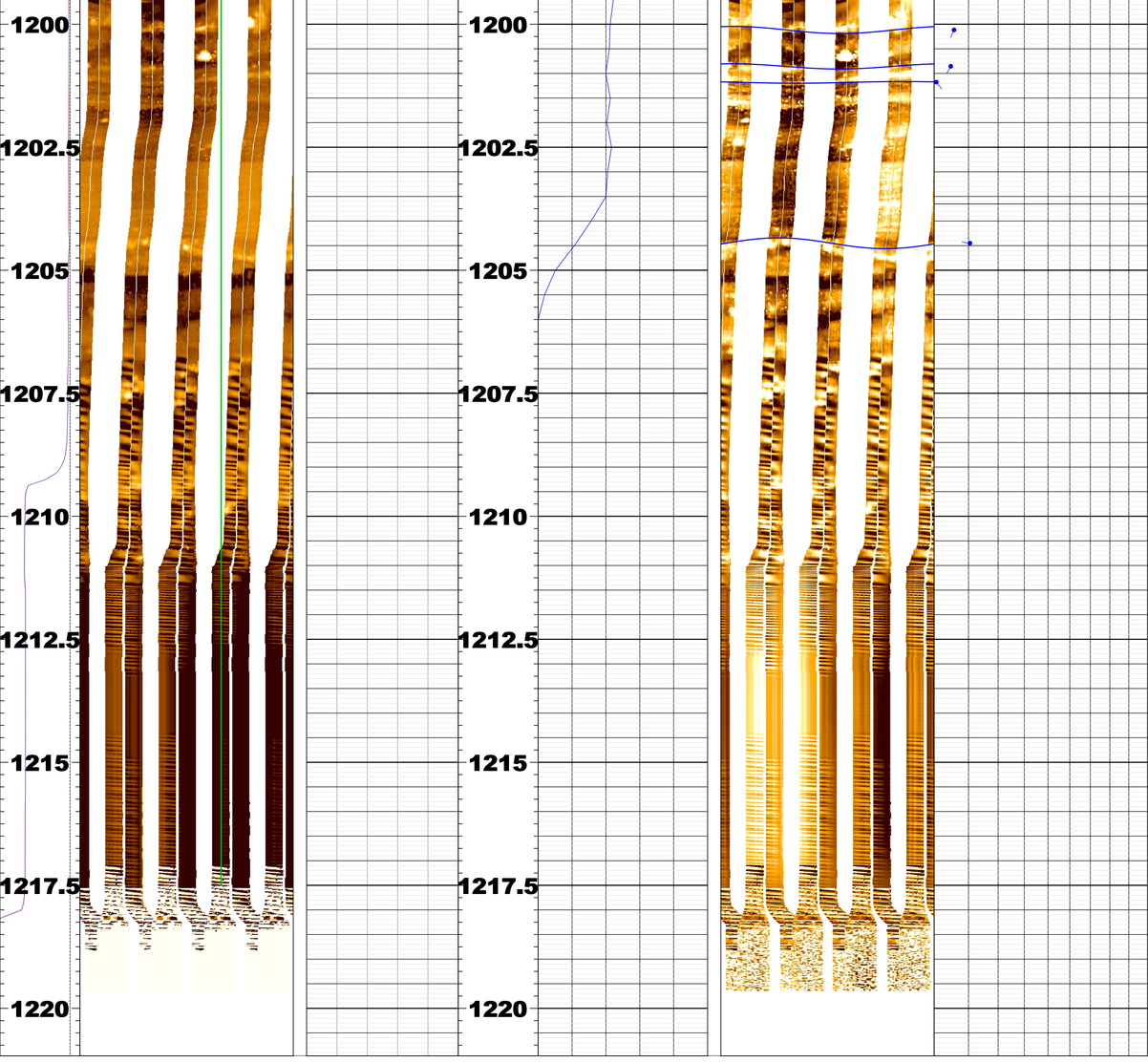
1200
1202.5
1205
1207.5
1210
1212.5
1215
1217.5
1220
1200
1202.5
1205
1207.5
1210
1212.5
1215
1217.5
1220

Schlumberger

CrEX-1

Preliminary Processed FMI

COMPANY:	Los Alamos National Laboratory		
WELL:	CrEX-1		
FIELD:	LANL		
RIG:	New Mexico		
COUNTRY:	USA		
Date Logged:	07-Aug-2014	Date Processed:	20 October
Surface Elevations:	Longitude: 106° 15' 28"	Latitude: 35° 51' 28"	
	KB: 6831 ft	DF: 6836 ft	GL: 6831 ft

FOLD HERE: The well name, location and borehole reference data were furnished by the customer.

Svc. Order #:	Interpretation Center:	Analyst: HANSARD	Process Date: 20

Remarks:

Appendix D

Aquifer Testing Report

D-1.0 INTRODUCTION

This appendix describes the hydrogeological analysis of the aquifer tests at well CrEX-1 located in Mortandad Canyon within the existing chromium plume. The primary objective of the analysis was to determine the hydraulic properties of the zones screened by CrEX-1.

Conceptual Hydrogeology

The CrEX-1 screened intervals consist of a 50-ft-long screen from 990 ft to 1040 ft below ground surface (bgs) and a 20-ft-long screen from 1070 ft to 1090 ft bgs. There is a 30-ft blank zone between the two screens.

CrEX-1 was completed in the Puye Formation (Tpf, 809 ft to 1054 ft bgs), mixed Miocene deposits (Tjpf and Tcar, 1054 ft to 1070 bgs), and Miocene pumiceous sediments (Tjfp, 1070 ft to 1155 ft bgs). Because only the upper 50-ft screen was pumped, the aquifer test provides information about the properties of the Puye Formation and mixed Miocene deposits.

On October 3, 2014, following well installation, well development, installation of the packer between the upper and lower screens, and aquifer testing, depth to water was 997.2 ft bgs in the completed well. The upper screen of CrEX-1 straddles the regional water table. This allows for effective assessment of the uppermost portion of the regional aquifer next to the regional water table where the highest contaminant concentrations are expected. As a result, the effective screen length is about 43 ft (from the water table to the bottom of the upper screen, which is at 1040 ft bgs).

The pumping of CrEX-1 produced a maximum drawdown of about 6.2 m (~20 ft) within the pumped upper screen. However, the well specific capacity did not decline with the increase of the pumping rate (and the respective increase of the pumping drawdown; see below). This suggests that borehole skin effects caused a portion of the drawdown. Skin effect is an increase in the pressure drop at the pumping well when compared with aquifer pressure adjacent to the well. The increased pressure drop is thought to be caused by extra flow resistance near the wellbore because of imperfect hydraulic connection between the well and the aquifer. As a result, the drawdown in the aquifer adjacent to the well is expected to be much lower than the one observed within the pumped borehole. Nevertheless, the pumping caused a decline in the regional water table, and it is likely that vadose zone groundwater flow impacted the drawdowns observed in CrEx-1. Therefore, unconfined (phreatic) groundwater flow is occurring near the pumped well. However, the observed drawdowns are still small compared with the aquifer thickness (>100 ft), so it is acceptable to use analyses that interpret the flow as confined. In addition, analyses accounting for unconfined groundwater flow were also performed using Moench methodology (1997, 600136).

Aquifer Testing

CrEX-1 was tested from October 1 through 4, 2014. Testing consisted of a five-step pumping test on October 1 and a 24-h constant-rate pumping test that started on October 3.

The pumping rates during the five-step test and the 24-h pumping test are shown in Figure D-1.0-1. The figure also shows the water-level fluctuations measured in CrEX-1. The pumping rates were relatively steady. The water level declined and rebounded very fast when pumping was turned on and off. The initial over-shooting of the water levels during recovery after the pump was turned off potentially suggests groundwater recharge from the vadose zone. The water level also returned relatively fast to prepumping conditions after the pump was turned off. This suggests that the aquifer is relatively well producing, and borehole skin effects may be impacting the observed drawdowns within the pumping well.

D-2.0 AQUIFER-TEST INTERPRETATION

Drawdown and recovery data can be analyzed using a variety of methods. The Theis equation (1934-1935, 098241) describes drawdown around a well as follows (Equation D-2.0-1):

$$s = \frac{Q}{4\pi T}\int_u^\infty \frac{e^{-x}}{x}dx = \frac{Q}{4\pi T}W(u) = \frac{Q}{4\pi T}W\left(\frac{r^2}{4at}\right) = \frac{Q}{4\pi T}W\left(\frac{r^2 S}{4Tt}\right) \qquad \textbf{Equation D-2.0-1}$$

where *s* is drawdown (in m), *Q* is discharge rate (in m^3/d), *T* is transmissivity (in m^2/d), *a* is hydraulic diffusivity (characterizing the speed of propagation of hydraulic pressures in the subsurface) (in m^2/d), *S* is storage coefficient (dimensionless [-]), *t* is pumping time (in d), and *r* is the distance from the pumping well (in m).

The Cooper-Jacob method (1946, 098236) provides a simplification of the Theis equation. The Cooper-Jacob equation describes drawdown around a pumping well as follows (Equation D-2.0-2):

$$s = \frac{2.303Q}{4\pi T} log_{10}\frac{2.25at}{r^2} = \frac{2.303Q}{4\pi T} log_{10}\frac{2.25Tt}{r^2 S} \qquad \textbf{Equation D-2.0-2}$$

The Cooper-Jacob equation is valid whenever the *u* value in the Theis equation above is less than 0.05. For small radius values (e.g., corresponding to borehole radii), *u* is less than 0.05 at very early pumping times and, therefore, is less than 0.05 for most or all measured drawdown values. Thus, for the pumped well, the Cooper-Jacob equation usually can be considered a valid approximation of the Theis equation. According to the Cooper-Jacob method, the time-drawdown data are plotted on a semilog plot, with time plotted on the logarithmic scale. Then a straight line of best fit is constructed through the data points and transmissivity is calculated using Equation D-2.0-2:

$$T = \frac{2.303Q}{4\pi\Delta s} \qquad \textbf{Equation D-2.0-3}$$

where Δs is the slope of the straight line on the semilog plot (typically estimated as a change over one log cycle of the graph) (in m). The Cooper-Jacob method also allows for estimation of the hydraulic diffusivity *a* (and respectively of the storage coefficient *S*). However, these estimates are typically highly unreliable when drawdowns are observed at the pumping well. The hydraulic diffusivity and the storage coefficient can be estimated reliably only when based on drawdowns observed at an observation well near the pumping well.

The recovery data are analyzed using the Theis recovery method, which is a semilog analysis method similar to the Cooper-Jacob method described above. In this method, the only difference is that the residual drawdown is plotted on a semilog plot versus the ratio *t/t'*, where *t* is the time since pumping began, and *t'* is the time since pumping stopped. A straight line of best fit is constructed through the data points, and *T* is calculated from the slope of the straight line as in the Cooper-Jacob method above. The recovery data are particularly useful compared with drawdown data. Because the pump is not running, data responses associated with temporal discharge rate fluctuations are eliminated. The result is that the recovery data set is generally "smoother" and easier to analyze.

More complicated analytical solutions are available to account for drawdown impacts caused by vadose zone flow, partial well penetration, aquifer leakage, etc. Some of these analytical solutions are available in simulation codes such as WELLS (http://wells.lanl.gov) and AQTESOLV (http://www.aqtesolv.com). For example, the codes allow for analyses using the Moench method (1997, 600136); this method is applied to analyze the drawdown data as well.

D-3.0 DATA ANALYSIS

This section presents the data obtained during the aquifer tests and the results of the analytical interpretations. Data are presented for drawdown and recovery for the five-step test and 24-h constant-rate pumping test.

Five-Step Variable-Rate Aquifer Test

The specific capacity data obtained from the CrEX-1 five-step pumping test are summarized in Table D-3.0-1. The table also includes specific capacity data obtained during the 24-h constant-rate pumping test. Note that these values are approximate because the pumping drawdowns did not reach equilibration at the end of the pumping period during all the tests. During the step tests, the specific capacity varied between about 100 m^2/d and 120 m^2/d (~5.5 gallons per minute [gpm]/ft and 6.6 gpm/ft). The step-test data demonstrate that the specific capacity of the well does not seem to depend on the pumping rate, which suggests the well is well developed.

24-Hour Constant-Rate Aquifer Test

Figure D-3.0-1 shows a semilog plot of the drawdown data recorded during the 24-h constant-rate pumping test conducted at an average pumping rate of 517.6 m^3/d (~94.9 gpm). The test data show a well-defined drawdown curve with short-term, temporary equilibration of the water-level decline midway through the test (Figure D-3.0-1); there might also be a second, very short equilibration period close to the end of the test. The temporary equilibration may be caused by (1) vadose zone recharge (delayed yield effects), (2) three-dimensional groundwater flow effects (because of vertical expansion of the cone of depression), (3) recharge boundary effects, or (4) fluctuations in municipal water-supply pumping. It is important to note that the drawdowns did not equilibrate at the end of the 24-h constant-rate pumping test. However, based on the general understanding of the hydrogeologic conditions at the site, equilibration is expected at later pumping times.

Based on analysis of the drawdown curve in Figure D-3.0-1, two periods can be characterized with straight lines matching the drawdown data (there is potentially a third period at the end of the pumping test, but clearly the slope of the third period matches the slope of the second period). The first straight-line match defines the transmissivity of the aquifer in close vicinity to the well. The estimated aquifer transmissivity close to CrEX-1 is 510 m^2/d (41,000 gpd/ft). The second straight-line slope defines lower transmissivity. The transmissivity is lower because, at later pumping times, the cone of depression has reached a portion of the aquifer with lower transmissivity. This potentially suggests aquifer heterogeneity. The second (late-time) straight-line slope characterizes the effective aquifer properties impacting the groundwater flow towards CrEX-1. The estimated effective aquifer transmissivity in the vicinity of CrEX-1 is about 360 m^2/d (30,000 gpd/ft).

Figure D-3.0-2 presents analysis of the drawdown data performed using the Moench method (1997, 600136), assuming unconfined groundwater flow; the analysis was performed using the code AQTESOLV. The analysis produced better overall representation of the drawdown data and better characterization of the late-time data. As a result, the estimated transmissivity value is consistent with the late-time estimate given above, assuming confined conditions. The estimated effective aquifer transmissivity is 340 m^2/d, assuming unconfined conditions.

Figure D-3.0-3 shows CrEX-1 drawdown recovery after the 24-h constant-rate pumping test. The drawdown recovery was plotted on a semilog plot versus the ratio t/t', where t is the time since pumping began, and t' is the time since pumping stopped. The recovery at late times (in Figure D-3.0-3, time increases from left to right) shows two well-defined straight-line periods separated by a period of temporal

drawdown equilibration. As stated above, the temporary equilibration may be caused by (1) vadose zone recharge (delayed yield effect), (2) three-dimensional groundwater flow effects (because of vertical expansion of the cone of depression), (3) boundary effects, or (4) fluctuations in municipal water-supply pumping. However, in Figure D-3.0-3, both straight lines have very similar slopes and defined transmissivity values of 480 m^2/d and 490 m^2/d, respectively (39,000 gpd/ft and 40,000 gpd/ft, respectively). These transmissivity estimates are between the transmissivity estimates based on the drawdown data and are expected to represent the effective aquifer properties impacting the groundwater flow towards the well during drawdown recovery of CrEX-1. In conclusion, it can be assumed that the value of 490 m^2/d (40,000 gpd/ft) is the current best estimate of the aquifer transmissivity in the area near CrEX-1. This transmissivity value is very similar to the estimate obtained by a recent R-28 aquifer test analysis conducted in 2014 (LANL 2014, 255110).

The saturated thickness corresponding to the transmissivity value is not known to estimate hydraulic conductivity. The saturated thickness is impacted by the pumping because the pumping causes a decline in the regional water table. Assuming the saturated thickness is the length of the initial saturated screened interval (~43 ft; before the pumping started) minus half the observed drawdown (~10 ft), the estimated average hydraulic conductivity is about 49 m/d or 161 ft/d. This estimate is uncertain, but the value of hydraulic conductivity is consistent with the estimate obtained for R-28 (~120 ft/d).

The CrEX-1 transmissivity and hydraulic conductivity estimates suggest that the well is tapping a highly permeable zone in the regional aquifer. This helps achieve the CrEX-1 objective of hydraulic capture of contaminated groundwater.

D-4.0 REFERENCES

The following list includes all documents cited in this appendix. Parenthetical information following each reference provides the author(s), publication date, and ER ID or ESH ID. This information is also included in text citations. ER IDs were assigned by the Environmental Programs Directorate's Records Processing Facility (IDs through 599999), and ESH IDs are assigned by the Environment, Safety, and Health (ESH) Directorate (IDs 600000 and above). IDs are used to locate documents in the Laboratory's Electronic Document Management System and, where applicable, in the master reference set.

Copies of the master reference set are maintained at the NMED Hazardous Waste Bureau and the ESH Directorate. The set was developed to ensure that the administrative authority has all material needed to review this document, and it is updated with every document submitted to the administrative authority. Documents previously submitted to the administrative authority are not included.

Cooper, H.H., Jr., and C.E. Jacob, August 1946. "A Generalized Graphical Method for Evaluating Formation Constants and Summarizing Well-Field History," *American Geophysical Union Transactions,* Vol. 27, No. 4, pp. 526-534. (Cooper and Jacob 1946, 098236)

LANL (Los Alamos National Laboratory), March 2014. "Summary Report for the 2013 Chromium Groundwater Aquifer Tests at R-42, R-28, and SCI-2," Los Alamos National Laboratory document LA-UR-14-21642, Los Alamos, New Mexico. (LANL 2014, 255110)

Moench, A.F., June 1997. "Flow to a Well of Finite Diameter in a Homogenous, Anisotropic Water Table Aquifer," *Water Resources Research,* Vol. 33, No. 6, pp. 1397–1407. (Moench 1997, 600136)

Theis, C.V., 1934-1935. "The Relation Between the Lowering of the Piezometric Surface and the Rate and Duration of Discharge of a Well Using Ground-Water Storage," *American Geophysical Union Transactions,* Vol. 15-16, pp. 519-524. (Theis 1934-1935, 098241)

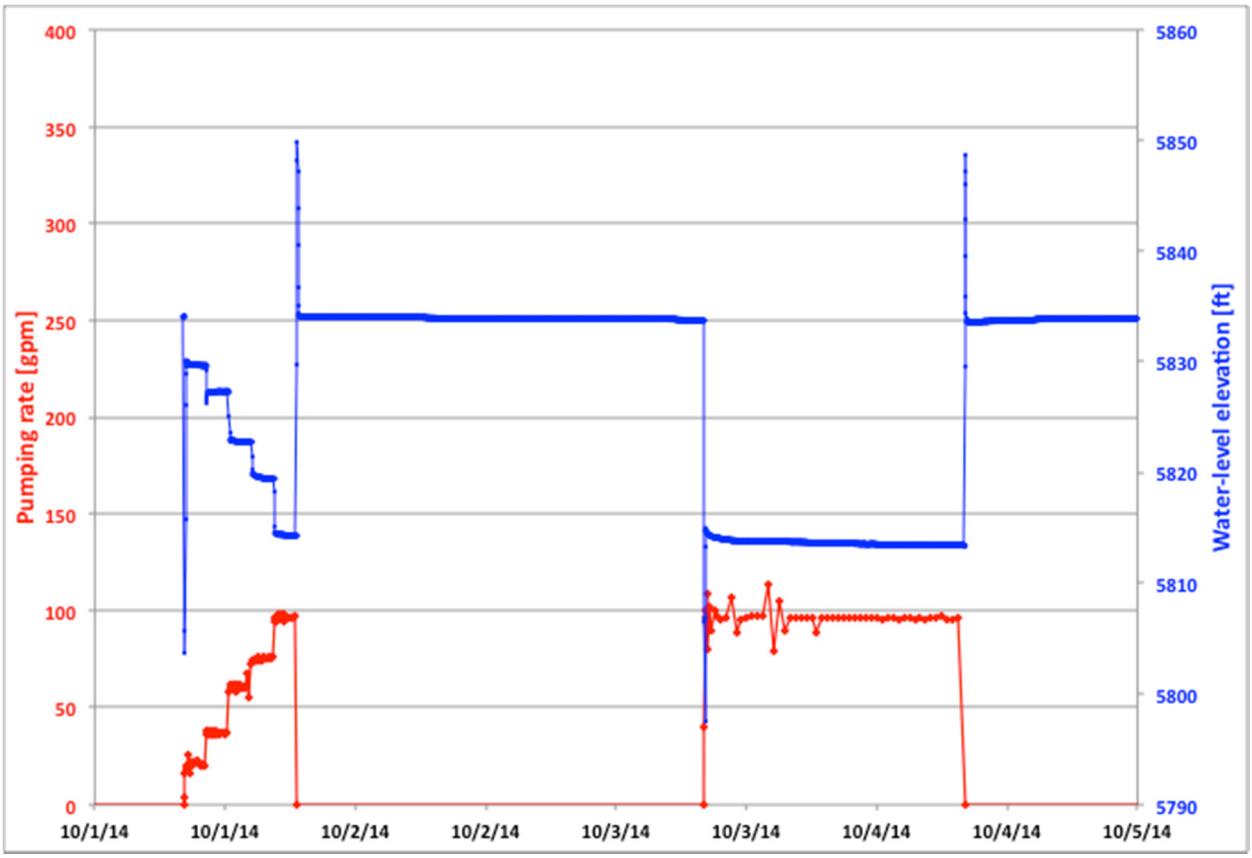

Figure D-1.0-1 Change in pumping rates (in red, left y-axis) and water-level elevations (in blue, right y-axis) during the five-step test and the 24-h pumping test over time

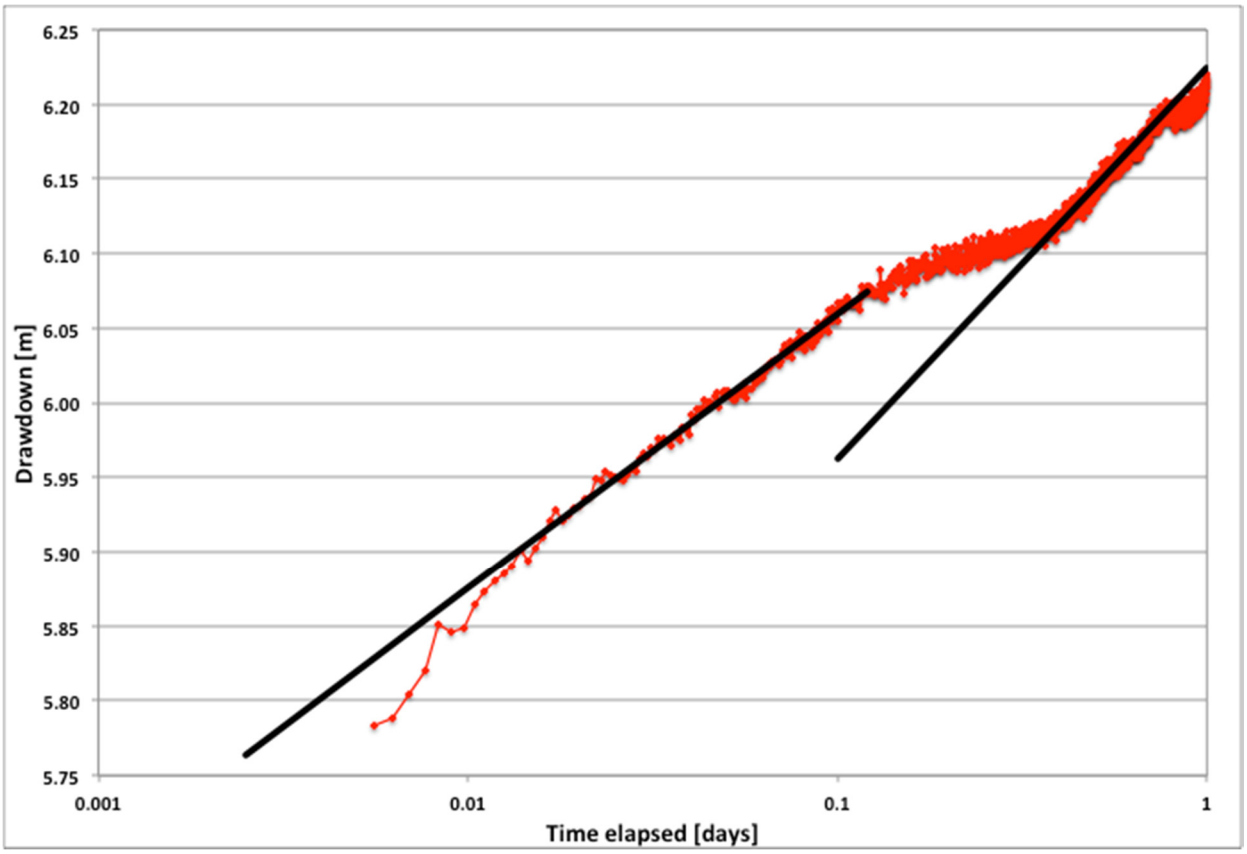

Note: The analysis of the drawdown data was performed using the Cooper-Jacob method, assuming confined groundwater flow.

Figure D-3.0-1 CrEX-1 drawdown versus time during the 24-h constant-rate pumping test

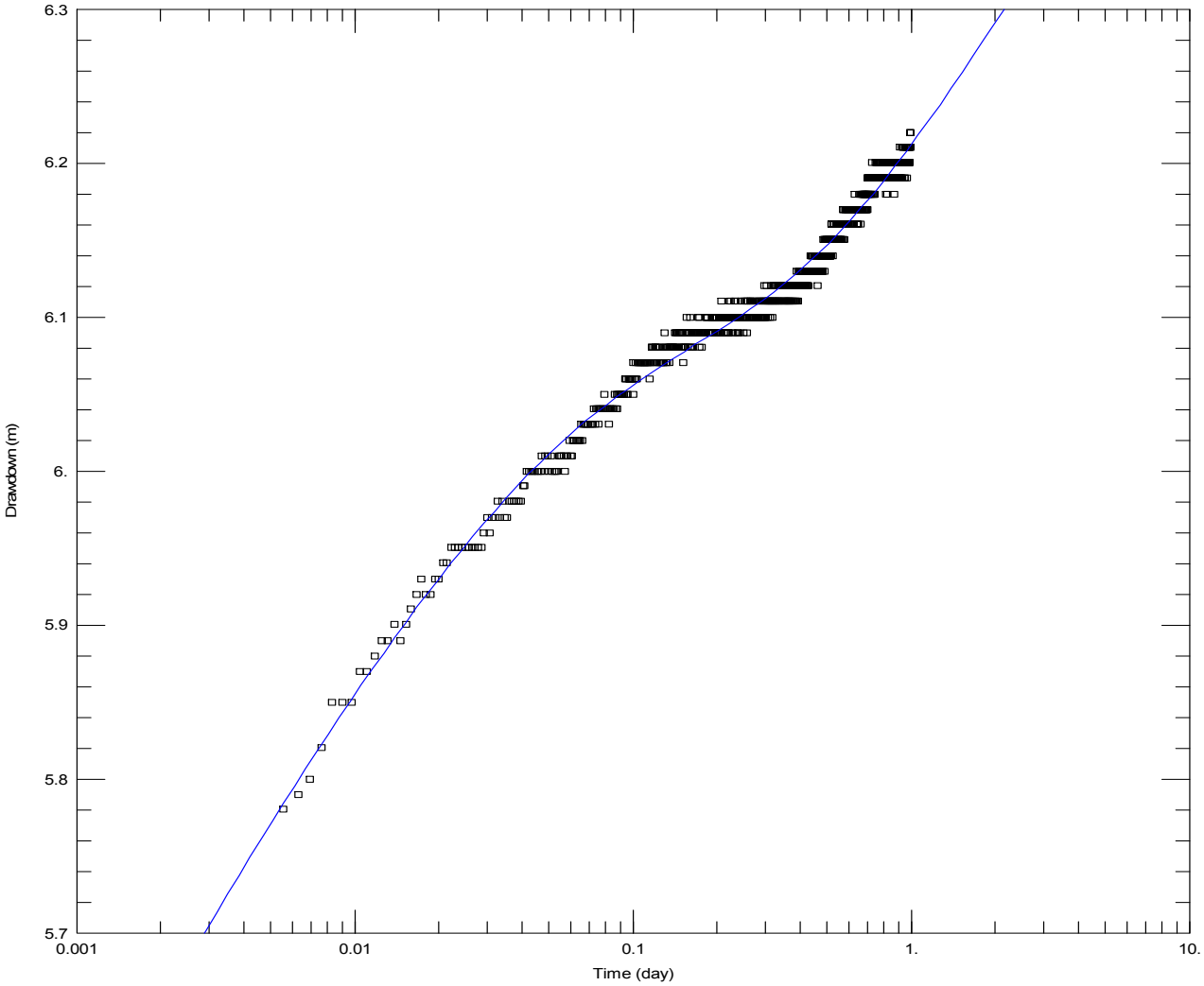

Note: The analysis of the drawdown data was performed using the Moench method (1997, 600136), assuming unconfined groundwater flow; the analysis was performed using the code AQTESOLV.

Figure D-3.0-2 CrEX-1 drawdown versus time during the 24-h constant-rate pumping test

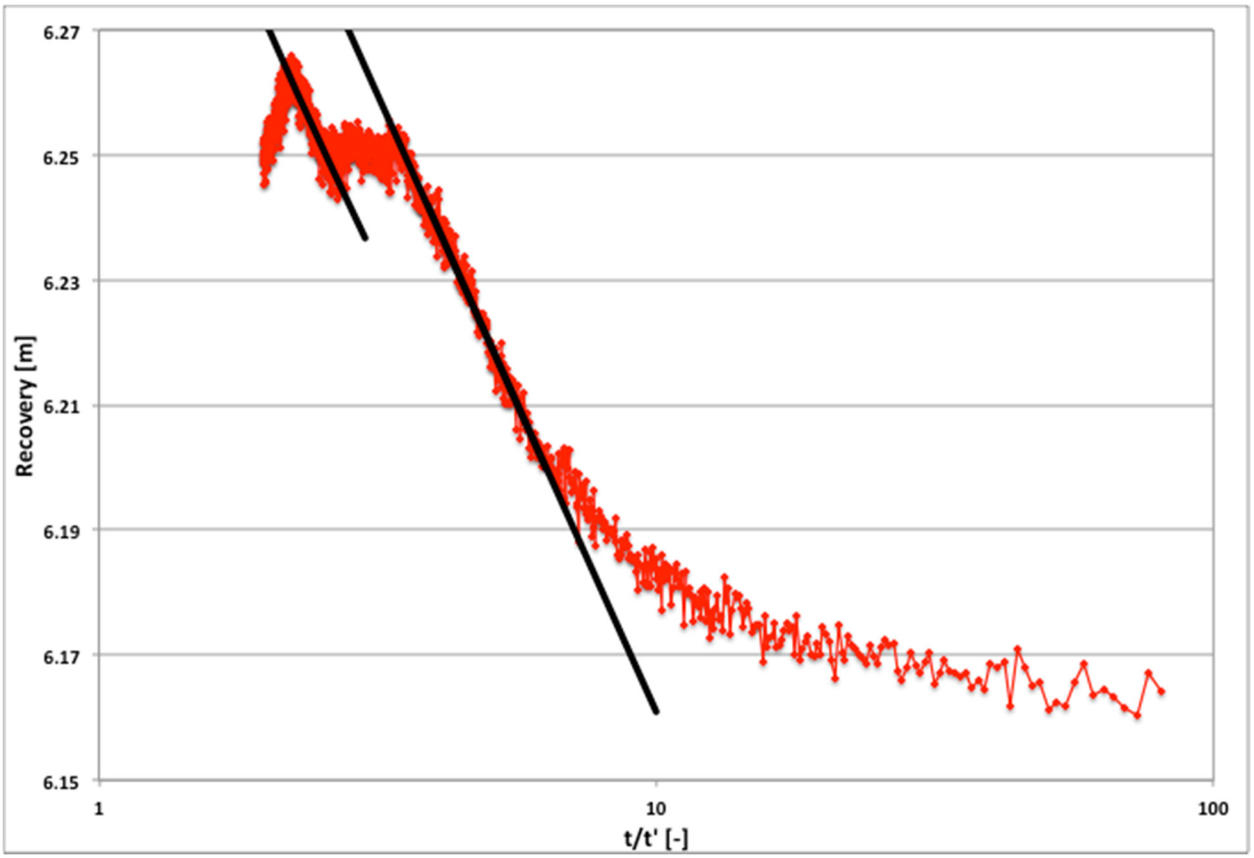

Notes: The drawdown recovery was plotted on a semilog plot versus the ratio *t/t'*, where *t* is the time since pumping began, and *t'* is the time since pumping stopped. Effectively, the time increases from left to right.

Figure D-3.0-3 CrEX-1 drawdown recovery after the 24-h constant-rate pumping test

Table D-3.0-1
Summary of Specific Capacity Data Obtained from CrEX-1 Aquifer Tests

Test	Average Pumping Rate (gpm)	Average Drawdown (ft)	Average Specific Capacity (gpm/ft)	Average Pumping Rate (m^3/d)	Average Drawdown (m)	Average Specific Capacity (m^2/d)
Step test #1	20.5	3.7	5.48	111.6	1.14	98.1
Step test #2	35.7	5.6	6.39	194.5	1.70	114.3
Step test #3	60.3	10.3	5.85	328.8	3.15	104.5
Step test #4	74.8	11.3	6.63	407.5	3.44	118.5
Step test #5	96.2	16.2	5.95	524.2	4.92	106.5
24-h test	94.9	20.1	4.73	517.6	6.12	84.5